

Sheffield Hallam University

A study of triorganotin biocides in antifouling coatings.

CAMPBELL, Stewart James.

Available from the Sheffield Hallam University Research Archive (SHURA) at:

<http://shura.shu.ac.uk/19421/>

A Sheffield Hallam University thesis

This thesis is protected by copyright which belongs to the author.

The content must not be changed in any way or sold commercially in any format or medium without the formal permission of the author.

When referring to this work, full bibliographic details including the author, title, awarding institution and date of the thesis must be given.

Please visit <http://shura.shu.ac.uk/19421/> and <http://shura.shu.ac.uk/information.html> for further details about copyright and re-use permissions.

POLYTECHNIC LIBRARY
POND STREET
SHEFFIELD S1 1WB

TELEPEN

100305425 0



Sheffield City Polytechnic Library

REFERENCE ONLY

ProQuest Number: 10694302

All rights reserved

INFORMATION TO ALL USERS

The quality of this reproduction is dependent upon the quality of the copy submitted.

In the unlikely event that the author did not send a complete manuscript and there are missing pages, these will be noted. Also, if material had to be removed, a note will indicate the deletion.



ProQuest 10694302

Published by ProQuest LLC (2017). Copyright of the Dissertation is held by the Author.

All rights reserved.

This work is protected against unauthorized copying under Title 17, United States Code
Microform Edition © ProQuest LLC.

ProQuest LLC.
789 East Eisenhower Parkway
P.O. Box 1346
Ann Arbor, MI 48106 – 1346

**A STUDY OF TRIORGANOTIN BIOCIDES
IN ANTIFOULING COATINGS**

Stewart James Campbell BSc

A thesis submitted in partial fulfilment of the
requirements of the Council for National Academic Awards for the
degree of Doctor of Philosophy

September 1990

Sponsoring

Establishment: Sheffield City Polytechnic

Collaborating

Establishment: Admiralty Research Establishment, Poole



Abstract

A Study of Triorganotin Biocides in Antifouling Coatings

by

Stewart Campbell

The technique of tin-119m Mößbauer and NMR spectroscopy has been used to study the chemical and structural changes undergone by a series of triorganotin biocides when dispersed in an antifouling paint and a polyurethane system.

In the antifouling paint, based on the Hypalon polymer, tri-n-butyltin chloride, tri-n-butyltin acetate and *bis*-(triphenyltin) oxide are essentially unmodified. *Bis*-(tri-n-butyltin) oxide, in contrast, was entirely converted into two new species, one of which was identified as tri-n-butyltin chloride. The second component was thought to be a sulphonate ester. However, synthesis of such compounds and subsequent spectroscopic analysis did not support this theory.

Triphenyltin acetate experienced some dephenylation when incorporated into the paint, with a diphenyltin species detected by Mößbauer spectroscopy and GC analysis. Triphenyltin chloride suffered more extensive dephenylation, the dried paint containing the mono- and diphenyltin species.

The organotin release-rate of eight Hypalon paint samples has been determined using a flow system and analysis of the effluent by graphite furnace atomic absorption spectrometry. All eight samples were shown to have release-rates significantly less than that required for an effective antifouling coating.

Incorporation of triorganotin biocides into the polyurethane resulted in physical changes to the polymer and in certain cases, chemical transformations in the organotin. *Bis*-(tri-n-butyltin) oxide is entirely converted into new species in the polyurethane. From work carried out on model systems, the likely products are N-stannylcarbamate derivatives, which are thought to be catalysts in polyurethane formation. It is also suggested that the extensive and undesirable foaming observed in such polyurethanes, is due to the formation of isocyanate oligomers which act as branch points for polymer cross-linking.

Tri-n-butyltin chloride, *bis*-(triphenyltin) oxide and triphenyltin chloride all catalyze the polyurethane reaction, the latter increasing the setting time rather than reducing it. Mößbauer and infrared evidence from model studies suggests that dative bonding between triorganotins and isocyanates is occurring, *via* the oxygen of the isocyanate group. It is these complexes which are proposed to be the catalytic species. The relative merits of the triorganotins are discussed with respect to their potential as effective antifouling agents in the polyurethane system.

Table of Contents

1. Marine Fouling and its Prevention	1
1.1. Introduction	1
1.2. The Fouling Problem	1
1.3. Toxicology	3
1.4. Antifouling Systems	6
1.4.1. Paints	7
1.4.2. Elastomeric Systems	10
1.4.3. Organotin Polymer Systems	12
1.5. Environmental Aspects	16
1.5.1. The Environmental Impact of Organotins	16
1.5.2. Degradation of Organotins in the Environment	18
1.6. Summary	20
1.7. Research Aims	20
References	23
2. Mößbauer Spectroscopy	27
2.1. The Mößbauer Effect	27
2.2. Line Width	27
2.3. Recoil Energy Loss	28
2.4. Doppler Broadening	30
2.5. The Solid State	32
2.6. The Hyperfine Interactions	34
2.6.1. The Isomer Shift	35
2.6.2. Quadrupole Splitting	39
2.6.3. The Magnetic Interaction	43
2.7. The Mößbauer Experiment	45
2.7.1. The Source	45
2.7.2. The Absorber	46
2.7.3. Detectors	48
2.7.4. Cryogenics	50
2.7.4.1. The Liquid Nitrogen Cryostat	51
2.7.5. The Drive System	52
2.7.6. Data Handling	53
2.8. Mößbauer Spectroscopy and it's Application to Organotin Chemistry.....	54
2.8.1. Theoretical Mößbauer Studies on Organotin Compounds	55
2.8.2. Characterization of Organotin Compounds by Mößbauer Spectroscopy	57
2.8.3. Combined X-Ray Crystallography/Mößbauer Spectroscopy	59
2.8.4. Combined Mößbauer and NMR/Infrared Spectroscopy	60
2.8.5. The Study of Organotins in Complex Systems	70
References	72
3. Mößbauer Studies of Triorganotin Biocides in Hypalon Paint	77
3.1. Introduction	77
3.2. Discussion of the Results of the Tri-n-Butyltin Study	79
3.2.1. Initial Studies of the Fate of <i>Bis</i> -(Tri-n-Butyltin) Oxide.....	79
3.2.2. Initial Studies of the Fate of Tri-n-Butyltin Acetate	85
3.2.3. Initial Studies of the Fate of Tri-n-Butyltin Chloride.....	86
3.2.4. Initial Studies of the Fate of <i>Bis</i> -(Tri-n-Butyltin) Carbonate.....	90
3.3. Discussion of the Results of the Triphenyltin Study	91
3.3.1. Initial Studies of the Fate of <i>Bis</i> -(Triphenyltin) Oxide.....	91
3.3.2. Initial Studies of the Fate of Triphenyltin Acetate	93
3.3.3. Initial Studies of the Fate of Triphenyltin Chloride.....	94
3.4. Conclusions from Initial Studies of the Fate of Triorganotin Compounds in Hypalon Paint	95
3.4.1. The Fate of Tri-n-Butyltin Compounds in Hypalon Paint	95
3.4.2. The Fate of Triphenyltin Compounds in Hypalon Paint	96
3.5. Model Reactions of Tri-n-Butyltin and Triphenyltin Biocides with Sulphonyl Chlorides	99

3.5.1.	Introduction	99
3.5.2.	The Reaction Between <i>Bis</i> -(Tri- <i>n</i> -Butyltin) Oxide and Methanesulphonyl Chloride	101
3.5.3.	The Reaction Between Tri- <i>n</i> -Butyltin Chloride and Methanesulphonyl Chloride	104
3.5.4.	The Reaction Between <i>Bis</i> -(Tri- <i>n</i> -Butyltin) Oxide and Benzenesulphonyl Chloride	104
3.5.5.	The Reaction Between Tri- <i>n</i> -Butyltin Chloride and Benzenesulphonyl Chloride	105
3.5.6.	The Reaction Between <i>Bis</i> -(Triphenyltin) Oxide and Methanesulphonyl Chloride	105
3.5.7.	The Reaction Between Triphenyltin Chloride and Methane- /Benzenesulphonyl Chloride	112
3.5.8.	The Reaction Between <i>Bis</i> -(Triphenyltin) Oxide and Benzenesulphonyl Chloride	112
3.6.	Conclusions from the Sulphonyl Chloride Model Study	118
3.7.	Studies of Tri- <i>n</i> -Butyltin and Triphenyltin Stearates	123
3.8.	Studies of Tri- <i>n</i> -Butyltin and Triphenyltin Dithiocarbamates	124
3.9.	Experimental Details	126
3.9.1.	Möbbauser Spectroscopy	126
3.9.2.	General Information	126
3.9.3.	Experimental Methods	126
	References	132
4.	Release-Rate Studies	134
4.1.	Introduction	134
4.2.	Determination of Trace Levels of Organotin Compounds	137
4.2.1.	Electrochemical Techniques	138
4.2.2.	High Performance Liquid Chromatography	139
4.2.3.	High Performance Thin Layer Chromatography	141
4.2.4.	Atomic Absorption Spectrometry	141
4.2.5.	Combined Gas Chromatography/Mass Spectrometry	150
4.3.	Release-Rate Study	151
4.3.1.	Determination of Release-Rates	155
4.4.	Discussion of Release-Rate Results	160
	References	161
5.	Polyurethanes As Antifouling Coatings	163
5.1.	Introduction	163
5.2.	Chemistry of Polyurethane Formation	163
5.2.1.	Secondary Reactions	165
5.2.2.	Isocyanate Polymerization Reactions	165
5.2.3.	Cross-Linking Reactions	167
5.2.4.	Isocyanates in Polyurethane Manufacture	168
5.2.5.	Polyols in Polyurethane Manufacture	170
5.3.	Additives	172
5.3.1.	Catalysts	172
5.3.2.	Other Polyurethane Additives	180
5.4.	Effect of Triorganotin Biocides on the Polyurethane Foams	181
5.5.	Initial Studies of Triorganotin Biocides in the Polyurethane Foams	182
5.5.1.	The <i>Bis</i> -(Tri- <i>n</i> -Butyltin) Oxide Containing Polyurethane	186
5.5.2.	The Tri- <i>n</i> -Butyltin Chloride Containing Polyurethane	188
5.5.3.	The Tri- <i>n</i> -Butyltin Acetate Containing Polyurethane	188
5.5.4.	The <i>Bis</i> -(Triphenyltin) Oxide Containing Polyurethane.....	191
5.5.5.	The Triphenyltin Chloride Containing Polyurethane	194
5.6.	Conclusions of the Initial Study	194
5.7.	Model Studies of Reactions Between Triorganotin Compounds and Isocyanates .	195
5.7.1.	The Reaction Between <i>Bis</i> -(Tri- <i>n</i> -Butyltin) Oxide and Phenyl Isocyanate	196
5.7.2.	The Reaction Between <i>Bis</i> -(Tri- <i>n</i> -Butyltin) Oxide and 1,6-Diisocyanatohexane.....	196
5.7.3.	The Reaction Between <i>Bis</i> -(Tri- <i>n</i> -Butyltin) Oxide and 1,4-Phenylene Diisocyanate	196

5.7.4.	The Reaction Between Tri-n-Butyltin Acetate and Phenyl Isocyanate	197
5.7.5.	The Reaction Between Tri-n-Butyltin Acetate and 1,4-Phenylene Diisocyanate/1,6-Diisocyanatohexane	197
5.7.6.	The Reaction Between Tri-n-Butyltin Chloride and Phenyl Isocyanate	197
5.7.7.	The Reaction Between Tri-n-Butyltin Chloride and 1,6-Diisocyanatohexane	198
5.7.8.	The Reaction Between Tri-n-Butyltin Chloride and 1,4-Phenylene Diisocyanate	198
5.8.	Discussion of Results from the Initial Study	199
5.9.	Further Model Reactions	204
5.9.1.	The Room Temperature Reaction Between <i>Bis</i> -(Tri-n-Butyltin) Oxide and Phenyl Isocyanate	204
5.9.2.	The Room Temperature Reaction Between <i>Bis</i> -(Tri-n-Butyltin) Oxide and 1,6-Diisocyanatohexane	209
5.9.3.	The Room Temperature Reaction Between <i>Bis</i> -(Tri-n-Butyltin) Oxide and 1,4-Phenylene Diisocyanate	212
5.10.	Discussion of Results of the Room Temperature Reactions Between <i>Bis</i> - (Tri-n-Butyltin) Oxide and the Isocyanates	215
5.11.	Triorganotin Reactions with DND	216
5.11.1.	The Reaction Between <i>Bis</i> -(Tri-n-Butyltin) Oxide and DND.....	216
5.11.2.	The Reaction Between Tri-n-Butyltin Chloride and DND	222
5.11.3.	The Reaction Between Tri-n-Butyltin Acetate and DND	222
5.11.4.	The Reaction Between <i>Bis</i> -(Triphenyltin) Oxide and DND.....	227
5.11.5.	The Reaction Between Triphenyltin Chloride and DND	229
5.12.	Discussion and Conclusion of the Model Studies	231
	References	233
6.	Summary of Conclusions and Suggestions for Future Work	234
6.1.	Conclusions from Studies of Triorganotins in Hypalon Paint	234
6.2.	Conclusions from Release-Rate Studies	235
6.3.	Conclusions from Studies of Triorganotins in Polyurethane Foams	235
	Courses and Conferences Attended	237
	Acknowledgements	238

1. Marine Fouling and its Prevention

1.1. Introduction

Stationary or mobile structures when immersed in seawater are subject to fouling by marine flora and fauna. The most practical way of dealing with this problem is to apply a coating which contains substances poisonous to marine foulants. Triorganotin compounds have proved to be very effective toxicants in these systems, with around 3 500 tons per annum being used for this purpose.

1.2. The Fouling Problem

The fouling of surfaces in seawater follows a broad general pattern. Initially a surface quickly becomes covered with a layer of slime, composed of bacteria, diatoms, protozoa and algal spores. Sedentary organisms such as plant spores and animal larvae form a secondary layer. The principal foulants then attach; these can include seaweeds, barnacles, tubeworms, mussels, sponges and sea anemones. Other species can also cause problems such as *Teredo* (shipworm) and *Limnoria* (gribble) which bore into structures. They are not strictly fouling species, but their presence is obviously detrimental.

Settlement of these organisms on submerged surfaces may lead to a number of economically serious problems [2]. A build up of fouling on ships' hulls leads to an increase in drag which, together with the increased weight, means that vessels must use more fuel to maintain cruising speed. Monaghan *et al* [3] estimated that in six months a vessel needs to expend around 40% more fuel to maintain its cruising speed, which may be reduced by up to one knot [4]. Removal of fouling and repainting of the vessel means time spent in dry dock. This results in a loss of revenue for merchant ships and a reduction in defensive capability for navies. In 1971 Bollinger [5] estimated that the total cost to US commercial and naval shipping was over one billion dollars per annum. A more

recent estimate by Gitlitz in 1981 [6] showed that "moderate" fouling of a supertanker would result in one million dollars extra expenditure per annum for fuel alone.

The functioning of scientific and military hardware can be adversely affected by fouling. Sonar equipment may suffer range loss, signal distortion and increased background noise levels due to the presence of hard-shelled macro organisms on their outer housings.

The need for protection is obvious, and several methods have been tried. Copper cladding was the first recorded antifoulant in the 8th Century B.C., and its use carried on to the 18th Century. An alternative to expensive copper sheets was the incorporation of arsenic and mercury salts into pitches and waxes. By the turn of this century copper (I) oxide was the primary antifouling agent, mostly in paints, and remained so until the 1960's.

In 1954 Van der Kirk and Luijten [7] published their findings on the biocidal activity of organotin compounds. Their research showed that triorganotins were more active than copper (I) oxide and could thus be used in much lower concentrations. (In fact, the superiority of organotin compounds was discovered by a DuPont chemist, Tisdale [8], in the early 1940's. The company patented certain formulations using triphenyltin linoleate as a cotoxicant with organolead compounds). The relative merits of copper (I) oxide and the triorganotin compounds are discussed fully in the following sections.

An ideal antifouling coating is one which releases toxicant at a rate sufficient to maintain, next to the hull, a thin layer of water in which marine organisms cannot survive. The toxicant should be effective at low concentrations and should be specific against target biota. The protection offered should be long lasting and not cause hull corrosion. Finally, the coating should be easy and safe to apply and not pose any environmental problems.

1.3. Toxicology

Organotin compounds can be represented by the general formula R_nSnX_{4-n} , where R is an alkyl or aryl group and X is anionic or $-OR'$. The number of tin—carbon bonds has a profound effect on the biological activity of the molecule. In general the highest activity occurs when $n = 3$, *i.e.* triorganotin compounds [7]. (The toxicity of di- and monoorganotin compounds is much lower). It was also found that within this family the nature of the R group provided biocidal specificity, see Table 1.1.

Table 1.1 Biocidal Specificity of Triorganotin Compounds [7].

Species	R in most active R_3SnX cpd.
Insects	Methyl
Mammals	Ethyl
Gram -ve bacteria	n-Propyl
Gram +ve bacteria, fish, algae, fungi, molluscs, plants	n-Butyl
Fish, algae, fungi, molluscs	Phenyl
Fish, mites	Cyclohexyl

Any increase in the n-alkyl chain length beyond four results in a sharp drop in biological activity, trioctyltin compounds being essentially non-toxic [9].

Blunden *et al* [10] claimed that the nature of the X group has little effect upon the toxicity of the triorganotin, with two exceptions. Firstly, X itself may be biologically active and secondly the structure of X may allow the formation of a five-coordinate chelated monomer. The latter will reduce the biocidal activity. However, recent work by Kuthubutheen *et al* [11] suggests that the toxicity of a triorganotin depends upon the hydrophilicity of X. As X becomes more hydrophilic, so the activity increases. They also demonstrated that $n-Bu_3SnX$

compounds were more toxic than the $i\text{-Bu}_3\text{SnX}$ analogues, and this is thought to be due to steric factors. It was also found that in general triaryltins were more selective than trialkyltins.

As can be seen from Table 1.1, fouling species are most susceptible to tri- n -butyltin and triphenyltin compounds, which are usually abbreviated to TBT and TPT respectively. The most widely used toxicants are *bis*-(tri- n -butyltin) oxide (TBTO), tri- n -butyltin acetate, chloride and fluoride (TBTOAc, TBTCI and TBTF), *bis*-(triphenyltin) oxide (TPTO), and triphenyltin chloride and fluoride (TPTCl and TPTF).

The toxicity of the R_3SnX series is related to the total molecular surface area [12] and to the octanol:water partition coefficient, K_{ow} . The higher the value of K_{ow} the higher the hydrophobicity of the R_3SnX species, and the greater its toxicity. Cell membranes, which are mainly fat-based, are more permeable to R_3SnX compounds with high K_{ow} values.

The acute toxicity of the triorganotin derivatives is thought to be due to their ability to bind to certain proteins which results in derangement of mitochondrial functions [13]. Mößbauer studies [14,15] indicated that Et_3SnX binds to protein sites with tetrahedral or *cis*-five-coordinate geometry (quadrupole splitting $< 2.3\text{mm s}^{-1}$). A possible binding site is shown in Figure 1.1(a):

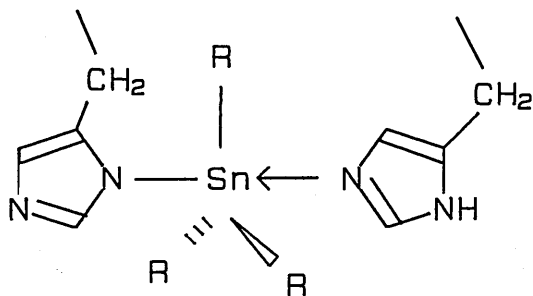


Figure 1.1(a)

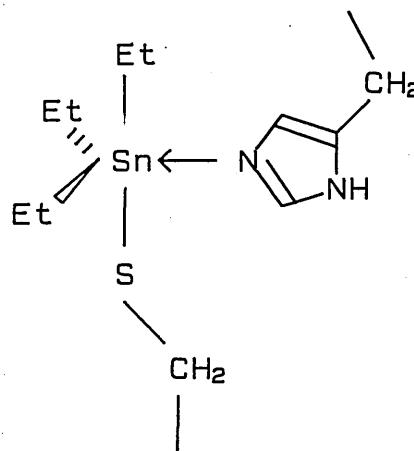


Figure 1.1(b)

Figure 1.1(a) Proposed Binding of Et_3SnX with Histidine Residues in a Protein and 1.1(b) Proposed Binding of Et_3SnBr with Histidine and Cysteine Residues in a Protein.

Et_3SnBr was found to bind with cat haemoglobin [16] *via* a histidine and cysteine residue as shown in Figure 1.1(b).

Studies of the effect of triorganotin on various species ranging from microorganisms [11] to fish [17, 18, 19] have been carried out. Environmental levels of triorganotin, although they may be low, can produce sub-lethal or lethal effects due to the ability of most marine organisms to bioconcentrate toxicants. The resultant ecological problems will be discussed in Section 1.5.

In man, the symptoms of triorganotin poisoning are headache, nausea and vomiting. The effects are reversible with the exception of neuronal destruction in the brain caused by certain trimethyltin derivatives [20].

The relative toxicities of four biocides to algae and barnacles are shown in Table 1.2:

Table 1.2 Comparative Antifouling Activity of Four Biocides. [13]

Compound	Algae/LC₅₀ in ppm	Barnacle/LC₅₀ in ppm
Cu ₂ O	1 – 50	1 – 10
R ₃ SnX	0.01 – 5	0.1 – 1
R ₃ PbX	0.1 – 1	0.1 – 1
RHgX	0.1 – 1	0.1 – 1

As can be seen from Table 1.2, R₃SnX compounds are generally an order of magnitude more active than copper (I) oxide and as toxic as triorganoleads and organomercurials. The latter two have been banned for many years because of their broad spectrum toxicity. However, triorganotins are now the subject of legislation because of their environmental impact. This will be reviewed in Section 1.5.

In a recent paper, Renni *et al* [21] claimed that the use of polymeric salt derivatives of thiocarbamic acid as co-toxicants with R₃SnX/Cu₂O compounds enhanced the overall effectiveness of the coating.

1.4. Antifouling Systems

A substrate is required that will slowly release the toxicant at a sufficient rate to prevent fouling. Three approaches have been taken using (i) paints, (ii) elastomers and (iii) organotin polymers.

1.4.1. Paints

A paint consists of four basic components; vehicle, solvent, pigment and additives. The vehicle provides film continuity and adhesion to the substrate. The solvent is necessary for the purpose of application. Pigments add properties to the paint that cannot be obtained from the vehicle alone, such as colour, gloss and hardness. Additives modify the properties of the vehicle/pigment mixture.

Conventional antifouling paints can be divided into two groups according to the mechanism of toxicant release into seawater: (i) soluble matrix and (ii) contact. The binder employed in the former type is soluble in seawater and as it slowly dissolves fresh toxicant comes to the surface. Rosin, a naturally occurring acidic resin, is the main component of the binder in these paints. Contact paints have a binder of vinyl resin or chlorinated rubber, both of which are insoluble. These paints rely on a leaching/diffusion action to bring the toxicant to the surface. For this reason, contact paints require greater toxicant loadings than do soluble matrix paints.

Prior to the 1960's, most antifouling paints used copper (I) oxide as the toxicant [22]. Copper (I) oxide is only slightly soluble in seawater, so paints had to contain a high loading, usually 85–92% in the dry paint. Such high toxicant contents meant that physical properties such as tensile strength, peel resistance and abrasion resistance were seriously reduced. Also, a protective layer was necessary between the hull and the paint to prevent the formation of a galvanic couple. A cosmetic problem was also evident, since antifouling paints based on copper (I) oxide were always red in colour. Despite these limitations, a well formulated paint could provide a foul-free life of up to 18 months in temperate waters [22].

Van der Kirk and Luijten's discovery [7] of the higher activity of triorganotins combined with their better aqueous solubility meant that paint loadings of the toxicant could be reduced tenfold. Therefore the physical properties would be virtually unaffected, no corrosion problems would exist and paints could be any colour. A typical contact paint composition is detailed in Table 1.3 [23].

Table 1.3 Composition of Antifouling Contact Paint.

	parts by mass
Red iron oxide	20.0
Talc	8.5
Zinc oxide	9.4
Bentone 27	0.7
Methanol 95%	0.2
Bu ₃ SnF	15.7
Parlon S-20 (50% in xylene)	13.8
WW Gum rosin (60% in xylene)	23.0
Xylene	8.7

The effectiveness of these paints depends upon the controlled release of the triorganotin biocide. Several factors can influence the rate of leaching and these are listed in Table 1.4 [24].

Table 1.4 Principal Factors Influencing Leaching of Organotin Antifoulants.

Total percentage solubles.	Pigment volume concentration.
Paint resin:rosin ratio.	Solvent characteristics, <i>e.g.</i> relative polarity, rate of evaporation.
Level of toxicant.	Other additives, <i>e.g.</i> zinc oxide, organic biocides.
Solubility of toxicant in seawater.	Adsorption of toxicant on pigment.
Film thickness.	
Type of resin.	
Compatibility of toxicant with resin and other film components.	

Water sensitive pigments such as zinc oxide and rosin permit greater water diffusion into the film, assisting mobility of the toxicant at the surface. Different organotin biocides require changes in the paint formulation, such as the resin:rosin ratio and level of zinc oxide, to allow sufficient toxicant to be present at the surface at all times. The level of toxicant, film permeability and thickness are important factors in determining the life of a coating. In addition, the performance of a paint will depend on external factors which affect the rate of fouling such as water temperature and salinity, the season and the nature of the fouling species.

The minimum rate at which triorganotins must leach from a paint film in order to prevent fouling vary depending on the nature of the R group. For *bis*-(tri-n-butyltin) oxide, Bennett and Zedler [25] claimed that $1-2 \mu\text{g cm}^{-2} \text{ day}^{-1}$ was required to prevent fouling. However, later work by De la Court and De Vries [26] showed that less than $5 \mu\text{g cm}^{-2} \text{ day}^{-1}$ was insufficient. In the same paper, a figure of $1-2 \mu\text{g cm}^{-2} \text{ day}^{-1}$ was reported to be necessary for TPTF.

A recent development in the formulation of organotin antifouling paints involves the technique of microencapsulation of the toxicant prior to incorporation in the coating [27]. Static immersion tests with a vinyl/rosin base paint containing 14% by mass of tri-n-butyltin chloride microcapsules provided zero fouling over a four year period [28].

The present study has been examining the incorporation of various triorganotins into Hypalon¹ paint. Hypalon was first produced in the 1930's by substituting chloro- and chlorosulphonyl- side groups into polyethene. The polyethene used has an average molecular weight of 20 000 and contains approximately one chlorine atom for every seven carbon atoms and one chlorosulphonyl group for every ninety carbon atoms. Hypalon paints are of the contact type.

1. Hypalon is a registered trademark of DuPont

1.4.2. Elastomeric Systems

Organotin elastomeric systems were developed in response to the fouling problems encountered by rubber or metallic domes used to protect sonar equipment. Antifouling paints have a short active life due to surface cavitation arising from the transmission of acoustic signals. This problem was solved by the BF Goodrich Company when biocide was added directly to the rubber [22].

Elastomers in their original state are macromolecules of essentially no strength or useful physical properties. To produce a usable material, it is necessary to cross-link the smaller macromolecules, creating very large macromolecules. This is accomplished by use of a cross-linking agent ("curative") and vulcanization ("curing"), *i.e.* heating the elastomer and curative to some temperature for a given period of time to induce a chemical reaction. Sulphur is a common curative for isoprenes (rubbers); isocyanates are used in the formation of polyurethanes. Accelerators and activators are employed to improve the rate of cure and to enhance the physical characteristics of the elastomer. Other components include; softeners and peptizing agents which aid mixing; fillers, normally inorganic, which may be reinforcing or simply bulk increasing; protective agents such as antioxidants and special additives, which include pigments and the antifoulants themselves. As with paints, *bis*-(tri-*n*-butyltin) oxide is a common toxicant in elastomeric systems. However, studies by Allen and Brooks *et al* [29] showed that in addition to *bis*-(tri-*n*-butyltin) oxide, *bis*-(tri-*n*-butyltin) carbonate, and tri-*n*-butyltin stearate, (TBTO)₂CO and TBTSt, undergo conversion to tri-*n*-butyltin chloride upon incorporation into neoprene rubber. This process occurs *via* reaction with hydrogen chloride arising from dehydrochlorination of the base polymer under curing conditions, see Section 2.8.5. Table 1.5 provides a generalized comparison of antifouling (AF) rubbers with conventional paints [30].

Table 1.5 Comparison of Antifouling Rubbers and Paints.

<u>Property</u>	<u>AF Rubber</u>	<u>AF Paint</u>
Toxicant	TBTO, TBTS, TBTF or TBTOAc	Cu_2O or R_3SnX
Toxicant Content	2–10%	85–95% Cu_2O 30–55% R_3SnX
Loss Mechanism	Diffusion/dissolution	Leach or exfoliation
Application state	Solid sheets	Liquid paint
Film thickness	1.5–3.2mm	0.05–0.30mm
Maximum working life (in tropical waters)	6 years	18 months, usually around 6 months
Ease of application	Depends on object, hulls difficult	Relatively simple
Abrasion resistance	Relatively good	Relatively poor

TBTS is *bis*(tri-n-butyltin) sulphide.

A typical neoprene formulation is described in Table 1.6 [24].

Table 1.6 Neoprene 351 Formulation.

<u>Component</u>	<u>Formulation</u> (parts by weight)
Neoprene WRT100	100.0
FEF Carbon black	14.5
Phenyl- β -naphthylamine	2.0
Zinc oxide	5.0
Lauric acid	3.0
Magnesium oxide	4.0
Ethylene thiourea	0.75
Mercaptobenzothiazyl disulphide	1.0

Part of the work described in this thesis has been concerned with the incorporation of triorganotin compounds into polyurethane systems. This work is discussed in Chapter 5.

1.4.3. Organotin Polymer Systems

These are the latest development in antifouling coatings. In general, these formulations incorporate a triorganotin carboxylate group chemically bound to the backbone of the binder, which is usually an acrylate polymer. Attack by seawater on the paint film causes hydrolysis of the organotin-ester linkage, thus releasing the biocide. The depleted layer now has free carboxylate groups. With its low integral strength it is easily eroded by the motion of seawater to expose a fresh layer. These are known as self-polishing coatings, see Figure 1.2 [24]:

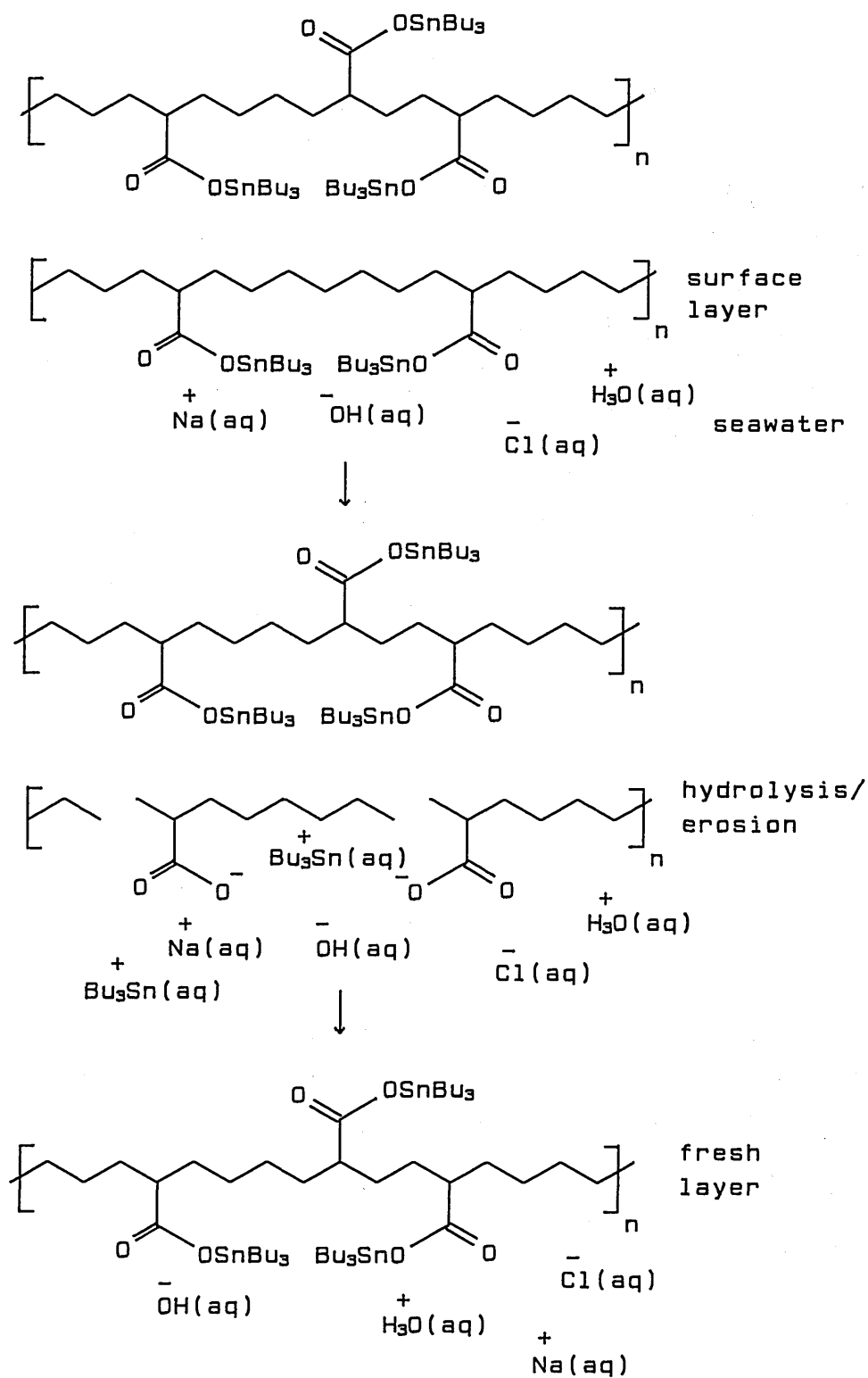


Figure 1.2 Schematic of Antifoulant Release by a Self-Polishing Coating.

Christie [31] has described the development of a commercial coating based on a copolymer of tri-n-butyltin methacrylate with methyl methacrylate. By controlling the polymer composition and pigmentation and by using retarders, the rate at which the coating ablates can be regulated. Several advantages have been claimed for these coatings:

- (i) a lifetime proportional to the thickness applied,
- (ii) controllable erosion rate/toxicant delivery,
- (iii) no removal and disposal of depleted paint,
- (iv) efficient utilization of toxicant and
- (v) continuous replacement of active surface.

The US Navy has carried out its own development work on these systems [32]. A typical example of the polymers produced is shown in Figure 1.3, where x, y and z represent repeating monomer units and R is butyl, propyl, methyl or benzyl. The polymer backbone can be based on an acrylic, vinyl, or polyester monomer or an epoxy resin:

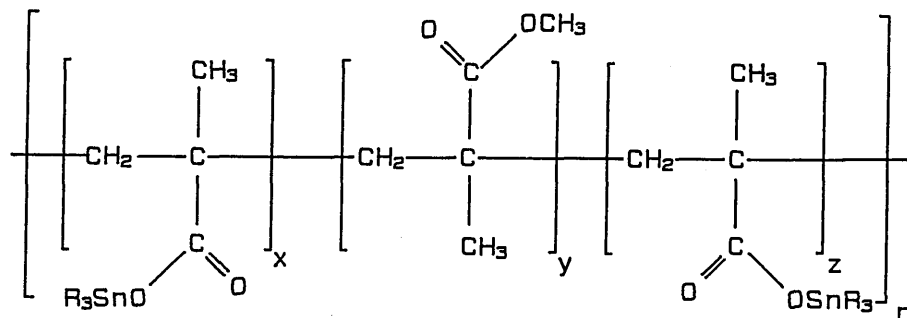
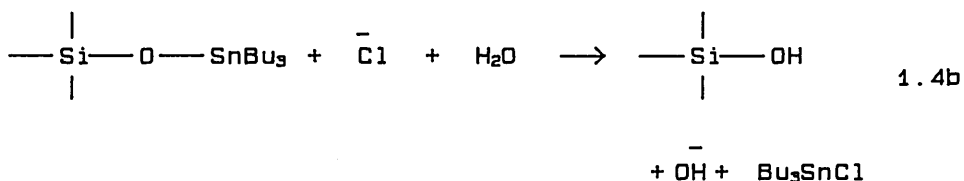
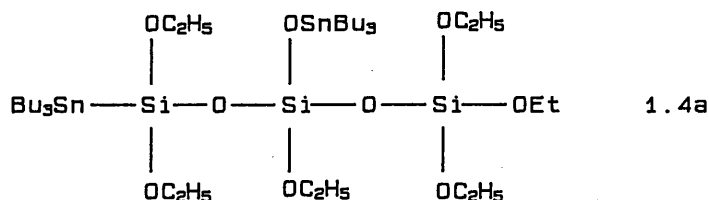


Figure 1.3 A Typical Triorganotin Polymer.

Excellent antifouling performance was reported for a copolymer of tri-n-butyltin methacrylate/tripropyltin methacrylate/methyl methacrylate in raft panel tests. Cologer [33] has noted that in ship tests, organotin polymer paints exhibit superior long-term antifouling capability, exceeding three years, with a much lower organotin content than conventional paints.

Karpel [34] described the development of a different organotin polymer system. The triorganotin moieties are bonded to a siloxane pre-polymer, as shown in Figure 1.4 (a):



**Figure 1.4 (a) Tri-n-Butyltin Siloxane Pre-polymer and 1.4(b)
Hydrolysis of Tri-n-Butyltin Siloxane Polymer.**

The mechanism for the release of the triorganotin is hydrolysis and is shown in Figure 1.4 (b). By varying the organotin:siloxane ratio it is possible to alter the release rate.

Organotin polysiloxanes have quite different properties from the organotin acrylates. The latter are usually linear polymers which are applied in solution, *i.e.* a paint. The polysiloxanes however, provide a resin that moisture cures as the solvent evaporates which allows the formation of a three-dimensional network. When fully cured, the resin is hydrophobic, but hydrolysis of the

tri-n-butyltin moieties causes the polymer to become hydrophilic. Water can then penetrate the matrix and release more toxicant. Polysiloxanes, unlike the acrylates, are insoluble in seawater and therefore not self-polishing. The performance of these coatings was not reported. However, some Japanese patents [35, 36, 37] based on siloxane or siloxane/acrylate block polymers have shown a minimum two year foul-free lifetime.

1.5. Environmental Aspects

1.5.1. The Environmental Impact of Organotins

In his detailed review of the subject, Maguire [28] describes tri-n-butyltins as perhaps the most acutely toxic chemicals to aquatic organisms ever deliberately introduced into water. It was during the last decade that the full environmental impact of triorganotins was realized.

In the 1970's the Pacific Oyster, *C. gigas*, was introduced into Europe for cultivation following the mass mortalities of endemic oysters [38]. In France, the introduction was partly successful, but in Britain attempts at farming failed, especially on the east coast. The shells of the oysters became thicker and were malformed with a corresponding decrease in flesh weight. Similar abnormalities were observed in the French oysters, where an association between the incidence of shell malformations and the proximity of marinas or boat moorings was noted by Alzieu *et al* [39]. When high levels of organotins were found in oyster tissue, the French government brought forward legislation banning the use of triorganotin based antifouling paints on craft of less than 25 metres. Waldock and Thain [40] showed that *C. gigas* could concentrate tri-n-butyltins from water or sediment by up to 10 000 times. Similar bioconcentration factors have been observed by Bately *et al* [41] for the Sydney Rock Oyster, leading to similar deformities.

In general, a tri-n-butyltin level of around $0.2 \mu\text{g l}^{-1}$ will produce mortality amongst adult *C. gigas*, but half that amount will prove fatal at the larval stage. Most oysters and mussels in US coastal waters are now reported to be contaminated with tri-n-butyltin and its degradation products [42].

The Dog Whelk, *N. lapillus*, also suffered a decline in numbers, notably along the south coast of England during the 'seventies and 'eighties. Detailed accounts on the cause of the drop in numbers of *N. lapillus* have been published [43-47]. It was found that female whelks were developing male characteristics, (a penis and vas deferens), a deformity termed as "imposex". The greatest incidence of imposex was found in areas of high boating activity [43]. The levels of tri-n-butyltin needed to induce the deformity are as low as 1.0 ng l^{-1} [48]. However, in waters containing about $0.03 \mu\text{g l}^{-1}$ of tri-n-butyltins, (typical for the more polluted bays in the south of England), females became sterile after about 18 months [44]. On the east coast of the USA the same phenomena has been observed in the Common Mud Snail, *N. obsoletus* [48]. The sensitivity of *N. lapillus* to tri-n-butyltin has led to its use as an indicator of water purity [47].

Bushong *et al* [49] performed tri-n-butyltin toxicity experiments on selected Chesapeake Bay invertebrates and fish. It was found that a 72 hour exposure to $1.1 \mu\text{g l}^{-1}$ tri-n-butyltin constituted an LC_{50} , (the concentration which produces a 50% fatality rate in a population), for all but one of the invertebrates tested. The fish were generally more resistant; 96 hour LC_{50} around $25 \mu\text{g l}^{-1}$. Tri-n-butyltin concentrations of greater than $1.1 \mu\text{g l}^{-1}$ were found in the Bay, the implications of which are obvious.

The levels of tri-n-butyltin in waters around the world have been examined by many workers and reviewed by Maguire [28]. Table 1.7 shows the ranges of worldwide organotin concentrations in estuarine surface microlayers, sediments and water.

Table 1.7 Comparison of Organotin Concentration Ranges in Estuarine Surface Microlayer, Water and Sediment.

Organotin Species	Surface Microlayer / ngSndm⁻³	Water / ngSndm⁻³	Sediment / μgSndm⁻³
Bu ₃ Sn ⁺	0 - 2000	0 - 600	0 - 11000
Bu ₂ Sn ²⁺	0 - 450	0 - 275	0 - 8500
BuSn ³⁺	20 - 165	0 - 310	0 - 700

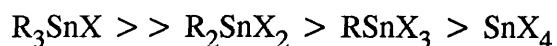
Concern at these levels has led to controls being applied to the use of organotin based antifouling paints. The UK government in February 1987 announced its intention to introduce restrictions on the use of the paints under the Control of Pollution Act (1974) [50]. This now includes a complete ban on the retail sale of paint formulations containing tri-n-butyltin antifoulants. Since then, regulations have been tightened still further so that all formulations containing aquatic biocides require prior approval by ministers before they can be sold or used.

1.5.2. Degradation of Organotins in the Environment

This can be defined as the progressive removal of the organic groups from the tin atom:



It was stated in Section 1.3 that the biological activity of tin compounds is in the order:



(R₄Sn is only toxic if metabolized to R₃SnX). In theory the triorganotin after exerting its biocidal activity, would degrade into increasingly non-toxic products. This is in marked contrast to the end products of lead and mercury in

the environment. They are readily methylated by bacteria to highly stable organometallics. Both MePb^+ and MeHg^+ have a high affinity for the sulphhydryl, (—S—H), group which occurs in proteins. Coordination of alkylleads and alkylmercurials with the sulphhydryl group can lead to a disruption of normal cell activity [51]. Alkylmercurials also concentrate, particularly in brain tissue, causing cerebral disorders and eventually death.

The half-life of tri-n-butyltin has been measured in several areas. In San Diego Bay, $t_{1/2}\text{Bu}_3\text{Sn}^+$ has been estimated to be between 6–19 days [52]. A similar half-life has been calculated for Bu_3Sn^+ in estuarine waters off the Georgia (US) coast and in a Californian marina [53,54]. The marina study used ^{14}C labelled tri-n-butyltin. It was found that the principal metabolite was di-n-butyltin, (DBT), which degraded more slowly to monobutyltin, (MBT) and $^{14}\text{CO}_2$. Waite *et al* [55] discovered very similar behaviour of tri-n-butyltin in the Rivers Bure and Yare in the Norfolk Broads. These results should be compared with the half-life of Bu_3Sn^+ in polluted waters.

For example, Maguire and Tkacz [56] found that in Toronto harbour, the half-life of Bu_3Sn^+ was several months. In Sakaisenbokou harbour, one of the most polluted areas in Osaka Bay, Japan, a similar half-life was observed [57]. The reason for these differences in the half-life of Bu_3Sn^+ is the availability of various degradation pathways, *viz*, biological, photochemical and chemical routes. The latter is thought to be negligible; biological degradation is the most rapid pathway followed by photochemical breakdown [28].

The majority of organotin degradation is carried out by microorganisms, either in the water or in the sediment where the biocides tend to accumulate [58]. Barnes *et al* [59] showed that ^{14}C -labelled triphenyltin acetate in soil was converted to inorganic tin and carbon dioxide. Since similar degradation did not occur in sterile soil, thus it was concluded that microorganisms were metabolising the organotin. Barug and Vonk [60] obtained similar results with ^{14}C -labelled *bis*-(tri-n-butyltin) oxide. In polluted waters the low levels of microorganisms leads to an increased persistence of organotins.

Photochemical degradation, caused mainly by UV radiation, is only important in clear waters. Only organotins in the surface layer of turbulent and polluted waters will degrade by this route. A study with Me_3SnCl demonstrated that it could be sequentially degraded, the final product being hydrated tin (IV) chloride [61]. The relative degradation rates were $\text{Me}_3\text{Sn}^+ > \text{Me}_2\text{Sn}^{2+} > \text{MeSn}^{3+}$. Maguire *et al* [62] showed that UV radiation induced breakdown of the Bu_3Sn^+ moiety in *bis*-(tri-*n*-butyltin) oxide. The half-life of Bu_3Sn^+ was approximately 90 days, *cf.* 6–19 days in clean, non-sterile water.

1.6. Summary

Triorganotin-based antifouling compositions offer superior performance when compared to other systems. Unfortunately, significant ecological damage has been caused by these compounds in the estuaries and bays of Australia, Europe, Japan, North America and New Zealand. Legislation is now established in most of these areas restricting the use of triorganotin systems, especially on smaller craft.

However, they can be safely used on vessels which spend a relatively large proportion of their time on the open sea. This includes oil tankers, container ships, naval vessels and oil rigs; so a large market still exists for antifouling systems, mostly based on triorganotin biocides.

1.7. Research Aims

There is a need to develop new antifouling coatings which provide long-term protection with minimal environmental impact. Triorganotin compounds, especially the tri-*n*-butyltins and triphenyltins, offer the best available performance of any marine biocide. As is evident from Section 1.2, a considerable amount of research is currently underway to develop enhanced antifouling coatings.

The aim of this research project was to examine in detail two potential antifouling coatings, Hypalon paint and a polyurethane foam, both of which have triorganotin compounds incorporated therein. Of particular interest are the chemical and structural changes which the triorganotins may undergo when a component of these matrices. Since the biological activity of these compounds is highly sensitive to their chemical nature, it is essential that they are available for release into the water as the active species.

To conduct such a study it is necessary to have a technique which is capable of examining the organotin compounds *in situ*. Mößbauer spectroscopy allows this to be achieved and it has been successfully applied to the study of organotins in a variety of matrices (see Section 2.8.5).

The useful parameters to be gained from the Mößbauer spectra of organotins are the Isomer Shift (δ) and the Quadrupole Splitting (ΔE_Q). These parameters, along with the theoretical and practical aspects of Mößbauer spectroscopy are discussed in Chapter 2.

The Mößbauer experiment offers several advantages over more conventional spectroscopic techniques:

- (i) it provides structural information on both amorphous and crystalline systems,
- (ii) the isomer shift usually provides unambiguous distinction between the tin oxidation states,
- (iii) the quadrupole splitting is sensitive to the stereochemistry around the tin atom and also to ligand electronegativity and
- (iv) the technique is non-destructive.

When studying the incorporation of the biocides into the polyurethane, not only is transformation of the triorganotins possible, but also changes in the polymer may occur. Many organotin compounds are known to catalyze the reactions of isocyanates with hydroxyl groups and indeed, are commonly used in the

industrial manufacture of polyurethanes. Therefore, the effect of the triorganotin biocides on the physical nature of the polyurethane has been of particular interest.

Other techniques used to provide complementary data have included infrared spectroscopy, mass spectrometry, (MS) and ^{119}Sn nuclear magnetic resonance, (NMR), spectroscopy. The latter is particularly useful in the study of the solution properties of triorganotin compounds, which often vary from their solid state properties. The ^{119}Sn chemical shift of a compound usually provides a good indication of the coordination number of the tin atom.

Another important factor to be considered with any antifouling coating is the rate at which the toxicant is released into the water. As was stated in Section 1.4, an antifouling coating using *bis*-(tri-*n*-butyltin) oxide needs to release at least $5 \mu\text{g Sn cm}^{-2} \text{ day}^{-1}$ to maintain a foul-free surface. Levels much above this will lead to an unnecessary waste of toxicant (and shorter working life) and could cause environmental problems. The ideal system would release a minimum level of toxicant, sufficient to prevent fouling over extended periods, say 2–3 years.

The rate at which triorganotins are released from eight Hypalon paint samples has been examined in detail. This has involved the construction of a flow system in which the levels of organotin compounds released from the paint could be determined under controlled conditions. The effluent was collected and after extraction and matrix modification, the amount of tin present was determined by graphite furnace atomic absorption spectrometry (GFAAS). The methodology and results obtained are presented in Chapter 4.

Chapter 1 References.

1. Bennett, R.F., Ind. Chem. Bull., 1983, 2, 171.
2. Fischer, E., Proc. 1976 Internat. Contr. Rel. Pestic. Symp., Akron, 1976, 21.
3. Monaghan, C.P., Kulkarni, V.I., Ozcar, M. and Good, H.L., Environmental Fate of Organotin Antifoulants, Chemical Speciation of Toxicants in Aqueous Solutions, US Govt. Rep. Tech. Rep. No.2, AD-A087374, 1980.
4. Mearns, R.D., J. Oil Col. Chem. Assoc., 1973, 56, 353.
5. Bollinger, E.M., Proc. 1st Contr. Rel. Pestic. Symp. Akron, 1974, 19.
6. Gitlitz, M.H., J. Coat. Technol., 1981, 57, 46.
7. Van der Kerk, G.J.M. and Luijten, J.G.A., J. Appl. Chem., 1954, 4, 314.
8. Tisdale, W.H., British Patent No. 578312, 1946.
9. Smith, P.J., Toxicological Data on Organotin Compounds, ITRI Publ. No. 538, 1978.
10. Blunden, S.J., Smith, P.J. and Sugavanam, B., Pestic. Sci., 1984, 15, 253.
11. Kuthubutheen, A.J., Wickneswari, R. and Kumar Das, V.G., Appl. Organomet. Chem., 1989, 3, 231.
12. Cooney, J.J. and Wuertz, S., J. Ind. Microbiol., 1989, 4, 375.
13. Evans, C.J. and Hill, R., Organotin-Based Antifouling Systems, Reprinted from Rev. Si, Ge, Sn and Pb Compds., 1983, Freund Publishing and references therein.
14. Farrow, B.G. and Dawson, A., Eur. J. Biochem., 1978, 86, 85.
15. Elliot, B.M., Aldridge, W.N. and Bridges, J.W., Biochem. J., 1979, 177, (2), 461.
16. Taketa, F., Siebenlist, K., Kasten-Jolly, J. and Palosaari, N., Archiv. Biochem. Biophys., 1980, 203, 466.
17. Pinkney, A.E., Wright, D.A. and Hughes, G.M., J. Fish Biol., 1989, 34, 665.

18. Soloman, R., Lear, S., Cohen, R., Spokes, K., Silva, P., Silva, P., Silva, M., Soloman, H., and Silva, P., Toxicol. Appl. Pharmacol., 1989, 100, 307.
19. Martin, R.C., Dixon, D.G., Maguire, R.J., Hodson, P.V. and Tkacz, R.J., Aquat. Toxicol., 1989, 15, 37.
20. Aldridge, W.N., Brown, A.W., Bierley, J.B., Vershoyle, R.D. and Street, B.W., Lancet, 1981, 2, 692.
21. Renni, L., Gombach, M.L. and Cinti, G., Adv. Org. Coat. Sci Technol. Ser., 1988, 10, 209.
22. Cardarelli, N., Controlled Release Pesticide Formulations, CRC Press, 1976.
23. Gitlitz, M.H., J. Coat. Technol., 1981, 53, 46.
24. Blunden, S.J., Cusack, P.A. and Hill, R., The Industrial Uses of Tin Chemicals, The Royal Society of Chemistry, 1985.
25. Bennett, R.F. and Zedler, R.J., J. Oil Col. Chem. Assoc., 1966, 49, 928.
26. De la Court, F.H. and De Vries, H.J., Proc. 4th Int. Congress Marine Corrosion and Fouling, 1976, 113.
27. Maile, J.B., Maile, A. and Porter, R.P., US Patent 4263887, 1981.
28. Maguire, R.J., Appl. Organomet. Chem., 1987, 1, 475.
29. Allen, D.W., Bailey, S., Brooks, J.S. and Taylor, B., Chem. Ind., 1985, 826.
30. Bollinger, E.H., Proc. 1st Contr. Rel. Pestic. Symp., 1974, 19.1.
31. Christie, A.O., J. Oil Col. Chem., 1977, 60, 348.
32. Montemarano, J.A. and Dyckman, E.J., J. Paint Technol., 1975, 47, 59.
33. Cologer, C.P., Naval Eng. J., 1984, 96, 25.
34. Karpel, S., Pigment Resin Technol., 1988, 13.
35. Yamamori, N., Nippon Paint Co. Ltd. Patent, 1989.
36. Imazaki, H., Koho Japanese Patent 01 161 071, 1989.
37. Anon., Kokai Tokkyo Koho Japanese Patent 01 121 373, 1989.
38. Lewis, J. A., Surf. Coat. Aust., 1988, 25, (11), 18.

39. Alzieu, C., Thibaud, Y., Heral, M. and Boutier, B., Rev. Trav. Inst. Pech. Marit., 1980, 44, 301.
40. Waldock, M.J. and Thain, J.E., Mar. Poll. Bull., 1983, 14, (11), 411.
41. Batley, G.E., Mann, K.J., Brockbank, C.I. and Maltz, A., Aust. J. Mar. Freshwater Res., 1989, 40, 39.
42. Wade, T.L., Garcia-Romero, B. and Brooks, J.M., Environ. Sci. Technol., 1988, 22, 1488.
43. Bryan, G.W., Gibbs, P.E., Hummerstone, G.L. and Burt, G.R., J. Mar. Biol. Assoc. UK, 1986, 66, 611.
44. Bryan, G.W., Gibbs, P.E., Burt, G.R., and Hummerstone, G.L., J. Mar. Biol. Assoc. UK, 1987, 67, 525.
45. Bryan, G.W., Gibbs, P.E., Burt, G.R., J. Mar. Biol. Assoc. UK, 1988, 68, 733.
46. Gibbs, P.E., Pascoe, P.L. and Burt, G.R., J. Mar. Biol. Assoc. UK, 1988, 68, 715.
47. Bailey, S.K. and Davies, I.M., J. Mar. Biol. Assoc. UK, 1989, 69, 335.
48. Smith, B.S., J. Appl. Toxicol., 1981, 1, 22.
49. Bushong, S.J., Lenwood, W.H., Hall, W.S., Johnson, W.E. and Herman, R.L., Wat. Res., 1988, 22, (8), 1027.
50. Waldock, M.J., Thain, J.E. and Waite, M.E., Appl. Organomet. Chem., 1987, 1, 287.
51. Chemistry in the Environment, Readings from Scientific American, comp. Hamilton, C.L., W.H. Freeman and Co., 1973.
52. Seligman, P.F., Valkirs, A.O. and Lee, R.F., Environ. Sci. Technol., 1986, 20, 1229.
53. Lee, R.F., Valkirs, A.O. and Seligman, P.F., Environ. Sci. Technol., 1989, 23, 1515.
54. Seligman, P.F., Valkirs, A.O., Stang, P.M. and Lee, R.F., Mar. Poll. Bull., 1988, 19, (10), 531.

55. Waite, M.E., Evans, K.E., Thain, J.E. and Waldock, M.J., Appl. Organomet. Chem., 1989, 3, 383.
56. Maguire, R.J. and Tkacz, R.J., J. Agric. Food Chem., 1985, 33, 947.
57. Hattori, Y., Kobayashi, A., Nonaka, K., Sugimae, A. and Nakamoto, M., Wat. Sci. Tech., 1988, 20, (617), 71.
58. Kram, M.L., Stang, P.M. and Seligman, P.F., Appl. Organomet. Chem., 1989, 3, 523.
59. Barnes, R.D., Bull, A.T. and Poller, R.C., Pestic. Sci., 1973, 4, 305.
60. Barug, D. and Vonk, J.W., Pestic. Sci., 1980, 11, 77.
61. Blunden, S.J., J. Organomet. Chem., 1983, 248, 149.
62. Maguire, R.J., Carey, J.H. and Hale, E.J., J. Agric. Food Chem., 1983, 31, 1060.

2. Mößbauer Spectroscopy

2.1. The Mößbauer Effect

While studying the resonant emission and absorption of γ -photons of ^{191}Ir , Rudolph Mößbauer discovered the effect which was to bear his name [1]. The high energy of the γ -photons emitted means that the nuclei recoil to such an extent that resonant absorption is lost. By raising the temperature it was possible to regain some resonance due to Doppler broadening of the emission and absorption linewidths. However, Mößbauer observed that as the temperature of the source and absorber were decreased, resonant absorption increased. The essence of Mößbauer's discovery was the phenomenon of recoilless emission and absorption of γ -ray photons with highly resolved energies. In 1961 he was awarded the Nobel Prize and since then the Mößbauer effect has been developed into a technique capable of providing an insight into the structure and coordination chemistry of over forty elements.

To understand the nature of resonant recoilless γ -ray photon emission and absorption a variety of factors have to be considered.

2.2. Line Width

The natural linewidth of any transition is given by the Heisenberg Uncertainty Principle:

$$\Gamma = (h/2\pi)/\Delta t$$

where Δt is the lifetime of the excited state.

For ^{119}Sn , $\Delta t = 18.3$ ns, so;

$$\Gamma = 1.05 \times 10^{-34} \text{ Js} / 18.3 \times 10^{-9} \text{ s}$$

$$= 5.74 \times 10^{-27} \text{ J} \equiv 3.58 \times 10^{-8} \text{ eV}$$

The energy of the ^{119}Sn transition from the excited to the ground state is 23.875 KeV and hence the theoretical resolution is 7×10^{11} . This is much greater than any other known spectroscopic technique.

2.3. Recoil Energy Loss

When any nucleus emits a photon of energy momentum must be conserved :

$$E_R \quad \leftarrow \quad \bullet \quad \text{~~~~~} \nearrow \quad h\nu$$

$$\text{and } p_{\text{nucleus}} = p_{\text{photon}}$$

For a γ -photon $E = h\nu = hc/\lambda$ and $p = E/c = h/\lambda$. Since the nucleus is comparatively massive it is reasonable to assume non-relativistic mechanics:

$$p_{\text{nucleus}} = mv \quad \text{and} \quad E_R = \frac{1}{2}mv^2$$

$$\text{so } E_R = p^2/2m$$

If we assume $E_R \ll E_0$, where E_0 is the transition energy, then E_{photon} is equal to E_0 , so that;

$$E_R = \frac{E_0^2}{2mc^2} \quad \text{since } p=E/c$$

If $A =$ mass number of the decaying nucleus, then the recoil energy can be written in the form;

$$E_R = \frac{5.37 \times 10^{-10} E_0^2}{A} \quad \text{or} \quad \frac{5.37 \times 10^{-4} E_0^2 (\text{KeV})}{A}$$

$$\text{Hence for } ^{119}\text{Sn}, \quad E_R = \underline{0.003 \text{ eV}}$$

Thus $E_R \ll E_0$, but $E_R \gg \Gamma$

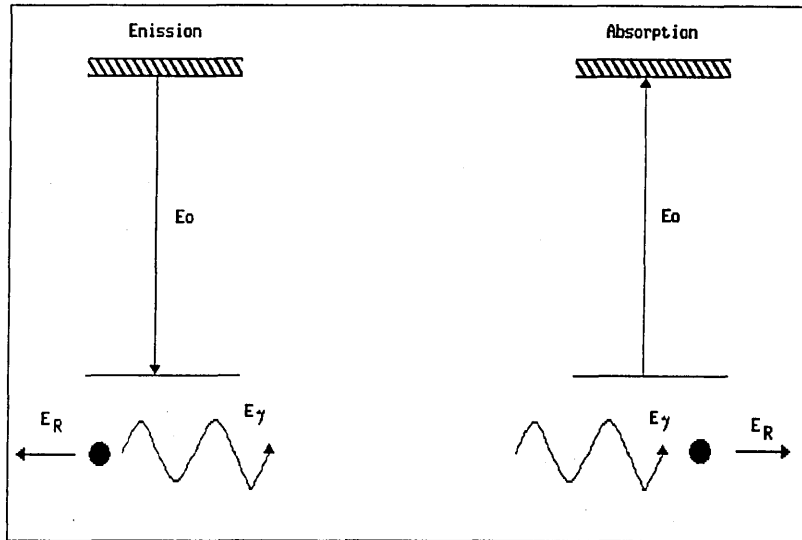


Figure 2.1 Emission and Absorption of γ -Rays.

But because $E_R = 0.003\text{eV}$ and $\Gamma = 3.58 \times 10^{-8}\text{eV}$, resonance is not observed, see Figure 2.2:

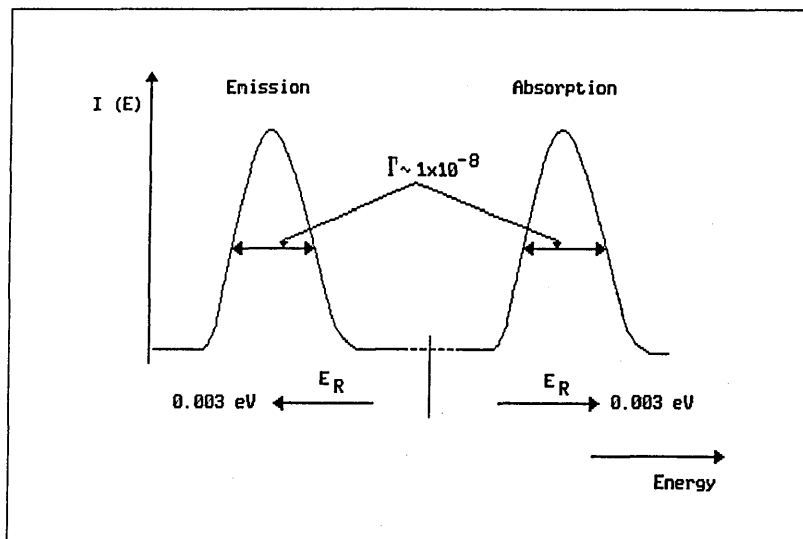


Figure 2.2 Emission and Absorption Linewidths.

Compare this with, for example, infrared transitions where E_0 is 0.01–1 eV; $\Gamma = 10^{-5}$ eV and $E_R = 10^{-12}$ eV which leads to nearly complete overlap of emission and absorption lines.

2.4. Doppler Broadening

So far it has been assumed that the emitting and absorbing nuclei have been stationary. However, above absolute zero all nuclei will have Random Thermal Velocity. In a gas this can be calculated from:

$$E_{\text{kinetic}} = \frac{1}{2} m v_T^2 = \frac{3}{2} K T \quad \text{Equation 2.1}$$

where $K =$ Boltzmann's constant.

Such velocities will lead to Doppler Broadening. The Doppler Shift is given by:

$$\Delta E = \frac{v_T E_0}{c} \quad \text{Equation 2.2}$$

In the gaseous state the velocity of the emitting nucleus will be random with respect to the absorber. Thus, for a free nucleus approximation the broadening, \bar{D} , is given by:

$$\bar{D} = \frac{2v_T E_0}{c} \quad \text{Equation 2.3}$$

v_T can be calculated from Equation 2.1

$$e.g. \text{ at } 300\text{K} \quad E_{\text{kin}} = (3/2) \times 1.38 \times 10^{-23} \text{ JK}^{-1} \times 300\text{K}$$

$$= \underline{6.21 \times 10^{-21} \text{J}}$$

$$E_{\text{kin}} = \frac{1}{2} m v_T^2$$

$$\text{so } v_T = \sqrt{(2 \cdot E_{\text{kin}} / m)} \text{ and mass } ^{119}\text{Sn atom} = 1.99 \times 10^{-25} \text{kg}$$

$$= \frac{\sqrt{(2 \times 6.21 \times 10^{-21} \text{J})}}{1.99 \times 10^{-25} \text{kg}}$$

$$= \underline{249.8 \text{ ms}^{-1}}$$

$$\text{so } \bar{D} = \frac{2 \times 250 \text{ms}^{-1} \times 23.875 \times 10^3 \text{eV}}{3 \times 10^8 \text{ms}^{-1}} = \underline{0.04 \text{eV}}$$

This can be applied to the 3-d case. Note that Doppler broadening is dependant on the recoil energy.

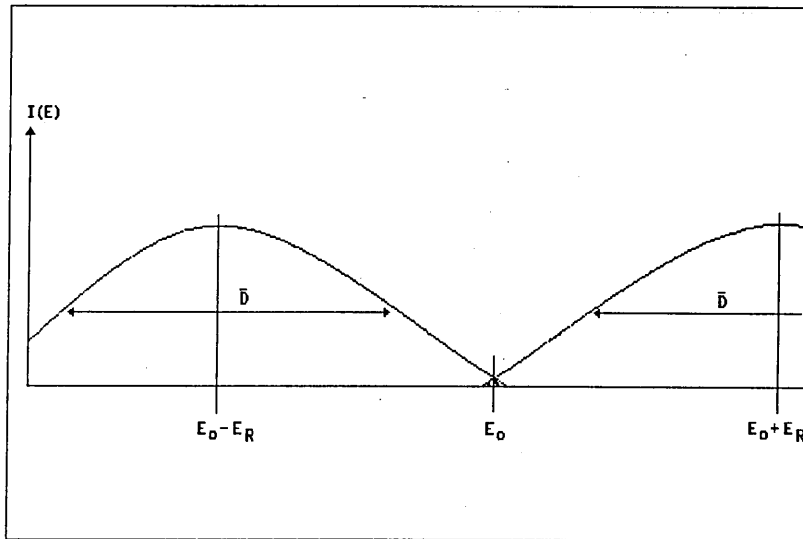


Figure 2.3 Overlap of Spectral Lines Due to Doppler Broadening.

The amount of overlap is very small and because of this broad linewidth the resolution is poor. Mößbauer discovered how to effectively eliminate recoil energy and Doppler broadening to produce narrow linewidths and then to bring about resonance fluorescence. To understand how this can be achieved it is necessary to consider the structure of the solid state.

2.5. The Solid State

Einstein proposed that solids are quantum mechanical systems and their energies should, therefore, be quantized. Transitions are said to occur through phonon interactions. The lattice is a complex vibrational system depending upon the structure and force constants. The very simple Einstein model for the vibrational properties of the lattice describes it as a series of quantized oscillators with a minimum energy transition of $E_E = \frac{1}{2}h\omega_E$.

Consider the decay schemes of ^{57}Co and ^{58}Co :

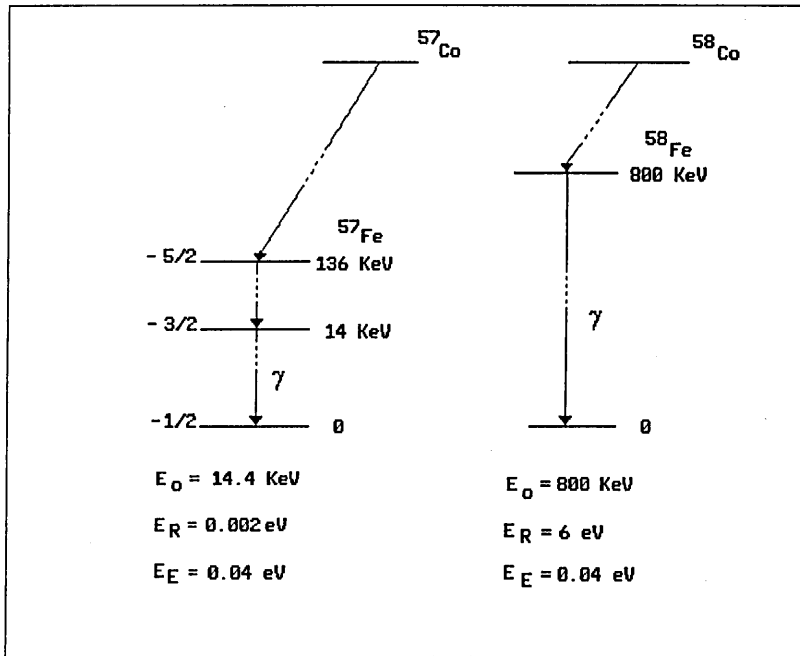


Figure 2.4 Decay Schemes of ^{57}Co and ^{58}Co .

When an ^{57}Fe nucleus emits a γ -ray photon, the recoil energy is less than that of the first vibrational transition. The γ -ray is said to be emitted *via* a zero phonon transition and does not experience recoil. The emitting nucleus is effectively "frozen" into the lattice which absorbs the recoil energy. For the 800KeV transition of ^{58}Fe , the recoil energy is much greater than $\hbar\omega_E$ and many phonons are involved in the transition. The emitted photon loses recoil energy and is Doppler broadened.

The probability of emission without recoil, f , is given by:

$$f = \exp \left[\frac{-4 \Pi \langle x^2 \rangle}{\lambda^2} \right]$$

where $\langle x^2 \rangle$ is the mean square vibrational amplitude of the emitting/absorbing nucleus and λ is the wavelength of the γ -ray. In order to observe a significant recoil free fraction, E_0 must be less than 150 KeV. It is this equation which restricts the observation of the Mößbauer effect to certain elements. It has yet to be observed in any element below ^{40}K , due to their high energy transitions.

With a finite probability of recoilless emission and absorption of γ -ray photons, resonance fluorescence can occur. If source and absorber nuclei are identical this will be observed, the resulting linewidth being twice that of the source linewidth. When the source and absorber are non-identical resonance may be destroyed because the chemical nature affects the nuclear energy levels. Although the differences are minute, using the Mößbauer effect it is possible to observe such changes in the nuclear energy levels. These are known as the Hyperfine Interactions.

2.6. The Hyperfine Interactions

These are the result of interactions between a nucleus and the electron environment. Mößbauer spectroscopy is essentially applied to the study of the hyperfine interactions which may provide information on the electronic, chemical and magnetic states of the atom. There are three hyperfine interactions:

- (i) the isomer shift;
- (ii) the quadrupole interaction and
- (iii) the magnetic interaction.

In the Mößbauer experiment a single line (*i.e.* highly monochromatic) γ -ray source with a large f -factor and narrow linewidth is used. The nuclear energy levels in the Mößbauer atoms of the absorber will in general be different from those in the source. Hence, there will be no resonant absorption until the γ -ray source is Doppler shifted over a suitable velocity range. The Doppler velocity at which resonant absorption occurs provides a measure of the hyperfine splitting.

2.6.1. The Isomer Shift

This is a result of the interaction between nuclear and electronic charges, *i.e.* the effect of the finite nuclear size on the Coulomb energy. The Coulomb energy itself is related to the electron density at the nucleus. The only orbitals with a finite probability of existing within the nucleus are the s-electron orbitals. For Sn the total electron density in the 1s to 4s orbitals is constant. The electron density of the 5s (valence) orbital depends upon the oxidation state of the atom.

The isomer shift is a measure of the difference in the electrostatic interaction in the nuclear radii of the ground and excited states, see Figure 2.5;

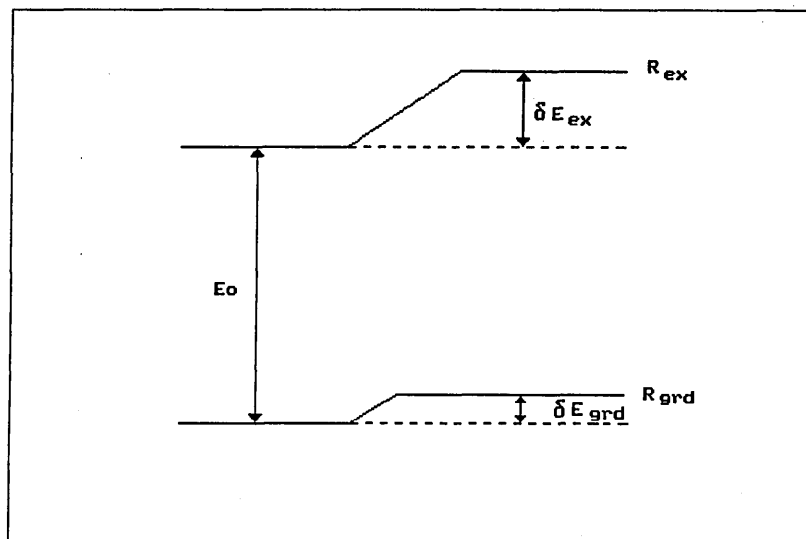


Figure 2.5 Formation of the Isomer Shift.

The difference, $\delta E_{\text{ex}} - \delta E_{\text{grd}}$ is equal to:

$$\frac{2\pi Z e^2 \{\psi(0)\}^2 (R_{\text{ex}}^2 - R_{\text{grd}}^2)}{5}$$

where Z is the atomic number, e is the electronic charge and $\{\psi(0)\}^2$ is the s-electron density at the nucleus. The source and absorber contain the same isotope with the same nuclear radii, but different s-electron densities, see Figure 2.6;

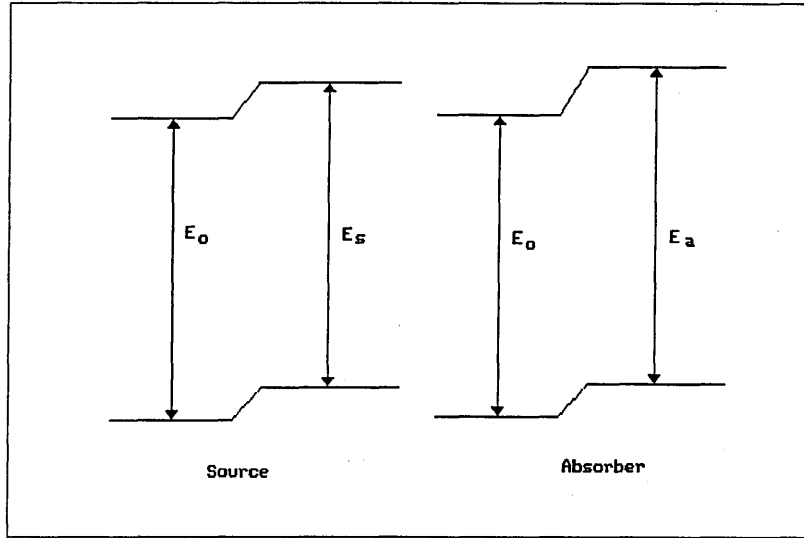


Figure 2.6 Source and Absorber Nuclear Energy Levels.

$$E_S = E_0 + \frac{2\pi}{5} Ze^2 \{\psi(0)\}^2 (R_{ex}^2 - R_{grd}^2)$$

$$E_A = E_0 + \frac{2\pi}{5} Ze^2 \{\psi(0)\}^2 (R_{ex}^2 - R_{grd}^2)$$

Isomer shift, $\delta = E_A - E_S$

Hence, $\delta = \frac{2\pi Ze^2}{5} | \{\psi(0)\}_A^2 - \{\psi(0)\}_S^2 | (R_{ex}^2 - R_{grd}^2)$ Equation 2.4

The difference in the nuclear radii are very small, (approx. 0.1%), so that the square can be neglected and Equation 2.4 can be rewritten;

$$\delta = \frac{4\pi Ze^2 R^2}{5} | \frac{\delta R}{R} | (\{\psi(0)\}_A^2 - \{\psi(0)\}_S^2)$$

For ^{119}Sn $\delta R/R$ is positive (+1.8) so that as s-electron density at the absorber nucleus increases so does the isomer shift. The magnitude of $\delta R/R$ was only firmly established in the mid-'seventies by Roggweiller and Kundig [2]. Prior to this values for $\delta R/R$ ranged from 0.74 to 3.3. Even the sign was in doubt until the late 'sixties. The isomer shift is measured relative to a standard source, which for ^{119}Sn Mößbauer spectroscopy is usually calcium or barium stannate, *i.e.* $\text{Sn}[\text{Kr}] 4d^{10}5s^05p^0$. The ranges of δ for tin compounds are shown below;

divalent Sn	δ 2.3 to 4.4mms ⁻¹
metallic Sn	δ approx. 2.5mms ⁻¹
Sn^{4+} and Sn^{IV}	δ -0.4 to 2.0mms ⁻¹

Consider the tin halides[3], Table 2.1;

Table 2.1 Isomer Shifts of Selected Tin Halides.

	<u>δ/mms^{-1}</u>		<u>δ/mms^{-1}</u>		<u>δ/mms^{-1}</u>
SnF_2	3.60	SnF_4	-0.40		
SnCl_2	4.06	SnCl_4	0.84	SnCl_6^{2-}	0.50
SnBr_2	3.97	SnBr_4	1.05	SnBr_6^{2-}	0.84
SnI_2	3.85	SnI_4	1.55	SnI_6^{2-}	1.23

All recorded at 77K relative to BaSnO_3 [3]

The initial assumption that Sn(II) has an outer configuration of $5s^2$ is not valid. Many Sn(II) compounds show marked covalent character, including the halides, and X-ray studies reveal that SnCl_2 and SnF_2 form halide bridged polymers[4], see Figure 2.7;

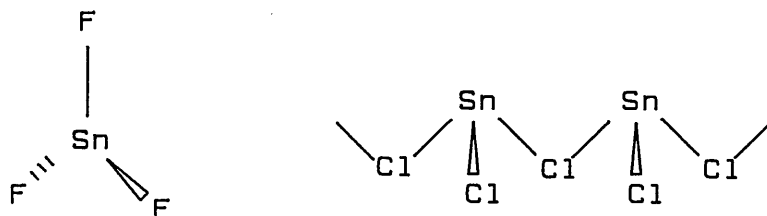


Figure 2.7 Structure of Tin (II) Halides.

The angle at which the Sn-halogen bonds lie suggests the use of p-orbitals in bonding. The values for δ in the tin (II) halides do not change as might be expected. These relatively unstable compounds have complicated and variable structures when compared to the tin (IV) halides. Apart from SnF_4 , these are four-coordinate moieties with the Sn $5sp^3$ hybridized. Because of the reduction in s-electron density this causes the isomer shifts of these compounds to be much smaller than those of tin (II) halides. SnF_4 is, in fact, six-coordinate *i.e.* $5sp^3d^2$ hybridized and the extra shielding caused by the d-orbitals means that the isomer shift of SnF_4 is therefore much lower than expected. This argument also explains the values of δ for the SnX_6^{2-} compounds.

To a first approximation, δ is dependent only on s-electron density, but this can be altered by hybridization and/or shielding effects.

2.6.2. Quadrupole Splitting

So far it has been assumed that the nucleus is spherical with uniform charge density. This is true when the nuclear spin state, I , = 0 or $\frac{1}{2}$. However, when $I > \frac{1}{2}$ deviation from spherical symmetry occurs and the nucleus has a finite quadrupole moment, see Figure 2.8:

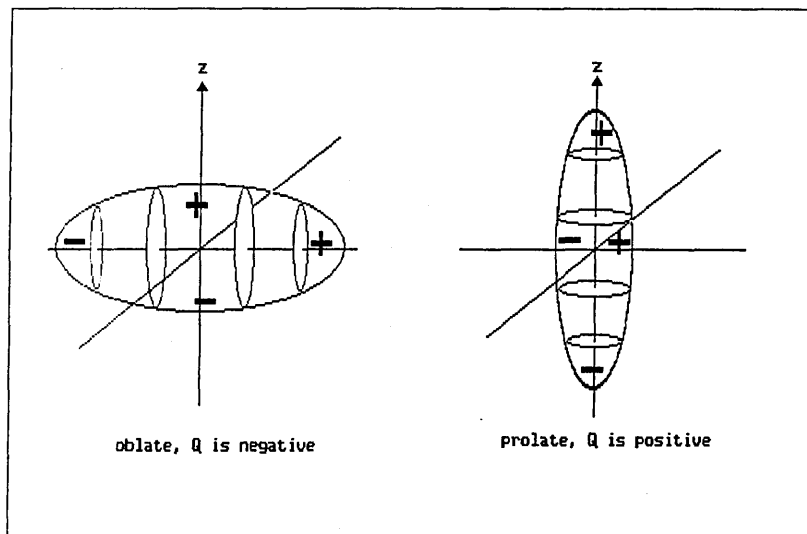


Figure 2.8 Nuclei with Non-Spherical Symmetry.

The nuclear quadrupole moment, eQ , is a measure of the deviation of the nucleus from spherical symmetry. The Electric Field Gradient, EFG, at the nucleus is defined by the second derivative of the electric potential;

$$\frac{\partial^2 V}{\partial x^2}, \quad \frac{\partial^2 V}{\partial y^2}, \quad \frac{\partial^2 V}{\partial z^2}$$

or V_{xx} , V_{yy} , V_{zz} . The coordinates are chosen such that;

$$|V_{zz}| \gg |V_{yy}| \gg |V_{xx}| \text{ and } V_{xx} + V_{yy} + V_{zz} = 0$$

The asymmetry parameter η is given by ;

$$\eta = \frac{V_{xx} - V_{yy}}{V_{zz}} \quad \text{so } 0 < \eta < 1$$

The interaction of the nuclear quadrupole moment with the principal component of the EFG splits the nuclear state into sublevels given by:

$$E_Q = \frac{eqQ}{4I(2I-1)} \{3m_I^2 - I(I+1)\} \{1 + (\eta^2/3)\}^{1/2}$$

Where I is the spin state of the level and m_I is the magnetic quantum number (I, I-1, ..0.. -I)

It is important to note that m_I is squared, so states with different signs will not be split. This results in the partial removal of degeneracy.

Consider ^{119}Sn , where eqQ and η are finite (*i.e.* EFG is non-zero):

if a constant, $k = eqQ(1 + \eta^2/3)^{1/2}$, and $\eta = 0$, then $k = eqQ$

$$\text{when } I = 1/2 \quad E_Q = 0$$

$$\text{when } I = 3/2 \quad E_Q(m_I) = \frac{k\{3m_I^2 - I(I+1)\}}{4I(2I - 1)}$$

$$\text{so} \quad E_Q(m_I) = \frac{k(3m_I^2 - 15/4)}{12}$$

$$E_Q \pm 1/2 = \frac{k(3/4 - 15/4)}{12} \quad E_Q \pm 3/2 = \frac{k(27/4 - 15/4)}{12}$$

$$\text{therefore: } E_Q \pm 1/2 = -k/4 \quad \text{and } E_Q \pm 3/2 = k/4$$

So the quadrupole splitting $\Delta E_Q = E_Q(I \pm 3/2) - E_Q(I \pm 1/2)$

$$= k/2 = (eqQ)/2$$

Figure 2.9. shows how the partial removal of the degeneracy of the $I=3/2$ energy level results in a quadrupole splitting:

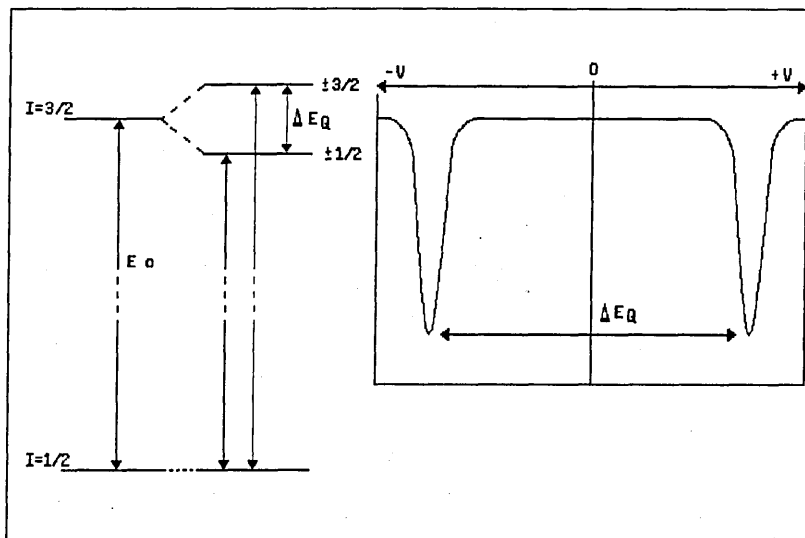
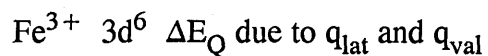
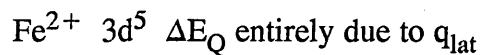


Figure 2.9. Formation of Quadrupole Splitting.

The EFG at the nucleus has two contributions:

- (i) non-cubic electron distribution in partially filled valence orbitals of the Mößbauer atom, q_{val} , and
- (ii) charges on ligands surrounding the Mößbauer atom in non-cubic symmetry, q_{lat} , *e.g.*



The quadrupole splitting in tin compounds may be expected to vary as a function of the unequal occupancy of the 5p and 5d orbitals. Using the tin (IV) halides as an example [3];

	$\Delta E_Q/\text{mms}^{-1}$
SnF_4	1.66
SnCl_4	0.00
SnBr_4	0.00
SnI_4	0.00

All measured at 77K [3].

It would be expected that these compounds would show no quadrupole splitting as a symmetrical arrangement of identical ligands surrounds the tin atom. However, SnF_4 has a significant quadrupole splitting, the reason for this being described in 2.6.1. The tin atom is six-coordinated, surrounded by two *trans*-non-bridging and four bridging fluorine atoms. The difference in the Sn—F bond lengths leads to a finite value for q_{val} .

For organotin (IV) compounds the magnitude of the EFG is determined by:

(i) stereochemistry of the compound; if it is a regular tetrahedron or octahedron, there will be no EFG;

(ii) differences in σ - and/or π -bonding between various ligands, which includes unequal occupancy of both 5p and 5d orbitals.

For the lighter elements the distinction between different types of bonding is much easier to make. For example, five-coordinate tin can only be approximately represented by $5sp^3d$. A further aspect which causes confusion is the lack of a measurable quadrupole splitting for a compound such as Ph_3SnH .

However, in general, a decrease in the electronegativity of the ligand leads to a reduction in the quadrupole splitting [3]:

	$\Delta E_Q/\text{mms}^{-1}$
Me_3SnF	3.47
Me_3SnCl	3.32
Me_3SnBr	3.28
Me_3SnI	3.05

All data recorded at 77K [3].

As coordination number and ligand electronegativity increase so does the EFG and therefore ΔE_Q .

2.6.3. The Magnetic Interaction

Certain systems may experience an internal and/or external magnetic field. The interaction of the nuclear magnetic dipole moment, μ , with a magnetic field, B , at the nucleus splits the nuclear states where $I > 0$ into $(2I+1)$ sublevels:

$$E_m = -g\mu_N B m_I$$

where $m_I = I, I-1, \dots, 0, \dots, -I$, μ_N is the nuclear magneton and g is the gyromagnetic ratio. So for ^{57}Fe metal, which has an internal magnetic field, complete removal of degeneracy is observed, as shown in Figure 2.10:

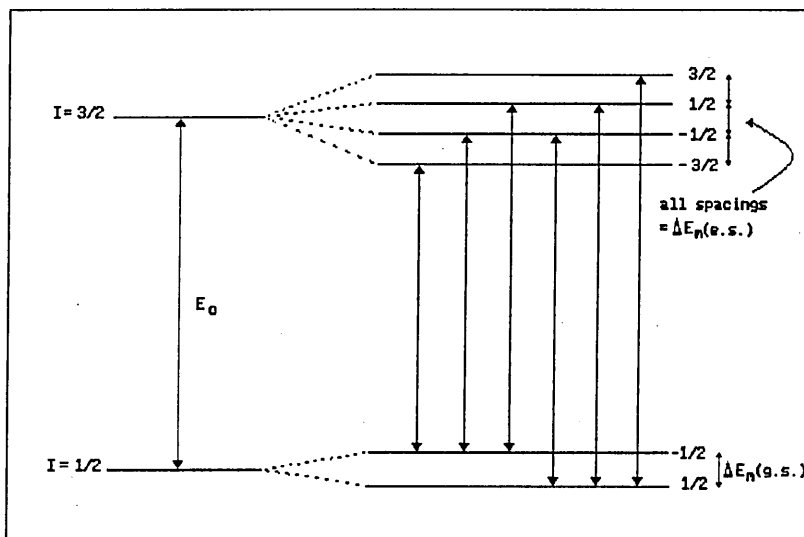
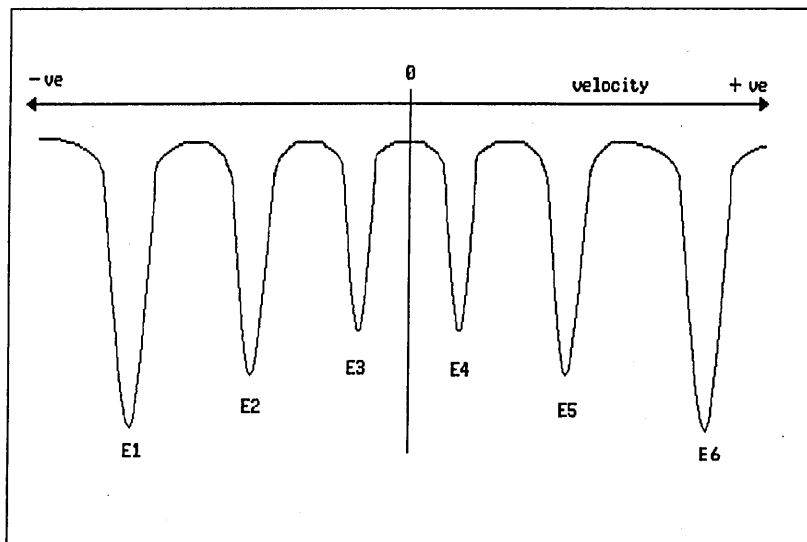


Figure 2.10 Splitting of the Nuclear Energy Levels in α - ^{57}Fe .

Allowed transitions, $\Delta m = 0, \pm 1$ means that a six line spectrum is observed, with relative intensities of 3:2:1:1:2:3 as shown in Figure 2.11:



$E1, E6 = 10.624\text{mms}^{-1}$, $E2, E5 = 6.152\text{mms}^{-1}$ and
 $E3, E4 = 1.680\text{mms}^{-1}$

Figure 2.11 The Spectrum of α -Fe at 298K when $H_{\text{ext}} = 0$.

This magnetic, or Zeeman, splitting is of no consequence in the study of organotin compounds. However, the spectrum of α -Fe with its well defined line spacings is used to calibrate the Mößbauer spectrometer.

2.7. The Mößbauer Experiment

The presence of the hyperfine interactions means that the source and absorber energy levels will not be the same. To carry out a Mößbauer experiment a number of components are required:

- (i) source/energy modulation system,
- (ii) absorber,
- (iii) detector,
- (iv) recording system and
- (v) cryogenic system (not always necessary).

2.7.1. The Source

As already mentioned in 2.1, the Mößbauer effect has been recorded in over 40 elements. Of these, ^{57}Fe and ^{119}Sn have been studied the most. Mößbauer atoms have low energy, soft, γ -rays ($< 150\text{KeV}$, see Section 2.5). The excited state should be easily accessible, preferably by spontaneous decay of a parent isotope with a relatively long half-life. The decay scheme of ^{119}Sn is shown in Figure 2.12:

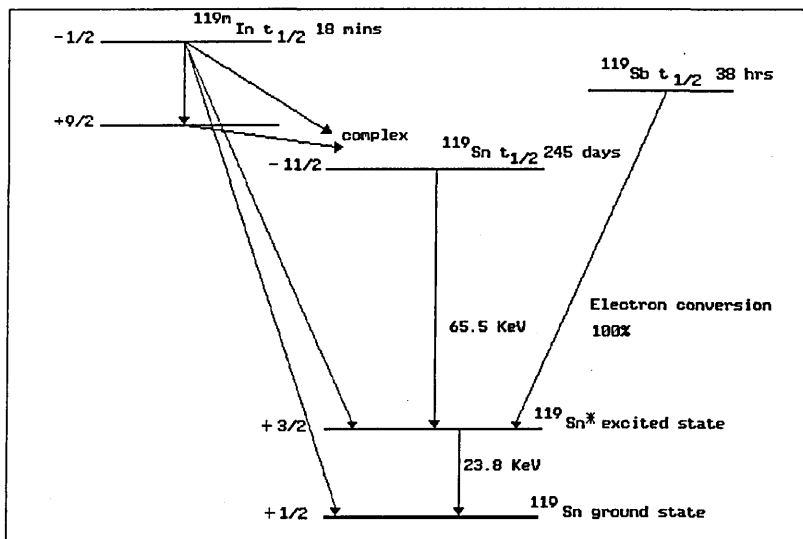


Figure 2.12 Decay Scheme of ^{119}Sn .

The excited states of ^{119}Sn can be populated in three ways;

- (i) from $^{119\text{m}}\text{In}$, but $t_{1/2}$ is only 18 minutes,
- (ii) from ^{119}Sb , but $t_{1/2}$ is only 38 hours, or
- (iii) from $^{119\text{m}}\text{Sn}$, where $t_{1/2}$ is about 245 days, which provides a reasonable working life.

The source is prepared by neutron bombardment of a matrix enriched in ^{118}Sn which increases the specific activity of the resultant metastable nucleide. This also means a lower concentration of ^{119}Sn is present which reduces self-absorption. Standard source materials are SnO_2 or Group II stannates. The source used in this study was 15mCi CaSnO_3 .

2.7.2. The Absorber

In the majority of Mößbauer experiments the absorber is the material under investigation. When studying organotin compounds it is necessary to maintain the sample at low temperature (80K) because of their low recoil-free fraction. The thickness of the absorber is another important factor to take into consideration.

Because of uncertainty in the energy of the transitions, the linewidth is not infinitely sharp, and the distribution of energies is given by:

$$I(E) = \text{const.} \cdot \frac{\Gamma}{2\pi} \cdot \frac{1}{(E - E_0)^2 + (\Gamma/2)^2}$$

This formula leads to the so-called Lorentzian lineshape. Deviations from this ideal occur if the absorber thickness is too great. The effective absorber thickness can be calculated:

$$t_A = \beta \cdot \sigma_0 \cdot f_A \cdot n_A$$

where β is the partial strength of the absorption line, σ_0 is the maximum absorber cross-section, f_A is the recoil free fraction of the absorber and n_A is the number of resonant nuclei per cm^2 in the absorber.

If $t_A < 5$ then the lines are Lorentzian and weaker as t_A decreases. If $t_A \gg 5$ the lines begin to broaden and are no longer Lorentzian. In practice t_A should be between 1 and 5.

e.g. t_A for 2.5% tri-n-butyltin chloride in a polyurethane foam;

$\beta = 0.5$ because a quadrupole doublet is observed;

$\sigma_0 = 1.40313 \times 10^{-18} \text{ cm}^2$ and $f_A \approx 0.3$ (at 80K)

weight of sample = 2.56g = 0.023g Sn

isotopic abundance $^{119}\text{Sn} = 8.58\%$ so 0.023g Sn contains:

$$\underline{0.002\text{g } ^{119}\text{Sn}}$$

number of resonant atoms = $(0.002/119) \times 6.023 \times 10^{23} = 1.01 \times 10^{19}$ atoms

area of sample = 1.8 cm^2 , so 5.64×10^{18} resonant atoms cm^{-2} :

$$\text{so } t_A = \underline{1.2}$$

Such spectra would take several days to accumulate, those of neat organotins a few hours.

2.7.3. Detectors

Consider the γ -ray energy spectra of ^{57}Co and ^{119}Sn :

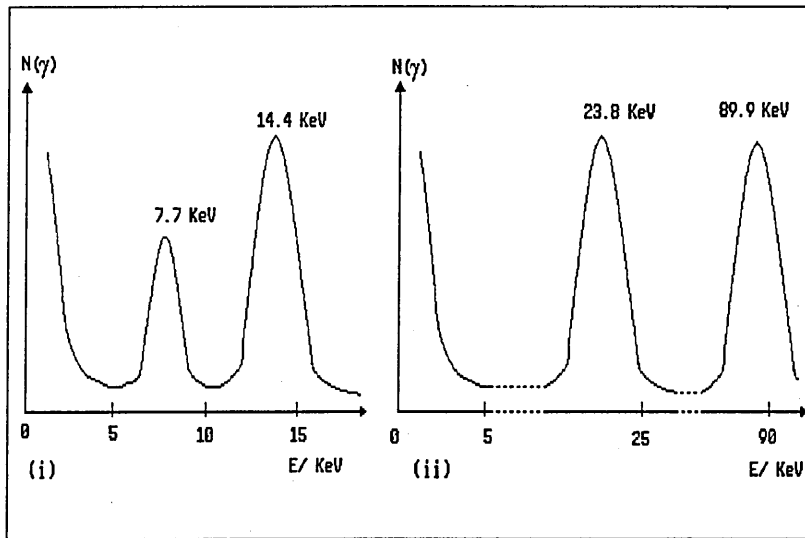


Figure 2.13 γ -Ray Energy Spectra of ^{57}Co and ^{119}Sn .

The γ -ray energy spectrum of ^{57}Co shows that near to the 14.4 KeV Mößbauer line there is a 7.7 KeV X-ray line. To prevent the latter being counted it is necessary to have a detector with good resolution. In practice a proportional counter is used, this is shown schematically in Figure 2.14;

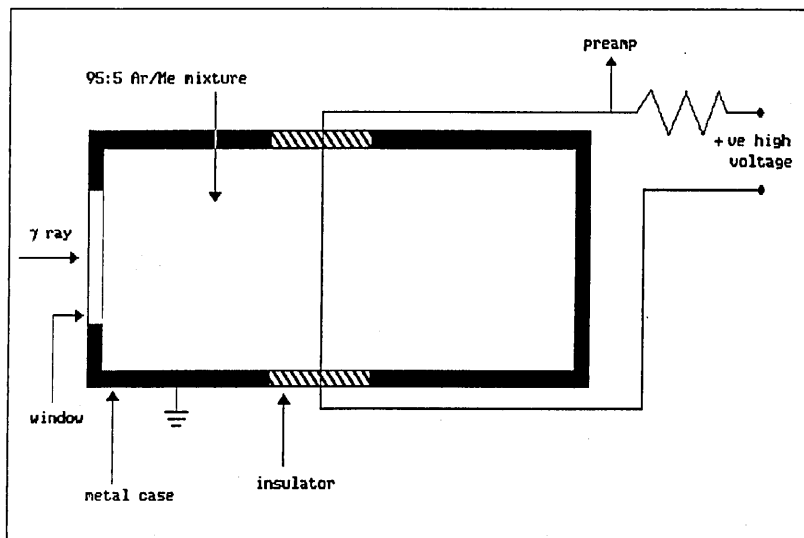


Figure 2.14 Schematic of the Proportional Counter.

After passing through the detector window, the γ -ray may collide with a gas atom or molecule and eject a valence electron. The kinetic energy of this electron will be nearly equal to that of the γ -ray photon. The electron dissipates its energy by ionizing other gas atoms/molecules. The positive ions will be attracted towards the metal walls, the electrons will accelerate towards the wire, thus causing more ionization. The arrival of many electrons in a short time interval (approximately $0.1\mu\text{s}$) causes a drop in the p.d. and a measurable signal. The p.d. takes a further period, approximately $0.1\mu\text{s}$, to recover, so that the detector has a "dead time" when counting is not possible.

Resolution is not such a problem with ^{119}Sn , so it is possible to use a scintillation counter which operates at higher efficiencies than the proportional counter, but with lower resolution. The scintillation counter is shown schematically in Figure 2.15;

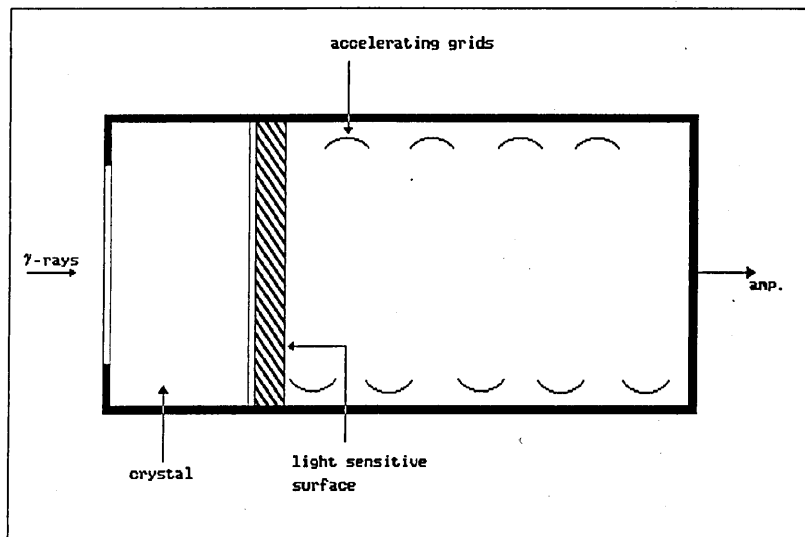


Figure 2.15 Schematic of the Scintillation Counter.

The crystal is usually thallium doped sodium iodide. Incident γ -rays cause emission of visible light when in collision with the crystal. The secondary rays strike the light-sensitive surface of the photomultiplier tube causing electrons to be emitted. The amplification at each accelerating grid leads to a measurable signal.

2.7.4. Cryogenics

As has already been stated in Section 2.7.2, organotin compounds have low f values at room temperature and it is necessary to cool them down during a Mößbauer experiment. Two systems are available, a liquid nitrogen cryostat and a closed cycle displax helium cryostat. The former has a minimum operating temperature of 77K, the latter 12K.

2.7.4.1. The Liquid Nitrogen Cryostat

This was used for the majority of the Mößbauer experiments in this study, the cryostat maintaining the absorber at 80K. The cryostat is shown in Figure 2.16;

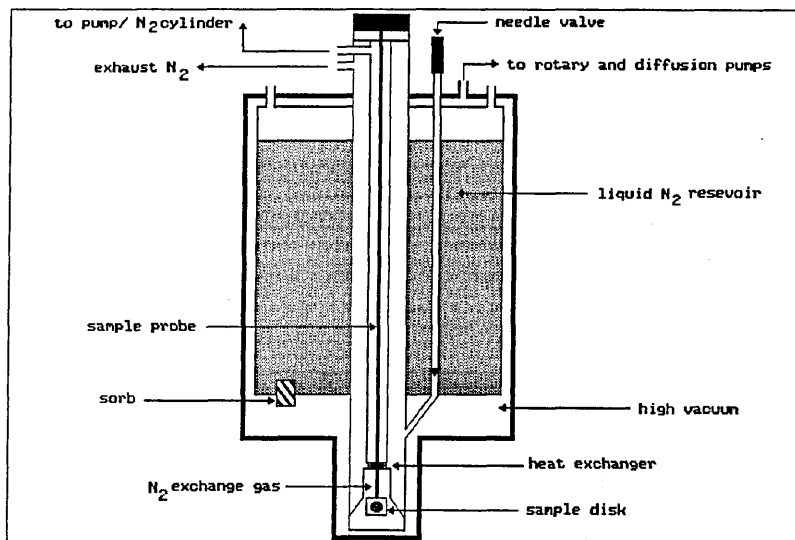


Figure 2.16 Schematic of the Liquid Nitrogen Cryostat.

The cryostat contains a reservoir of liquid nitrogen maintained by a high vacuum (10^{-5} to 10^{-6} torr). When the needle valve is opened, nitrogen flows to the heat exchanger cooling the copper contact ring on the sample probe, which in turn cools the absorber. The presence of an exchange gas (usually N_2) in the sample chamber is needed for effective operation. Liquid nitrogen will maintain a base absorber temperature of 77K, and the use of a temperature controller allows temperatures in the range 300K to 80K to be achieved. A platinum sensor on the heat exchanger allows the temperature controller to monitor the power supply necessary to remain at the preset temperature, usually 80K.

The cryostat contains a sorb which helps to preserve a high vacuum. Periodically the cryostat has to be re-evacuated and the sorb is heated in order to degas it.

The sample is cooled in liquid nitrogen before being placed inside the cryostat. The probe must be aligned with the mylar windows of the cryostat, which have the source and detector on either side.

2.7.5. The Drive System

As already discussed in the section on the hyperfine interactions, source and absorber will in general be in non-identical chemical environments. Because of this, resonant fluorescence will not occur unless the source γ -ray energy is modified in some way. This can be conveniently achieved by mounting the source on a transducer and utilizing the Doppler effect:

$$E_{\gamma} = E_s(1 + v_D/c)$$

where E_{γ} is the energy of the modulated γ -ray; E_s is the energy of the γ -ray and v_D is the Doppler velocity.

It is found that Doppler velocities of the order of $\pm 6 \text{ mms}^{-1}$ are sufficient to record the Mößbauer spectra of organotin compounds.

The transducer is linked to a Canberra MultiChannel Analyzer, MCA, and each channel corresponds to a particular source velocity. A feedback loop reduces velocity errors to a minimum. Before the spectrum is recorded it is necessary to select the appropriate γ -ray. This can be accomplished using a Single Channel Analyzer, SCA. The MCA in the Pulse Height Analysis, PHA, mode performs this task. Upper and lower level discriminators are used to set the window, which is usually about 150 channels wide.

When switched to the time mode the MCA scans through the channels, normally 512, with approximately $200 \mu\text{s}$ dwell time in each channel. Synchronization between the MCA and transducer means that each storage channel corresponds to one Doppler velocity. Spectra are recorded using a constant acceleration waveform, as shown in Figure 2.17:

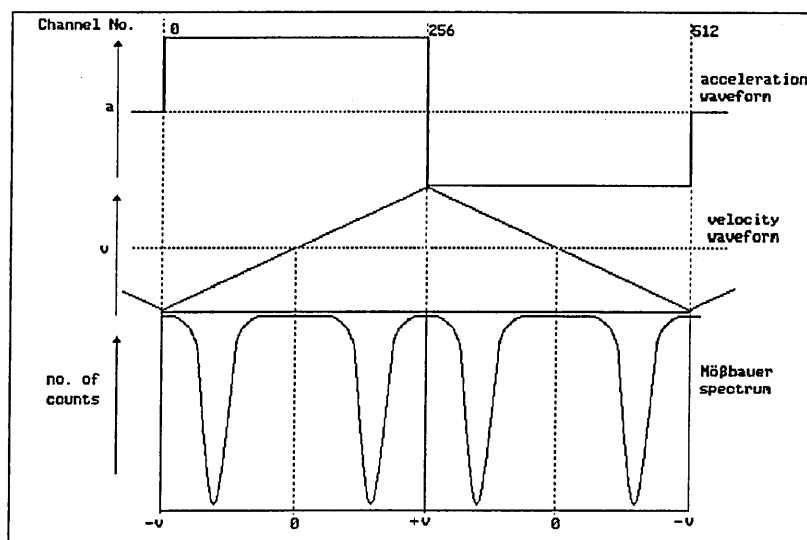


Figure 2.17 Relationship of Acceleration and Velocity Waveforms with the Mößbauer Spectrum.

Since each velocity is passed through twice on one 0-512 scan, a mirror image of the spectrum is recorded. Once a satisfactory resolution of the peak(s) has been achieved, the two halves can be folded to produce a single spectrum. The recent installation of IBM AT computers has led to the replacement of the Canberra MCA's.

2.7.6. Data Handling

This consists of folding the mirror images and then fitting Lorentzian lines to the spectrum. The recorded data used to be sent to the buffer of a microcomputer from the MCA and then stored on floppy disk. Using a Kermit program the data would then be transferred to the IBM mainframe. A suite of folding, fitting and plotting programs could then be used to manipulate the raw data. However, along with the IBM AT's came the introduction of an Apollo

570 minicomputer system. The latter contains enhanced versions of all the mainframe programs and data can be transferred directly to it from the IBM.

The data handling programs include:

(i) MOSFOLDN: this program can deal with up to 1024 data points.

The data can be folded about a set point or at the channel number corresponding to the minimum χ^2 value;

(ii) CALIBRATE: this is a modified version of MOSFITN (see below) and will only fit an α -Fe or sodium nitroprusside (SNP) spectrum. A parameter file, CAL_PARFE, contains the initial estimates for the line positions in channel numbers. These can be obtained from the relevant FOLDED_DATA file. From the initial estimates and using standard values for the splitting of α -Fe (Section 2.6.3) or SNP, CALIBRATE calculates the calibration constant. The maximum and minimum Doppler velocities are calculated for different centres;

(iii) MOSFITN: this program is based upon a non-linear least squares regression routine. As with CALIBRATE, a parameter file is required, *e.g.* MOSFITN_PARQ. Parameter files can be modified to fit any number of singlets, doublets or sextets, or any combination of the three. When a satisfactory fit has been accomplished the fitted data file and a plot of the spectrum can be obtained.

2.8. Mößbauer Spectroscopy and it's Application to Organotin Chemistry

The first paper on the Mößbauer effect in tin was published in 1960 [6]. Since that time the increasing importance of organotins in science and industry is reflected in the number of papers published. For convenience these will be divided into five categories;

(i) theoretical;

(ii) analysis by Mößbauer spectroscopy alone;

(iii) combined X-ray crystallography/Mößbauer spectroscopy;

(iv) combined ^{119}Sn NMR/infrared with Mößbauer spectroscopy and

- (v) analysis of real, or complex systems.

2.8.1. Theoretical Mößbauer Studies on Organotin Compounds

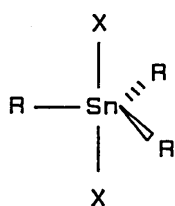
In 1963, Gol'danskii *et al* [7] published results which indicated that certain triorganotin species, including Ph_3SnCl , had asymmetric line areas. Line asymmetry can arise from anisotropic recoilless radiation or from partial orientation of the crystallites. Gol'danskii claimed the former was true in Ph_3SnCl , and the model was developed mathematically by Karyagin [8]. However, Shpinel *et al* [9] found that grinding Ph_3SnCl with graphite resulted in the loss of line asymmetry, proving that partial orientation of the crystallites was the cause of Gol'danskii's observation. However, the so-called Gol'danskii-Karyagin effect has been observed in polymeric compounds such as Me_3SnF , Ph_3SnF and Me_3SnCOOH [10].

In 1969, Herber *et al* [11] published the results of a study of organotin (IV) compounds. They claimed that it was possible to differentiate between tetrahedral, sp^3 , hybridized and trigonal bipyramidal, sp^3d , or octahedral, sp^3d^2 , tin atoms. Simply dividing the quadrupole splitting by the isomer shift gave a value, ρ . If $\rho < 1.8$, the tin atom is sp^3 hybridized; if $\rho > 2.1$, the tin atom is sp^3d or sp^3d^2 hybridized. Between 1.8 and 2.1 there is some ambiguity, but the Herber rule provides a very useful indication of the coordination number of organotin (IV) compounds.

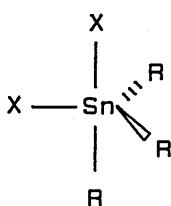
Research activity in the mid-'sixties to 'seventies focused on correlating the observed Mößbauer parameters with the structure of organotin compounds. Parish and Platt [12] concluded that an imbalance in the polarity of the σ — bonds between Sn—L was the dominant factor in the formation of an EFG large enough to produce a quadrupole splitting. Devooght *et al* [13] carried out a more rigorous study into the correlation of the quadrupole splitting and isomer shift of some trialkyltin halides with molecular structure. In particular, they

were interested in the larger than expected quadrupole splittings in certain trialkyltin halides. They concluded that back donation of electron density from Sn5p orbitals may be occurring.

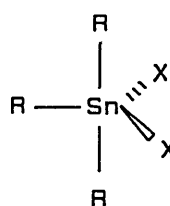
Bancroft *et al* [14] advanced the interpretation of five-coordinate organotin spectra by calculating a series of partial quadrupole splittings, p.q.s. . Using these values it is possible to calculate the p.q.s. of three five-coordinate isomers:



(I) *trans*-



(II) *cis*-



(III) *mer*-

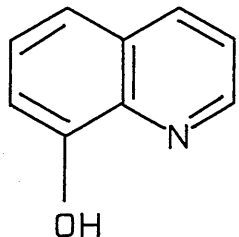
Figure 2.19 Structural Isomers of R_3SnX_2 .

The derived expressions for ΔE_Q (I), (II) and (III) are;

$$\Delta E_Q(I) = 2[X]^{tba} + 2[X']^{tba} - 3[R]^{tbe}$$

$$\Delta E_Q(II) \approx \frac{2[R]^{tba} - 8[R]^{tbe} + 2[X]^{tba} + 5[X]^{tbe}}{\sqrt{13}}$$

$$\Delta E_Q(III) \approx \frac{-8[R]^{tba} - [R]^{tbe} + 7[X]^{tbe}}{\sqrt{7}}$$

	$[\text{pqs}]^{\text{fba}}/\text{mms}^{-1}$	$[\text{pqs}]^{\text{fbe}}/\text{mms}^{-1}$
	Ph -0.89	-0.98
	oxin -0.05	+0.04

$$\Delta E_{\text{Q}}(\text{I}) = 2.74 \text{mms}^{-1},$$

$$\Delta E_{\text{Q}}(\text{II}) = 3.17 \text{mms}^{-1} \text{ and}$$

$$\Delta E_{\text{Q}}(\text{III}) = 1.71 \text{mms}^{-1}.$$

The observed quadrupole splitting for $\text{Ph}_3\text{Sn}(\text{oxin})$ is 1.75mms^{-1} , which is in good agreement with the value for the *mer*- isomer.

Recent work in this area has centred on two Italian workers, Barbieri and Silvestri [15-19], who have attempted to find a relationship between Mößbauer isomer shifts and the atomic charge on the tin atom, Q_{Sn} . By using semiempirical values of Q_{Sn} , linear correlations have been found in some homologous series. However, all models so far used to explain observed parameters necessitate assumptions and simplifications which lead to discrepancies.

2.8.2. Characterization of Organotin Compounds by Mößbauer Spectroscopy

Mößbauer spectroscopy has been used to characterize known and novel organotin compounds. Work of this type really began in the early seventies, with studies by Fitzsimmons and co-workers in particular [20,21,22]. Organotin dithiocarbamates, mixed alkyl/aryltins and trialkyltin halides with adducts such as metal carbonyls and nitrogen heterocycles have all been characterized using Mößbauer spectroscopy [23 - 29].

A good example of how the technique can be used was presented by Barbieri *et al* [30,31]. They found that the 2-mercaptoethanesulphonate complex $[\text{Ph}_2\text{Sn}(\text{SCH}_2\text{CH}_2\text{SO}_3)_2]^{2-}$ exhibited significant antileukemia activity in mice. The activity was thought to be due to the Ph_2Sn (IV) moiety, with the ligand being responsible for transportation across the cell membranes.

The configuration of the diorganotin (IV) *bis*(2-mercaptoethane-sulphonates), $[\text{R}_2\text{Sn}(\text{SCH}_2\text{CH}_2\text{SO}_3)_2]^{2-}$ (R = Me, Ph) as sodium and guanadinium salts, in the solid state and in aqueous solutions of the Me_2Sn (IV) derivatives was studied.

The p.q.s. of the various possible tetrahedral and trigonal bipyramidal structures were calculated by computer and compared to the observed quadrupole splittings. It was found that in the solid state and in aqueous solution both the sodium and the guanadinium salts exhibit tetrahedral geometries.

The effect of HEPES buffer on the dimethyltin derivative in aqueous solution was also studied. The structure of HEPES is shown below in Figure 2.20;

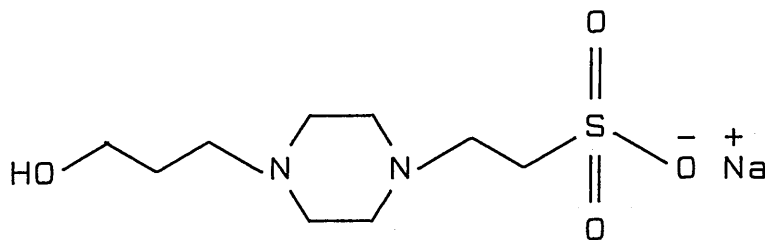


Figure 2.20 Structure of HEPES.

There is evidence to suggest that coordination between tin centres and the tertiary nitrogen of HEPES can mimic the bonding assumed to occur in organotin-protein systems. It was found that one mole of HEPES formed a trigonal bipyramidal species with $[\text{Me}_2\text{Sn}(\text{SCH}_2\text{CH}_2\text{SO}_3)_2]^{2-}$.

Finally, it was noted that lysis of the tin—sulphur bonds in the complex of dimercaptoethanesulphonate occurs at room temperature in a matter of days, thus releasing the active R_2Sn (IV) moiety.

The investigation was extended to include $R_2Sn[SCH_2CH(NH_3^+)COO^-]_2$ and $R_2Sn[SC(CH_3)_2CH(NH_3^+)COO^-]_2$. These two complexes behaved in exactly the same manner as the dimercaptoethanesulphonate species.

As with all analytical methods there are limitations and more reliable information is obtained by comparing results from complementary techniques.

2.8.3. Combined X-Ray Crystallography/ Mößbauer Spectroscopy

Mößbauer spectroscopy and X-ray crystallography are both solid-state techniques and the information gained is of a similar nature. For example, in a study by Allen *et al* [32] on dimethylchlorotin acetate, the Mößbauer parameters were;

$$\delta = 1.38 \pm 0.02 \text{mms}^{-1}$$

$$\Delta E_Q = 3.56 \pm 0.02 \text{mms}^{-1} \text{ and}$$

$$\rho = 2.6$$

Data recorded at 80K using a $BaSnO_3$ source[32].

These figures suggest that the tin atom is at least five-coordinate. The X-ray data confirmed this and showed that the Me_2SnCl units are linked together by acetate bridges to give polymeric chains. Several other studies of a similar nature have been published [33-40].

A recent paper by Tudela *et al* [40] has shown that Mößbauer spectroscopy can be used to find errors in published X-ray crystal structure. By using p.q.s. values it was possible to show that the Sn—Cl bond length in tetrachloro- *bis* (1,3-diethylthiourea) tin (IV) had been calculated incorrectly. Redetermination of the X-ray structure was carried out and found to be in agreement.

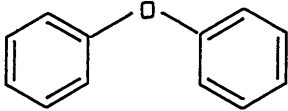
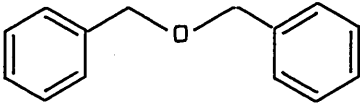
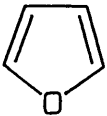
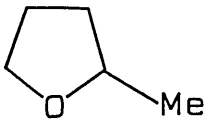
2.8.4. Combined Mößbauer and NMR/ Infrared Spectroscopy

The organotin chemist is fortunate in that the ^{119}Sn isotope is amenable not only to Mößbauer, but also to NMR spectroscopy. Before the 1960's the major technique for characterizing novel compounds was infrared spectroscopy, which still retains an important role. However, the advent of routine ^{119}Sn Mößbauer and NMR experiments means that complete structure determinations are often possible. There are many references in the literature to the use of combinations of Mößbauer with NMR and/or infrared spectroscopy to characterize organotin compounds [42-65]. In the majority of these, the infrared and Mößbauer techniques have been used to study the solid state, and NMR to study solution state properties.

Blunden *et al* [50] studied the interaction between two tin (IV) halides, SnCl_4 and SnBr_4 , with a series of cyclic and aromatic ethers in the solid state and in solution. Ethers are present in coal, and tin (IV) halides have proved to be good coal liquefaction catalysts, but the mechanism is not well understood.

A selection of the ^{119}Sn NMR results are shown in Table 2.2:

Table 2.2 ^{119}Sn NMR Data for Selected Tin Halide–Ether Adducts.

Ether	SnX_4	Ether: SnX_4	$\delta(^{119}\text{Sn})$ ppm
/	SnCl_4	/	-149
/	SnBr_4	/	-637
	SnCl_4	1:1	-150
	SnBr_4	1:1	-638
Ph_2O			
	SnCl_4	1:1	-181
		10:1	-602
	SnBr_4	1:1	-696
Bz_2O		10:1	-835
	SnCl_4	1:1	-149
	SnBr_4	1:1	-637
Furan			
	SnCl_4	1:1	-334
		10:1	-604
	SnBr_4	1:1	-755
2-MeTHF		10:1	-1317

All data recorded in CCl_4 .

^{119}Sn NMR shifts are indicative of coordination number. An increase is accompanied by a change in $\delta(^{119}\text{Sn})$ to lower frequencies. Hence, in tetrachloromethane, SnCl_4 and SnBr_4 have chemical shifts of -149 and -637

ppm respectively, but in methanol they are -600 and -1307 ppm. This is due to the formation of a six-coordinate $\text{SnX}_4 \cdot 2\text{MeOH}$ species. The above results show that furan and Ph_2O do not coordinate with SnX_4 , but Bz_2O and 2-MeTHF do.

The solid state work was restricted to 1,4-dioxane and methyltetrahydrofuran 1:1 adducts with SnCl_4 as these were the only stable complexes to be isolated, see Table 2.3;

Table 2.3 Mößbauer Data of Selected Tin Halide:Ether Adducts.

Compound	δ/mms^{-1}	$\Delta E_Q/\text{mms}^{-1}$
SnCl_4	0.78	0.00
$\text{SnCl}_4:1,4\text{-dioxane (I)}$	0.41	0.90
$\text{SnCl}_4:2[2\text{-MeTHF (II)}$	0.49	1.26
$\text{SnCl}_4:2[3\text{-MeTHF (III)}$	0.44	1.12
$\text{SnCl}_4:[2,2,5,5\text{-Me}_4\text{THF (IV)}$	0.62	0.00

All data recorded at 80K. Isomer shifts are relative to CaSnO_3 with an error in δ and ΔE_Q of $\pm 0.05\text{mms}^{-1}$.

Octahedral tin (IV) halide adducts with *trans*- O-donor ligands have measurable quadrupole splittings, whereas those with *cis*- geometries do not. From this it was concluded that the structures of (II) and (III) are:

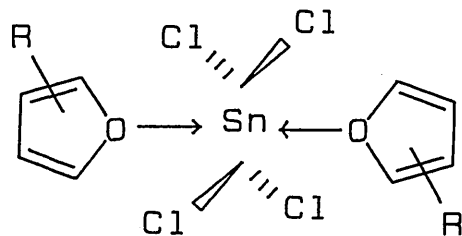


Figure 2.21 Adduct of SnCl_4 with (II) or (III).

The two 1:1 adducts (I) and (IV) show rather different properties to one another, the former showing evidence of an EFG, the latter none. $\text{SnCl}_4 \cdot \text{Ph}_3\text{PO}$, $\text{SnCl}_4 \cdot \text{NMe}_3$ and $\text{SnBr}_4 \cdot \text{NMe}_3$ all behave in the same way as (IV). It is surprising that these compounds have no measurable quadrupole splitting, but it should be noted that no linewidths were reported. The possibility exists that there may be a small EFG which would produce unresolved splitting.

The structure of (I) was given as a normal 1:1 adduct or possibly a pseudo 1:2 adduct, Figure 2.22:

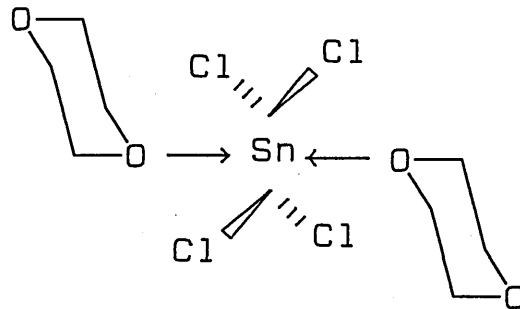


Figure 2.22 1:1 Adduct of SnCl_4 : 1,4-Dioxane.

Davies *et al* [58] studied the structure of dialkoxide dioxastannolanes, initially by X-ray crystallography, and then by ^{119}Sn Mößbauer and NMR spectroscopy. The compounds are formed by reaction of dialkyltin oxides with 1,2-diols:

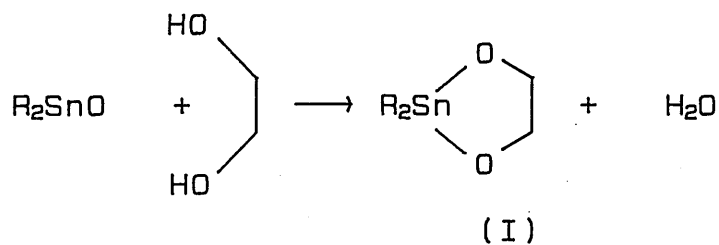


Figure 2.23 Reaction of Dialkyltin Oxides with 1,2-Diols.

Of interest in the study was 2,2-di-n-butyl-1,3,2-dioxastannolane ($\text{R}=\text{Bu}$). Measurements of molecular weight in solution indicated that the product was dimeric, *i.e.*

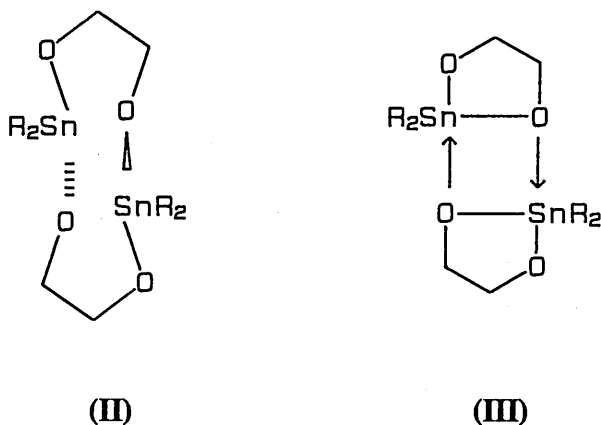


Figure 2.24 Dimers of 2,2-Di-n-Butyl-1,3,2-Dioxastannolane.

Möbbauser studies of the solid state showed that (I) was at least five-coordinate, so that association of the type shown in (III) is occurring. X-ray crystallography showed that the compound is in fact polymeric:

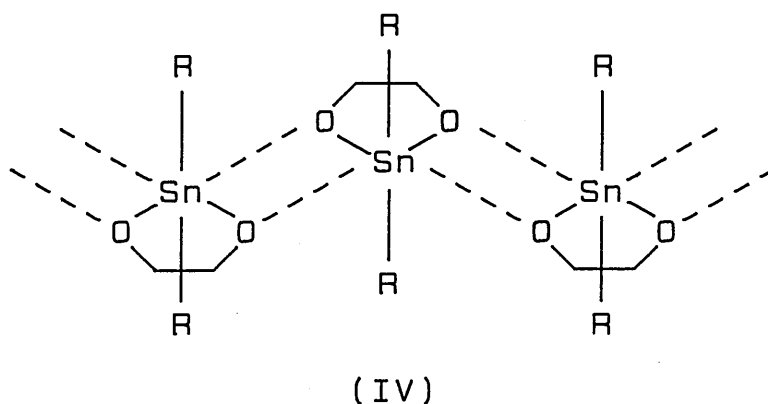
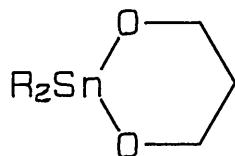


Figure 2.25 Structure of 2,2-Di-n-Butyl-1,3,2-Dioxastannolane in the Solid State (IV).

An analogous compound,



, showed similar behaviour.

Using an equation of Sham and Bancroft [59] it was possible to predict the quadrupole splitting of (IV):

$$|\Delta E_Q| = 4(S) (1 - 3\sin^2\theta \cos^2\theta)^{1/2}$$

where $S = \text{p.q.s. of the R group } (-1.03\text{mms}^{-1})$ and

$$\theta = (180 - \angle \text{R—Sn—R})/2$$

From the X-ray study $\text{R—Sn—R} = 138.6^\circ$, hence $\theta = 20.7$ and $|\Delta E_Q| = 3.37\text{mms}^{-1}$, which is in poor agreement with the observed value of 3.00mms^{-1} .

When (I) was studied by ^{119}Sn NMR, (with tetraphenyltin as comparison) the following results were obtained:

	solution/ δ ppm	solid/ δ ppm
Ph_4Sn	-120	-120
(I)	-189	-230

The solid state NMR shows an upfield shift caused by a change from five- to six-coordination, (Ph_4Sn is four-coordinate in solution and solid state). This study, as with many others shows that the interpretation of Mößbauer spectra is rarely straightforward.

A series of complexes of the type $[\text{R}_2\text{SnCl}_2\widehat{\text{N}}\widehat{\text{N}}]$, where $\text{R} = \text{Me, Et or n-Pr}$ and $\widehat{\text{N}}\widehat{\text{N}} = \text{various bi- and tridentate ligands}$ were examined by Visalakshi *et al* [57]. Such complexes, formed by the Lewis acid-base interaction of organotins with nitrogen are generally six-coordinate, often with distorted octahedral geometry. There exists the possibility of *cis/trans*- isomerism. The ligands of interest in this study are shown in Figure 2.26;

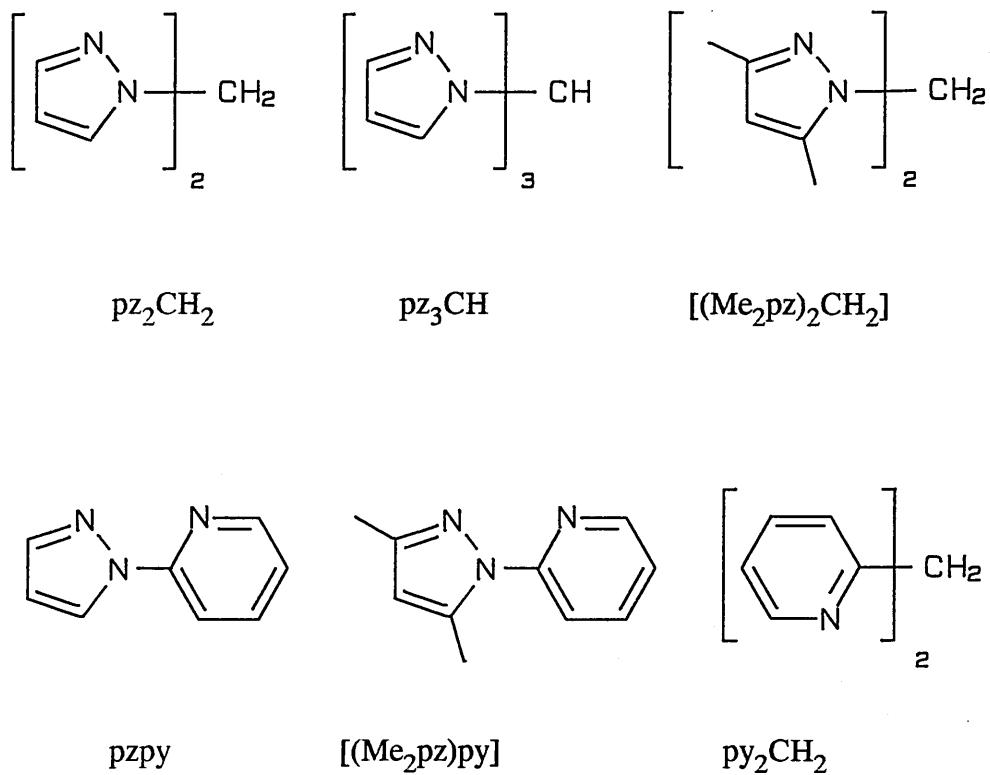


Figure 2.26 Bi- and Tridentate Ligands.

1:1 adducts of these ligands were formed with the R_2SnCl_2 moieties. The molar conductances were in the range of $2\text{-}20 \Omega^{-1} \text{cm}^2\text{mol}^{-1}$, indicating that they are non-conducting electrolytes. There are three possible geometrical isomers of $[\text{R}_2\text{SnCl}_2(\widehat{\text{N N}})]$, see Figure 2.27:

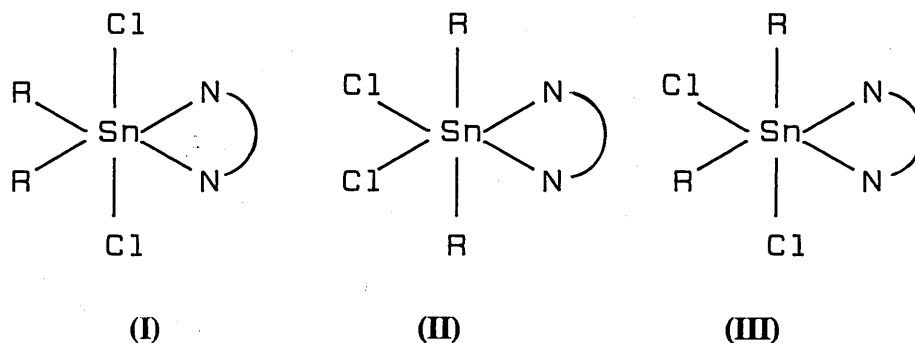


Figure 2.27 Geometrical Isomers of $[R_2SnCl_2(\widehat{N-N})]$.

Infrared spectroscopy in the $600-200\text{ cm}^{-1}$ region where Sn—C, Sn—Cl and Sn—N vibrations occur, was used to provide stereochemical information.

When $R = \text{Me}$, a single $\nu\text{Sn—C}$ band should be observed for the linear *trans*-R complex, II. However, if a non-linear *trans*-R stereochemistry or *cis*-arrangement is present, then two bands should be observed. In fact Visalakshi found that two Sn—C stretching bands were present and it was thought likely to be due to a non-linear *trans*-structure.

It was also reported that in $R_2\text{SnCl}_2$, $\nu\text{Sn—Cl}$ was $\approx 335\text{ cm}^{-1}$, but in $[R_2\text{SnCl}_2(\widehat{N-N})]$ it was $< 310\text{ cm}^{-1}$. This lowering of stretching frequency is due to an increase in the Sn—Cl bond length. This in turn is a result of a change from $5sp^3 \rightarrow 5sp^3d^2$ hybridization and the input of electron density from the ligand nitrogens. The Mößbauer parameters of a selection of these complexes are shown in Table 2.4.

Table 2.4 Mößbauer Parameters of Selected Complexes.

Species	δ/mms^{-1}	$\Delta E_Q/\text{mms}^{-1}$	ρ
[Me ₂ SnCl ₂]	1.54	3.33	2.16
[Me ₂ SnCl ₂ .pz ₂ CH ₂]	1.44	4.12	2.86
[Me ₂ SnCl ₂ .(Me ₂ pz) ₂ CH ₂]	1.43	3.95	2.76
[Me ₂ SnCl ₂ .pz ₃ CH]	1.51	3.75	2.48
[Me ₂ SnCl ₂ .(Me ₂ pz)py]	1.46	4.02	2.75
[Me ₂ SnCl ₂ .py ₂ CH ₂]	1.40	3.99	2.85

All data recorded at 78K with an error $\pm 0.05\text{mms}^{-1}$, relative to BaSnO₃.

Hexacoordinate tin complexes with *trans*- R groups have quadrupole splittings of $\approx 4\text{mms}^{-1}$, whereas those with *cis*- R groups have quadrupole splittings of $\approx 2\text{mms}^{-1}$. Thus the combined Mößbauer and infrared evidence suggests an asymmetric *trans*- R structure for these compounds.

The ¹¹⁹Sn NMR spectra of the complexes which dissolved in CDCl₃ were recorded and the chemical shifts are shown in Table 2.5.

Table 2.5 ¹¹⁹Sn NMR Data of Selected Complexes.

Species	$\delta^{119}\text{Sn}/\text{ppm}$
Me ₂ SnCl ₂	140
Et ₂ SnCl ₂	122
[Me ₂ SnCl ₂ (pz ₂ CH ₂)]	119
[Et ₂ SnCl ₂ (pz ₃ CH)]	107
[Me ₂ SnCl ₂ (Me ₂ pz)CH ₂]	117
[Me ₂ SnCl ₂ pz.py]	33
[Et ₂ SnCl ₂ (Me ₂ pz)py]	-73

It can be inferred from the above data that in CDCl_3 solution, the pz_2CH_2 , pz_3CH and the $(\text{Me}_2\text{pz})_2\text{CH}_2$ complexes dissociate to give R_2SnCl_2 plus the ligand. However the upfield shift (wrongly described by the authors as a downfield shift) of the two pyridine based complexes indicates that they are not dissociated in CDCl_3 solution. This may be rationalized by the fact that pyridine ligands are stronger π -acceptors than the pyrazoles and hence form a stronger bond.

2.8.5. The Study of Organotins in Complex Systems by Mößbauer Spectroscopy

It is in this area that Mößbauer spectroscopy can provide unique chemical and structural data. Prior to its development it would have been difficult to study, for example, the nature of an organotin dispersed within a solid matrix. The majority of organotin compounds produced worldwide ($\approx 35\ 000$ tons p.a.) are used for PVC stabilization, followed by antifouling agents in paints and catalysts for the polyurethane industry. This is reflected in the work published to date [67 - 74].

Of particular relevance to this research was the study of the fate of triorganotin compounds dispersed in neoprene systems by Allen *et al* [70,72]. It was found that the curing of *bis*-(tri-n-butyltin) oxide, tri-n-butyltin stearate and *bis*-(tri-n-butyltin) carbonate in neoprene gave rise to the formation of tri-n-butyltin chloride in all three cases. Soxhlet extraction of the polymers and analysis by ^{119}Sn NMR confirmed this finding. It was proposed that the conversion occurs by reaction with hydrogen chloride, which forms by dehydrochlorination of the base polymer during curing.

When triphenyltin derivatives were incorporated into the neoprene they were subject to drastic degradation. The Mößbauer spectra were complex and the presence of SnO_2 which, with its relatively high recoil free fraction and broad linewidth, made interpretation difficult. Soxhlet extraction of the neoprene to

provide samples for ^{119}Sn NMR was unsuccessful, indicating that the phenyltins were bound to the polymer. (However, it should be noted that phenyltin compounds are particularly insoluble in most solvents).

Two neoprene samples originally containing triphenyltins were refluxed with n-propylmagnesium chloride. The resulting tetraorganotins were extracted and analyzed by G.C. All stages of dephenylation were shown to be present in the gas chromatograms. Dephenylation was thought to occur in the presence of hydrogen chloride produced during curing.

Chapter 2 References.

1. Mößbauer, R.L., Z. Physik, 1958, 151, 124.
2. Roggweiller, P. and Kundig, W., Phys. Rev. B, 1975, 11, 4179.
3. Greenwood, N.N. and Gibb, T.C., Mößbauer Spectroscopy, Chapter 14, Chapman and Hall, 1971.
4. Massey, A.G., The Typical Elements, Chapter 7, Penguin Books, 1972.
5. Stevens, J. and Stevens, V., Mößbauer Data Effect Index, 1980, 3, (4), 99.
6. Barloutard, R., Cotton, E., Picou, J-L. and Quidort, J., C.R. Hebd. Seances Acad. Sci., 1960, 99.
7. Gol'danskii, V.I., Makarov, E.F. and Khrapov, V.V., Phys. Lett., 1963, 3, (7), 344.
8. Karyagin, S.V., Doklady Akad. Nauk. SSSR, 1963, 148, 1102.
9. Shpinel, V.S., Aleksandrov, A.Y., Ryasnin, G.K. and Okhlobystin, O.Y., Soviet Physics J.E.T.P., 1965, 21, 47.
10. Stöckler, H.A. and Sano, H., Chem. Phys. Letters, 1968, 2, 448.
11. Herber, R.H., Stöckler, H.A. and Reichle, W.T., J. Chem. Phys., 1969, 42, (7), 2447.
12. Parish, R.V. and Platt, R.H., J. Chem. Soc. (A), 1969, 2145.
13. Devooght, J., Gielen, M. and Lejeune, S., J. Organomet. Chem., 1970, 21, 333.
14. Bancroft, G.M., Kumar Das, V.G., Sham, T.K. and Clark, M.G., J. Chem. Soc. Dalton Trans., 1976, 643.
15. Barbieri, R., and Silvestri, A., Inorganica Chim. Acta, 1981, 47, 201.
16. Barbieri, R. and Silvestri, A., J. Chem. Soc. Dalton Trans., 1984, 1019.
17. Silvestri, A., Inorg. Chim. Acta, 1988, 142, 5.
18. Barbieri, R., Rivarola, E., Silvestri, A., Huber, F. and Aldridge, W.N., Procs. Alma Ata Mößbauer Conf., 1988, 5, 1573.
19. Fitzsimmons, B.W., Seeley, N.J. and Smith, A.W., J. Chem. Soc. (A), 1969, 143.

20. Fitzsimmons, B.W., Owusu, A.A., Seeley, N.J. and Smith, A.W., J. Chem. Soc. (A), 1970, 935.
21. Ensling, J., Gutlich, P., Hassellbach, K.M. and Fitzsimmons, B.W., J. Chem. Soc. (A), 1970, 1940.
22. Barbieri, R., Pellerito, L., Bertazzi, N. and Stocco, G.G., Inorg. Chim. Acta, 1974, 11, 173.
23. Crowe, A.J., Smith, P.J. and Harrison, P.G., J. Organomet. Chem., 1981, 201, 327.
24. Barbieri, R., Silvestri, A., Van Koten, G. and Noltes, J.G., Inorg. Chim. Acta, 1980, 40, 267.
25. Smith, P.J., Hill, R., Nicolaidis, A. and Donaldson, J.D., J. Organomet. Chem., 1988, 252, 149.
26. Cusack, P.A. and Patel, B.N., Inorg. Chim. Acta, 1984, 86, 1.
27. Frampton, C.S. and Silver, J., Inorg. Chim. Acta, 1986, 112, 203.
28. Katada, M., Uchida, Y., Iwai, K., Sano, H., Sakai, H. and Maeda, Y., Bull. Chem. Soc. Jpn., 1987, 60, 911.
29. Barbieri, R., Silvestri, A. and Huber, F., Appl. Organomet. Chem., 1988, 2, 457.
30. Barbieri, R., Silvestri, A. and Huber, F., Appl. Organomet. Chem., 1988, 2, 525.
31. Allen, D.W., Nowell, I.W., Brooks, J.S. and Clarkson, R.W., J. Organomet. Chem., 1981, 219, 29.
32. Harrison, P.G., Phillips, R.C. and Richards, J.A., J. Organomet. Chem., 1976, 114, 47.
33. Tse, J.S., Collins, M.J., Lee, F.L. and Gabe, E.J., J. Organomet. Chem., 1986, 310, 169.
34. Molloy, K.C., Quill, K., Cunningham, D., McArdle, P. and Higgins, T., J. Chem. Soc. Dalton Trans., 1989, 267.
35. Molloy, K.C., Waterfield, P.C. and Mahon, F., J. Organomet. Chem., 1989, 365, 61.

36. Cunningham, D., Fitear, P., Molloy, K.C. and Zuckerman, J.J., J. Chem. Soc. Dalton Trans., 1983, 1523.
37. Einstein, F.W.B., Jones, C.H.W., Jones, T. and Sharma, R.D., Can. J. Chem., 1983, 61, 2611.
38. Calogero, S., Valle, G. and Russo, U., Organomet., 1984, 3, 1205.
39. Ng, S.W., Chin, K.L, Wei, C., Kumar Das, V.G. and Butcher, R.J., J. Organomet. Chem., 1989, 376, 277.
40. Tudela, D., Kahn, M.A. and Zuckerman, J.J., J. Chem. Soc. Comm., 1989, 558.
41. Ford, B.F.E., Liengne, B.V. and Sans, J.R., Chem. Comm., 1968, 1333.
42. DeVries, J.L.F.K., and Herber, R.H., Inorg. Chim., 1972, 11, (10), 2458.
43. Brown, J.M., Chapman, A.C., Harper, R., Mowthorpe, D.J., Davies, A.G. and Smith, P.J., J. Chem. Soc. Dalton Trans., 1972, 3, 338.
44. Petridis, D. and Fitzsimmons, B.W., Inorg. Chim. Acta, 1974, 11, 105.
45. Calogero, S., Furlan, P., Peruzzo, V. and Plazzogna, G., Inorg. Chim. Acta, 1977, 22, 55.
46. Phillips, J.E. and Herber, R.H., J. Organomet. Chem., 1984, 268, 39.
47. Grätz, K., Huber, F., Silvestri, A., Alonzo, G. and Barbieri, R., J. Organomet. Chem., 1985, 290, 41.
48. Saxena, A., Tandon, J.P. and Crowe, A.J., Polyhedron, 1985, 4, (6), 1085.
49. Blunden, S.J., Searle, D. and Smith, P.J., Inorg. Chim. Acta, 1985, 98, 185.
50. Frampton, C.S., Roberts, R.M.G., Silver, J., Warmsley, J.F. and Yavari, B., J. Chem. Soc. Dalton Trans., 1985, 169.
51. Rivarola, E., Silvestri, A., Alonzo, G., Barbieri, R. and Herber, R.H., Inorg. Chim. Acta, 1985, 99, 87.
52. Molloy, K.C., Quill, K., Blunden, S.J. and Hill, R., Polyhedron, 1986, 5, (4), 959.

53. Wang, X., Liu, X., Xiao, L., Wang, Y., Yian, Q., Xia, Y., Wang, S., Acta. Chim. Sinica, 1986, 1, 29.
54. Donaldson, J.D., Grimes, S.M., Pellerito, L., Girasolo, M.A., Smith, P.J., Cambria, A. and Fama, M., Polyhedron, 1987, 3, 383.
55. Blunden, S.J. and Hill, R., Inorg. Chim. Acta., 1984, 87, 83.
56. Visalakshi, R., Jain, V.K., Kulshrestha, S.K., Rao, G.S., Inorg. Chim. Acta, 1986, 118, 119.
57. Davies, A.G., Price, A.J., Dawes, H.M. and Hursthouse, M.B., J. Chem. Soc. Dalton Trans., 1986, 297.
58. Sham, T.K. and Bancroft, G.M., Inorg. Chem., 1975, 14, 2281.
59. Sandhu, G.K., Gupta, R., Sandhu, S.S., Moore, L.S. and Parish, R.V., J. Organomet. Chem., 1986, 311, 281.
60. Blunden, S.J., Patel, B.N., Smith, P.J. and Sugavanam, B., Appl. Organomet. Chem., 1987, 1, 241.
61. Smith, P.J. and Bhagwati, P.N., Recl. Trav. Chim. Pay-Bas., 1988, 107, 167.
62. Bamgboye, T.T., Inorg. Chim. Acta, 1988, 145, 243.
63. Bamgboye, T.T. and Bamgboye, O.A., Inorg. Chim. Acta, 1988, 144, 249.
64. Molloy, K.C., Blunden, S.J. and Hill, R., J. Chem. Soc. Dalton Trans., 1988, 1259.
65. Kothiwal, A.S., Singh, A., Rai, A.K. and Mehrotra, R.C., Indian J. Chem., 1988, 27A, 507.
66. Allen, D.W., Brooks, J.S., Clarkson, R.W., Mellor, M.T.J. and Williamson, A.G., Chem. Ind., 1979, 663.
67. Allen, D.W., Brooks, J.S., Clarkson, R.W. and Mellor, M.T.J., J. Organomet. Chem., 1980, 199, 299.
68. Brooks, J.S., Clarkson, R.W. and Allen, D.W., J. Organomet. Chem., 1983, 243, 411.

69. Lagunov, V.A., Polozenko, V.I., Sinani, A.B. and Stepanov, V.A., Fiz. Tverd. Tela. (Leningrad), 1983, 25, (6), 186.
70. Allen, D.W., Bailey, S., Brooks, J.S. and Taylor, B.F., Chem. Ind., 1985, 826.
71. Allen, D.W., Brooks, J.S. and Unwin, J., Chem. Ind., 1985, 524.
72. Allen, D.W., Bailey, S. and Brooks, J.S., Chem. Ind., 1986, 62.
73. Bailey, S., PhD Thesis, 1987, Sheffield City Polytechnic.

3. Mößbauer Studies of Triorganotin Biocides in Hypalon Paint

3.1. Introduction

The samples of Hypalon paint containing biocides supplied by the Admiralty Research Establishment were not amenable to study by Mößbauer spectroscopy due to their very low tin content, containing only 0.2% w/w as the organotin in the wet paint. The work described in this chapter was carried out using samples prepared by incorporating a significantly greater amount of triorganotin agent into the paint.

A range of tri-n-butyltin- and triphenyltin- compounds has been incorporated into the paint at concentrations of 10% w/w respectively. The Mößbauer spectra of both wet and dry paint samples have been recorded for each biocide.

The Mößbauer data for the tri-n-butyltin studies are presented in Table 3.1.

Table 3.1 Mößbauer Data for Tri-n-Butyltin- Containing Hypalon Paints.

sample	phase	$\delta/$ mms ⁻¹	$\Delta E_Q/$ mms ⁻¹	$\Gamma_1/$ mms ⁻¹	$\Gamma_2/$ mms ⁻¹	%R.A.	ρ	χ^2
pure TBTO	Q1	1.21	1.52	1.18	1.18	100.0	1.3	1.2
pure TBTOAc	Q1	1.40	3.54	1.02	0.92	100.0	2.5	0.4
pure TBTCI	Q1	1.51	3.43	1.04	1.04	100.0	2.2	1.0
pure (TBTO) ₂ CO	Q1	1.39	2.68	1.04	1.04	60.0	1.9	0.4
	Q2	1.42	3.64	0.80	0.80	40.0	2.6	
wet paint/TBTO	Q1	1.21	1.80	1.40	1.40	64.1	1.5	0.5
	Q2	1.48	2.76	1.18	1.18	35.9	1.9	
wet paint/TBTOAc	Q1	1.45	3.62	1.04	1.04	100.0	2.5	0.3
wet paint/TBTCI	Q1	1.52	3.24	1.06	1.06	100.0	2.1	0.4
wet paint/ (TBTO) ₂ CO	Q1	1.39	2.72	1.04	1.04	61.3	2.0	0.4
	Q2	1.42	3.64	0.80	0.80	39.7	2.5	
dry paint/TBTO	Q1	1.30	1.70	1.36	1.36	11.0	1.3	0.3
	Q2	1.49	3.48	1.04	1.04	89.0	2.3	
dry paint/TBTOAc	Q1	1.39	3.44	1.06	1.06	100.0	2.5	0.5
dry paint/TBTCI	Q1	1.53	3.17	1.10	1.12	100.0	2.0	2.6
dry paint/ (TBTO) ₂ CO	Q1	1.39	2.70	1.00	1.00	50.3	1.9	0.3
	Q2	1.42	3.64	0.80	0.80	49.7	2.6	

1. All spectra recorded at 80K with an error of $\pm 0.02\text{mms}^{-1}$ for pure compounds and $\pm 0.05\text{mms}^{-1}$ for paint samples. Isomer shifts are relative to CaSnO_3 .

2. %R.A. is the relative area of each phase, *i.e.* quadrupole doublet.

3. $\rho = \Delta E_Q / \delta$.

4. TBTO is *bis*-(tri-n-butyltin) oxide,

TBTOAc is tri-n-butyltin acetate,

TBTCI is tri-n-butyltin chloride and

(TBTO)₂CO is *bis*-(tri-n-butyltin) carbonate.

3.2. Discussion of the Results of the Tri-n-Butyltin Study

3.2.1. Initial Studies of the Fate of *Bis*-(Tri-n-Butyltin) Oxide in Hypalon Paint

The Mößbauer spectrum of pure *bis*-(tri-n-butyltin) oxide consists of a single quadrupole doublet. Applying the Herber rule [1], ρ is 1.26 and thus *bis*-(tri-n-butyltin) oxide is a four-coordinate (*i.e.* discrete) molecule, as shown in Figure 3.1:

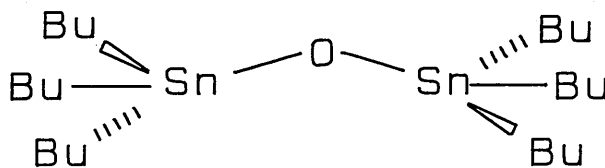


Figure 3.1 Structure of *Bis*-(Tri-n-Butyltin) Oxide in the Pure State.

(It is important to note that *bis*-(tri-n-butyltin) oxide as well as other compounds analyzed in this study by Mößbauer spectroscopy are liquid at 25°C. When the spectra are recorded at 80K the samples will be frozen liquids or solutions and the parameters will relate to the solid state not to the room temperature state. All the liquid samples were rapidly plunged into the liquid nitrogen to effect rapid freezing).

Initial studies of the *bis*-(tri-n-butyltin) oxide system were complicated by the ability of the organotin to absorb atmospheric carbon dioxide to form the carbonate, *bis*-(tri-n-butyltin) carbonate. This problem was overcome by warming the *bis*-(tri-n-butyltin) oxide to around 80°C and bubbling dinitrogen through the liquid for six hours.

The Mößbauer spectrum of the *bis*-(tri-*n*-butyltin) oxide in the wet paint suggested that two tin species were present. One was probably unreacted *bis*-(tri-*n*-butyltin) oxide, the other had parameters which did not correlate to any known literature values.

The Mößbauer spectrum of the related dried paint sample was initially fitted as one quadrupole doublet. (Figure 3.2(a)) However, when fitted as two doublets, χ^2 decreased from 0.5 to 0.3. (Figure 3.2(b))

It must be noted that the relative areas of absorption lines in Mößbauer spectra are not necessarily directly proportional to the concentration of the tin species. The area of any given phase depends on the recoil free fraction, f , of the tin nucleus, which may vary from compound to compound.

The major doublet has an isomer shift similar to that for tri-*n*-butyltin chloride. However, the quadrupole splitting, although similar to that of tri-*n*-butyltin chloride in the pure state, is much higher than that of tri-*n*-butyltin chloride in the dried paint.

The parameters of the other doublet, Q1, observed in the Mößbauer spectrum of the dried paint sample originally containing *bis*-(tri-*n*-butyltin) oxide are sufficiently different from those of the pure compound to suggest that a second new species has been formed. However, assignment of Q1 was not possible by comparison with literature values. Like *bis*-(tri-*n*-butyltin) oxide, this species would appear to be four-coordinate, (ρ 1.3), tin (IV).

A twelve hour Soxhlet extraction of approximately 2g of the dried paint sample in dichloromethane followed by ^{119}Sn NMR on the extract failed to detect any signals in the spectrum. A more exhaustive seven day Soxhlet extraction was then carried out on a 5g sample. The ^{119}Sn NMR spectrum of this extract exhibited two very weak signals at 155.6 ppm and -2.8 ppm (Figure 3.3). The former signal corresponds to tri-*n*-butyltin chloride, $\delta(^{119}\text{Sn})$ 153 ppm but the latter signal could not be identified. A possible candidate is mono-*n*-butyltin trichloride for which $\delta(^{119}\text{Sn})$ -3.0 ppm, in the pure state; when dissolved in carbon tetrachloride, $\delta(^{119}\text{Sn})$ 6.0 ppm [4].

The Mößbauer and ^{119}Sn NMR spectra correlate well, both indicating the presence of two new species in the dry paint, one of which is tri-n-butyltin chloride. It should also be noted that the ^{119}Sn NMR spectrum exhibited very weak signals.

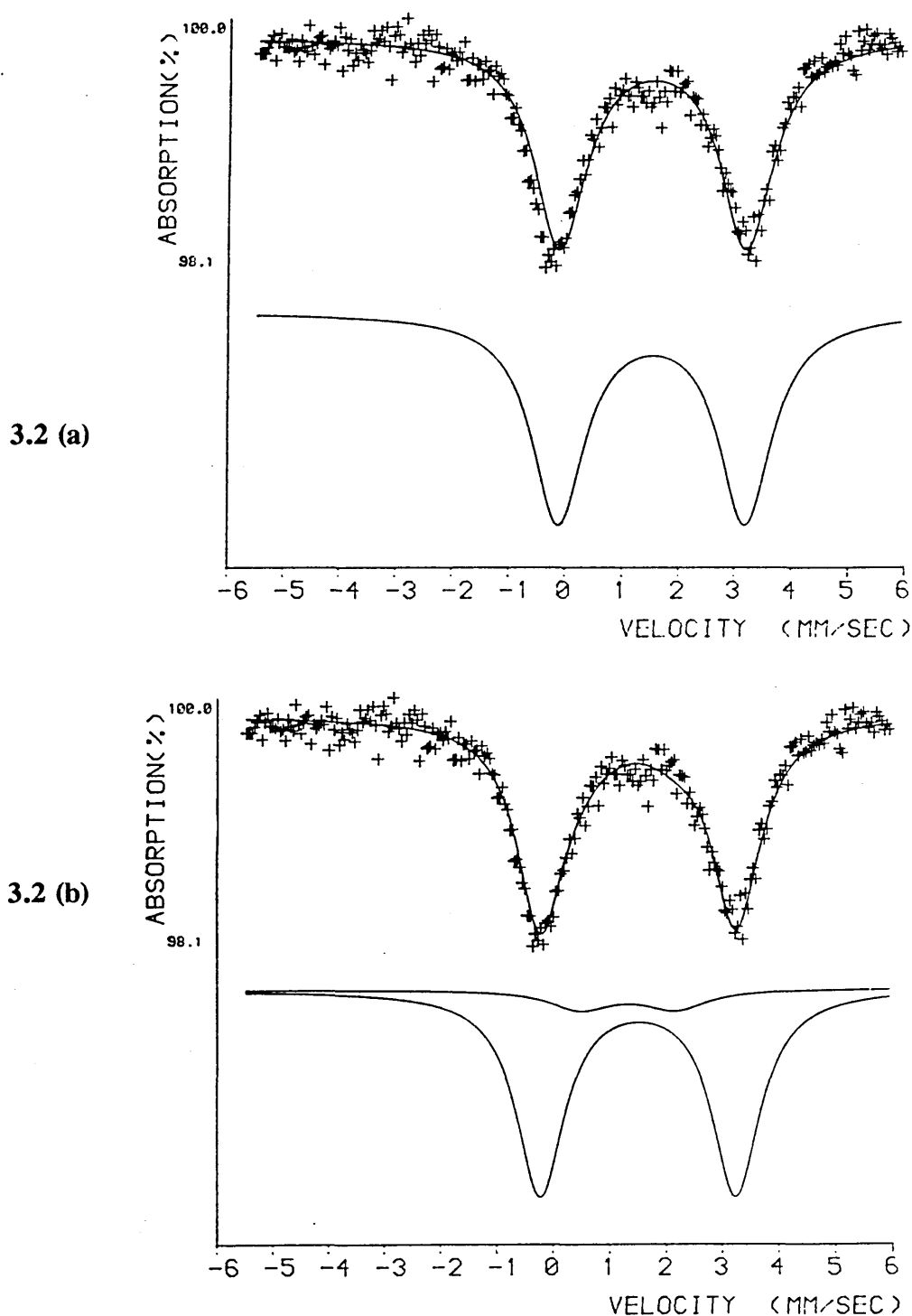


Figure 3.2 (a) Mößbauer Spectrum of Dry Hypalon Paint Originally Containing *Bis*-(Tri-n-Butyltin) Oxide, Fitted as One Doublet and 3.2 (b) as Two Doublets.

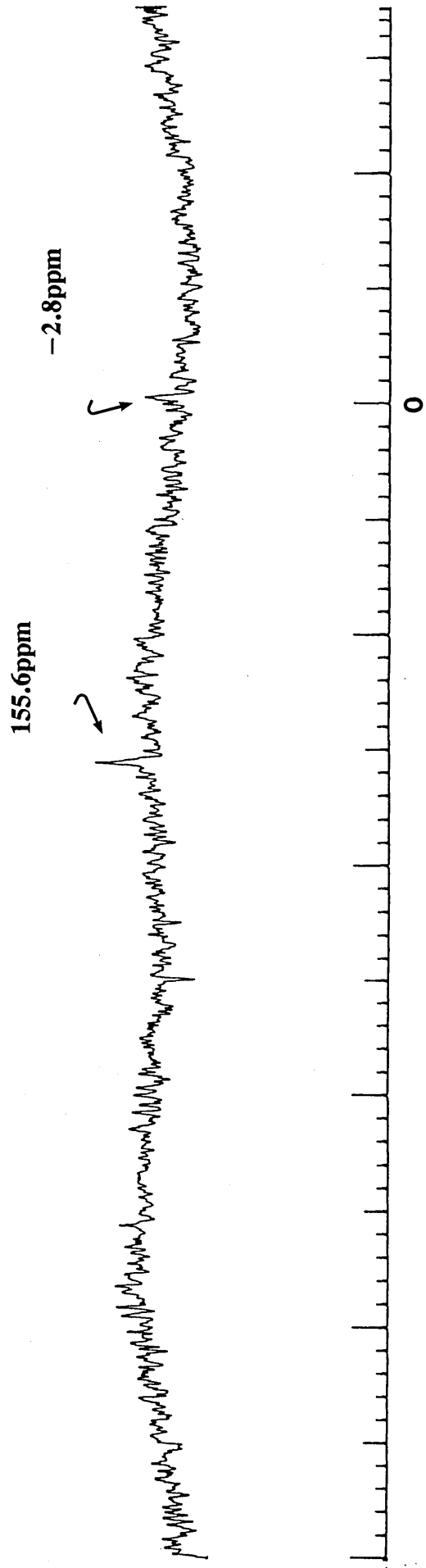
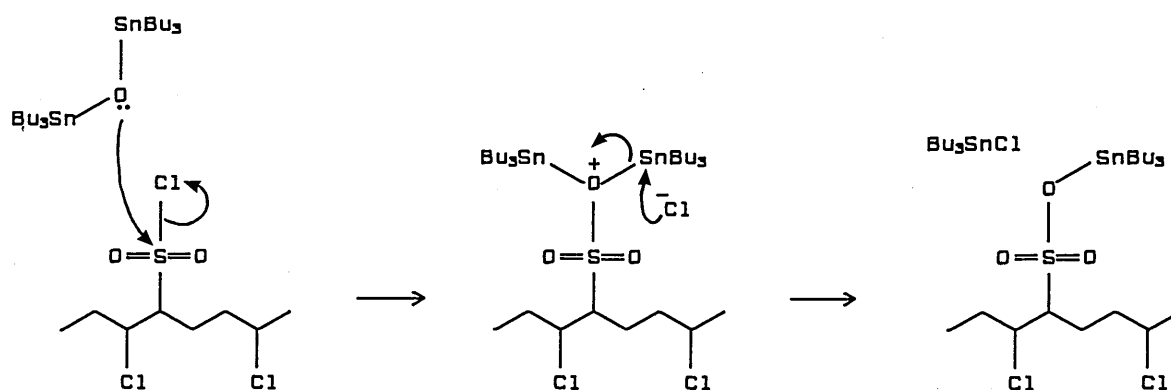


Figure 3.3 ^{119}Sn NMR Spectrum of the Soxhlet Extract of Dry Hypalon Paint Originally Containing *Bis*-(Tri-*n*-Butyltin) Oxide.

This in turn means that the organotin species present may be bound to the paint. Such binding is almost certain to reduce the organotin biocide release-rate from the paint and thus its efficiency as an antifouling coating. It was concluded, therefore, that *bis*-(tri-*n*-butyltin) oxide reacts with some component(s) of the paint to yield tri-*n*-butyltin chloride plus one other species, both likely to be bonded to the paint. In the pure state tri-*n*-butyltin chloride is five-coordinate with the dative bond being made by a lone pair from the chlorine of another tri-*n*-butyltin chloride molecule (Figure 3.6). It is not unreasonable to suggest that in the dried paint the fifth coordination site may be occupied by a polymer bound chlorine atom or chlorosulphonyl group. The intensity of the NMR signals would tend to suggest that such bonds are relatively strong. It is further suggested that *bis*-(tri-*n*-butyltin) oxide may in fact react with the chlorosulphonyl- side groups to yield tri-*n*-butyltin chloride, as suggested in Scheme 3.1;



Scheme 3.1 Proposed Scheme Between *Bis*-(Tri-*n*-Butyltin) Oxide and Hypalon Bound Chlorosulphonyl Groups.

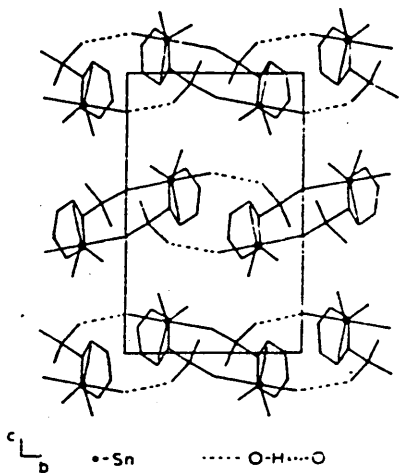


Figure 3.4 Structure of Trimethyltin Benzenesulphonate Monohydrate. [5]

It was therefore thought that the unidentified component, Q1, in the Mößbauer spectrum of the Hypalon paint originally containing *bis*-(tri-*n*-butyltin) oxide might be due to a sulphonate ester.

This possibility was examined in a series of model reactions, described in Section 3.5.

3.2.2. Initial Studies of the Fate of Tri-*n*-Butyltin Acetate in Hypalon Paint

The quadrupole splitting of pure tri-*n*-butyltin acetate is 3.54mms^{-1} and ρ 2.5, which is indicative of a five-coordinate tin structure. Using the partial quadrupole splitting, pqs, data from Bancroft's work [6], it was possible to calculate the theoretical quadrupole splitting if the *trans*- isomer (see Section 2.8.1):

$$\begin{aligned}
 [\text{OAc}]^{\text{tba}} &= +0.075\text{mms}^{-1} \text{ and } [\text{Bu}]^{\text{tbe}} = -1.13\text{mms}^{-1} \\
 \Delta E_{\text{Q}(\text{trans})} &= 2[\text{OAc}]^{\text{tba}} + 2[\text{OAc}]^{\text{tba}} - 3[\text{Bu}]^{\text{tbe}} \\
 &= \underline{3.60\text{mms}^{-1}}
 \end{aligned}$$

This is in good agreement with the observed value of 3.54mms^{-1} and it can be assumed that the fifth coordination site is occupied by a *trans*- intermolecular carbonyl oxygen—tin dative bond, see Figure 3.5:

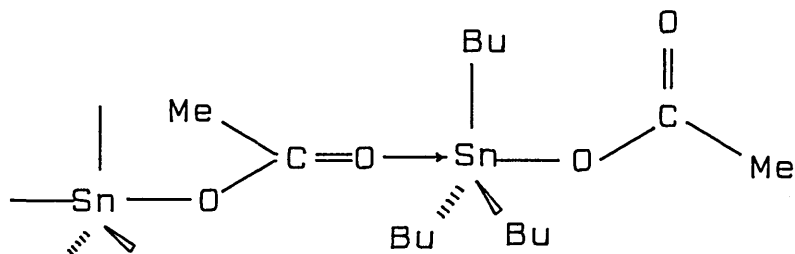


Figure 3.5 Intermolecular Bonding in Pure Tri-n-Butyltin Acetate.

The magnitude of the isomer shift for the tin species present in the wet and dry paint samples formulated with tri-n-butyltin acetate is the same as for the pure compound, within experimental error. However, the quadrupole splittings observed for the paint sample are different than for the pure compound. This may be due to a dilution effect, but the acetate is essentially unmodified.

3.2.3. Initial Studies of the Fate of Tri-n-Butyltin Chloride When Incorporated into Hypalon Paint

In the pure state, tri-n-butyltin chloride appears to have a five-coordinate intermolecularly associated polymeric structure (ρ 2.2). Bancroft's data enables the calculation of the pqs of the of the three possible structural isomers [5], as shown in Figure 3.6:

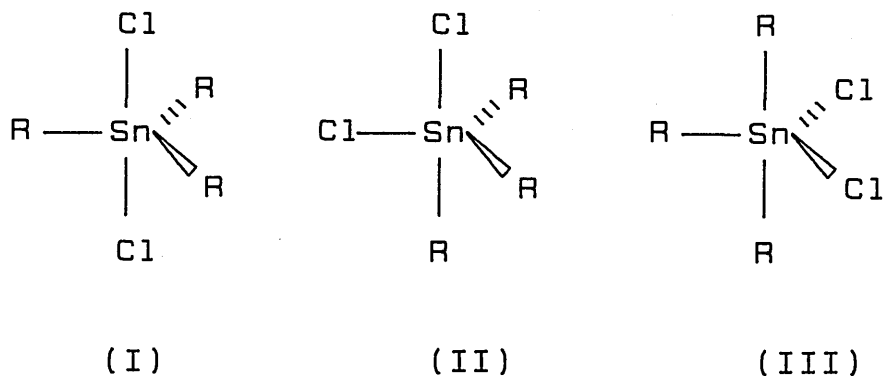


Figure 3.6 Structural Isomers of R_3SnCl_2 .

$$\Delta E_Q(\text{I}) = 2[\text{Cl}]^{\text{tba}} + 2[\text{Cl}]^{\text{tba}} - 3[\text{Bu}]^{\text{tbe}}$$

$$\Delta E_Q(\text{II}) \approx \frac{2[\text{Bu}]^{\text{tba}} - 8[\text{Bu}]^{\text{tbe}} + 2[\text{Cl}]^{\text{tba}} + 5[\text{Cl}]^{\text{tbe}}}{\sqrt{13}}$$

$$\Delta E_Q(\text{III}) \approx \frac{-8[\text{Bu}]^{\text{tba}} - [\text{Bu}]^{\text{tbe}} + 7[\text{Cl}]^{\text{tbe}}}{\sqrt{7}}$$

where:

$$[\text{Bu}]^{\text{tbe}} \text{ (trigonal bipyramidal equatorial)} = -1.13 \text{mms}^{-1}$$

$$[\text{Bu}]^{\text{tba}} \text{ (trigonal bipyramidal apical)} = -0.94 \text{mms}^{-1}$$

$$[\text{Cl}]^{\text{tbe}} \text{ (trigonal bipyramidal equatorial)} = +0.20 \text{mms}^{-1}$$

$$[\text{Cl}]^{\text{tba}} \text{ (trigonal bipyramidal apical)} = 0.00 \text{mms}^{-1}$$

this gives:

$$\Delta E_{Q(\text{I})} = 3.39 \text{mms}^{-1},$$

$$\Delta E_{Q(\text{II})} = 2.26 \text{mms}^{-1} \text{ and}$$

$$\Delta E_{Q(\text{III})} = 3.80 \text{mms}^{-1}.$$

In the pure state, the observed quadrupole splitting is 3.43mms^{-1} , which is in good agreement with the *trans*- isomeric structure.

In the wet and dry paint samples, the isomer shift of tri-n-butyltin chloride is the same as that in the pure state. In the wet paint spectrum, the quadrupole splitting is reduced which may be due to a dilution effect. Brooks *et al* [2] observed that when di-n-butyltin dichloride was incorporated into PVC at progressively lower concentrations the quadrupole splitting decreased. This was thought to be due to a change from a six- to a five-coordinate species. When tri-n-butyltin chloride was diluted in n-hexane ($0.19 - 3.00 \text{mol dm}^{-3}$ concentration range), no decrease in the quadrupole splitting was observed [3]. A range of tri-n-butyltin chloride solutions in petroleum spirit (boiling point $40 - 60^\circ\text{C}$) were prepared and their Mößbauer spectra were recorded, as shown in Table 3.2:

Table 3.2 Mößbauer Results of Tri-n-Butyltin Chloride Dilution Study.

	δ/mms^{-1}	$\Delta E_Q/\text{mms}^{-1}$
Pure tri-n-butyltin chloride	1.51	3.43
25% tri-n-butyltin chloride	1.50	3.36
10% tri-n-butyltin chloride	1.50	3.36
5% tri-n-butyltin chloride	1.51	3.40

All data recorded at 80K with an error of $\pm 0.05\text{mms}^{-1}$. Isomer shifts are relative to CaSnO_3 .

From these results it is evident that the dilution of tri-n-butyltin chloride in petroleum spirit does not reduce the quadrupole splitting. For comparison, a 10% w/w dilution of tri-n-butyltin chloride in graphite was also prepared. The Mößbauer spectrum of this sample revealed an isomer shift of 1.59mms^{-1} and a quadrupole splitting of 3.49mms^{-1} . Such deviations from the pure state parameters would tend to suggest that tri-n-butyltin chloride molecules may be involved in some type of bonding with the carbon layers in graphite, perhaps involving a π -interaction.

In the dried paint spectrum the quadrupole splitting was expected to increase from the value of 3.24mms^{-1} in the wet paint spectrum. However, this was not the case, the quadrupole splitting decreasing further to 3.17mms^{-1} . (The isomer shift is unchanged). The partial quadrupole splitting calculations show that the quadrupole splitting is very sensitive to structural isomerism. It is suggested that there may be a preferred orientation of tri-n-butyltin chloride within the paint which results in the lower than expected quadrupole splitting. It must be noted, however, that the tri-n-butyltin chloride formed from the *bis*-(tri-n-butyltin) oxide does not experience such a decrease in quadrupole splitting. This discrepancy cannot be readily accounted for.

A sample of the dried paint (approximately 5g) containing tri-n-butyltin chloride was Soxhlet extracted for seven days in an experiment similar to that performed in the *bis*-(tri-n-butyltin) oxide paint sample.

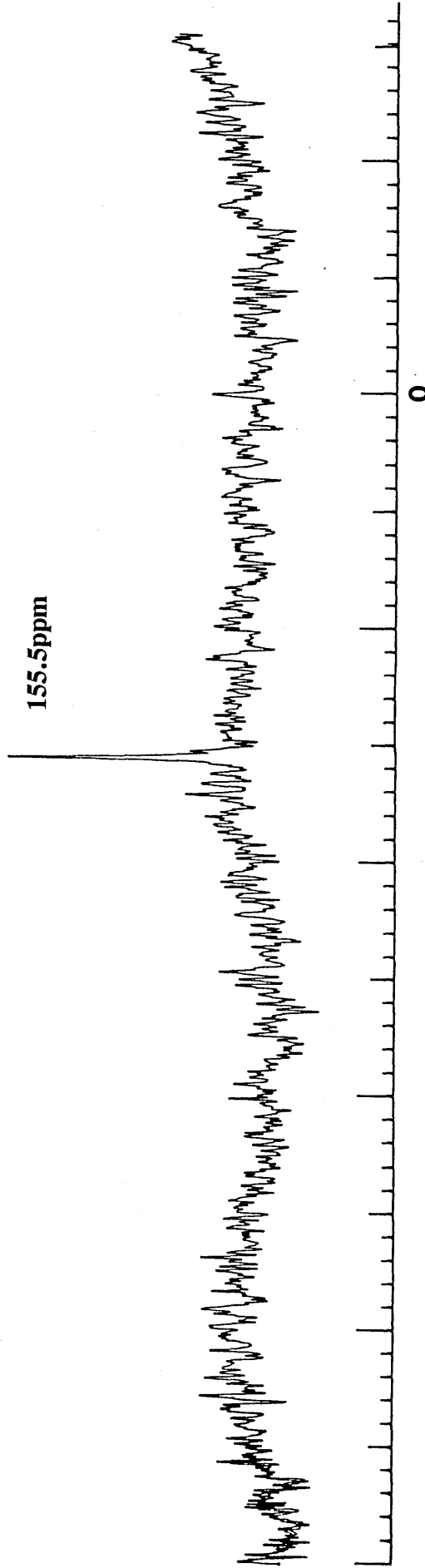


Figure 3.7 ^{119}Sn NMR Spectrum of the Soxhlet Extract of Dry Hypalon Paint Containing Tri-n-Butyltin Chloride.

The ^{119}Sn NMR spectrum of the extract was recorded and revealed one weak signal $\delta(^{119}\text{Sn})155.5$ ppm, consistent with tri-n-butyltin chloride, (Figure 3.7). The important feature to note is the rather low intensity of the signal, despite the fact that the tri-n-butyltin chloride has not reacted with Hypalon. As has already been suggested, some binding of the organotin appears to have occurred.

3.2.4. Initial Studies on the Fate of *Bis*-(Tri-n-Butyltin) Carbonate When Incorporated into Hypalon Paint

The Mößbauer spectrum of *bis*-(tri-n-butyltin) carbonate exhibits two unresolved doublets (Figure 3.8). Applying the Herber rule, ρ is 1.9 and 2.6 for Q1 and Q2, respectively. There are thought to be two distinct tin sites in pure *bis*-(tri-n-butyltin) carbonate, *i.e.* four- and five-coordinate tin atoms. The structure of the carbonate is probably polymeric since it is a highly viscous liquid.

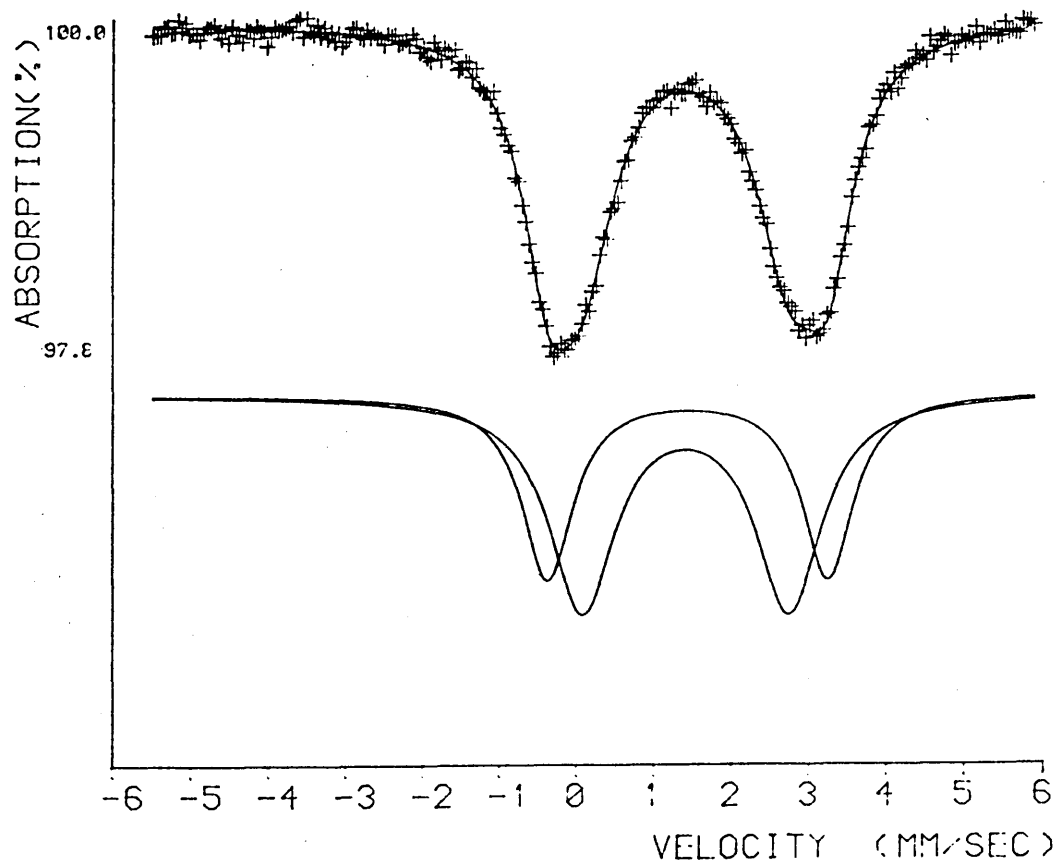


Figure 3.8 Mößbauer Spectrum of Pure *Bis*-(Tri-n-Butyltin) Carbonate.

When incorporated into Hypalon paint and during the subsequent drying process, it appears that *bis*-(tri-*n*-butyltin) carbonate is unchanged. There is, however, one anomaly. In the pure state and in the wet paint, the ratios of the two doublets are approximately 3:2, whereas in the dry paint the ratio is 1:1. This would indicate a higher proportion of five-coordinate tin sites in the latter or a different recoil-free fraction for the two tin sites in the different systems.

3.3. Discussion of the Results of the Triphenyltin Study

The incorporation of three triphenyltin compounds at a 10% w/w level in Hypalon paint was carried out and the resulting materials studied by Mößbauer spectroscopy. The results are shown in Table 3.3.

3.3.1. Initial Studies of the Fate of *Bis*-(Triphenyltin) Oxide In Hypalon Paint

In the pure state *bis*-(triphenyltin) oxide exists as a discrete four-coordinate moiety, [7] see Figure 3.9:

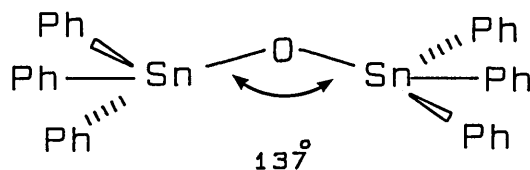


Figure 3.9 Structure of Pure *Bis*-(Triphenyltin) Oxide.

Table 3.3 Mößbauer Data for Triphenyltin- Containing Hypalon Paints.

sample	phase	$\delta/$ mms^{-1}	$\Delta E_Q/$ mms^{-1}	$\Gamma_1/$ mms^{-1}	$\Gamma_2/$ mms^{-1}	%R.A.	ρ	χ^2
pure TPTO	Q1	1.09	1.33	0.95	0.95	84.9	1.2	0.6
	Q2	1.16	2.66	1.13	1.13	15.1	2.3	
pure TPTOAc	Q1	1.27	3.26	1.00	1.00	100.0	2.6	0.8
pure TPTCl	Q1	1.33	2.56	0.97	0.97	100.0	1.9	0.5
wet paint/TPTO	Q1	1.10	1.43	1.30	1.30	57.4	1.3	0.5
	Q2	1.20	3.00	0.90	0.90	42.6	2.5	
wet paint/TPTOAc	Q1	1.27	3.26	1.07	1.07	100.0	2.6	0.6
wet paint/TPTCl	Q1	1.33	2.56	0.99	0.99	100.0	1.9	0.4
dry paint/TPTO	Q1	1.11	1.37	0.93	0.93	82.6	1.2	0.5
	Q2	1.52	2.49	1.03	1.03	13.8	1.6	
dry paint/TPTOAc	Q1	1.06	1.59	1.18	1.18	32.9	1.5	0.4
	Q2	1.26	3.29	0.90	0.90	67.1	2.6	
dry paint/TPTCl	Q1	1.06	1.60	1.22	1.22	25.9	1.5	0.6
	Q2	1.24	2.87	1.00	1.00	74.1	2.3	

1. All spectra recorded at 80K with an error of $\pm 0.02 \text{mms}^{-1}$ for pure compounds and $\pm 0.05 \text{mms}^{-1}$ for paint samples. Isomer shifts are relative to CaSnO_3 .

2. %R.A. is the relative area of each phase, *i.e.* quadrupole doublet.

3. $\rho = \Delta E_Q / \delta$.

4. TPTO is *bis*-(triphenyltin) oxide,

TPTOAc is triphenyltin acetate and

TPTCl is triphenyltin chloride.

A fresh batch of this compound was purchased from Aldrich for the study. When the spectrum was fitted as one doublet, χ^2 was 0.9, rather high for a pure compound. When refitted as two doublets, χ^2 was reduced to 0.5. The compound, specified as 97% pure, appeared to be contaminated with a five-coordinate species having ρ 2.3. By analogy with *bis*-(tri-*n*-butyltin) oxide, it was thought that the contaminant was likely to be *bis*-(triphenyltin) carbonate. In the Mößbauer spectrum of the wet paint, two quadrupole doublets were again present, with isomer shifts the same as those in the pure state. The quadrupole splittings were, however, greater in the wet paint, which cannot be readily accounted for. In the dry paint, the major doublet is due to unreacted *bis*-(triphenyltin) oxide. (This compound is a weaker Lewis base than *bis*-(tri-*n*-butyltin) oxide and hence is less likely to react with the chlorosulphonyl groups on the polymer.) The second compound could not be identified by its Mößbauer parameters.

When the dried paint was extracted overnight in dichloromethane and the ^{119}Sn NMR spectrum was recorded two weak signals were apparent, $\delta(^{119}\text{Sn})$ -8.9 and -83.9 ppm respectively (1:3 integral ratio). The literature value for *bis*-(triphenyltin) oxide is $\delta(^{119}\text{Sn})$ -80.6 ppm [4] which is in good agreement with $\delta(^{119}\text{Sn})$ -83.9 ppm. The only other triphenyltin compound with a similar chemical shift is triphenyltin hydroxide, $\delta(^{119}\text{Sn})$ -86.0 ppm, though its formation is difficult to account for. Assignment of the -8.9 ppm signal could not be made from the available literature.

3.3.2. Initial Studies of the Fate of Triphenyltin Acetate in Hypalon

Paint

X-ray studies on Ph_3SnX species, where X is an acetate group, have shown that they are five-coordinate polymers in the pure state [8,9,10]. Using data from Bancroft *et al* [6], the quadrupole splitting of the *trans*- structural isomer was calculated to be 3.24mms^{-1} , which is in close agreement with the observed value of 3.26mms^{-1} .

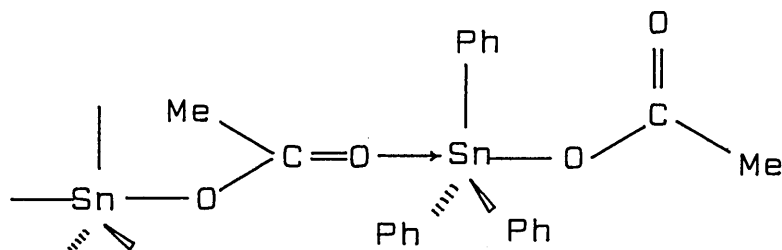


Figure 3.10 Structure of Triphenyltin Acetate in the Pure State.

In the wet paint, the Mößbauer parameters suggest that unreacted triphenyltin acetate is present. The quadrupole splitting does not decrease, suggesting that the intermolecular dative carbonyl—tin bond is relatively strong.

In the dry paint, the major doublet corresponds to unreacted triphenyltin acetate, the less intensive doublet having parameters which do not correspond closely to known triphenyltin values in the literature.

The ^{119}Sn NMR spectrum of the paint extract was devoid of signals. This may be due to binding of the organotins to the paint, or the fact that triphenyltin compounds are rather insoluble in dichloromethane.

3.3.3. Initial Studies of the Fate of Triphenyltin Chloride in Hypalon

Paint

The structure of triphenyltin chloride has been determined by X-ray crystallography [11]. The molecules are discrete, with a slightly distorted tetrahedral geometry about the tin atom. The Mößbauer spectrum of triphenyltin chloride confirms this finding ($\rho 1.9$).

As with triphenyltin acetate, triphenyltin chloride is unchanged in the wet paint. However, again in the dry paint, as with triphenyltin acetate, some chemical changes appear to have occurred. There does not appear to be any unreacted triphenyltin chloride present. In fact there are two new species, one of which has parameters which correspond to those of the unknown in the dry paint

spectrum of triphenyltin acetate. The other doublet, which was expected to be due to triphenyltin chloride, has parameters which do not correlate well with any known triphenyltin values in the literature.

The ^{119}Sn NMR spectrum of the dichloromethane extract of the dried paint exhibited a weak signal at $\delta(^{119}\text{Sn}) -45.5$ ppm, comparable with the literature value of triphenyltin chloride $\delta(^{119}\text{Sn}) -48.0$ ppm [4]. This discrepancy is difficult to account for and highlights the difficulties which can arise in correlating Mößbauer and NMR data.

3.4. Conclusions from Initial Studies of the Fate of Triorganotin Compounds in Hypalon Paint

3.4.1. The Fate of Tri-n-Butyltin Compounds in Hypalon Paint

The addition of *bis*-(tri-n-butyltin) oxide, tri-n-butyltin acetate, tri-n-butyltin chloride and *bis*-(tri-n-butyltin) carbonate to Hypalon paint causes modification of the four compounds to varying extents. *Bis*-(tri-n-butyltin) oxide is entirely converted into two new species, one identified as tri-n-butyltin chloride from the Mößbauer data and confirmed by ^{119}Sn NMR spectroscopy. The second component could not be readily identified, but was thought to be a tri-n-butyltin sulphonate ester.

The low concentrations of tin species in the extract studied by ^{119}Sn NMR spectroscopy indicated that the tin compounds are becoming bound to the paint in some way. This also appeared to be the case in the tri-n-butyltin chloride containing paint sample. If such binding is occurring, then the release rates of the organotin may well be affected.

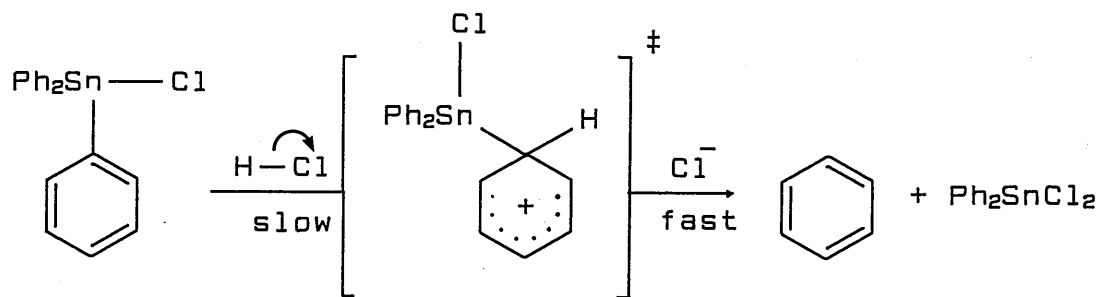
The reaction of the *bis*-(tri-n-butyltin) oxide with pendant chlorosulphonyl groups on the Hypalon polymer (as suggested in Scheme 3.1) would lead to a polymer bound tin sulphonate ester and tri-n-butyltin chloride. Such a reaction would correlate well with the observed data. Consequently, a series of model reactions was carried out to explore this possibility (Section 3.5).

The other three tri-*n*-butyltins are not chemically changed to new organotin species, but it would appear that their structure/coordination chemistry at tin is different in the paint from that in the pure state.

3.4.2. The Fate of Triphenyltin Compounds in Hypalon Paint

In general, the results from the triphenyltin studies are more complex than those of the tri-*n*-butyltin work. Like *bis*-(tri-*n*-butyltin) oxide, *bis*-(triphenyltin) oxide appears to be contaminated in the neat state (perhaps by the carbonate). Unlike *bis*-(tri-*n*-butyltin) oxide, however, *bis*-(triphenyltin) oxide seems unchanged on incorporation into Hypalon paint. This may be due, as already stated, to its weaker Lewis base characteristics. The contaminant in *bis*-(triphenyltin) oxide readily reacts with the paint to form a four-coordinate organotin (IV) species.

Similarities exist between the behaviour of triphenyltin acetate and triphenyltin chloride. Both are unmodified in the wet paint, it is during or after solvent evaporation when reactions seem to occur, as evidenced by the appearance of two quadrupole doublets in the Mößbauer spectrum in each case. The second component in the former is unchanged triphenyltin acetate. It was noted from work by Bailey [3], that triphenyltin compounds readily undergo dephenylation in the presence of halogen acids and halocarbons, *e.g.* neoprene (Scheme 3.3):



Scheme 3.3 Protodestannylation of Triphenyltin Chloride with HCl.

Since the polymer contains many chloro– side groups, it is not unreasonable to suggest that some dephenylation may occur in Hypalon paint. The Mößbauer parameters of the di- and monophenyltin chlorides are shown in Table 3.4.

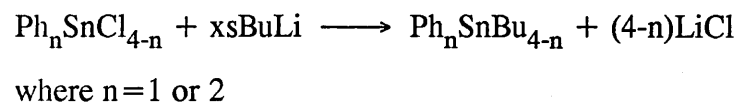
Table 3.4 Mößbauer Data for Di- and Monophenyltin Chlorides in the Pure State.

	δ/mms^{-1}	$\Delta E_Q/\text{mms}^{-1}$
Ph_2SnCl_2	1.37	2.86
PhSnCl_3	1.10	1.75

All data recorded at 80K relative to a BaSnO_3 source with an experimental error of $\pm 0.02\text{mms}^{-1}$ [3].

If these parameters are compared to those of the two doublets in the dry paint sample originally containing the triphenyltin chloride a reasonable match is observed. To confirm the identity of the two species as the di- and monophenyltin moieties a derivatization/extraction experiment was performed.

The paint sample was refluxed for four hours with butyllithium:



Reaction 3.1 Derivatization of Phenyltins.

The resulting stannanes should be soluble in ether and thus should be released from the paint. The authentic stannanes were made from butyllithium and the di- and monophenyltin chlorides. All the samples were then analysed by GC under the following conditions:

Column: 3% OV-1 Chromosorb WHP 80/100 mesh
Carrier: N₂ at 20 mlmin⁻¹
Injection Temp: 350°C **Detector Temp:** 350°C

	1	2
Oven temp/°C	210.0	230.0
Iso time/min	1.5	0.5
Ramp rate/°Cmin ⁻¹	20.0	20.0

Chromatograms are shown in Figure 3.11. The monophenyltin stannane has a t_R of 1.33 min, the diphenyltin stannane has a t_R of 2.38 min. The chromatogram of the Hypalon extract is surprisingly uncomplicated, but contains an obvious major product *i.e.* the monophenyltin butylstannane. There is also a trace of the diphenyltin stannane present.

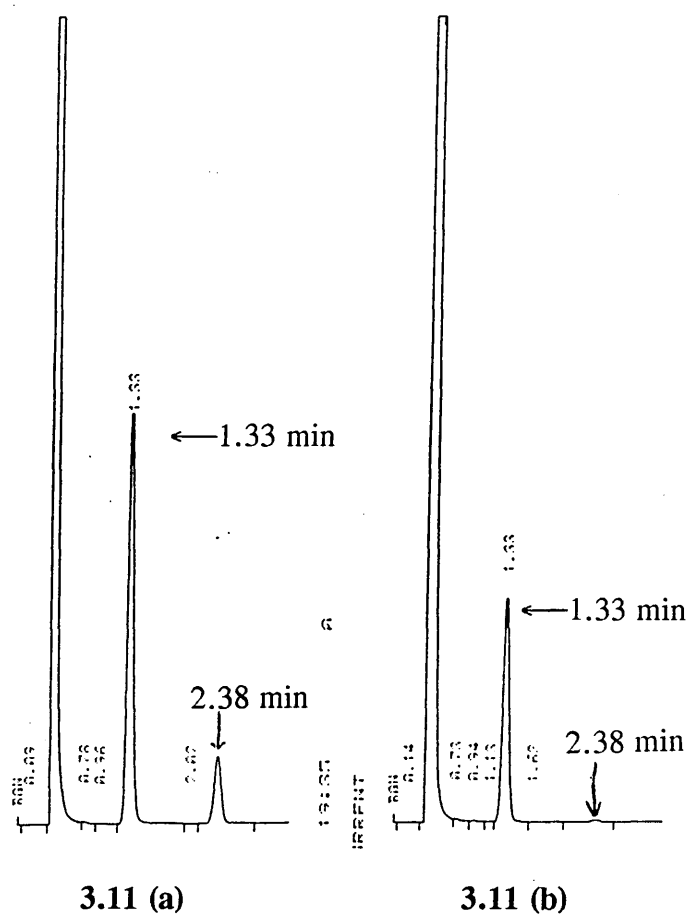


Figure 3.11 (a) Gas Chromatogram of the Di-n-Butyldiphenyltin and Tri-n-Butylphenyltin Standards and 3.11 (b) Extract of Butylated Hypalon Paint Originally Containing Triphenyltin Chloride.

The results of this experiment confirm that on incorporation into the Hypalon paint, triphenyltin chloride is converted to the di- and monophenyltin chlorides. Further, the second component in the spectrum of dry paint sample originally containing triphenyltin acetate is monophenyltin trichloride.

In the neoprene system *bis*-(triphenyltin) oxide as well as triphenyltin chloride and triphenyltin acetate was dephenylated, with the full range of breakdown products identified. In the Hypalon system dephenylation has not occurred to such a great extent. This may be rationalised simply by comparing the incorporation methods. While in the paint drying occurs at room temperature, the neoprenes are cured at 150°C which promotes the formation of hydrogen chloride. The reaction shown in Scheme 3.2 will proceed more vigorously with hydrogen chloride at 150°C than with chloro- side groups on a polyethene chain at 20°C.

3.5. Model Reactions of Tri-*n*-Butyltin and Triphenyltin Biocides with Sulphonyl Chlorides

3.5.1. Introduction

These reactions were carried out with two aims. The first was to identify the unknown species in the spectrum of the Hypalon sample originally containing *bis*-(tri-*n*-butyltin) oxide. The second was academic interest as no literature has been published in this area. Both tri-*n*-butyltins and triphenyltins were studied. Methanesulphonyl chloride and benzenesulphonyl chloride were readily available and were used in this study. All reactions were carried out under reflux conditions in chloroform for one hour (see Section 3.9 for full experimental details).

The Mößbauer data for the reaction products are shown in Table 3.5.

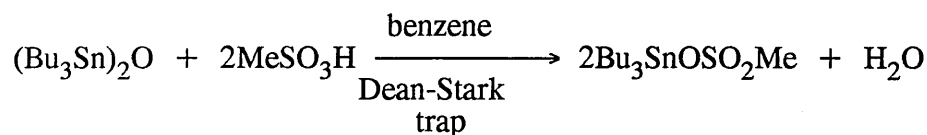
**Table 3.5 Mößbauer Data for the Products of the Triorganotin/
Sulphonyl Chloride Model Reactions.**

sample	phase	$\delta/$ mms^{-1}	$\Delta E_Q/$ mms^{-1}	$\Gamma_1/$ mms^{-1}	$\Gamma_2/$ mms^{-1}	%R.A.	ρ	χ^2
TBTO/MeSO ₂ Cl	Q1	1.36	1.02	0.99	0.98	19.1	0.8	0.6
	Q2	1.49	3.30	1.08	1.04	48.8	2.2	
	Q3	1.54	4.24	0.89	0.86	32.1	2.8	
TBTCI/MeSO ₂ Cl	Q1	1.51	3.39	1.12	1.12	100.0	2.3	0.6
TBTO/PhSO ₂ Cl	Q1	1.50	2.63	1.04	1.06	100.0	1.8	0.7
TBTCI/PhSO ₂ Cl	Q1	1.53	3.41	1.02	1.00	100.0	2.2	0.7
TPTO/MeSO ₂ Cl	S1	1.44		1.20		13.6		0.5
	Q1	1.28	2.60	0.98	1.00	61.1	2.0	
	Q2	1.38	4.00	0.88	1.06	25.3	2.9	
TPTCI/MeSO ₂ Cl	Q1	1.32	2.52	0.94	0.93	100.0	1.9	0.5
TPTO/PhSO ₂ Cl #1	Q1	1.23	3.61	0.85	0.99	45.5	2.9	1.0
	Q2	1.49	3.80	1.63	0.80	54.5	2.6	
TPTO/PhSO ₂ Cl #2	Q1	1.26	2.68	1.26	1.36	100.0	2.1	0.5
TPTO/PhSO ₂ Cl #2	Q1	1.26	2.68	1.26	1.36	100.0	2.1	0.5
#1 grd. graphite	Q1	1.33	3.80	0.98	1.02	100.0	2.9	0.7
#2 grd. graphite	Q1	1.24	2.74	1.06	1.15	100.0	2.2	1.4
TPTCI/PhSO ₂ Cl	Q1	1.30	2.50	1.08	0.94	100.0	1.9	0.5

1. All spectra recorded at 80K with an error of $\pm 0.05 \text{mms}^{-1}$. Isomer shifts are relative to CaSnO₃.
2. %R.A. is the relative area of each phase, *i.e.* quadrupole doublet or singlet.
3. $\rho = \Delta E_Q / \delta$.
4. TBTO and TPTO are *bis*-(tri-*n*-butyltin)- and *bis*-(triphenyltin) oxide,
5. TBTCI and TPTCI are tri-*n*-butyltin- and triphenyltin chloride and
6. MeSO₂Cl and PhSO₂Cl are methane- and benzenesulphonyl chloride.
7. grd. graphite \rightarrow samples ground with graphite prior to analysis.

3.5.2. The Reaction Between *Bis*-(Tri-*n*-Butyltin) Oxide and Methanesulphonyl Chloride

1:2 mol equivalents of the organotin and the sulphonyl chloride were heated together in chloroform. The product was a clear liquid, the Mößbauer spectrum of which consisted of three unresolved doublets (Figure 3.12(a)). The second doublet, Q2, had parameters which matched those of tri-*n*-butyltin chloride. The third doublet, Q3, had a large quadrupole splitting, with ρ 2.8, indicative of a highly coordinated tin site. This was thought to be the methanesulphonate ester of tri-*n*-butyltin. In order to confirm the identity of Q3 as the sulphonate ester, the compound was prepared by the reaction of *bis*-(tri-*n*-butyltin) oxide with methanesulphonic acid in benzene. The liberated water was removed by a Dean-Stark trap (Reaction 3.2).



Reaction 3.2 Azeotropic Formation of the Methanesulphonate Ester of Tri-*n*-Butyltin.

The product was a viscous, clear liquid with an unpleasant odour (common to all the sulphonate esters synthesized in this study). Microanalytical data supported the formation of the sulphonate ester.

The Mößbauer parameters are presented in Table 3.6. The quadrupole splitting and ρ values are of the order expected, but differ from Q3 for the *bis*-(tri-*n*-butyltin) oxide/methanesulphonyl chloride reaction product by more than experimental error.

The ^{119}Sn NMR spectrum of the sulphonyl chloride reaction product exhibited two signals, $\delta(^{119}\text{Sn})$ 121.2 and -8.2 ppm (N.B. no signal at $\delta(^{119}\text{Sn})$ 155 ppm due to tri-*n*-butyltin chloride), whereas the sulphonic acid reaction product

exhibited a single peak, $\delta(^{119}\text{Sn})$ 68.7 ppm. These data would tend to suggest that the methanesulphonate ester of tri-*n*-butyltin is not formed during the reaction between *bis*-(tri-*n*-butyltin) oxide and methanesulphonyl chloride.

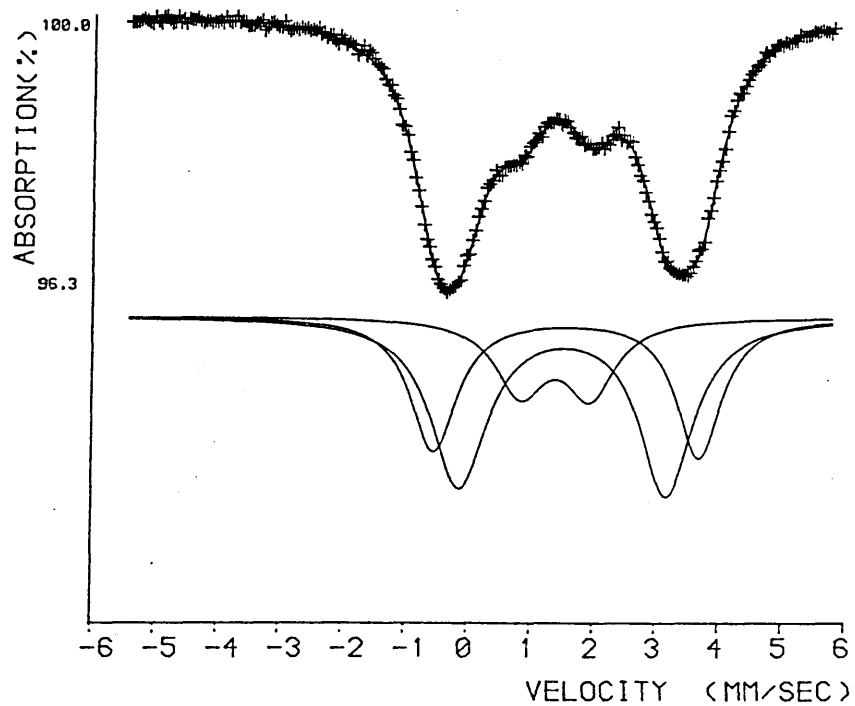
Table 3.6 Mößbauer Data for the Products of the Triorganotin Oxide/Sulphonic Acid Reactions.

sample	phase	$\delta/$ mms^{-1}	$\Delta E_Q/$ mms^{-1}	$\Gamma_1/$ mms^{-1}	$\Gamma_2/$ mms^{-1}	%R.A.	ρ	χ^2
TBTO/MeSO ₃ H	Q1	1.62	4.44	1.00	0.98	100.0	2.7	2.8
TBTO/PhSO ₃ H	Q1	1.64	4.48	0.98	0.98	100.0	2.7	1.1
TPTO/MeSO ₃ H	S1	0.01		1.32		5.2		
	Q1	1.04	1.07	0.88	1.66	11.7	1.0	2.4
	*Q2	1.45	4.16	0.92	1.20	83.1	2.9	
TPTO/PhSO ₃ H	S1	-0.02		1.60		17.2		
	Q1	1.15	2.18	1.13	0.82	5.8	1.9	11.3
	*Q2	1.47	4.19	1.09	1.35	77.0	2.9	

1. All spectra recorded at 80K with an error of $\pm 0.02\text{mms}^{-1}$. Isomer shifts are relative to CaSnO₃.
2. %R.A. is the relative area of each phase, *i.e.* quadrupole doublet or singlet.
3. $\rho = \Delta E_Q / \delta$.
4. TBTO and TPTO are *bis*-(tri-*n*-butyltin)- and *bis*-(triphenyltin) oxide,
5. TBTCI and TPTCI are tri-*n*-butyltin- and triphenyltin chloride and
6. MeSO₂H and PhSO₂H are methane- and benzenesulphonic acid.
7. The products of the TPTO reactions were ground with graphite prior to their spectra being recorded.
8. *Q2 These phases were also fitted using the PQH program.

It should be noted that one of the signals in the ¹¹⁹Sn NMR spectrum of the product of the sulphonyl chloride reaction ($\delta(^{119}\text{Sn})$ -8.2 ppm) is similar to that observed in the extract of Hypalon paint originally containing *bis*-(tri-*n*-butyltin) oxide ($\delta(^{119}\text{Sn})$ -2.8 ppm).

3.12 (a)



3.12 (b)

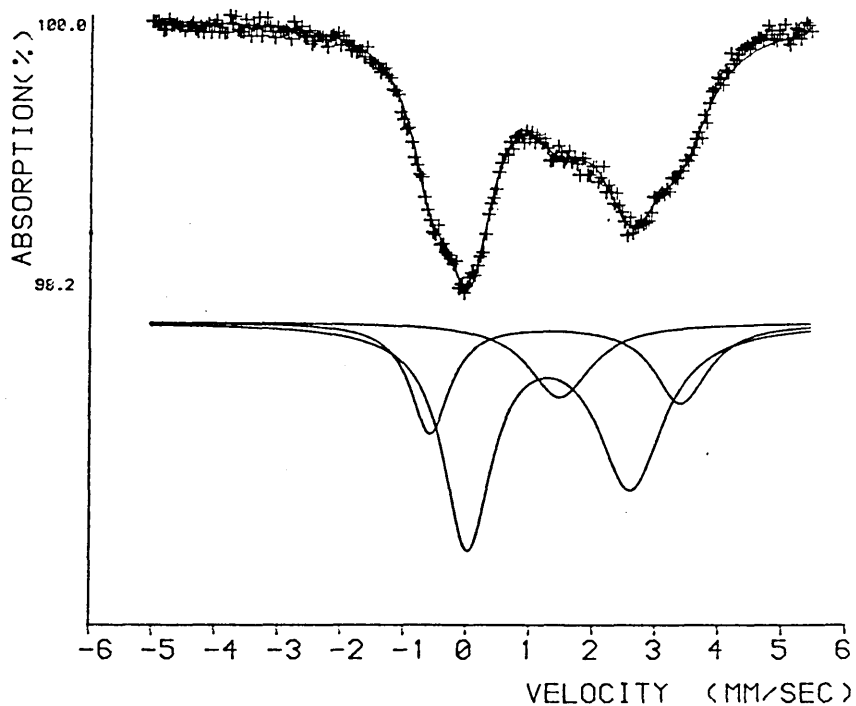


Figure 3.12 (a) Mössbauer Spectrum of the Product from the Reaction of *Bis*-(Tri-*n*-Butyltin) Oxide with Methanesulphonyl Chloride and 3.12 (b) Mössbauer Spectrum of the Product from the Reaction of *Bis*-(Triphenyltin) Oxide with Methanesulphonyl Chloride.

The presence of the third doublet in the sulphonyl chloride reaction product (Q1) should perhaps correspond to unreacted *bis*-(tri-*n*-butyltin) oxide, however the parameters of the doublet do not confirm this and identification of Q1 could not be made by comparison with literature values.

3.5.3. The Reaction Between Tri-*n*-Butyltin Chloride and Methanesulphonyl Chloride

Equimolar amounts of tri-*n*-butyltin chloride and methanesulphonyl chloride were heated together in chloroform. This experiment was carried out as a control, no reaction being expected. The product was a clear liquid whose Mößbauer and ^{119}Sn NMR parameters were the same as those of pure tri-*n*-butyltin chloride. Thus, no reaction occurs between these two substances.

3.5.4. The Reaction Between *Bis*-(Tri-*n*-Butyltin) Oxide and Benzenesulphonyl Chloride

1 mol equivalent of *bis*-(tri-*n*-butyltin) oxide was heated in chloroform with 2 mol equivalents of benzenesulphonyl chloride. The product was a viscous liquid whose Mößbauer spectrum consisted of a single quadrupole doublet. The parameters (ρ 1.8) suggest the formation of a four-coordinate species, *i.e.* not the benzenesulphonyl ester of tri-*n*-butyltin.

The authentic sulphonate ester was synthesized for comparison as in Reaction 3.1, with benzenesulphonic acid replacing methanesulphonic acid. The product was a pale pink liquid, less viscous than the methanesulphonate ester, but with very similar Mößbauer parameters (Table 3.6). Microanalytical data on the product confirmed that the benzenesulphonate ester has been synthesized.

The ^{119}Sn NMR spectrum of the benzenesulphonyl chloride reaction product exhibited two signals $\delta(^{119}\text{Sn})$ 125.5 and -11.2 ppm, *i.e.* very similar to that of the methanesulphonyl chloride reaction product. The ^{119}Sn NMR spectrum of the benzenesulphonic acid reaction product exhibited a single peak $\delta(^{119}\text{Sn})$ 80.8 ppm.

It is evident that the reaction between *bis*-(tri-*n*-butyltin) oxide and methane- or benzenesulphonyl chloride does not lead to the formation of the respective sulphonate ester, as was expected. The products of the reaction are the result of a mechanism not yet understood.

3.5.5. The Reaction Between Tri-*n*-Butyltin Chloride and Benzenesulphonyl Chloride

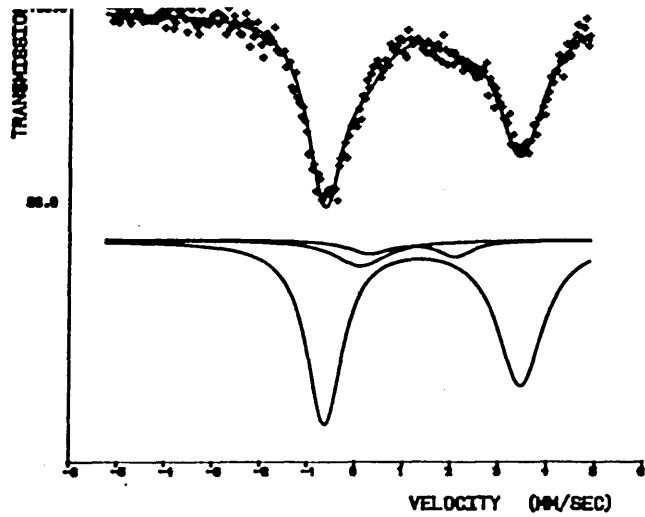
Equimolar quantities were heated under reflux conditions in chloroform. The product was a clear liquid whose Mößbauer and ^{119}Sn NMR parameters are consistent with the presence of tri-*n*-butyltin chloride. No reaction has, therefore, occurred between these substances.

3.5.6. The Reaction Between *Bis*-(Triphenyltin) Oxide and Methanesulphonyl Chloride

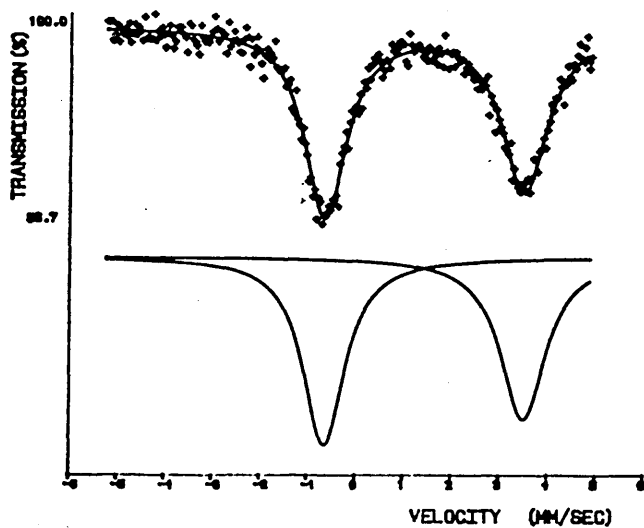
1 mol equivalent of *bis*-(triphenyltin) oxide and 2 mol equivalents of methanesulphonyl chloride were combined under reflux conditions in chloroform. The product of the reaction was a white solid, the Mößbauer spectrum of which consisted of a singlet and two quadrupole doublets (Figure 3.12(b)). The singlet has an isomer shift of 1.44mms^{-1} , the closest match being triphenyltin hydride, $\delta 1.39\text{mms}^{-1}$ [12], though it is difficult to account for the formation of the hydride in this reaction.

Q1 in the spectrum may be expected to correspond to triphenyltin chloride, but the parameters differ from those of pure triphenyltin chloride by more than experimental error. The cause of this discrepancy may be due to the product being an intimate mixture of three organotin species. The second quadrupole doublet, Q2, has a large quadrupole splitting of 3.75mms^{-1} , ($\rho 2.9$), indicative of a highly coordinated structure expected for the methanesulphonate ester of triphenyltin. The ^{119}Sn NMR spectrum of the mixture of products in d_6 -DMSO exhibited two broad signals, $\delta(^{119}\text{Sn}) -237.5$ and -255.2 ppm (*cf.* triphenyltin chloride $\delta(^{119}\text{Sn}) -224$ ppm).

3.13 (a)



3.13 (b)



3.13 (c)

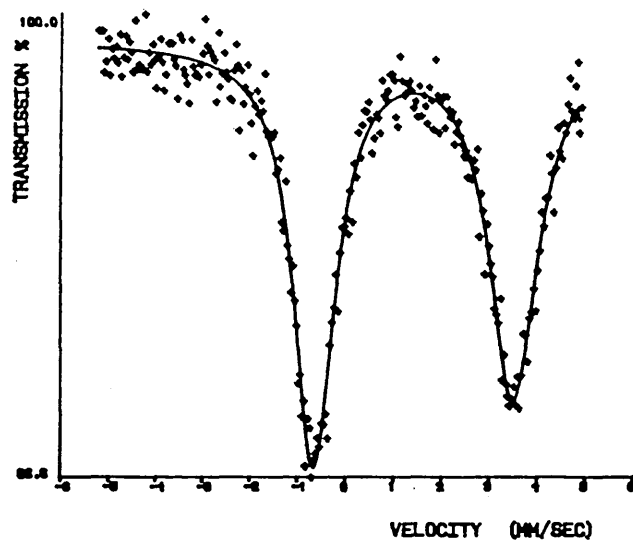
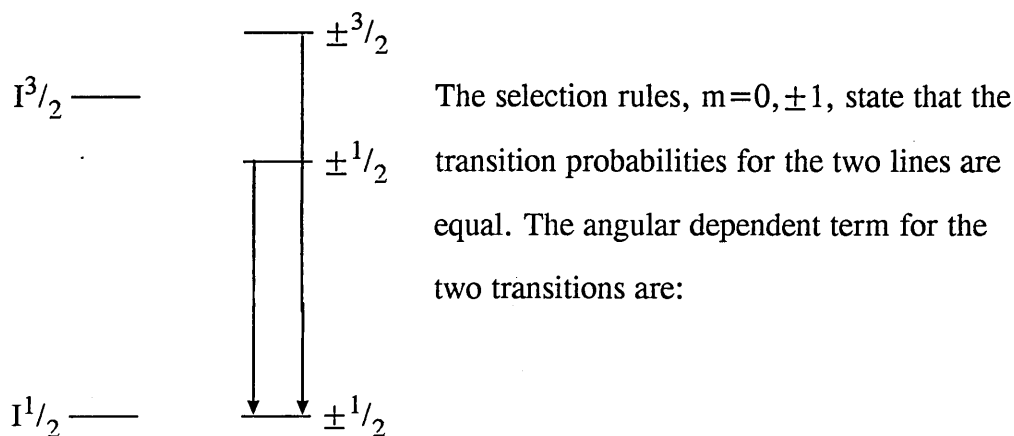


Figure 3.13 (a) Mössbauer Spectrum of the Product Containing the Methanesulphonate Ester of Triphenyltin (Q2) Ground with Graphite; 3.13 (b) Q2 from the above Spectrum Fitted as Two Singlets and (c) Q2 Fitted as One Doublet, note the Considerable Line Asymmetry.

The authentic sulphonate ester was synthesized from *bis*-(triphenyltin) oxide and methanesulphonic acid *via* Reaction 3.2. The product was a grey-white solid which melted at 275-280°C (*bis*-(triphenyltin) oxide m.p. 119-123°C).

The Mößbauer spectrum of the authentic sulphonate ester suggests that three species are present, one singlet and two doublets (Figure 3.13(a)). The singlet is probably due to a trace of tin (IV) oxide and Q1, unreacted *bis*-(triphenyltin) oxide or perhaps some dephenylation product. The major doublet Q2 was thought to arise from the sulphonate ester. Q2 showed line asymmetry, even when ground with alumina or graphite, (Figures 3.13 (b) and (c)), (S1 and Q1 have been subtracted for clarity). Possible sources of line asymmetry were mentioned in Chapter 2, *viz* partial orientation of crystalites or anisotropic recoilless radiation, the Gol'danskii-Karyagin effect.

The Gol'danski-Karyagin effect has its origins in the nuclear transitions, for tin, from the $I=3/2$ excited state to the $I=1/2$ ground state.



$$\begin{array}{lll} T_{1/2} & \pm 1/2 & \longrightarrow \pm 1/2 & 2 + 3\sin^2\theta \\ T_{3/2} & \pm 3/2 & \longrightarrow \pm 1/2 & 3(1 + \cos^2\theta) \end{array}$$

For a single crystal, the ratio $(2 + 3\sin^2\theta)/3(1 + \cos^2\theta)$ will be dependent upon θ . For a polycrystalline sample, however, the angular dependent terms are integrated over all angles:

$$\text{ratio} = \frac{\int_0^\pi T_{3/2} \sin\theta d\theta}{\int_0^\pi T_{1/2} \sin\theta d\theta} = 1$$

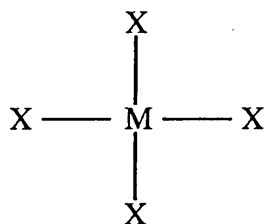
This means that for a randomly orientated polycrystalline sample the relative intensities for the two lines are unity.

The recoil free fraction, f , is given by:

$$f = \exp \left[\frac{-4 \Pi \langle x^2 \rangle}{\lambda^2} \right]$$

where $\langle x^2 \rangle$ is the mean square vibrational amplitude.

If we assume that the Mößbauer atom, M, is surrounded, say, by four equivalent bonds, then f is not angular dependent.



However, if one of the M—X bonds is replaced by an M—Y bond, where Y is of significantly different mass to X, then f will be angular dependent *i.e.* a function of θ :

$$\text{ratio} = \frac{\int_0^\pi T_{3/2} f(\theta) \sin\theta d\theta}{\int_0^\pi T_{1/2} f(\theta) \sin\theta d\theta} \neq 1$$

This means that the relative intensities of the two lines may not be equal in area, but they will have the same linewidth. This effect, first noted by Gol'danskii, has been observed in a few organotin compounds, notably polymeric trialkyl/aryl tin species such as Ph_3SnF [15,16] and Me_3SnF [17]. Since the methane-sulphonate ester of trimethyltin is likely to be polymeric and displays line

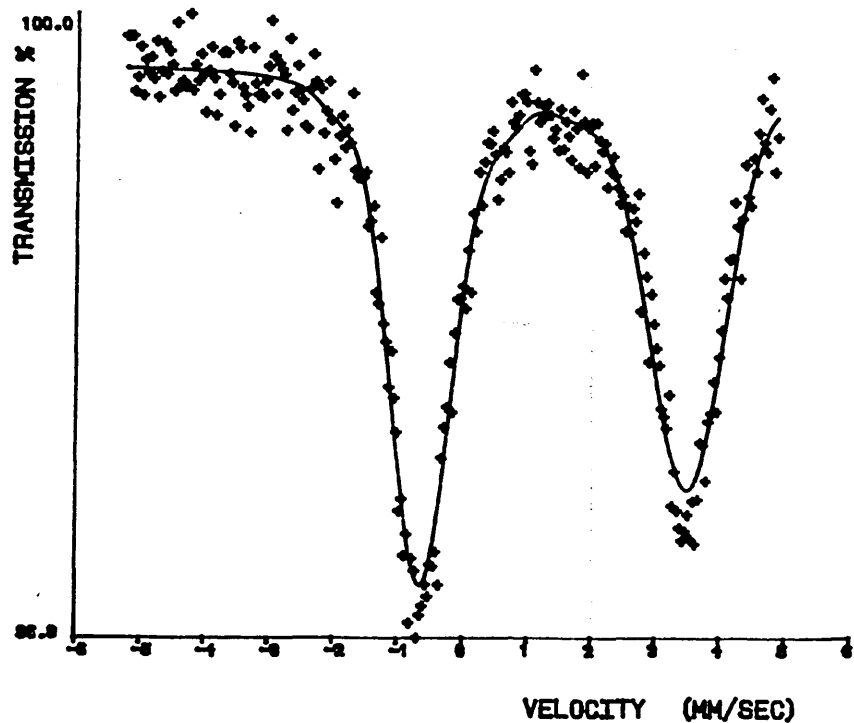
asymmetry even after grinding, the Gol'danskii-Karyagin effect may be at work. However, the linewidths are not equal, $\Gamma_1=1.03 \text{ mms}^{-1}$ and $\Gamma_2=1.23 \text{ mms}^{-1}$. Also, when fitted as two singlets, the areas of the two lines were almost equal, 51.6% to 48.4%. These results indicate that there is a distortion of quadrupole doublets *i.e.* a range of tin sites within the sample. A fitting program has been developed by Wivel *et al* [18] to cope with such asymmetric doublets. The algorithm, PQH, which runs from the MOSBAR suite, requires more fitting parameters than MOSFITN. Because of the greater number of variables, much more care is needed in the choice of the initial parameters. For each set of doublets a linear correlation between the isomer shift and quadrupole splitting is assumed:

$$\delta_x = \xi + \eta \times \Delta E_{Qx}$$

where ξ takes the value of δ_x when η is set to zero. η is the correlation coefficient for each set of doublets. Q2 was fitted using PQH over a range of quadrupole splittings from 0.00 \longrightarrow 8.00 mms^{-1} at 0.25 mms^{-1} intervals. The fitted data and the distribution plot are shown in Figure 3.14.

The implication of this computer fitting is that, in the solid state, the methane-sulphonate ester of trimethyltin contains a range of tin sites with quadrupole splitting ranging from 2.50 to 5.50 mms^{-1} . This can be tentatively explained in terms of variation in the coordination number and geometrical isomerism. If there is no intermolecular association, then the geometry around tin will be tetrahedral, with a relatively low quadrupole splitting. If the tin atom is five-coordinate then three isomers, *cis-*, *mer-* and *trans-* are possible (Figure 3.6). If there are six-coordinate tin atoms present, then two isomers are possible, facial (*fac-*) and meridional (*mer-*) (Figure 3.15).

3.14 (a)



3.14 (b)

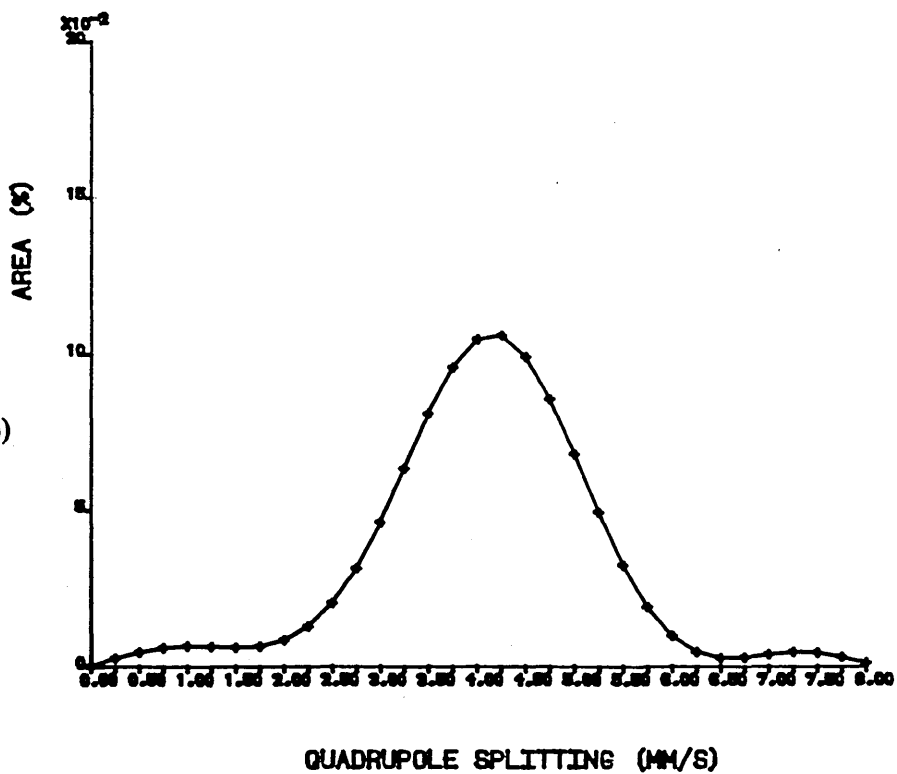


Figure 3.14 (a) PQH Fit of the Methanesulphonate Ester of Triphenyltin and 3.14 (b) the Distribution of Quadrupole Doublets in the Methane-Sulphonate Ester of Triphenyltin.

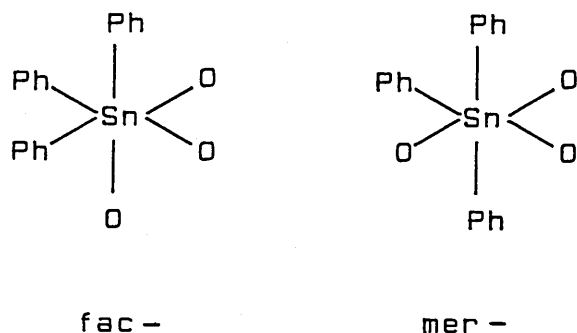


Figure 3.15 Geometrical Isomerism in Ph_3SnO_3 Systems.

The presence of the two geometrical isomers is unlikely to result in the wide distribution of quadrupole doublets observed. However, both isomers may be tetrahedrally and/or tetragonally distorted which could result in a large range of tin sites. The possibility of seven-coordinate tin sites cannot be ruled out, or indeed intramolecular Sn—O dative bonding as shown in Figure 3.16:

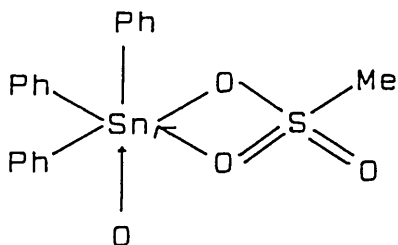


Figure 3.16 Proposed The Intramolecular Bonding in the Methane-Sulphonate Ester of Triphenyltin.

Any combination of these structures could produce a distribution of quadrupole doublets. It must be stressed that this explanation is purely speculative and confirmation is required from a different technique, *e.g.* X-ray crystallography.

The ^{119}Sn NMR spectrum of the authentic sulphonate ester in d_6 -DMSO exhibited three peaks, $\delta(^{119}\text{Sn})$ -237.7 , -254.8 and -523.3 ppm. The latter is significantly more intense than the other two and almost certainly corresponds to the sulphonate ester by virtue of its large chemical shift. This may be due to coordinate interactions between sulphonate ester molecules and the solvent.

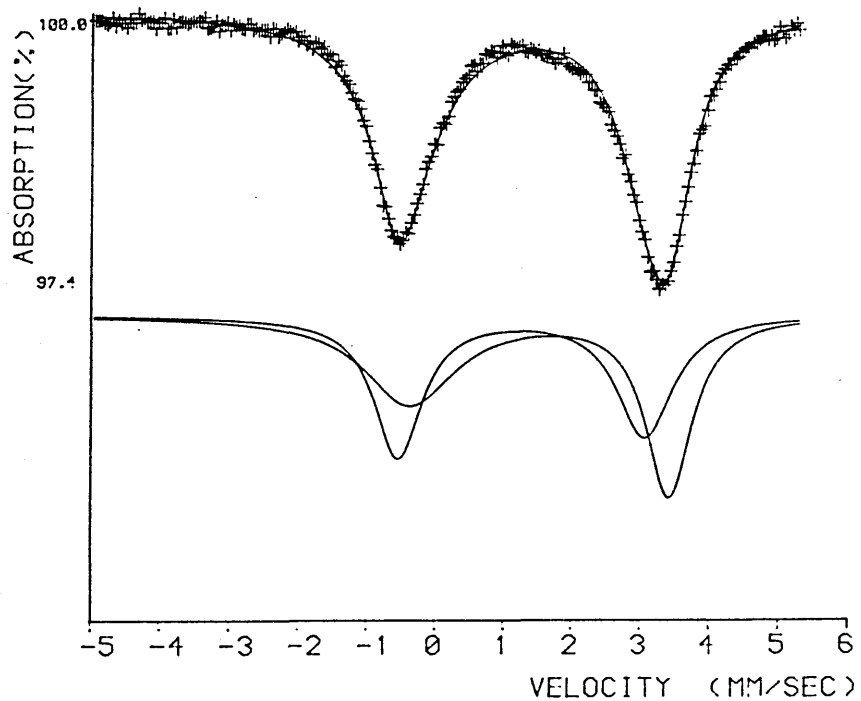
The signals at $\delta(^{119}\text{Sn})$ -237.7 and -254.8 ppm are identical to those observed in the ^{119}Sn NMR spectrum of the *bis*-(triphenyltin) oxide/methanesulphonyl chloride reaction product.

3.5.7. The Reaction Between Triphenyltin Chloride and Methane- and Benzenesulphonyl Chloride

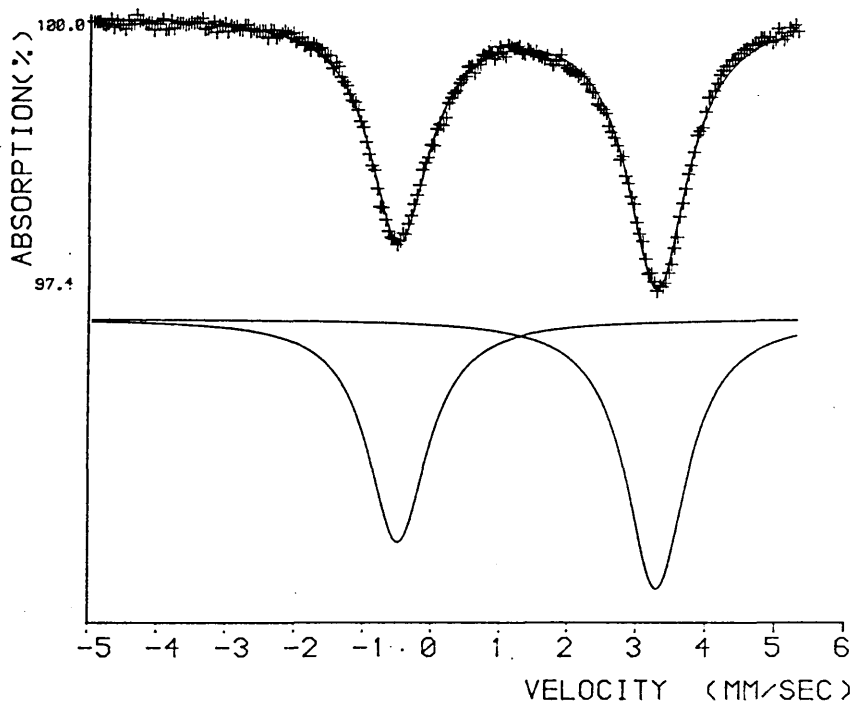
Equimolar quantities of the reactants were heated under reflux conditions in chloroform. A white solid was isolated in both experiments, whose melting points, Mößbauer and ^{119}Sn NMR parameters were consistent with those of triphenyltin chloride indicating that no reaction had occurred.

3.5.8. The Reaction Between *Bis*-(Triphenyltin) Oxide and Benzenesulphonyl Chloride

1 mol equivalent of *bis*-(triphenyltin) oxide was heated with 2 mol equivalents of benzenesulphonyl chloride in chloroform. Two products were isolated, a solid and an oil which crystallized on cooling in ice. The products will be referred to as solid #1 and solid #2 respectively. The best fit to the data for the Mößbauer spectrum of solid #1 was as two signals rather than as quadrupole doublets. Asymmetry in the absorption lines was evident (Figure 3.17); it was also noted that the linewidths of the two singlets were the same, within experimental error. The sample was ground with graphite and the Mößbauer spectrum was recorded (Figure 3.18(a)). The line asymmetry was eliminated and the spectrum fitted as one quadrupole doublet. These observations indicated that there is some degree of ordering in the crystal structure of solid #1.



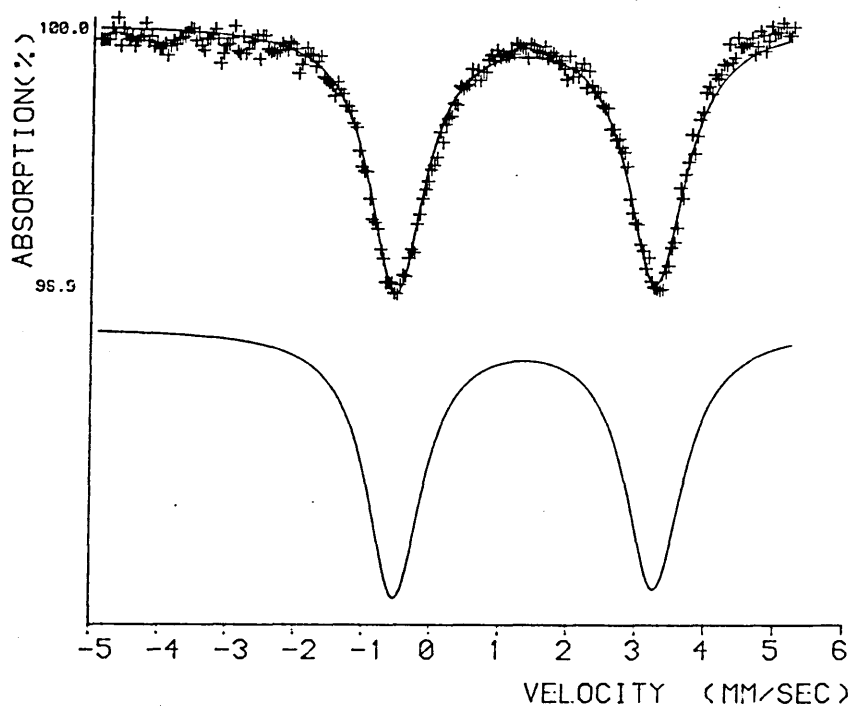
3.17 (a)



3.17 (b)

Figure 3.17 (a) Mössbauer Spectrum of Solid#1 from the Reaction Between *Bis*-(Triphenyltin) Oxide and Benzenesulphonyl Chloride, Fitted as Two Doublets and 3.17 (b) as Two Singlets.

3.18 (a)



3.18 (b)

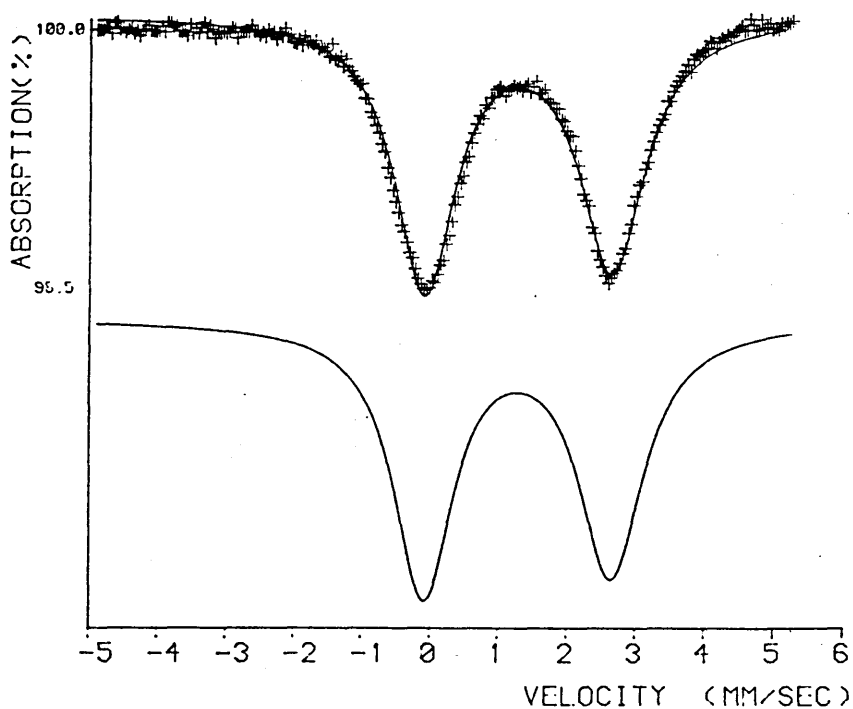


Figure 3.18 (a) Mössbauer Spectrum of Solid #1 from the Reaction Between *Bis*-(Triphenyltin) Oxide and Benzenesulphonyl Chloride, Ground with Graphite and Fitted as One Quadrupole Doublet and 3.18 (b) Solid #2 from the same Reaction, also Ground with Graphite.

The ^{119}Sn NMR spectrum of solid #1 contained two signals, one corresponding to triphenyltin chloride and the other (which was not identified) at $\delta(^{119}\text{Sn})$ -236.4 ppm.

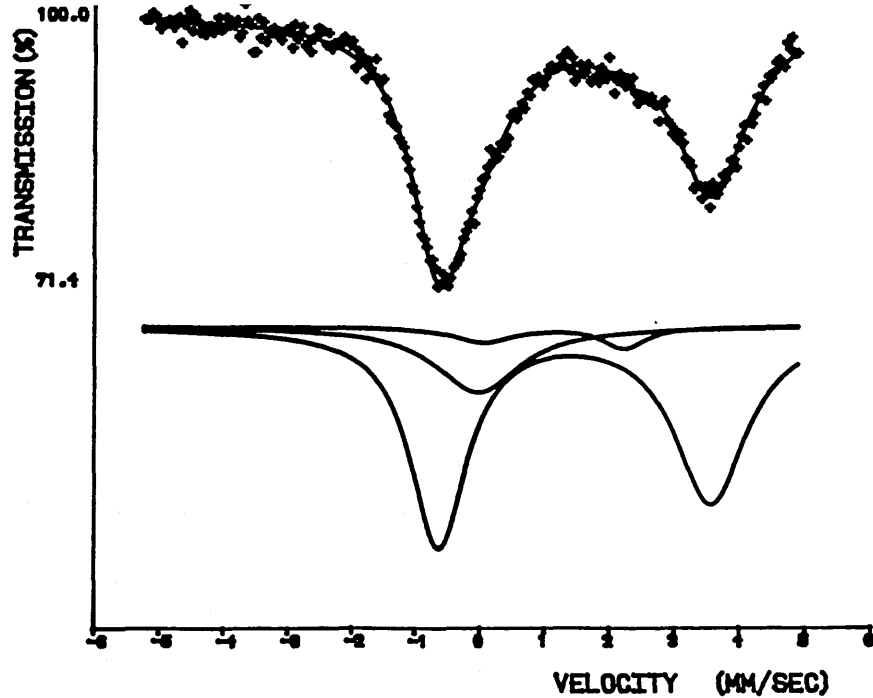
The Mößbauer parameters of solid #1, ΔE_Q 3.80 mms^{-1} and ρ 2.9 , suggest a high degree of coordination at the tin site as would be expected in the sulphonate ester. The benzenesulphonate ester of triphenyltin has been synthesized by Harrison *et al* [5] and the Mößbauer spectrum recorded, with δ 1.38 mms^{-1} and ΔE_Q 3.90 mms^{-1} , which is in reasonable agreement with the parameters for solid #1. The melting points were also found to be in agreement. The authentic benzenesulphonate ester was then synthesized from the reaction of *bis*-(triphenyltin) oxide and benzenesulphonic acid. The product of the reaction was a white solid with a melting point identical to solid #1. The Mößbauer spectrum consisted of three phases, one singlet and two doublets (Figure 3.19(a)). The singlet is probably due to a trace of SnO_2 . The first doublet, Q1, was not expected and did not correspond to unreacted *bis*-(triphenyltin) oxide. However, it appeared to be present in very low yield.

The major doublet, Q2, was isolated by phase subtraction of S1 and Q1 from the data (Figure 3.19(b)). As with the methanesulphonate ester of triphenyltin, the benzenesulphonate ester exhibited significant line asymmetry, even after grinding with graphite. Q2 was fitted using the PQH program and the spectrum and distribution plot are shown in Figure 3.20. A similar explanation to that proposed for the methanesulphonate ester is again suggested to account for the distribution of quadrupole doublets.

Microanalytical data on the product was in poor agreement with that expected for the sulphonate ester. However, the Mößbauer spectrum indicates that more than one species is present, which would account for the inaccuracy.

The ^{119}Sn NMR spectrum in d_6 -DMSO exhibited signals at $\delta(^{119}\text{Sn})$ -237.4 and -510.9 ppm (2:5 integral ratio). It should be noted that both the methane- and benzenesulphonate esters of triphenyltin exhibit signals around $\delta(^{119}\text{Sn})$ -500 ppm and less intense signals around $\delta(^{119}\text{Sn})$ -240 ppm.

3.19 (a)



3.19 (b)

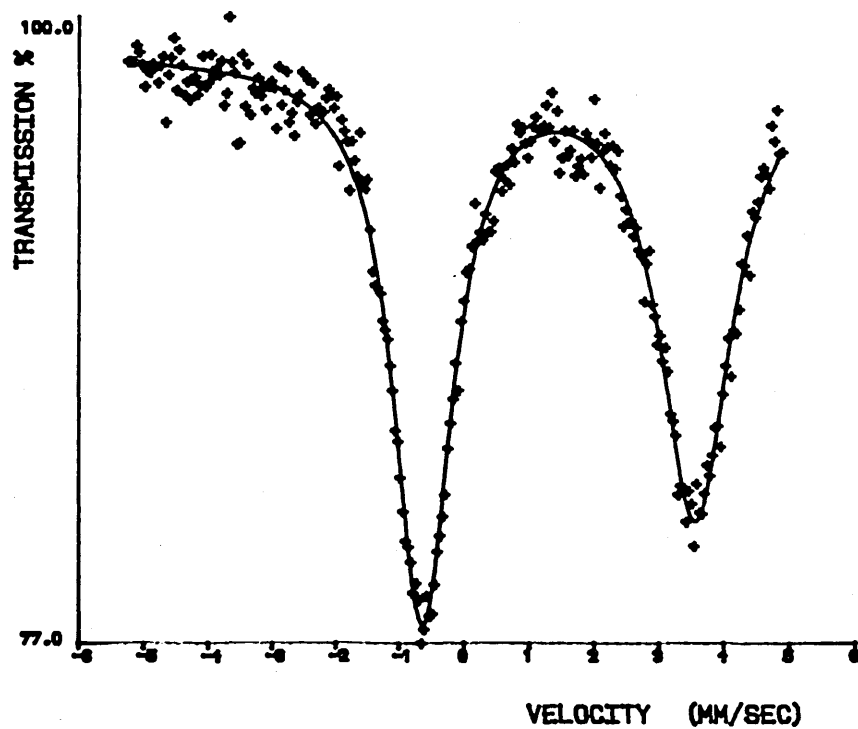
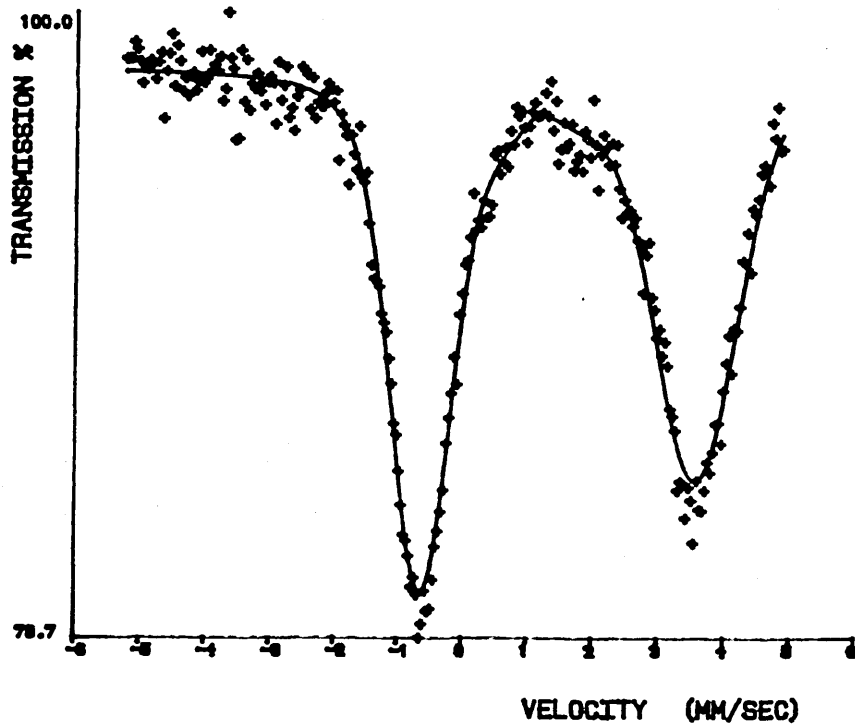


Figure 3.19 (a) Mössbauer Spectrum of the Product Containing the Benzenesulphonate Ester of Triphenyltin (Q2) Ground with Graphite and 3.19 (b) Q2 from the above Spectrum Fitted as One Doublet, note the Considerable Line Asymmetry.

3.20 (a)



3.20 (b)

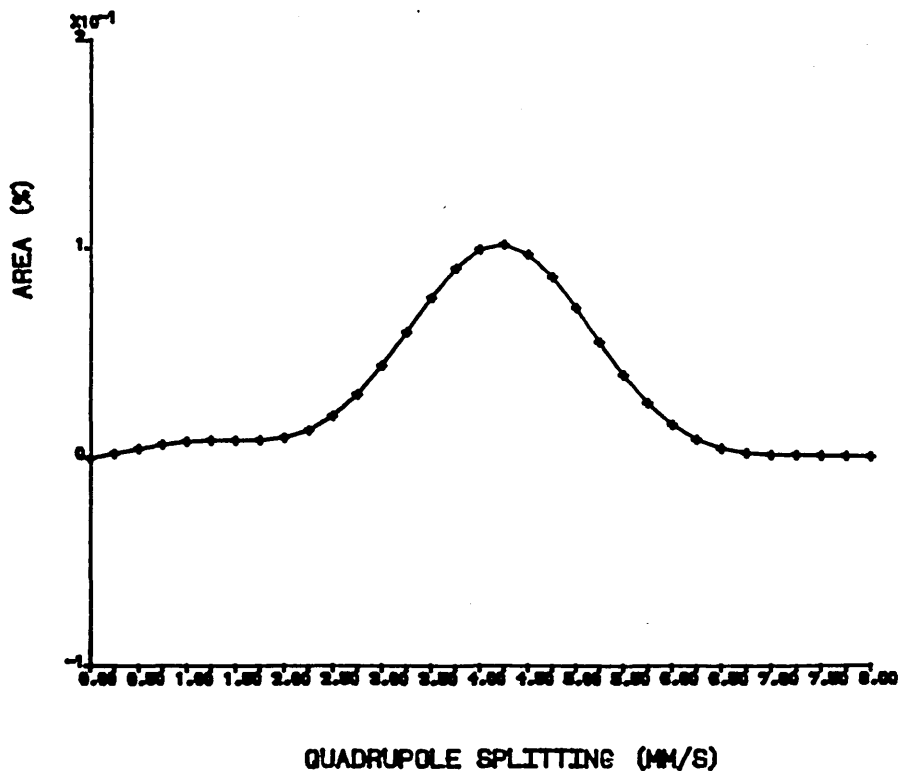


Figure 3.20 (a) PQH Fit of the Benzenesulphonate Ester of Triphenyltin and 3.20 (b) the Distribution of Quadrupole Doublets in the Benzene-Sulphonate Ester of Triphenyltin.

Solid #2 from the *bis*-(triphenyltin) oxide/benzenesulphonyl chloride reaction showed line asymmetry which was removed after grinding with graphite (Figure 3.18(b)). It was expected that solid #2 would be mainly triphenyltin chloride, but the Mößbauer parameters suggest a five-coordinate tin (IV) species is present ($\rho 2.2$). However, the ^{119}Sn NMR spectrum of solid #2 in d_6 -DMSO exhibited signals at $\delta(^{119}\text{Sn}) -117.6$ and -224.2 ppm (1:5 integral ratio). The latter signal corresponds to triphenyltin chloride, the former possibly being due to unreacted *bis*-(triphenyltin) oxide ($\delta(^{119}\text{Sn}) -121$ ppm). The melting point of solid #2 was below that of triphenyltin chloride. The discrepancy between the Mößbauer and ^{119}Sn NMR data is difficult to account for.

3.6. Conclusions from the Sulphonyl Chloride Model Studies

Bis-(tri-*n*-butyltin) oxide reacts with methanesulphonyl chloride to yield a product whose Mößbauer spectrum consists of three quadrupole doublets. One doublet is due to tri-*n*-butyltin chloride, the other two are due to tin (IV) four- and five/six-coordinate tin species respectively. The Mößbauer parameters of the authentic sulphonate ester (prepared independently) did not match those of the tin species observed in the Mößbauer spectrum of the sulphonyl chloride reaction product. The ^{119}Sn NMR spectrum of the latter exhibited two signals, neither of which could be identified from literature values or correlated with the observed signal in the ^{119}Sn NMR spectrum of the sulphonate ester. However, the signal at $\delta(^{119}\text{Sn}) -8.2$ ppm in the sulphonyl chloride reaction product spectrum is similar to the signal $\delta(^{119}\text{Sn}) -2.8$ ppm in the spectrum of the extract of Hypalon paint originally containing *bis*-(tri-*n*-butyltin) oxide.

Bis-(tri-*n*-butyltin) oxide also reacts with benzenesulphonyl chloride, the Mößbauer spectrum consisting of one quadrupole doublet. The parameters of the doublet do not correspond with those of the authentic sulphonate ester which was synthesized by reaction of *bis*-(tri-*n*-butyltin) oxide and benzenesulphonic acid.

The ^{119}Sn NMR spectra of the benzene- and methanesulphonyl chloride/*bis*-(tri-*n*-butyltin) oxide reaction products are almost identical with signals at approximately $\delta(^{119}\text{Sn})$ 120 and -10 ppm.

It is concluded that *bis*-(tri-*n*-butyltin) oxide does react with sulphonyl chlorides, but the expected products, tri-*n*-butyltin chloride and the corresponding sulphonate esters are not produced. The discrepancies between Mößbauer and ^{119}Sn NMR data, suggesting different numbers of components in the products, cannot be readily explained.

Tri-*n*-butyltin chloride did not react with the methane- or benzenesulphonate esters, as was expected.

Bis-(triphenyltin) oxide reacted with methanesulphonyl chloride to yield a product whose Mößbauer spectrum consisted of one singlet and two quadrupole doublets. The best match to the isomer shift of the singlet was triphenyltin hydride, though its formation cannot be readily explained. Triphenyltin chloride was an expected product, but the Mößbauer parameters of neither doublet supported this assumption. The second doublet, Q2, had parameters indicative of a highly coordinated tin site (ρ 2.9) and was thought to be the sulphonate ester. The latter was synthesized by the azeotropic method. The product had a ρ value identical to that of Q2 in the sulphonyl chloride reaction product, but the isomer shift and quadrupole splitting varied by more than experimental error.

The sulphonate ester from the azeotropic synthesis exhibited a distribution of quadrupole splittings in the Mößbauer spectrum. The Gol'danskii-Karyagin effect has been claimed for some triorganotin polymeric species in the literature, but no examples of distributions of quadrupole doublets have been reported for these compounds.

The ^{119}Sn NMR spectrum of the *bis*-(triphenyltin) oxide/methanesulphonyl chloride reaction product exhibited two broad peaks $\delta(^{119}\text{Sn})$ -237.5 and -255.2 ppm, neither of which could be identified from literature values. The ^{119}Sn NMR spectrum of the sulphonate ester from the azeotropic method consisted of three peaks. The major signal at $\delta(^{119}\text{Sn})$ -523.3 ppm was thought

to be due to the sulphonate ester. The other two weaker signals were virtually identical to those in the ^{119}Sn NMR spectrum of the *bis*-(triphenyltin) oxide/methanesulphonyl chloride reaction product. It is concluded that the sulphonate ester is not a major product of the sulphonyl chloride reaction. However, the sulphonyl chloride and azeotropic reaction products both contain two identical species in d_6 -DMSO.

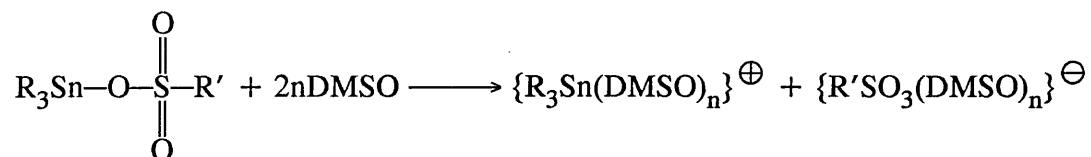
Bis-(triphenyltin) oxide reacted with benzenesulphonyl chloride to yield two solids, both of which exhibited line asymmetry due to partial orientation of crystallites.

The Mößbauer parameters and melting points of solid #1 and the benzenesulphonate ester of triphenyltin (as reported by Harrison *et al* [5]) were in good agreement. However, the sulphonate ester made by the azeotropic synthesis in this study had a higher isomer shift and quadrupole splitting than solid #1, although ρ is identical. The benzenesulphonate ester of triphenyltin, from the azeotropic route, exhibits a distribution of quadrupole doublets in the Mößbauer spectrum as does the methanesulphonate ester of triphenyltin. Both observations are suggested to arise from a distribution of tin coordination sites ranging from four to six or possibly seven. Geometrical isomerism and distortion of the five-, six- and seven-coordinate tin sites would lead to further variations in the quadrupole splitting. It is evident that the sulphonate esters of triphenyltin possess a different structural chemistry to those of tri-*n*-butyltin.

Solid #2 was expected to be triphenyltin chloride and the ^{119}Sn NMR spectrum confirmed this. However, the Mößbauer parameters of solid #2 did not correspond to those of triphenyltin chloride, but rather a five-coordinate tin (IV) species. Again, the discrepancy between Mößbauer and ^{119}Sn NMR data is not readily explained.

Triphenyltin chloride did not react with methane- or benzenesulphonyl chloride as was expected.

One consistent feature of the products of *bis*-(triphenyltin) oxide with methane-/benzenesulphonyl chlorides and methane-/benzenesulphonic acids is the appearance of a signal at $\delta(^{119}\text{Sn}) -237$ ppm in the NMR spectrum. It has been reported by Blunden and Hill [19] that certain triorganotin sulphonate esters ionize in aqueous solution. It is proposed that the sulphonate esters formed in this study dissociate in dimethylsulphoxide:



Reaction 3.3 Proposed Dimethylsulphoxide Solvolysis of $\text{R}_3\text{SnOSO}_2\text{R}'$.

The resultant $\{\text{R}_3\text{Sn}(\text{DMSO})_n\}^{\oplus}$ species is proposed to have a chemical shift of $\delta(^{119}\text{Sn}) -237$ ppm. A series of conductivity experiments were performed in order to confirm the existence of the proposed ions in the solution. The results are shown in Table 3.7.

Table 3.7 Conductivity of Triorganotin Sulphonate Esters.

	$\Lambda_m / \Omega^{-1}\text{cm}^2\text{mol}^{-1}$
$\text{Bu}_3\text{SnOSO}_2\text{Me}$	20.7
$\text{Bu}_3\text{SnOSO}_2\text{Ph}$	18.8
$\text{Ph}_3\text{SnOSO}_2\text{Me}$	25.0
$\text{Ph}_3\text{SnOSO}_2\text{Ph}$	25.5

All measurements recorded with 0.01M solutions in DMSO at 25°C.

Geary [20] has reviewed the relationship between conductivity behaviour in non-aqueous solvents and the chemical structure of the solute. For 1:1 electrolytes in DMSO, Λ_m is approximately $35 \Omega^{-1}\text{cm}^2\text{mol}^{-1}$. The observed

molar conductivities are in good agreement with this value. Indeed, lower values are expected due to the lower ionic mobilities of the proposed species compared with, for example, potassium thiocyanate, Λ_m 42 $\Omega^{-1}\text{cm}^2\text{mol}^{-1}$ [20]. The molar conductivities of the four triorganotin sulphonate esters were also determined in nitromethane, a low capacity donor solvent. Their solubility was much lower than in DMSO and no conductivity was observed.

It is concluded that in DMSO the four triorganotin sulphonate esters behave as 1:1 electrolytes. Thus, the ^{119}Sn NMR spectra which contain signals of approximately $\delta(^{119}\text{Sn}) -237$ ppm are thought likely to be due to the ionic $\{\text{Ph}_3\text{Sn}(\text{DMSO})_n\}^{\oplus}$ species. Since this peak is observed in the spectra of the products of *bis*-(triphenyltin) oxide with the methane-/benzenesulphonyl chlorides it is suggested that low concentrations of the respective sulphonate esters may be present.

One aim of the model study was to identify the tin species in the spectrum of the dry paint originally containing *bis*-(tri-*n*-butyltin) oxide. Comparison of the parameters of the unknown (Table 3.1) with those of the products of *bis*-(tri-*n*-butyltin) oxide in the model study (Table 3.5) indicates that the unknown has not been produced. However, several facts of academic interest have been established:

- (i) the reactivity of the *bis*-(triorganotin) oxides with sulphonyl chlorides, but resulting in products which are not necessarily the expected sulphonate esters;
- (ii) the very large quadrupole splittings of the authentic sulphonate esters and the line asymmetry observed in the triphenyltin sulphonate esters. The latter is ascribed to a distribution of tin sites within the sample and
- (iii) the 1:1 ionic dissociation of the triorganotin sulphonate esters in DMSO.

At this point, consideration was given to possible reactions of *bis*-(tri-*n*-butyltin) oxide species with other components of the paint, which were known to include stearic acid and N-pentamethylene thirum disulphide. The triphenyltin analogues were also synthesized.

3.7. Studies of Tri-*n*-Butyltin and Triphenyltin Stearates

The stearates were made by heating together under reflux the respective *bis*-(triorganotin) oxide with stearic acid in benzene for two hours. The water formed was removed using a Dean-Stark trap. Both stearates are white, amorphous solids. The Mößbauer parameters are shown in Table 3.8:

Table 3.8 Mößbauer Parameters of Triorganotin Stearates and Dithiocarbamates.

sample	phase	$\delta/$ mms ⁻¹	$\Delta E_Q/$ mms ⁻¹	$\Gamma_1/$ mms ⁻¹	$\Gamma_2/$ mms ⁻¹	%R.A.	ρ	χ^2
TBTstearate	Q1	1.44	3.58	0.99	0.95	100.0	2.5	0.5
TPTstearate	Q1	1.25	3.29	0.93	0.97	100.0	2.6	0.5
TBTdtc	Q1	1.44	2.16	1.03	1.04	100.0	1.5	0.7
TPTdtc	Q1	1.29	1.75	0.95	0.99	100.0	1.4	1.5

1. All spectra recorded at 80K with an error of $\pm 0.02\text{mms}^{-1}$. Isomer shifts are relative to CaSnO_3 .
2. %R.A. is the relative area of each phase, *i.e.* quadrupole doublet.
3. $\rho = \Delta E_Q / \delta$.
4. TBTstearate and TPTstearate are *bis*-(tri-*n*-butyltin)- and *bis*-(triphenyltin) stearate.
5. TBTdtc and TPTdtc are *bis*-(tri-*n*-butyltin)- and *bis*-(triphenyltin) dithiocarbamates.

The isomer shifts and quadrupole splittings of the triorganotin stearates are virtually identical to those of the respective acetates. The parameters of tri-n-butyltin stearate do not match those of the unknown observed in the dry paint spectrum originally containing *bis*-(tri-n-butyltin) oxide.

3.8. Studies of Tri-n-Butyltin and Triphenyltin Dithiocarbamates

A compound present in Hypalon paint is dipentamethylene thiuram disulphide, see Figure 3.21:

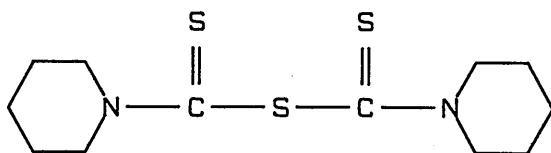
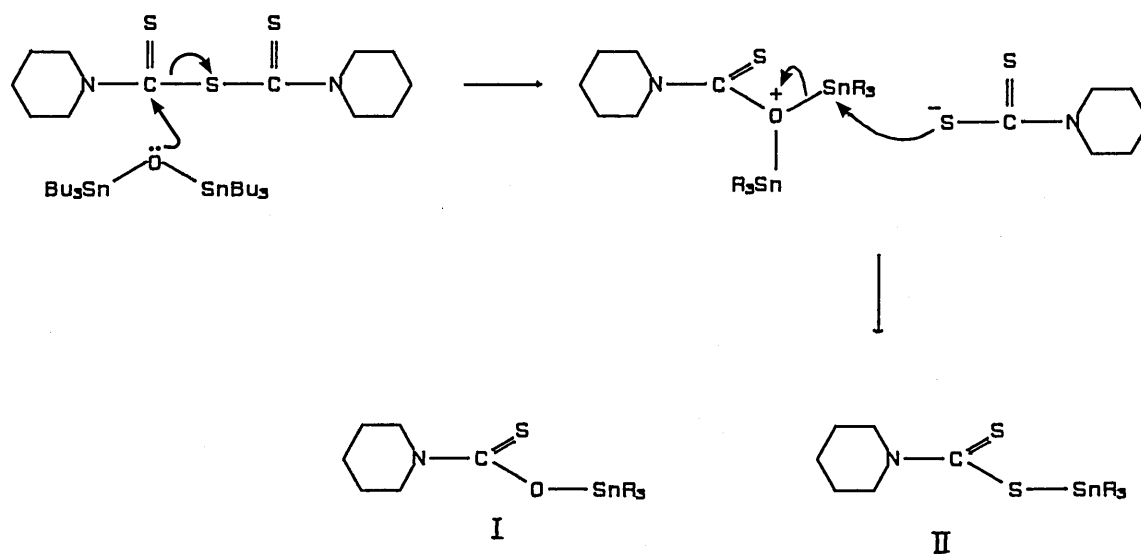


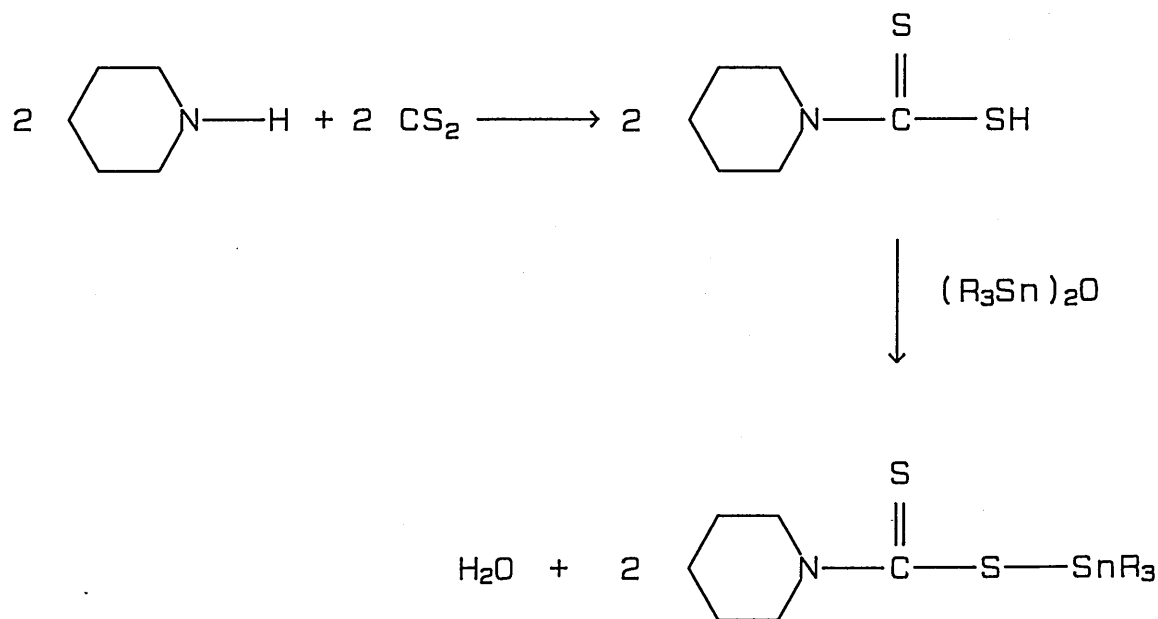
Figure 3.21 Structure of Dipentamethylene Thiuram Disulphide.

The following reaction between the *bis*-(triorganotin) oxide and the thiuram disulphide is proposed:



Scheme 3.4 Proposed Reaction Between $(R_3Sn)_2O$ and Dipentamethylene Thiuram Disulphide.

The two products would be expected to have very similar Mößbauer parameters. The synthesis of (II) was accomplished using the method of Shrivastava and Kumar [21]. The reaction is shown in Scheme 3.5:



Scheme 3.5 Synthesis of Triorganotin Dithiocarbamate.

The tri-*n*-butyltin dithiocarbamate (II) was a yellow oil, whereas the related triphenyltin dithiocarbamate was a white solid. The Mößbauer parameters of the two compounds are shown in Table 3.8. The parameters of the tri-*n*-butyltin dithiocarbamate does not correspond to those of the unknown species in the dry paint spectrum originally containing *bis*-(tri-*n*-butyltin) oxide. The identity of the minor component in the dry Hypalon paint sample originally containing *bis*-(tri-*n*-butyltin) oxide remains unidentified.

3.9. Experimental Details

3.9.1. Mößbauer Spectroscopy

Organotin samples were maintained at 80K using an Oxford Instruments Liquid Nitrogen Cryostat B27155 and an Oxford Instruments 3120 temperature controller.

The source, CaSnO_3 (15mCi), was mounted on an MVT4 velocity transducer linked to an Elscint MDF-N5 Driver. Detection of γ -rays was achieved by use of a Nuclear Enterprises Scintillation Counter, maintained at +1kV by a Nuclear Enterprises 4660 H.T. supply.

Spectra were recorded on one of two systems:

- (i) a Canberra Series 30 MCA with an Ortec 451 or 471 spectroscopy amplifier, or;
- (ii) an IBM AT fitted with EG&G Ortec MCA/MCS cards in conjunction with an Ortec 550 SCA and 427A delay amplifier, as well as an Ortec 451/471 spectroscopy amplifier.

3.9.2. General Information

^{119}Sn NMR spectra were recorded using a Bruker WP80 spectrometer. NMR data is given on the δ scale using tetramethyltin as the internal reference. Shifts to high field are negative in sign. Conductivity measurements were recorded on a Howe Conductivity Meter with a cell constant of 1.1 cm^{-2} . Melting points are uncorrected. Microanalyses were performed by Medac Ltd, Brunel University, Middlesex.

Reactions with sulphonyl chlorides were carried out under dinitrogen as they are moisture-sensitive.

3.9.3. Experimental Methods

The Preparation of Derivatized Phenyltins (3.4.2)

Triphenyltin chloride (3.85g, 0.01M) was placed in a 2-necked flask (200 ml) with dry diethyl ether (50g) at 0°C . Butyllithium (6 ml, 3M in hexane) was injected through a rubber septum. The mixture was heated to reflux conditions

for one hour. The reaction was quenched with excess sulphuric acid (2M). The mixture was transferred to a separating funnel and the aqueous layer drained off. The organic layer was washed, separated and dried. Rotary evaporation yielded clear crystals (3.2g, 78%) which melted at 35°C.

The above reaction was repeated with diphenyltin dichloride (3.44g, 0.01M) and double the quantity of the Grignard reagent. A clear liquid was isolated (2.5g, 64% yield).

The Reaction Between *Bis*-(Tri-*n*-Butyltin) Oxide and Methanesulphonyl Chloride (3.5.2)

Bis-(tri-*n*-butyltin) oxide (5.96g, 0.01 mol) and methanesulphonyl chloride (2.28g, 0.02 mol) were heated together in chloroform (100 ml) under reflux conditions for 1 hour. Solvent evaporation yielded a clear liquid, 7.81 g (95%).

$\delta^{119}\text{Sn}$ NMR (CDCl_3) 121.2 and -8.2 ppm.

Synthesis of the Methanesulphonate Ester of Tri-*n*-Butyltin (3.5.2)

Bis-(tri-*n*-butyltin) oxide (5.96g, 0.01mol) and methanesulphonic acid (1.92g, 0.02 mol) were heated together in benzene (100 ml) under reflux conditions using a Dean-Stark trap for 1 hour. A clear viscous liquid was isolated after rotary evaporation, 8.47g (93%).

$\delta^{119}\text{Sn}$ NMR (CDCl_3) 68.7 ppm. Microanalysis: found C, 41.89%; H, 7.90%. $\text{Bu}_3\text{SnOSO}_2\text{Me}$ requires C, 40.54%; H, 7.85%.

The Reaction Between Tri-*n*-Butyltin Chloride and Methanesulphonyl Chloride (3.5.3)

Tri-*n*-butyltin chloride (3.25g, 0.01mol) and methanesulphonyl chloride (1.14g, 0.01mol) were heated together in chloroform (50 ml) under reflux conditions for 1 hour. Solvent evaporation yielded a clear liquid, 4.30g (98%).

$\delta^{119}\text{Sn}$ NMR (CDCl_3) 153.0 ppm.

The Reaction Between Bis-(Tri-n-Butyltin) Oxide and Benzenesulphonyl Chloride (3.5.4)

Bis-(tri-n-butyltin) oxide (5.96g, 0.01mol) and benzenesulphonyl chloride (3.54g, 0.02mol) were heated together in chloroform (100 ml) under reflux conditions for 1 hour. Solvent evaporation yielded a clear viscous liquid, 8.74g (92%).

$\delta^{119}\text{Sn}$ NMR (CDCl_3) 125.5 and -11.2 ppm.

Synthesis of the Benzenesulphonate Ester of Tri-n-Butyltin (3.5.4)

Bis-(tri-n-butyltin) oxide (5.96g, 0.01mol) and benzenesulphonic acid (3.16g, 0.02mol) were heated together in benzene (100 ml) under reflux conditions, using a Dean-Stark trap, for 1 hour. A pale pink viscous liquid was isolated after rotary evaporation, 7.22g (79%).

$\delta^{119}\text{Sn}$ NMR (CDCl_3) 80.8 ppm. Microanalysis: found C, 49.61%; H, 7.23%. $\text{Bu}_3\text{SnOSO}_2\text{Ph}$ requires C, 48.35% and H, 7.21%.

The Reaction Between Tri-n-Butyltin Chloride and Benzenesulphonyl Chloride (3.5.5)

Tri-n-butyltin chloride (3.25g, 0.01mol) and benzenesulphonyl chloride (1.77g, 0.01mol) were heated together in chloroform (50 ml) under reflux conditions for 1 hour. Solvent evaporation yielded a clear liquid, 4.62g (92%).

$\delta^{119}\text{Sn}$ NMR (CDCl_3) 156.0 ppm.

The Reaction Between Bis-(Triphenyltin) Oxide and Methanesulphonyl Chloride (3.5.6)

Bis-(triphenyltin) oxide (7.16g, 0.01mol) and methanesulphonyl chloride (2.28g, 0.02mol) were heated together in chloroform (100 ml) under reflux conditions for 1 hour. Solvent evaporation yielded a white solid, 7.74g (82%).

$\delta^{119}\text{Sn}$ NMR (d_6 -DMSO) -237 and -225 ppm ($\approx 1:1$ integral ratio).

Synthesis of the Methanesulphonate Ester of Triphenyltin (3.5.6)

Bis-(triphenyltin) oxide (7.16g, 0.01mol) and methanesulphonic acid (1.92g, 0.02mol) were heated together in benzene (100 ml) under reflux conditions using a Dean-Stark trap for 1 hour. Solvent evaporation yielded a grey/white solid, 7.90g (87%), m.p. 275–280°C.

$\delta^{119}\text{Sn}$ NMR (d_6 -DMSO) –237.7, –254.8 and –523.3 ppm (1:1:3 integral ratios). Microanalysis: found C, 50.99%; H, 4.01%. $\text{Ph}_3\text{SnOSO}_2\text{Me}$ requires C, 51.27%; H, 4.08%.

The Reaction Between Triphenyltin Chloride and Methanesulphonyl Chloride (3.5.7)

Triphenyltin chloride (3.86g, 0.01mol) and methanesulphonyl chloride (1.14g, 0.01mol) were heated together in chloroform (50 ml) under reflux conditions for 1 hour. Solvent evaporation yielded a white solid, 3.44g (89%), m.p. 105–109°C.

$\delta^{119}\text{Sn}$ NMR (d_6 -DMSO) –224.4 ppm.

The Reaction Between *Bis*-(Triphenyltin) Oxide and Benzenesulphonyl Chloride (3.5.8)

Bis-(triphenyltin) oxide (7.16g, 0.01mol) and benzenesulphonyl chloride (3.54g, 0.02mol) were heated together in chloroform under reflux conditions for 1 hour. Solvent evaporation yielded a white solid and an oil which crystallised on cooling, solid #1 and solid #2 respectively. Solid #1, 3.84g, m.p. 250–253°C, solid #2, 3.33g, m.p. 248–253°C, total yield 67%.

Solid #1, $\delta^{119}\text{Sn}$ NMR (d_6 -DMSO) –225.0 and –236.4 ppm (1:3 integral ratio).

Solid #2, $\delta^{119}\text{Sn}$ NMR (d_6 -DMSO) –117.6 and –224.2 ppm (1:5 integral ratio).

Synthesis of the Benzenesulphonate Ester of Triphenyltin (3.5.8)

Bis-(triphenyltin) oxide (7.16g, 0.01mol) and benzenesulphonic acid (3.16g, 0.02mol) were heated together in benzene (100 ml) under reflux conditions using a Dean-Stark trap for 1 hour. Solvent evaporation yielded a white solid, 8.40g (81%), m.p. 250–253°C.

$\delta^{119}\text{Sn}$ NMR (d_6 -DMSO) –237.4 and –510.9 ppm (2:5 integral ratio).

Microanalysis: found C, 54.54%; H, 3.08%. $\text{Ph}_3\text{SnOSO}_2\text{Ph}$ requires C, 58.84% and H, 3.97%.

The Reaction Between Triphenyltin Chloride and Benzenesulphonyl Chloride

Triphenyltin chloride (3.86g, 0.01mol) and benzenesulphonyl chloride (1.77g, 0.01mol) were heated together in chloroform (50 ml) under reflux conditions for 1 hour. Solvent evaporation yielded a white solid, 3.53g (92%), m.p. 104–109°C. $\delta^{119}\text{Sn}$ NMR (d_6 -DMSO) –224.6 ppm.

Synthesis of Tri-*n*-Butyltin Stearate (3.7)

Bis-(tri-*n*-butyltin) oxide (5.96g, 0.01mol) and stearic acid (5.68g, 0.02mol) were heated together in benzene (100 ml) under reflux conditions using a Dean-Stark trap for 2 hours. Solvent evaporation yielded a white amorphous solid, 10.14g (87%) m.p. 30°C, $\delta^{119}\text{Sn}$ NMR (CDCl_3) 100 ppm.

Synthesis of Triphenyltin Stearate (3.7)

Bis-(triphenyltin) oxide (7.16g, 0.01mol) and stearic acid (5.68g, 0.02mol) were heated together in benzene (100 ml) under reflux conditions using a Dean-Stark trap for 2 hours. Solvent evaporation yielded a white amorphous solid, 11.54g (89%), m.p. 62–65°C. $\delta^{119}\text{Sn}$ NMR (CDCl_3) –115.8 ppm.

Synthesis of Tri-n-Butyltin-N-Pentamethylene Dithiocarbamate (3.8)

A solution of piperidine (20 mmol in chloroform, 5 ml) was slowly added to a solution of *bis*-(tri-n-butyltin) oxide (5.96g, 10mmol) and carbon disulphide (20mmol) in chloroform (15 ml). The reaction mixture was stirred at -20°C for 1 hour. The chloroform was evaporated off under a stream of dinitrogen and the product was extracted into diethyl ether. Evaporation of the solvent yielded a yellow oil, 3.21g (71%). $\delta^{119}\text{Sn}$ NMR (CDCl_3) 24.4 ppm.

Triphenyltin-N-Pentamethylene Dithiocarbamate (3.8)

As for tri-n-butyltin derivative, but *bis*-(triphenyltin) oxide (7.16g, 10 mmol) in solution. Solvent evaporation yielded a white solid, 3.99g (78%), m.p. $150-153^{\circ}\text{C}$. $\delta^{119}\text{Sn}$ NMR (CDCl_3) -190.9 ppm.

Chapter 3 References.

1. Herber, R.H., Stöckler, H.A., and Riechle, W.T., J. Chem. Phys., 1965, 42, (7), 2447.
2. Brooks, J.S., Allen, D.W. and Clarkson, R.W., J. Organomet. Chem., 1983, 243, 411.
3. Bailey, S., PhD Thesis, Sheffield City Polytechnic, 1987.
4. Smith, P.J. and Tupciauskas, A.P., Chemical Shifts of ^{119}Sn Nuclei in Organotin Compounds, from Annual Reports on NMR Spectroscopy, ed. Webb, G.A., Academic Press, 1978.
5. Harrison, P.G., Phillips, R.C. and Richards, J.A., J. Organomet. Chem., 1976, 114, 47.
6. Bancroft, G.M., Kumar Das, V.G., Sham, T.K. and Clark, M.G., J. Chem. Soc. Dalton Trans., 1976, 643.
7. Glidewell, C. and Liles, D.C., Acta Cryst., 1978, B34, 1693.
8. Bancroft, G.M., Davies, B.W., Payne, N.C. and Sham, T.K., J. Chem. Soc. Dalton Trans., 1975, 973.
9. King, T.J. and Harrison, P.G., J. Chem. Soc. Dalton Trans., 1974, 2298.
10. Tarkhova, T.N., Chapminov, E.V., Simonov, M.A. and Belov, N.W., Krystallografiya, 1977, 22, 1004.
11. Bokii, N.G., J. Struct. Chem., 1970, 11, 828.
12. Greenwood, N.N. and Gibb, T.C., Mössbauer Spectroscopy, Chapter 14, Chapman and Hall, 1971.
13. Gol'danskii, V.I., Makarov, E.F. and Khrapov, V.V., Phys. Lett., 1963, 3, (7), 344.
14. Karyagin, S.V., Doklady Akad. Nauk. SSSR, 1963, 148, 1102.
15. Stöckler, H.A. and Sano, H. Chem. Phys. Lett., 1968, 2, 448.
16. Stöckler, H.A. and Sano, H. Phys. Rev., 1968, 165, 406.
17. Herber, R.H. and Chandra, S., J. Chem. Phys., 1970, 52, 6054.
18. Wivel, C. and Morup, S., J. Phys., 1981, E14, 605.

19. Blunden, S.J. and Hill, R. Inorg. Chim. Acta, 1984, 87, 83.
20. Geary, W.J., Coord. Chem. Rev., 1971, 7, 81.
21. Srivastava, T.N. and Kumar, V., J. Organomet. Chem., 1976, 107, 55.

4. Release-Rate Studies

4.1. Introduction

The rate at which the triorganotin biocide is released from an antifouling coating will, together with the nature of the triorganotin, determine the effectiveness of that coating. Bollinger [1] has stated that there are three distinct mechanisms by which a biocide may pass from the matrix and into solution, *viz*, (i) leaching, (ii) exfoliation and (iii) diffusion.

(i) leaching: the antifouling agent is stationary within the coating until water permeates the matrix *via* the pore structure. The biocide is dissolved and may then migrate back through the insoluble matrix to the binder-water interface. Characteristics of porosity, such as pathlength, diameter and rate of growth with toxicant depletion will determine the loss rate. Another important factor (for all antifouling coatings) is the volume of water in contact with the surface area per unit time. De la Court [2] showed that settlement of marine organisms is only possible when the surface is stationary or the flow of water is very low. However, it is under such conditions that the biocide release-rate is at its lowest, regardless of the mechanism of toxicant loss:

(ii) exfoliation: this mechanism is only briefly mentioned by Bollinger [1], but described in more detail by Gitlitz [3]. The antifouling matrix is soluble in seawater and as it slowly dissolves fresh toxicant is exposed. The author claims that such systems show an exponential decay of toxicant release. However, Christie [4] stated that soluble matrix paints based on a tri-n-butyltin methacrylate/methyl methacrylate have a linear toxicant release-rate, see Figure 4.1:

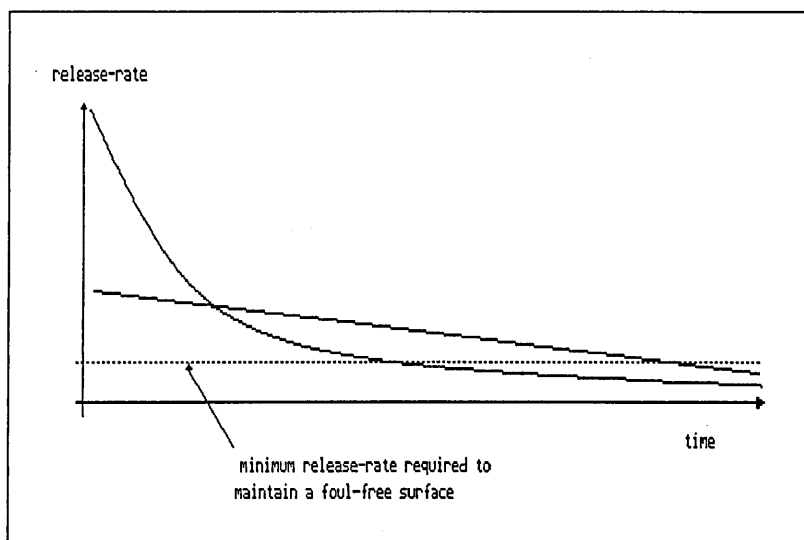


Figure 4.1 Exponential and Linear Decay of Toxicant Release-Rates.

To double the service life of an antifouling system with an exponential decay in toxicant release would require a coating four times thicker. For the tri-n-butyltin methacrylate/methyl methacrylate system any increase in film thickness will be almost directly proportional to the increase in service life. Also note that there is less toxicant waste with the latter system;

(iii) diffusion: this mechanism requires the biocide to be soluble in the coating, since the matrix itself lacks pore structure and is insoluble in seawater. Biocide molecules at the film surface/water interface diffuse into the water at a rate dependent upon their aqueous solubility, (*e.g.*, *bis*-(tri-n-butyltin) oxide ≈ 25 ppm, tri-n-butyltin fluoride < 10 ppm and triphenyltin fluoride < 1 ppm [3]). Partial depletion of the surface layers of the matrix creates a concentration gradient which leads to replenishment of the surface zone from the interior matrix "reservoir."

The rate-determining step is either toxicant diffusion through the matrix or aqueous dissolution, whichever is slower. For *bis*-(tri-n-butyltin) oxide in rubber, aqueous dissolution is slower. The loss rate is, therefore, proportional

to the difference between the toxicant concentration in the bulk water and the interfacial water concentration. Water turbulence is obviously an important factor.

The most widely used method to determine the efficiency of an antifouling coating is to immerse panels suspended on a raft in seawater [5]. The panels are examined periodically and photographic records are kept. The rafts are often octahedral in cross-section to provide different growing conditions for the marine foulants. Ship trials are obviously more realistic, but more expensive. They are usually only carried out after successful raft panel tests.

An alternative approach is rotor testing, in which panels are circulated at a pre-determined speed in continuously replenished water. This can not only provide information on release-rates, but also on the erosion-rate of the coating. In the present study the triorganotin toxicant release-rate from eight Hypalon paint samples was determined in the laboratory using a flow system, shown schematically in Figure 4.2:

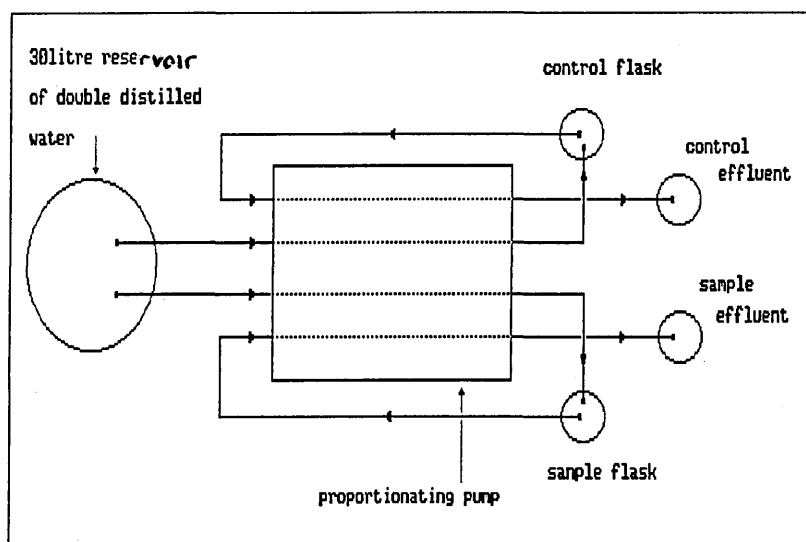


Figure 4.2 Schematic of Flow-Rate Apparatus.

A known area of paint sample (5 cm²) was placed in one conical flask. The arrangement is shown in detail in Figure 4.3:

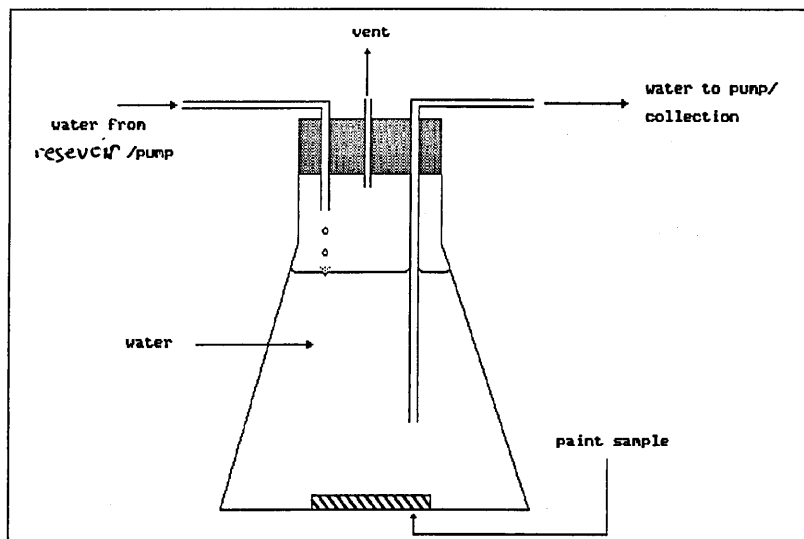


Figure 4.3 Schematic of Conical Flask Arrangement.

The paint was placed in the flask (250 ml) and covered with double-distilled water (200 ml). The pump, a Technion Autoanalyzer proportionating pump, was then started. Variations in flow-rate can be achieved by selecting tubing of different internal diameter (the pump works at a constant speed). A flow-rate of 120 mlh⁻¹ was used in this study. As is evident from Figures 4.2 and 4.3, the rate at which water enters the flask is exactly matched by the rate at which it is collected. A second, sample free flask, was used as a blank. The pump was operated continuously for the duration of the experiment.

4.2. Determination of Trace Levels of Organotin Compounds

A technique was then required to determine the triorganotin levels present in the effluent. It was expected that such levels would be low, probably in the ppb range. Several papers have been published describing various methodologies for determining trace levels of organotins. The main problem for the analyst is the

low, but environmentally significant levels of organotins, which have to be detected. The techniques used include electrochemical methods [6,7,8], high performance liquid chromatography, (HPLC), [9-12], high performance thin layer chromatography, (HPTLC), [13,14], atomic absorption/emission spectrometry, (AAS/AES), [15-32] and gas chromatography/mass spectrometry, (GC/MS), [33-37].

4.2.1. Electrochemical Techniques

Bond and McLachlan [6] developed a polarographic method specifically for *bis*-(tri-*n*-butyltin) oxide. They found that in non-aqueous solvents, *e.g.* THF, the presence of *bis*-(tri-*n*-butyltin) oxide resulted in an oxidation process at the mercury electrode:



On the time scale of the experiment the Sn—Hg—Sn complex was found to be unstable and additional electron transfer occurs (dissolved HgO reacts with the complex to yield an Sn(II) precipitate). The *bis*-(tri-*n*-butyltin) oxide/THF extracts were simply obtained by dissolving authentic paint samples in the solvent.

Van den Berg *et al* [7] developed a cathodic stripping voltammetric (CSV) method for determining inorganic tin. Authentic seawater samples were irradiated with UV lamps. Irradiation caused the decomposition of surface active organic compounds (a potential interference) and converted organotin compounds to inorganic Sn(II). The sample is then placed in a voltammetric cell and tropolone, Figure 4.4, is added (tropolone is commonly used as a tin complexing agent). The complex is adsorbed onto the mercury electrode at -0.8V for a known time (the concentration step). The voltage is then switched to -0.4V and the resultant current caused by loss of tin from the electrode is recorded using a potential scan. Although molybdenum was found to be an interference in the experiment, the authors claim a 3pM limit of detection, as tin.

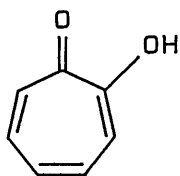
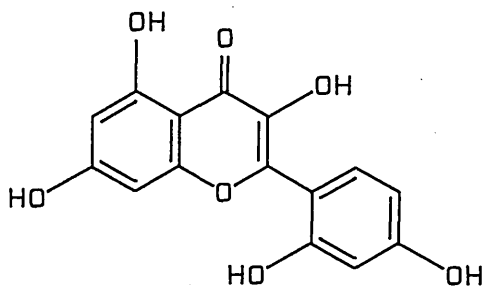


Figure 4.4 Structure of 2-Hydroxy-2,4,6-Cycloheptatrienone, Tropolone.

Carter *et al* [8] studied the polarographic response of tri-*n*-butyltin chloride as a function of the cell material. The response per unit concentration was found to decrease from polycarbonate > polyethene \approx glass \approx PTFE \approx PVC > silanized glass > nylon > perspex \approx waxed glass. Adsorption of the analyte onto the container walls was thought to be responsible. The implication for the analyst is that organotin solutions should ideally be kept in polycarbonate containers.

4.2.2. High Performance Liquid Chromatographic Techniques

The use of HPLC means that speciation of the organotins is possible, but a serious drawback is that detection is usually achieved by UV absorption. The *n*-butyltin species lack chromophoric groups and it is, therefore, not possible to detect them with conventional equipment. This problem has been overcome by Ebdon and co-workers by using detection by AAS [9], or by post-column derivatization of the organotin species followed by fluorimetric detection [10]. In the latter an initial pre-concentration step is carried out. Up to 500 ml of sample is passed through a short (4 cm) ODS packed column, which retains the organotin compounds. These can then be back-extracted with an eluent of methanol/water/ammonium acetate and through a second column. The eluent from the column is mixed with a fluorimetric reagent comprising of acetic acid, morin, (Figure 4.5) and a surfactant, Triton X-100.



**Figure 4.5 Structure of Morin,
2',3,4',5,7-Pentahydroxyflavone.**

Fluorescent complexes of morin and organotin compounds have already been shown to form, but these were found to be unstable [11]. Ebdon and Garcia-Alonso [10] showed that incorporation of surfactant into the eluent leads to micelle formation, in which the complex is stable. Detection of the tri-*n*-butyltin-morin complex was achieved by measurement of the emission line at 534 nm after excitation at 408 nm. The greatest sensitivity for the detection of this complex was at pH 5.2. The di-*n*-butyltin-morin complex gave the greatest response at pH 2.0, (with excitation/emission wavelengths of 420/504 nm), under which conditions the tri-*n*-butyltin complex does not form. Thus by varying the acidity of the fluorimetric reagent, speciation is possible. The limit of detection was found to be at the ng l^{-1} level, as tin.

Whang and Yang [12] found an elegant solution to the problem of triorganotin detection without the use of complex and expensive equipment such as fluorimeters. By using indirect photometric chromatography, IPC, the authors were able to detect tri-*n*-butyltin, tripropyltin, triethyltin and trimethyltin cations, as well as the UV-absorbing triphenyltin cations. The technique is based upon the addition of photometrically active counter ions into the mobile phase, Whang and Yang using benzyltrimethylammonium chloride (Figure 4.6).

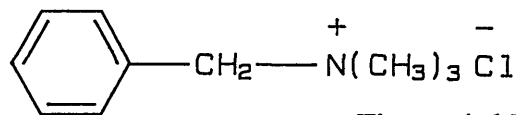


**Figure 4.6 Benzyltrimethylammonium
Chloride.**

In the column effluent the benzyltrimethylammonium ions substitute for the light-absorbing ions resulting in a decreased absorbance at the detector so that negative peaks are obtained (detection at 263 nm). The authors claim a ngml^{-1} limit of detection, as tin.

4.2.3. High Performance Thin Layer Chromatography

This technique has been used by Brown, Tomboulian and Walters [13,14]. It differs from conventional TLC in that the stationary phase consists of much finer silica gel and the analyte is deposited in lower concentrations. These two factors result in improved separation of the analyte.

The authors describe a method for the speciation and determination of trace levels of phenyltins. Using a mobile phase of acetic acid and chloroform, 30:70 v/v, the following retention factors were observed: Ph_4Sn 0.65, Ph_3SnCl 0.56, Ph_2SnCl_2 0.14 and PhSnCl_3 0.05. Inorganic tin did not migrate. Treatment of the plates with morin resulted in fluorescent species with all the spots except that of Ph_3SnCl . However, if the plate is subjected to UV radiation prior to treatment with morin, all the spots fluoresce. The concentration of tin can be determined by scanning densitometry, with a limit of detection at the ng level, as tin.

The advantage of HPTLC is the simultaneous sampling/analysis, which leads to increased precision and the high sample throughput. However, the equipment is expensive and requires a high level of operator skill.

4.2.4. Atomic Absorption Spectrometry

Atomic absorption spectrometry, AAS, is a technique which offers high elemental selectivity and sensitivity, especially graphite furnace AAS, GFAAS and quartz cell AAS. There are, however, two significant disadvantages. The first is that triorganotin species are rather volatile and matrix modification is required to prevent analyte loss prior to atomization. The second is that the technique can only determine total tin, unless the spectrometer can be interfaced

with a GC or similar separative apparatus. The latter is not easily achieved, but several workers have designed such systems and these will be reviewed later in this section.

Burns *et al* [15] examined the effects of coating the graphite tube with tantalum (V) oxide, prior to analysis. It was found that the precision was improved with the coated tube compared to an uncoated tube. Tantalum (V) oxide, being both acidic and oxidizing, was thought to digest the organotin compounds in the ashing stage ($\approx 800^{\circ}\text{C}$). The reduction in volatility which this produces results in increased reproducibility of the tin signal. Later work by Burns and co-workers [16] showed that tubes coated with molybdenum and vanadium salts also showed enhanced tin absorption signals.

Parks *et al* [17] discussed the problems of determining low levels of organotin species, which is hindered by their complicated decomposition behaviour in the furnace. The authors suggested three steps to enhance the determination of organotins by GFAAS.

The first was to use solvent extraction prior to analysis. Introduction of the samples into the furnace as aqueous, rather than organic samples, is preferable. However, authentic samples may contain interfering salts and preconcentration is usually essential if any signal is to be measured. The authors tested the extraction efficiency of toluene, methyl-*i*-butylketone (MIBK), chloroform and *n*-hexane. MIBK formed an emulsion with water, *n*-hexane extracted just 50% of the tri-*n*-butyltin and the chloroform extract appeared to react with the organotin in the furnace resulting in the premature loss of analyte. Toluene was found to be superior in every respect.

The second enhancement technique was to use a matrix modifier. As was noted by Burns *et al* [14,15], the presence of a highly oxidizing species in the furnace results in a signal improvement. Parks and co-workers found that ammonium dichromate increased the signal response approximately fifteen times, (up to 5 ng Sn), compared to an unmodified sample. However, aqueous ammonium dichromate and the toluene extract are immiscible, so that a third component,

propan-2-ol, was added to yield a homogeneous sample. The increase in sensitivity was thought to be due to the oxidation of the organotins to tin (IV) oxide. The latter species will only volatilize during the atomization stage (approximately 2300°C).

Physical enhancement was achieved by using a L'vov platform rather than the normal tube, see Figure 4.7(a) and (b):

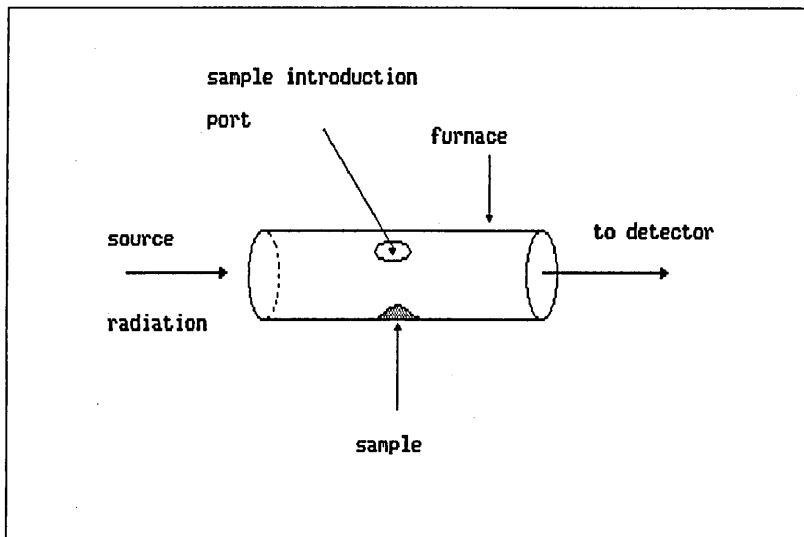


Figure 4.7(a) Standard Graphite Furnace.

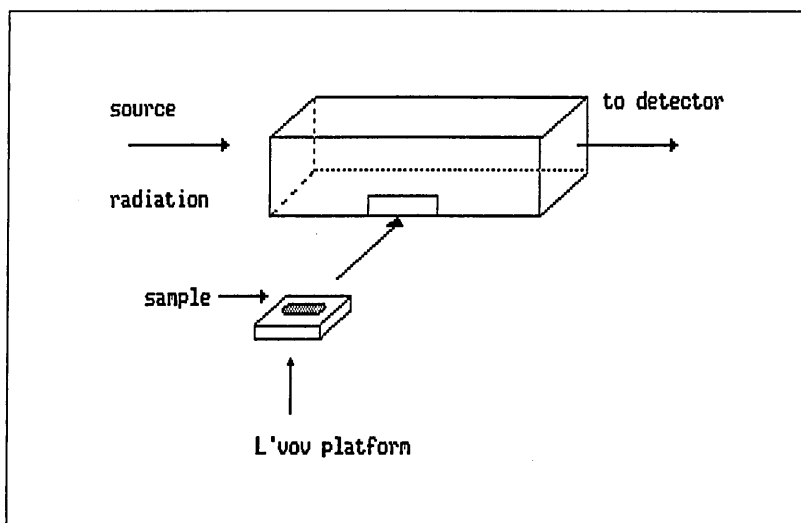
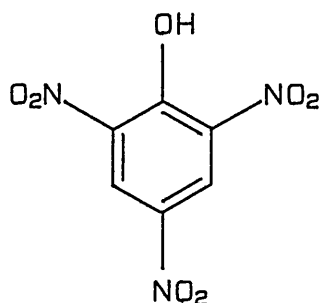


Figure 4.7(b) L'vov Platform and Furnace.

In the normal furnace, organic solvents are prone to "creeping" along the tube when heating begins. The L'vov platform contains a small cup in which the sample sits, reducing dispersion. By combining solvent extraction with matrix modification, physical enhancement and the use of an autosampler a 0.1 ppb limit of detection was achieved.

Pinel *et al* [18] obtained a limit of detection of 10 pgml^{-1} , or 0.01 ppb, as the organotin. The increase in sensitivity was made possible by two modifications to the method of Parks *et al* [17]. Firstly, the concentration step was improved by acidifying the aqueous sample and extracting with a tropolone solution (0.01% w/w in toluene). The second improvement was matrix modification with picric acid, Figure 4.8, rather than ammonium dichromate. Picric acid is a good oxidizing agent and is also miscible with toluene, which the dichromate is not.



**Figure 4.8 Picric Acid,
2,4,6-Trinitrophenol.**

Recovery of organotins from spiked samples was claimed to be good, but figures were not quoted. A concentration factor of approximately $200\times$ was reported for the extraction step.

Chamsaz and Winefordner [19] chemically modified the organotins and inorganic tin prior to solvent extraction. A solution of sulphuric acid, sodium iodide and ascorbic acid was added to the aqueous sample. Solvent extraction of the iodized organotins and inorganic tin was then carried out in benzene.

The authors used graphite tubes pyrolytically coated with molybdenum, tantalum, zirconium or tungsten salts. All the coated tubes provided greater sensitivity, (at least $3\times$), than the uncoated tube. It is thought that at atomization temperatures tin forms an involatile carbide, resulting in a lower than expected response. If the tube is coated with certain transition metals, these

will compete with tin, for the active carbon sites, thus increasing the observed signal. Tungsten and zirconium gave the best precision, with the former having the longest-life. The limit of detection is claimed to be sub-ppb, (as the organotin).

Apte and Gardener [20] attempted to develop an extraction method specific to tri-n-butyltin species. They found that adjusting the pH of the aqueous sample to greater than 8 reduced the amount of di-n-butyltin co-extracted. However, triphenyltin species were found to have very similar extraction behaviour to tri-n-butyltin species.

Apte and Gardener confirmed the findings of Chamsaz and Winefordner [19] with respect to the signal enhancement observed with tungsten coated tubes. The authors also claim that traces of water in the toluene extract increases the sensitivity, possibly by activating the tube surface in some way. A 4 ng l^{-1} , (4ppt), as tin, limit of detection is claimed.

A rather laborious concentration stage is reported by Chapman and Samuel [21] which begins by extracting five 1 litre aliquots of sample with a solution of tropolone in dichloromethane. After combining the extracts, concentrated acids are added and the mixture is fumed down to destroy the organic material. The residue is then taken up in sulphuric acid and analyzed for total tin.

An alternative method is also reported which allows speciation of n-butyltin compounds. The combined dichloromethane extracts, rather than being reduced with acid, are gently evaporated down to around 5 ml and then made up to 10 ml in a graduated flask. An aliquot of this solution is then evaporated down, almost to dryness, and then separated using reverse-phase paper chromatography. Treatment with trimethylpentane/acetic acid solution, drying, spraying with Catechol Violet and finally, irradiation with UV light, resulted in blue spots due to the organotins. To quantify the levels of tin, the chromatogram was cut up and the blue areas wet ashed as described previously.

The authors also noted that aqueous solutions of n-butyltins at the low ppm level made by dissolving the n-butyltin in a water miscible solvent followed by dilution with water may not be stable, especially at low temperatures.

Ferri *et al* [22] reported a preconcentration stage which relied not on liquid/liquid extraction, but adsorption of organotins on graphitized carbon black. The sample (up to a few litres) is pumped through a short column containing the graphite and the organotins are then eluted with a methanol/dichloromethane mixture. An enrichment factor of up to 80 000× was reported. Inorganic tin is not adsorbed onto the graphite and can be isolated from the eluent as a complex of pyrrolidinedithiocarbamate, see Figure 4.9, using solvent extraction.

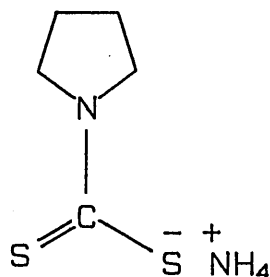


Figure 4.9 Ammonium Salt of 1-Pyrrolidinecarbodithioic Acid.

The tri-n-butyltin species were separated from the triphenyltin species on a short silica gel column. The former were then eluted with an n-hexane/ethyl acetate mixture (2:1) and the latter with ethyl acetate. The extracts were reduced in volume by warming and the residues taken up in acidified dichromate before analysis by GFAAS. A greater than 95% recovery of organotin species is claimed, with a limit of detection at the ng l^{-1} level and an error of $\leq 5\%$.

As has already been mentioned, AAS, and especially GFAAS, is a sensitive and selective technique. However, speciation of the organotins is not possible, unless a chromatographic separation precedes analysis. The paper by Ferri *et al* [22] reported such a procedure, but it was not an "on-line" method, *i.e.* there is no direct interface between the column and the furnace. Such interfacing requires specialized apparatus. One approach is to couple the GC column outlet to a quartz furnace, shown schematically in Figure 4.10;

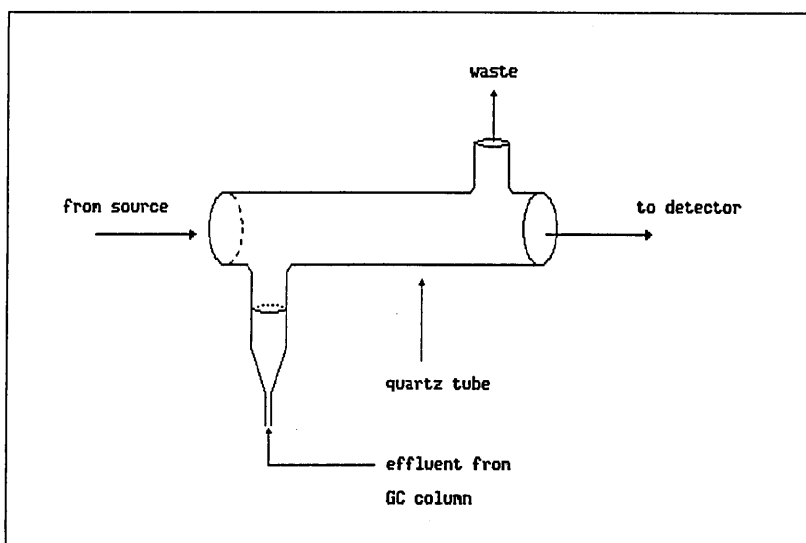


Figure 4.10 Schematic of GC Column/Quartz Tube Interface.

The quartz tube can be heated by a flame or electrothermally *via* heating coils wrapped around the furnace.

Clark *et al* [23] detailed a method based upon solvent extraction, hydride generation, GC separation and detection by quartz furnace AAS. The aqueous sample (100 cm³) is extracted with dichloromethane (20 cm³) containing tropolone and an internal standard, tripropyltin chloride. The organic extract is evaporated to dryness, acidified with HCl and taken up in ethanol. Aliquots of this mixture were then injected onto a GC column, the top of which is doped with solid NaBH₄. The n-butyltin species present and the internal standard are converted to the respective stannanes, which are separated as they pass through the column. The effluent flows into the quartz furnace where the tin species are detected (at low ppb level).

Astruc and Desauziers *et al* [24,25] compared two methods for determining tri-n-butyltin species in marine sediments. The first consisted of an acetic acid extraction/hydride generation/GC/quartz furnace AAS method, the second toluene-tropolone extraction/HPLC/GFAAS.

The hydride generation stage is achieved not on-column but in a reaction vessel where a solution of NaBH_4 is added to the acid extract. The resulting stannanes volatilize under reaction conditions and are purged from the vessel. A pyrex tube with an OV-101 stationary phase at 80K traps the purged stannanes. After a suitable trapping time the tube is heated, releasing successive stannanes into the quartz cell (electrically heated to 950°C). Limits of detection are in the low ppb range.

In the second method, the sample is shaken with a tropolone solution for an extended period (15 hours), after which the mixture is filtered and evaporated to 2 cm^3 . This aliquot is then injected into an HPLC, the separated organotins passing to an on-line GFAAS. The limit of detection is slightly higher than that of the previous method. The two independent techniques provided coherent results for various sediment samples.

Stallard *et al* [26] presented methods for determining sub-part per trillion, ppt, levels of n-butyltins in water (and sub-ppb levels in tissue and sediment). No sample preconcentration was performed, the aqueous aliquot being placed in a modified gas wash bottle. Sodium borohydride solution was then injected into the bottle, the stannanes evolved being purged and trapped at 80K on an OV-1 stationary phase. After trapping, the column was subjected to controlled heating to volatilize the stannanes. The lowering of the detection limit was due to the use of closed quartz tubes rather than the open-ended type normally employed. Stallard *et al* also experimented with the geometry of the tube/column interface and found it to be sensitive to the observed signal. Optimization of the geometry resulted in an longer residence time of the analyte in the lightpath and hence the improved limit of detection.

Alternative techniques have been reported by Maguire and Huneault [27] and Müller [28]. Both papers suggest the use of Grignard reagents, rather than hydride generation, to provide volatile tin species. The organotins are separated using a GC column which is interfaced to a flame photometric detector, FPD (*i.e.* AAS/AES).

On-line interfacing of HPLC/GFAAS is reported by Jewitt and Brinckman [29] and Nygren *et al* [30]. The use of HPLC means that the organotins can be separated as the ionic species, *i.e.* no derivatization is needed. Nygren *et al* reported a detection limit of 0.5 ng for tri-n-butyltin species with a linear response between 1 and 100 ng.

Krull *et al* [31] showed that it was possible to separate underivatized n-butyltins using GC. Detection of the tin species was accomplished by simultaneous FPD and direct current plasma AES, DCPAES. The latter is shown schematically in Figure 4.11:

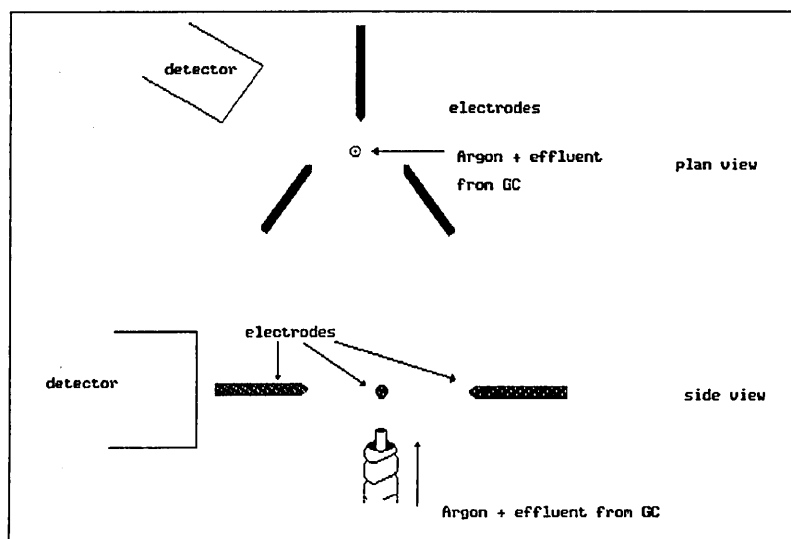


Figure 4.11 Schematic of DCPAES Arrangement.

An argon plasma is maintained between three electrodes. The effluent passes into the plasma and the intensity of the emission line at 303 nm is recorded by the detector. In FPD, the 365 nm emission line is monitored.

The authors used the technique to quantify n-butyltin levels in fish tissue, after an extraction stage. The limit of detection is reported to be around 5 ppb.

Brindle and Le [32] used a hydride generation/purge and trap/DCPAES technique to determine trace levels of tin in metallurgical samples. Transition metal interference was reduced if L-cysteine was present in the analyte solution.

4.2.5. Combined Gas Chromatography/Mass Spectrometry, GC/MS

It is clear from the preceding section that GC provides the analyst with a good technique for the separation of organotins. The use of a mass spectrometer as the GC detector allows quantification of the organotin species themselves and at detection limits comparable to the most sensitive AAS methods.

Gilmour *et al* [33] described a method for the detection of pg levels of methyltin compounds in sediments. The sample is derivatized in a hydride generator and the evolved stannanes are trapped cryogenically at the head of the GC column. Controlled heating resulted in the separation of the organotins and these were detected by the MS in the selected ion monitoring (SIM) mode at m/z 116, 118, 120, $[\text{Sn}]^+$, m/z 133, 135, $[\text{MeSn}]^+$, m/z 150, $[\text{Me}_2\text{Sn}]^+$ and m/z 165, $[\text{Me}_3\text{Sn}]^+$. Et_2SnCl_2 is used as an internal standard.

Because of the high sensitivity of the technique it is essential to use plastic equipment which does not contain organotin stabilizers.

Ruthenberg and Madetzki [34], in fact, developed a technique for the determination of two PVC stabilizers *viz*, mono- and dioctyltin chloride (MOTC and DOTC). It was thought that these compounds might diffuse out of the plastic used in food wrappings and pass into the human gut. Toxicological studies were carried out and a sensitive detection method was required.

The authors proposed a diethyl ether extraction from an acidified sample followed by the established hydride generation/purge and trap/GC method. However, it was found that the octyltin hydrides were not formed. A competitive reaction was thought to occur and tin-free aliphatic octyl species were detected. Butylation with a Grignard reagent proved successful and SIM monitoring at m/z 179 ($[(\text{C}_4\text{H}_9)_2\text{SnH}_2]^+$, the internal standard), m/z 347 $[(\text{C}_4\text{H}_9)_2\text{SnC}_8\text{H}_{17}]^+$, and m/z 403 $[\text{C}_4\text{H}_9\text{Sn}(\text{C}_8\text{H}_{17})_2]^+$, was carried out. Limits of detection were 5 ngml^{-1} for MOTC and 50 ngml^{-1} for DOTC.

Hugget *et al* [35] determined trace levels of tri-n-butyltin compounds in seawater, sediment and tissue. Extraction from (acidified) seawater with n-hexane/tropolone was followed by derivatization with n-hexylmagnesium

bromide and GC separation. Detailed experimental procedure is not reported, but a detection limit of $<1 \text{ ng l}^{-1}$ is claimed. The authors also report that most commercial supplies of Grignard reagents are contaminated with organotins, some by as much as several mg kg^{-1} .

The identification and quantification of tri-n-butyltin and its degradation products in seawater by GC/MS is reported by Greaves and Unger [36]. The usual solvent extraction/Grignard derivatization/GC method was used, followed by full scanning MS to identify all tin species. The retention times and observed m/z peaks were: tri-n-butyltin t_R 12 min, m/z 291 $[\text{Bu}_3\text{Sn}]^+$ and m/z 319 $[\text{Bu}_2\text{SnHex}]^+$; di-n-butyltin t_R 18 min, m/z 319 $[\text{Bu}_2\text{SnHex}]^+$ and m/z 347 $[\text{BuSnHex}_2]^+$; internal standard, tripropyltin t_R 21 min, m/z 347 $[\text{Pen}_2\text{SnHex}]^+$ and mono-n-butyltin t_R 23 min, m/z 347 $[\text{BuSnHex}_2]^+$ and m/z 375 $[\text{SnHex}_3]^+$. By using SIM at m/z 347, di- and mono-n-butyltins can be quantified (by comparison with tripropyltin), and followed by SIM at m/z 319 to quantify tri-n-butyltin (by comparison with di-n-butyltin). A limit of detection of $<2 \text{ ng l}^{-1}$ for the organotins is reported.

Krone *et al* [37] used a very similar methodology to that of Greaves and Unger [36] to determine the full range of n-butyltins in sediments and fish tissue. Tri-n-butyltin levels were determined by Hannah *et al* [38], again with a similar extraction/derivatization/GC/MS methodology. Significant levels of organotins were found by both groups of workers in the sediment and tissue samples.

4.3. Release-Rate Study

The technique adopted for the determination of organotins in the flow system effluent in this study was GFAAS. The method of Parks *et al* [17] was tried initially. However, it was found that addition of propan-2-ol to the toluene extract/aqueous dichromate did not result in a homogeneous solution, which resulted in rather poor results when compared to those of Parks *et al*. Also, the use of manual injection rather than by autosampler, decreased the precision limits.

Subsequently, the paper by Pinel *et al* [18] was published, using the toluene-tropolone extraction and picric acid matrix modifier. This method was adapted for use in the present study. The procedure for determining the tin content of the flow system effluent was as follows:

(i) preparation of aqueous tri-n-butyltin chloride standards, typically 0.0, 0.5, 2.5 and 5.0 ppb (as Sn) from a stock solution of tri-n-butyltin chloride in methanol (2.74g tri-n-butyltin chloride in 1000.0g methanol \equiv 1 part per 1000 as Sn).

(ii) extraction of acidified (2M HCl, 10 ml) standards, control and samples (all 500 ml) with tropolone solution (0.01% w/w in spectroscopic grade toluene, 5 ml). This consisted of mechanical shaking for 30 minutes and standing for 15 minutes. The majority of the aqueous layer was then discarded and the remaining mixture was transferred to a smaller (30 ml) separating funnel for a further 15 minutes. The aqueous layer was discarded and the toluene extract was dried in a phial with anhydrous sodium sulphite (1.0g).

(iii) after drying (20 minutes), the toluene extract was decanted into a clean beaker (5 ml) and made up to 4.50g with spectroscopic grade toluene. Prior to analysis, picric acid solution (5% w/w in spectroscopic grade toluene, 200 μ l) was added. This mixture was pipetted (20 μ l) into the L'vov platform and placed in the furnace.

(iv) instrumental operating conditions:

Parameter	Drying		Ashing		Atomization	
	1	2	3	4	5	6
Step Number	1	2	3	4	5	6
Temperature/ $^{\circ}$ C	150	200	700	750	2350	2350
Time/s	5	15	5	15	0	5

Instrument: IL 555 Temperature controller/IL 157 AAS.

Gas flow: 20 psi N₂

Integration time: 0.75 s

Lamp current: 5.5 mA

Integration mode: peak height

Lamp voltage: 800V

Clean stage: off

Wavelength: 235.5 nm

Bandwidth: 1.0 nm

The conditions described above differ slightly from those described in the paper, but were found to provide better sensitivity with the instrumentation used (which was dissimilar to that employed by Pinel *et al*).

(v) the average of five replicate readings was calculated for each standard/sample extract. A graph of tin concentration against absorbance was plotted and the samples were then quantified.

It was essential to perform daily calibration curves since the conditions of the furnace and platform are constantly altering (albeit slightly) with every run. A typical calibration curve is shown in Figure 4.12:

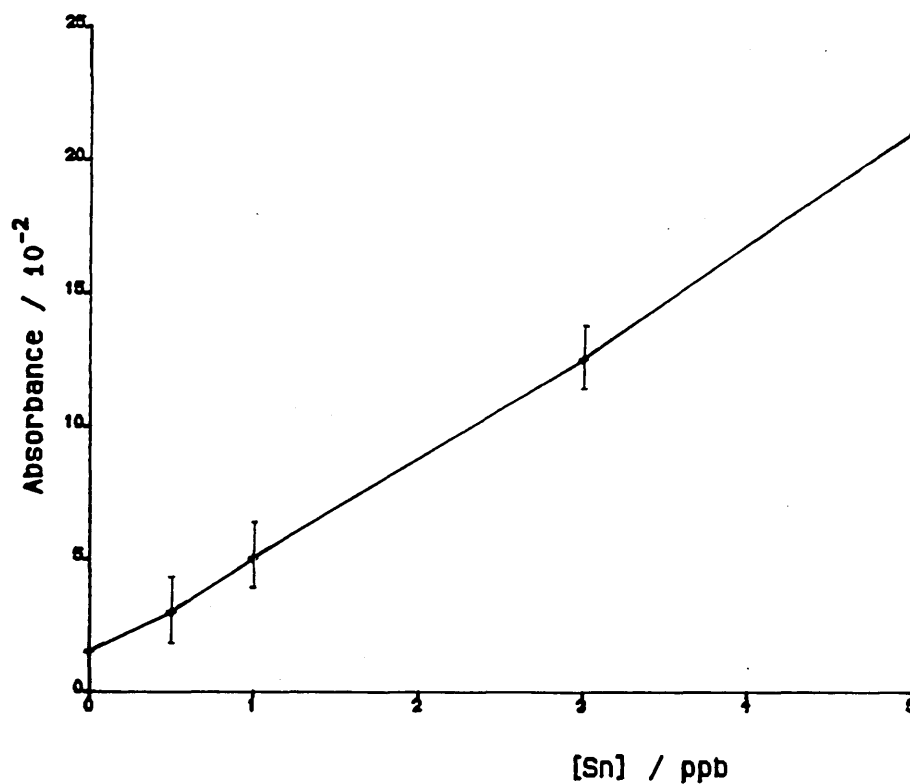


Figure 4.12 Plot of Tin Concentration Against Absorbance at 235.5 nm.

A limit of detection of 0.2 ppb was possible with an associated error of $\pm 10\%$. This compares rather poorly with Pinel *et al* [17] whose limit of detection was 0.01 ppb, but whose analyses were performed on superior instrumentation. Due to the number of samples, each paint was analyzed using the flow rate apparatus for the first five days and then transferred to a 600 ml beaker. The water (500 ml, double distilled) was changed daily. Plots of release-rates against time were collected for the eight samples and are shown in Figures 4.13 to 4.16.

The samples contained the following amounts of biocides, in g per 100g of wet paint:

Code	Bis-(Tri-n-Butyltin) Oxide	Tri-n-Butyltin Acetate	Diuron*
1A	0.04	0.04	0.00
1B	0.04	0.04	0.00
2A	0.04	0.04	0.04
2B	0.04	0.04	0.04
3A	0.10	0.10	0.00
3B	0.10	0.10	0.00
4A	0.10	0.10	0.10
4B	0.10	0.10	0.10

* Diuron is a pre-emergence biocide, see Figure 4.17:

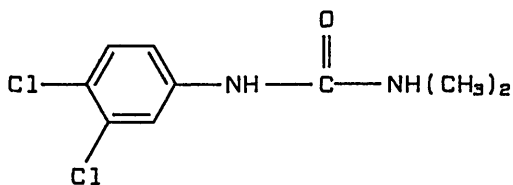


**Figure 4.17 Diuron,
3-(3,4-Dichlorophenyl)-1,1-
Dimethylurea.**

The "A" samples were allowed eight hours between coatings, whereas the "B" samples were touch dry when the second coat was applied.

4.3.1. Determination of Release-Rates

For the first five days of analysis, the paint samples (5 cm^2) were in the flow system operating at 120 mlh^{-1} . It took, therefore, 4.17 hours to collect the 500 ml required for analysis. The paint sample was 5 cm^2 , so overall a factor of $0.23\times$ on the observed level, in ppb, was needed to provide units of $\text{ppbSn/cm}^2/\text{day}$.

When the samples were placed in the static beaker system, the collection time was 24 hours and so observed ppb values were multiplied by 0.04 to provide units of $\text{ppbSn/cm}^2/\text{day}$. The limit of detection is indicated by a continuous line which is lower after the first five days due to the longer sampling time. All reported data is corrected against blank levels.

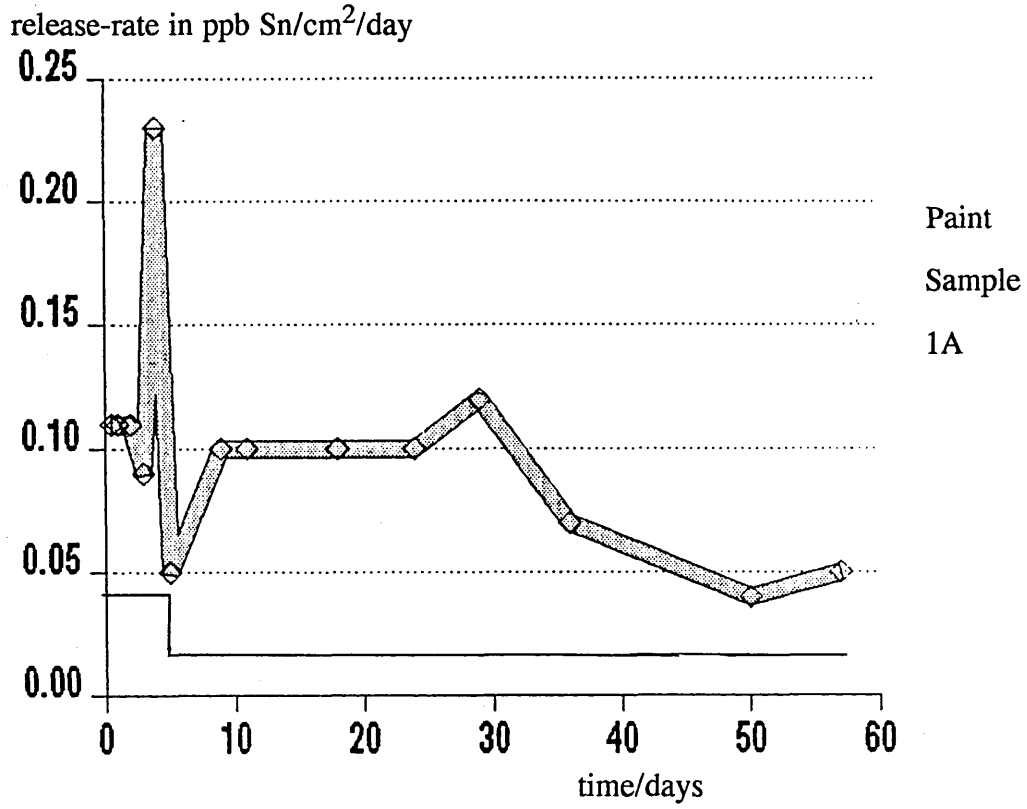
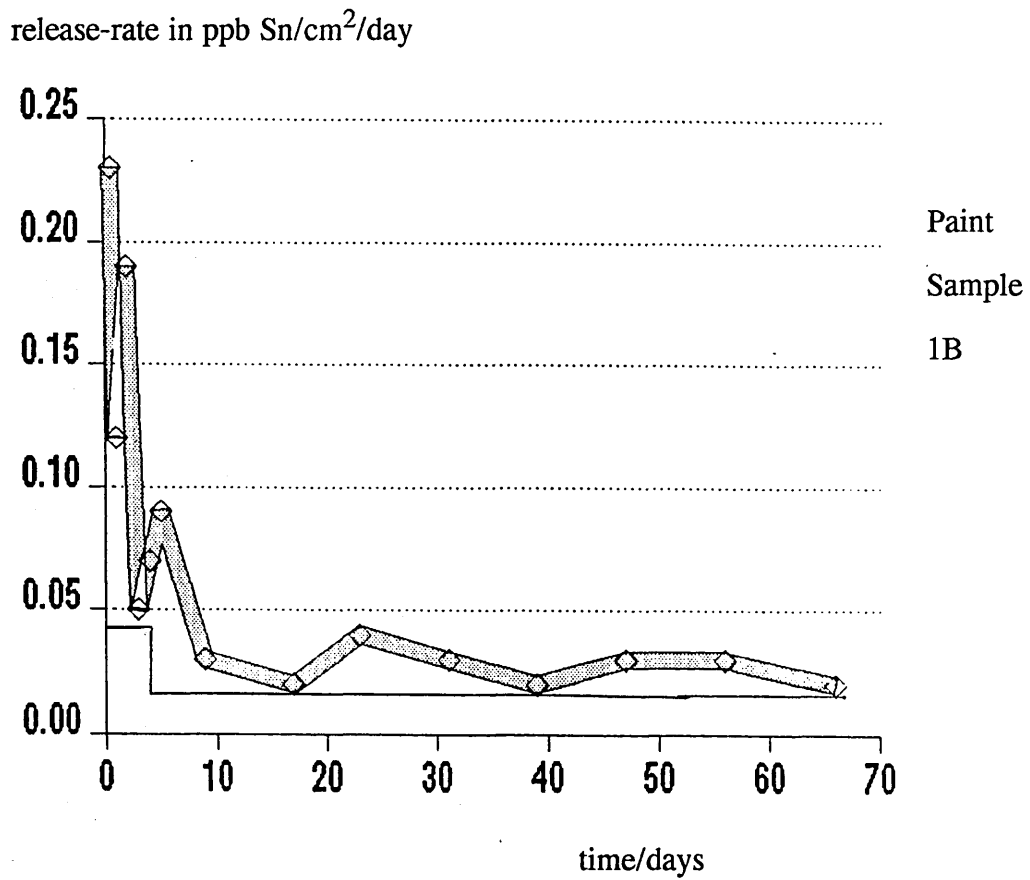


Figure 4.13 Organotin Release-Rates from Paint Samples 1A and 1B.



release-rate in ppb Sn/cm²/day

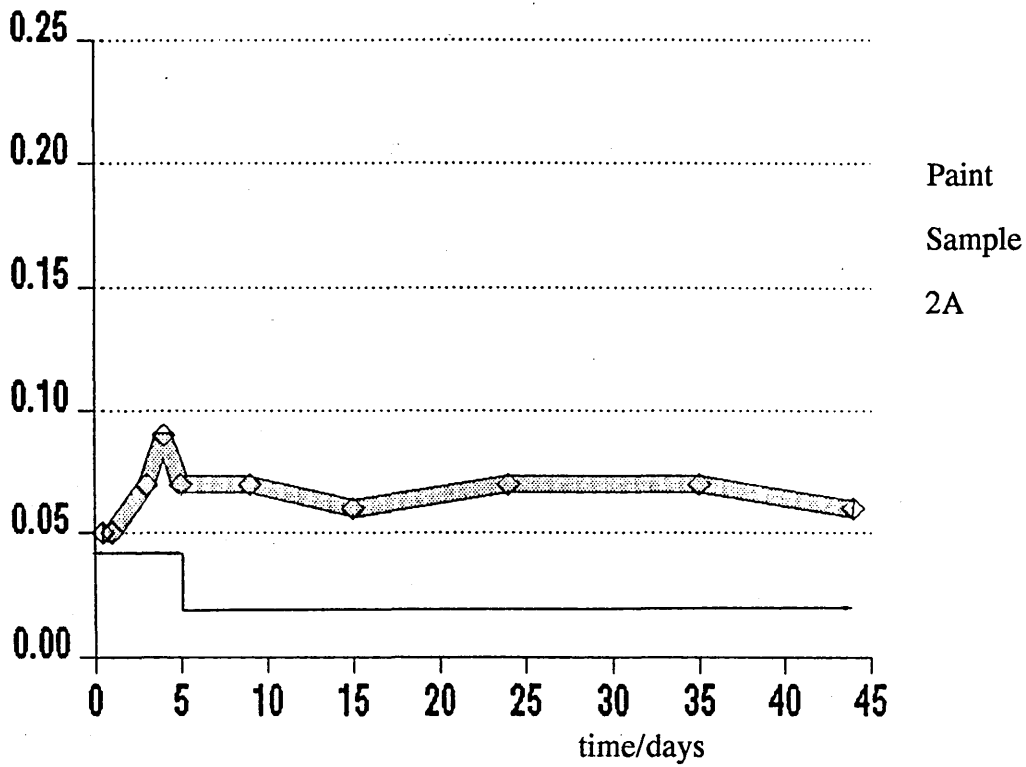
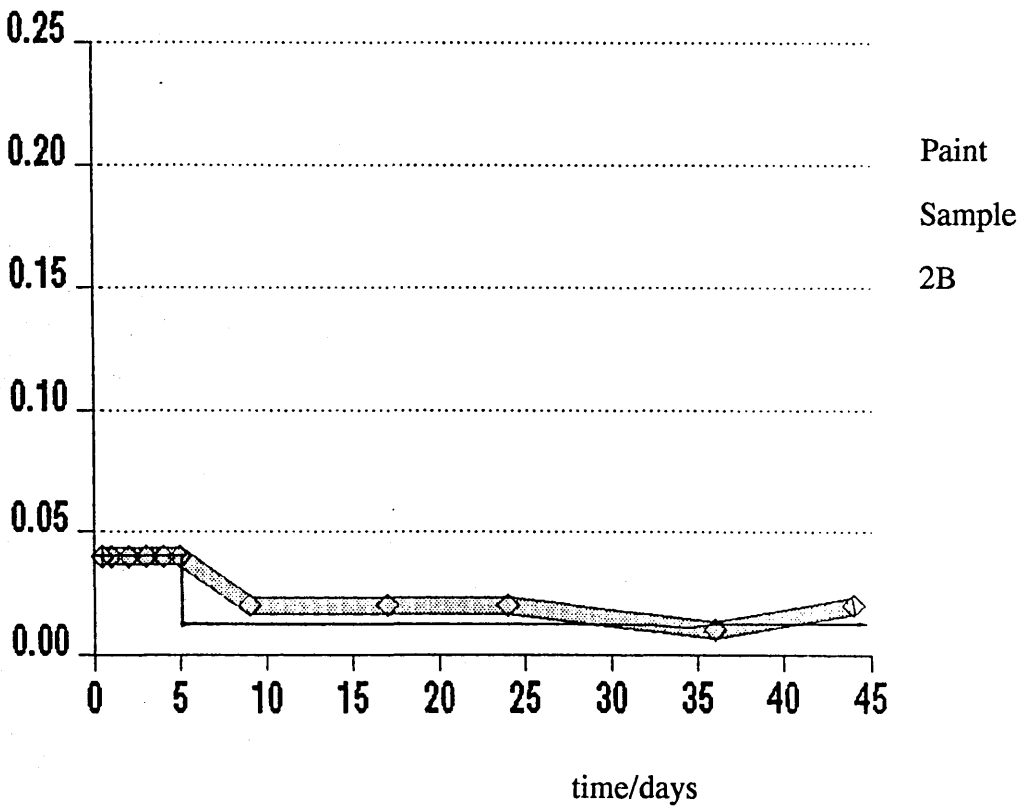


Figure 4.14 Organotin Release-Rates from Paint Samples 2A and 2B.

release-rate in ppb Sn/cm²/day



release-rate in ppb Sn/cm²/day

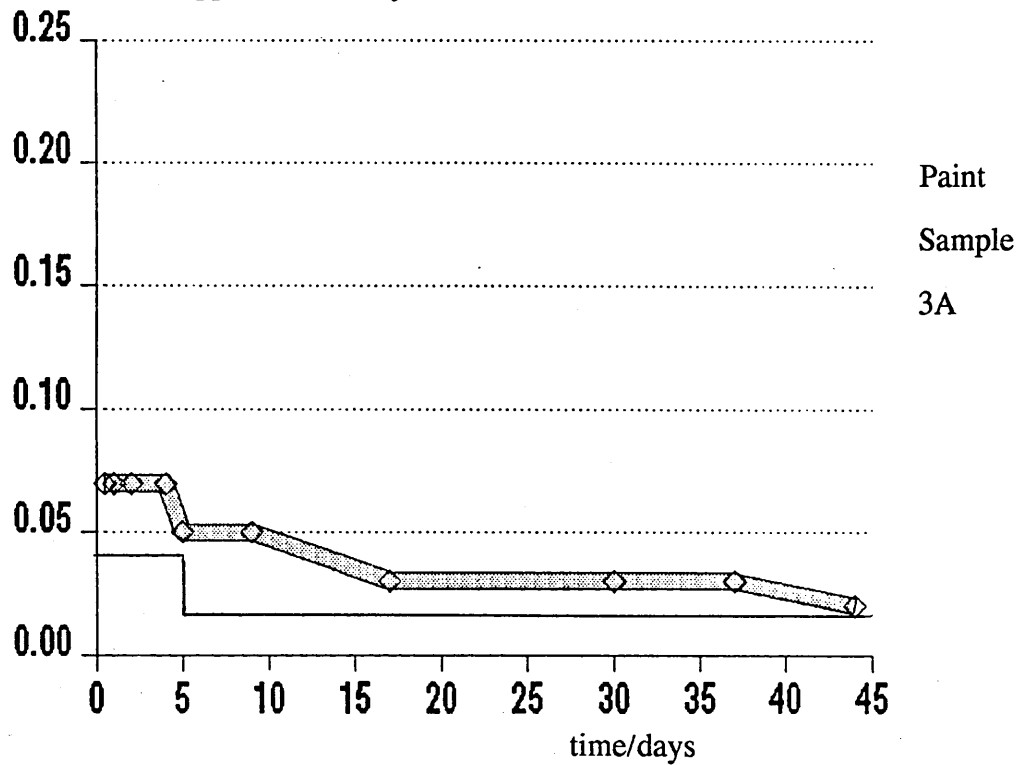
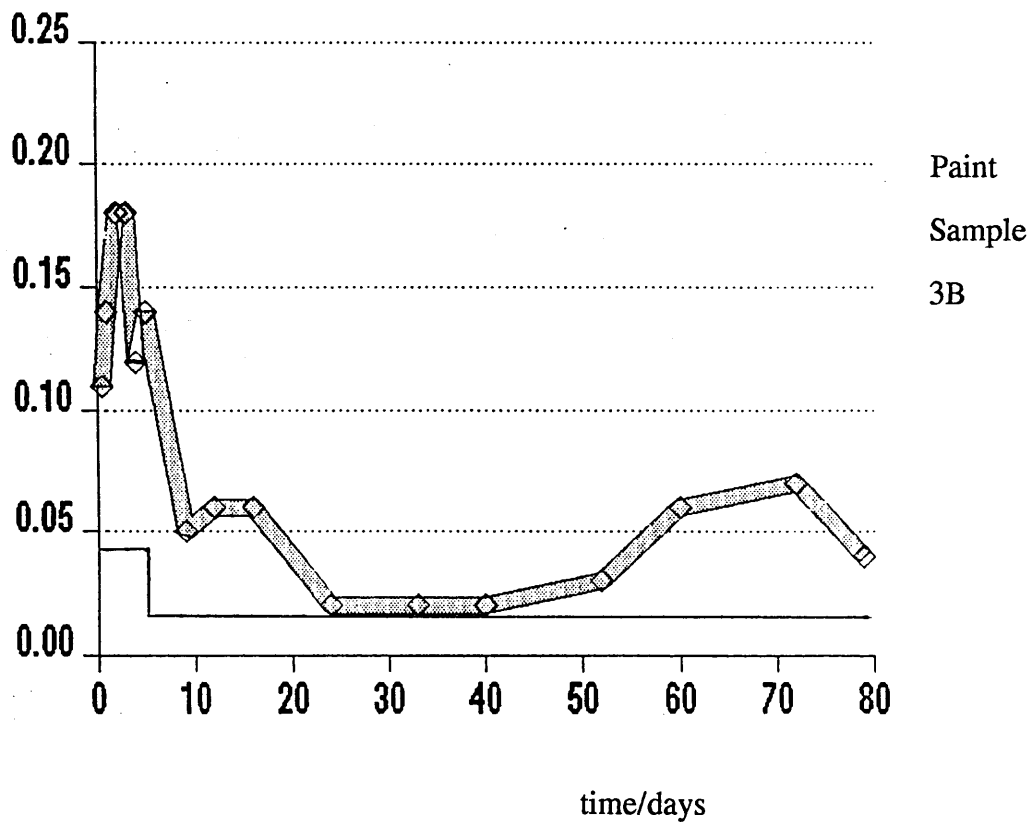


Figure 4.15 Organotin Release-Rates from Paint Samples 3A and 3B.

release-rate in ppb Sn/cm²/day



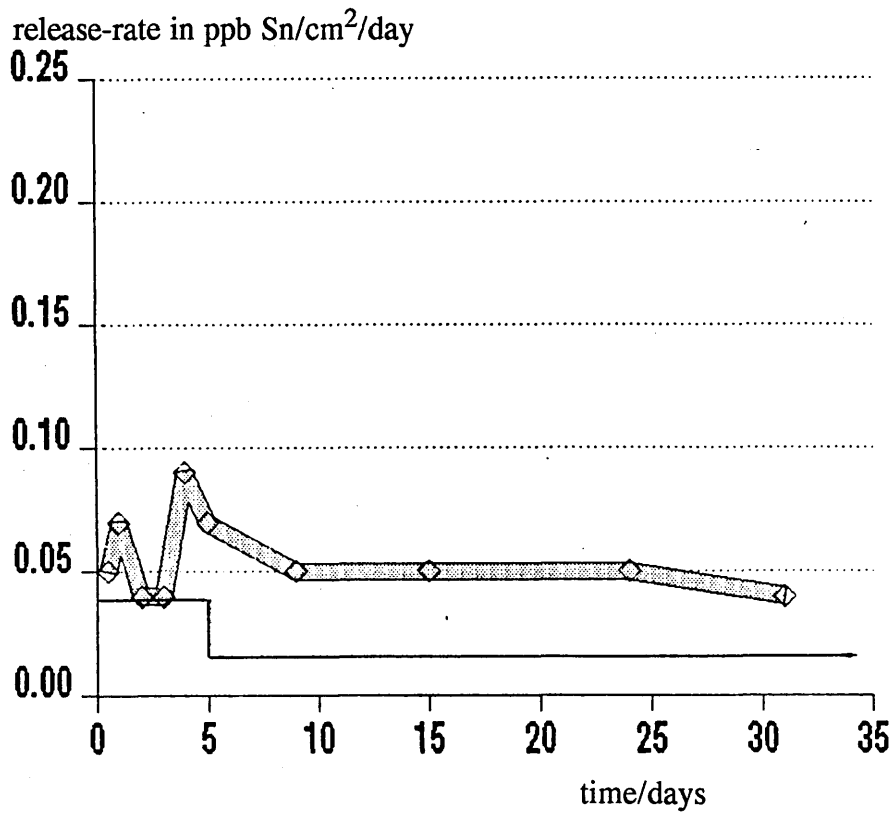
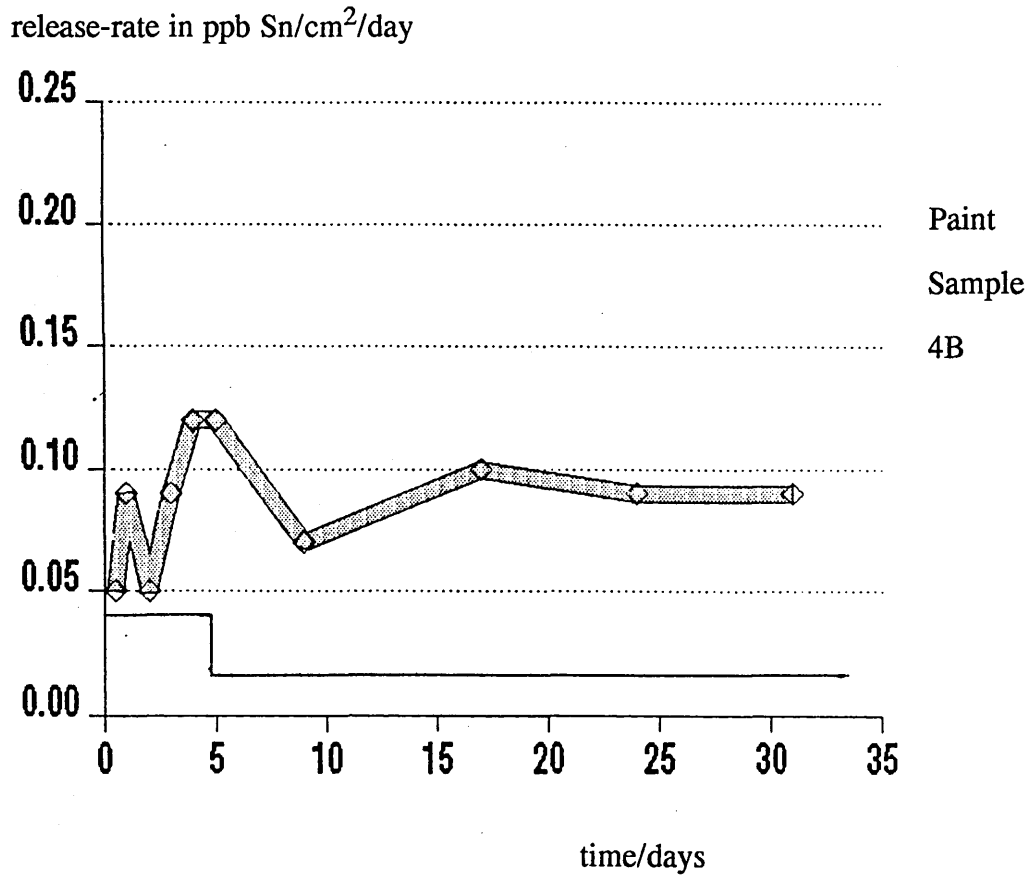


Figure 4.16 Organotin Release-Rates from Paint Samples 4A and 4B.



4.4. Discussion of Release-Rate Results

All the paint samples had similar release-rate levels, at around 0.05–0.10 ppb Sn/cm²/day, which is equivalent to approximately 0.05 μgSn/cm²/day. A figure of 5 μgSn/cm²/day (as *bis*-(tri-*n*-butyltin) oxide) has been claimed as the minimum value required to prevent fouling [39]. The eight paints studied are unlikely, therefore, to offer any significant protection against marine fouling, although raft panel tests are needed to confirm this finding.

The low release-rates observed for the eight samples may be due to the low organotin levels initially incorporated into the paints. However, it has been shown in Chapter 3 that Soxhlet extraction of the paints and subsequent analysis of the extracts by ¹¹⁹Sn NMR resulted in spectra with weak signals. It is proposed that some coordinate bonding of the organotins and their transformation products is occurring within the paint, which may be largely responsible for the low release-rates of the biocides.

Chapter 4 References.

1. Bollinger, E.H., Proc. 1stContr. Rel. Pestic. Symp. Akron, 1974, 19.1-19.10.
2. De la Court, F.H., J. Polym. Paint Col., 1988, 178, 494.
3. Gitlitz, M.H., J.Coat. Technol., 1981, 53, 678, 46.
4. Christie, A.O., J. Oil Col. Chem., 1977, 60, 348.
5. Blunden, S.J., Cusack, P.A. and Hill, R., The Industrial Uses of Tin Chemicals, The Royal Society of Chemistry, 1985, Chapter 4.
6. Bond A.M. and McLachlan, N.M., Anal. Chim. Acta, 1988, 204, 151.
7. Van den Berg, C.M.G., Khan, S.H. and Riley, J.P., Anal. Chim. Acta, 1989, 222, 43.
8. Carter, R.J., Turoczy, N.J. and Bond, A.M., Environ. Sci. Technol., 1989, 23, 615.
9. Ebdon, L., Hill, S. and Jones, P., Analyst, 1985, 110, 515.
10. Ebdon, L. and Garcia-Alonso, J.I., Analyst, 1987, 112, 1551.
11. Langseth, W., J. Chromatogr., 1984, 315, 351.
12. Whang, C.W. and Yang, L-L., Analyst, 1988, 113, 1393.
13. Tomboulian, P., Walters, S.M. and Brown, K.K., Mikrochim. Acta, 1987, II, 11.
14. Brown, K.K. Tomboulian, P., Walters, S.M., J. Res. Nat. Bur. Stand., 1988, 93, (3), 301.
15. Burns, D.T., Dadgar, D. and Harriot, M., Analyst, 1984, 109, 1099.
16. Donaghy, C., Harriot, M. and Burns, D.T. Anal. Proc., 1989, 26, 260.
17. Parks, E.J., Blair, W.R. and Brinckman, F.E., Talanta, 1985, 32, 633.
18. Pinel, R., Benabduallah, M.Z., Astruc, A. and Astruc, M., J. Anal. Atomic Spec., 1988, 3, 475.
19. Chamsaz, M. and Winefordner, J.D., J. Anal. Atomic Spec., 1988, 3, 119.
20. Apte, S.C. and Gardener, M.J., Talanta, 1988, 35, 7, 539.

21. Chapman, A.H. and Samuel, A., Appl. Organomet. Chem., 1988, 2, 73.
22. Ferri, T., Cardarelli, E. and Petronio, B.M., Talanta, 1989, 36, 4, 513.
23. Clark, S., Ashby, J. and Craig, P.J. Analyst, 1987, 112, 1781.
24. Astruc, A. Lavigne, R. Desauziers, V., Pinel, R. and Astruc, M., Appl. Organomet. Chem., 1989, 3, 267.
25. Desauziers, V., Leguille, F., Lavigne, R., Astruc, M. and Pinel, R., Appl. Organomet. Chem., 1989, 3, 469.
26. Stallard, M.O., Cola, S.Y. and Dooley, C.A., Appl. Organomet. Chem., 1989, 3, 105.
27. Maguire, R.J. and Huneault, H., J. Chromat., 1981, 209, 458.
28. Müller, M.D., Anal. Chem., 1987, 59, 617.
29. Jewett, K.L. and Brinckman, F.E., J.Chromat. Sci., 1981, 19, 583.
30. Nygren, O., Nilsson, C.A. and Frech, W., Anal. Chem., 1988, 60, 2204.
31. Krull, I.S., Panaro, K.W., Noonan, J. and Erickson, D., Appl. Organomet. Chem., 1989, 3, 295.
32. Brindle, I.D. and Le, X-C., Analyst, 1988, 113, 1377.
33. Gilmour, C.C., Tuttle, J.H. and Means, J.C., Anal. Chem., 1986, 56, 1848.
34. Ruthenberg, K. and Madetzki, C., Chromatographia, 1988, 26, 251.
35. Hugget, R.G., Unger, M.A., Espourteille, F.A. and Rice, C.D., J. Res. Nat. Bur. Stand., 1988, 93, (3), 277.
36. Greaves, J. and Unger, M.A., Biomed. Environ. Mass Spectro., 1988, 15, (10), 565.
37. Krone, C.A., Brown, D.W., Burrows, D.G., Bogar, R.G., Chan, S-L. and Varansai, V., Mar. Environ. Res., 1989, 27, (1), 1.
38. Hannah, D.J., Page, T.L., Pickston, L. and Taucher, J.A., Bull. Environ. Contam. Toxicol., 1989, 43, 22.
39. De la Court, F.H. and De Vries, H.J., Proc. 4th Int. Congress Marine Corrosion and Fouling, 1976, 113.

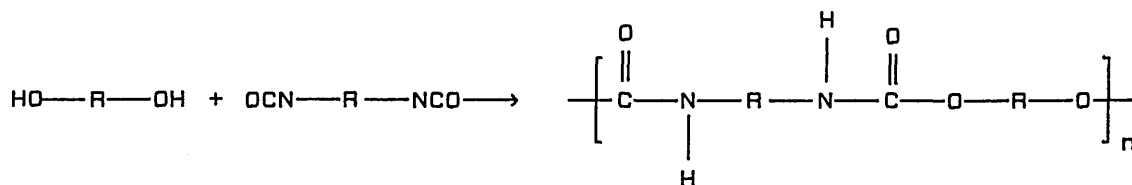
5. Polyurethanes As Antifouling Coatings

5.1. Introduction

Polyurethanes can take the form of rigid plastics, elastomers, foams of various densities and even threads. All polyurethanes are based on the exothermic reaction of polyisocyanates with polyols. Only a few isocyanates and a range of polyols with different molecular weights and functionalities are required to manufacture the full range of polyurethanes [1]. To date there is no literature evidence of polyurethanes being used^{as} antifouling coatings.

5.2. Chemistry of Polyurethane Formation

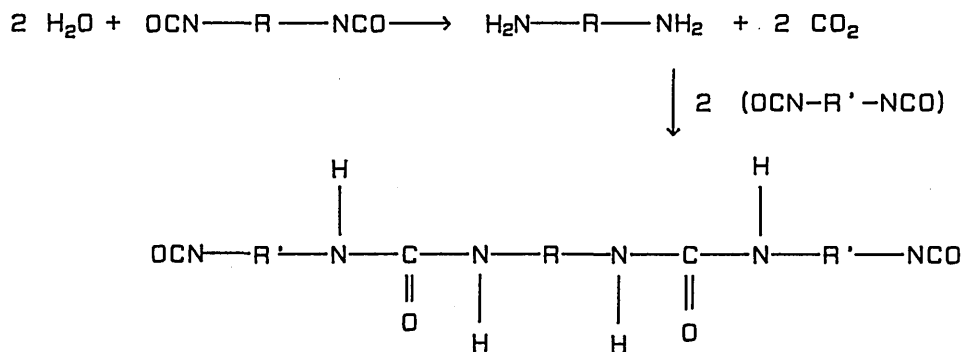
Polyurethanes are addition polymers formed by the reaction of di- or polyisocyanates with polyols, see Reaction 5.1:



Reaction 5.1 Formation of Polyurethanes.

The reaction is exothermic and its rate depends upon the structure of the polyol and the isocyanate. Aliphatic polyols with primary hydroxyl groups react about 10× faster than polyols with secondary hydroxyl groups. Phenols react more slowly still and on heating the reaction is reversed.

Isocyanates also react with water to yield a substituted urea and carbon dioxide. This reaction provides the gas for "blowing" in the manufacture of low density foam. The reaction, which yields a diisocyanatopolyurea, is shown overleaf:



Reaction 5.2 Reaction of Water with a Diisocyanate.

Diisocyanates with similarly reactive $-\text{NCO}$ groups such as 4,4'-diisocyanatophenylmethane, MDI, and *p*-phenylenediisocyanate, yield complex crystalline polymeric ureas. However, below 50°C , 2,4-toluenediisocyanate, 2,4-TDI, yields a dimeric urea, see Figure 5.1:

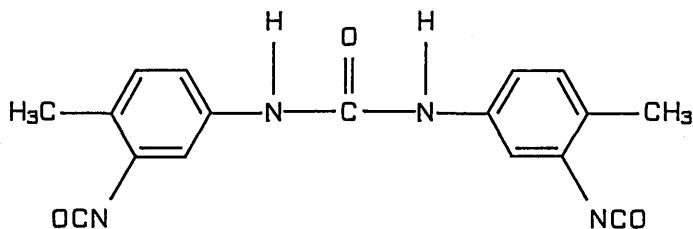
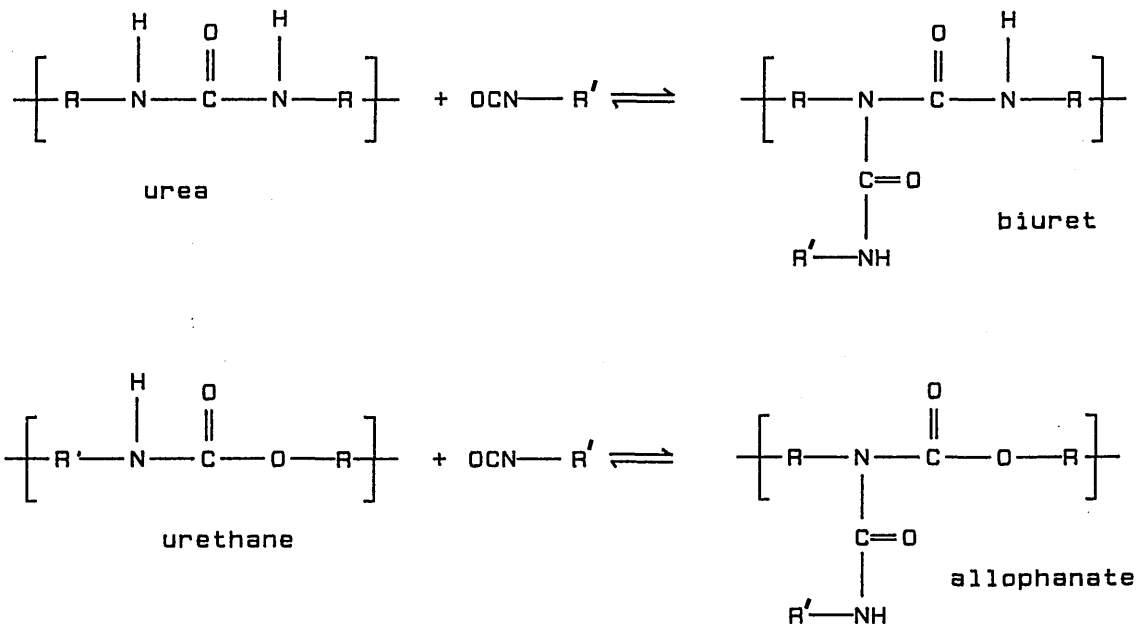


Figure 5.1 Dimeric Urea of 2,4-TDI.

As shown in Reaction 5.2, isocyanates react with amines and this reaction is important in polyurethane chemistry since diamines are used as chain extenders. The reaction of sterically hindered isocyanates with 1° amines at 25°C , in the absence of catalysts, is $\approx 100-1000\times$ faster than the reaction with 1° alcohols. Reactivity increases with the basicity of the amine. 3° amines do not react with isocyanates, but are catalysts for other isocyanate reactions.

5.2.1. Secondary Reactions

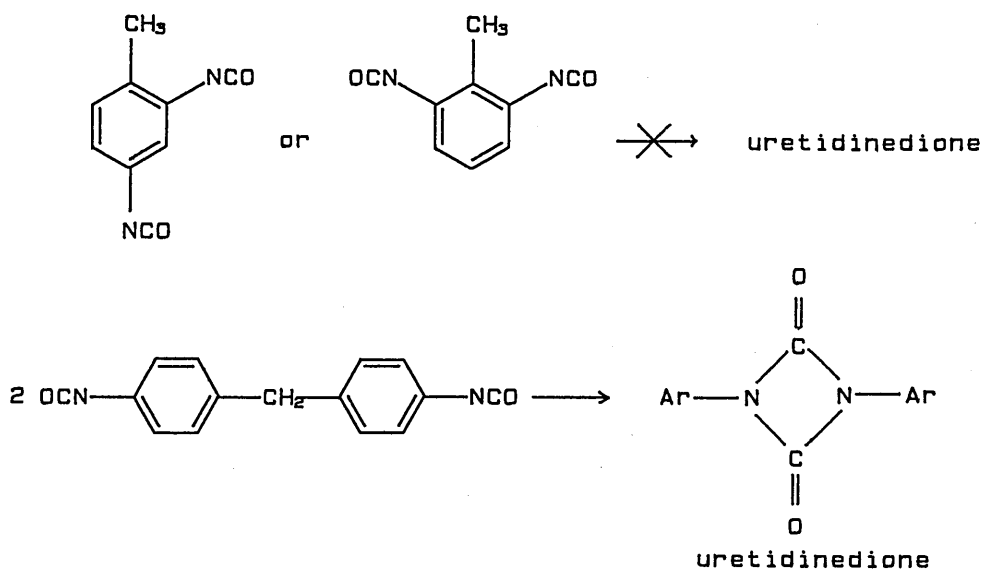
Isocyanates may react with active protons of the urethane and urea linkages to yield allophanates and biurets respectively, see Reaction 5.3. Both products result in an increase in polymer cross-linking.



Reaction 5.3 Formation of Allophanate and Biuret Linkages.

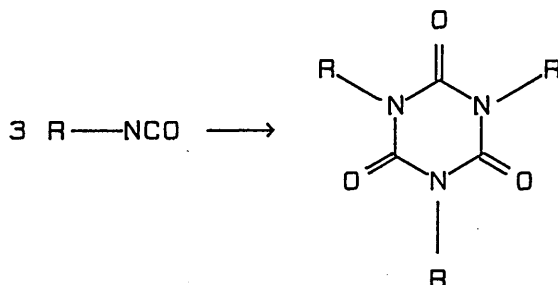
5.2.2. Isocyanate Polymerization Reactions

Isocyanates form oligomers, especially in the presence of basic catalysts to yield uretidinediones (dimers) and isocyanurates (trimers). Dimerization is restricted to aromatic isocyanates and is inhibited by *ortho*-substituents, see Reaction 5.4:



Reaction 5.4 Uretidinedione Formation.

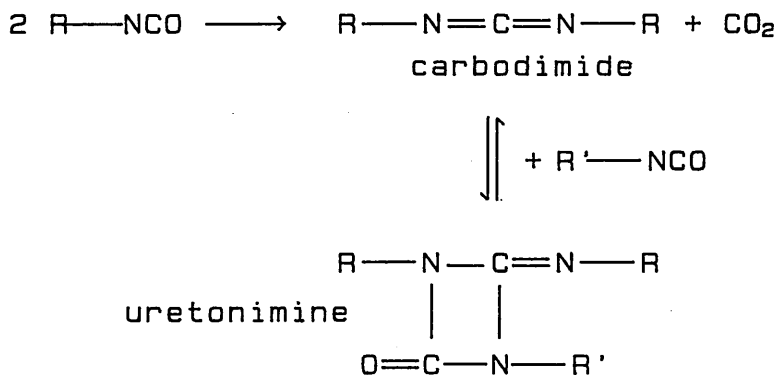
Isocyanurates form when aliphatic or aromatic isocyanates are heated:



Reaction 5.5 Isocyanurate Formation.

Isocyanurate formation in polyurethane manufacture is important since it provides very stable branch points, which unlike uretidinediones and allophanates, are thermally stable (isocyanurates in MDI or TDI foams show little degradation below 270°C).

In the presence of certain catalysts, isocyanates can condense with the elimination of carbon dioxide and a carbodiimide is produced. The latter can react (reversibly) with more isocyanate to yield a uretonimine:



Reaction 5.6 Uretonimine Formation.

All the reactions described so far are exothermic.

5.2.3. Cross-Linking Reactions

The structure of polyurethanes varies from rigid cross-linked polymers, to linear, highly extendable elastomers, see Figure 5.2.

Flexible foams and many elastomers have segmented structures consisting of long flexible chains, polyether or polyester oligomers, joined by relatively rigid aromatic polyurethane or polyurea segments. The physical properties depend largely on 2° or H-bonding of polar groups in the polymer chains, (N—H \rightarrow C=O groups of urethane and urea linkages). N—H groups can also H-bond with polyester C=O groups.

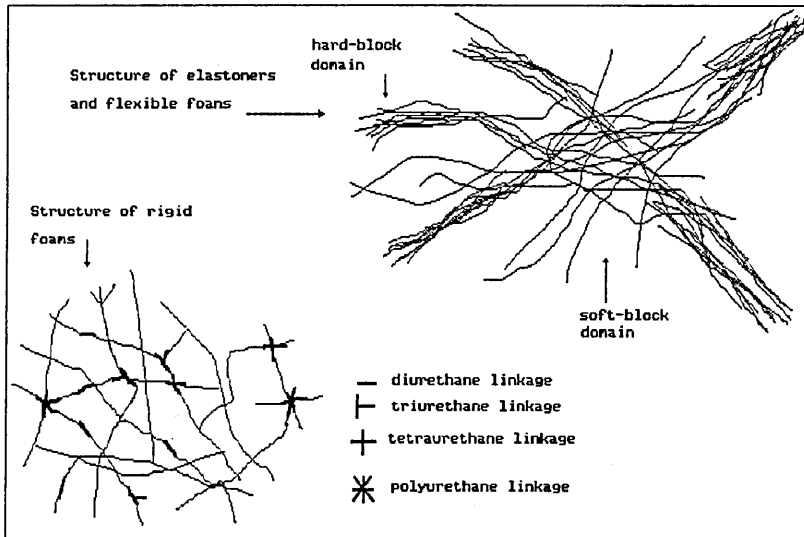


Figure 5.2 Schematic of Polyurethane Structure.

Rigid polyurethanes, in contrast, have a high degree of cross-linking. This results from the use of branched starting materials, such as polyfunctional alcohols, amines and isocyanates. Also, the use of excess isocyanate leads to isocyanurate formation.

5.2.4. Isocyanates in Polyurethane Manufacture

Most polyurethane production is based on TDI or MDI, the latter being the most commercially important. "Pure" MDI is mainly the 4,4'–isomer with small amounts of the 2,4'–, see Figure 5.3:

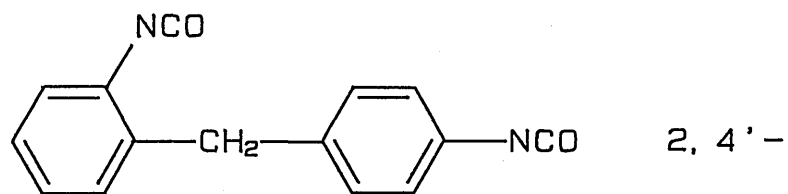
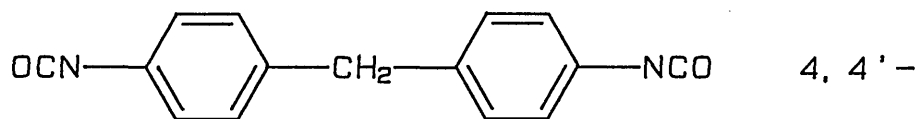


Figure 5.3 4,4' -and 2,4' -Isomers of MDI.

Pure MDI is a solid which melts at around 38°C, and tends to form an insoluble dimer on storage. To overcome this problem, MDI is reacted with a low weight aliphatic diol, see Figure 5.4:

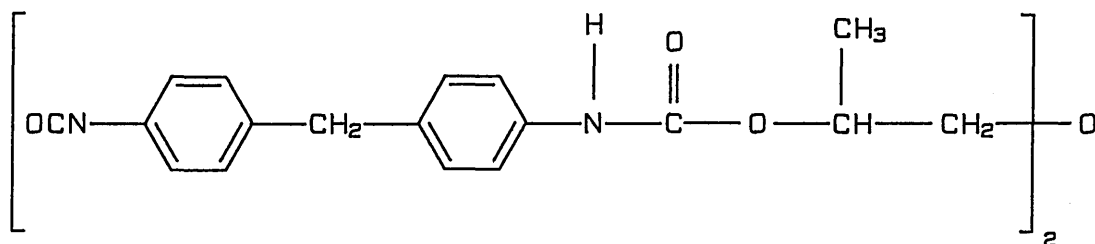


Figure 5.4 Modified MDI.

By dissolving the modified MDI in pure MDI, the melting point is lowered and the possibility of dimerization is reduced. The second method is to convert isocyanate linkages to uretonimine-linked trifunctional isocyanates:

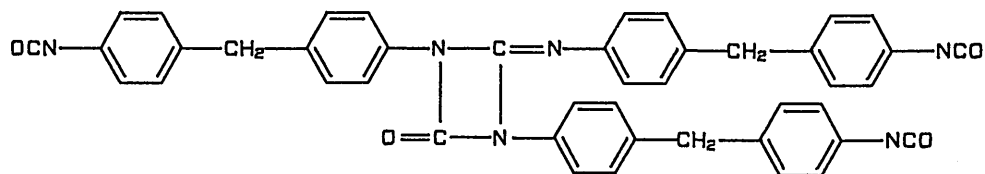


Figure 5.5 Modified MDI.

The isocyanate supplied by the ARE was polydiisocyanatediphenylmethane, or DND, an ICI trade name for MDI, see Figure 5.6:

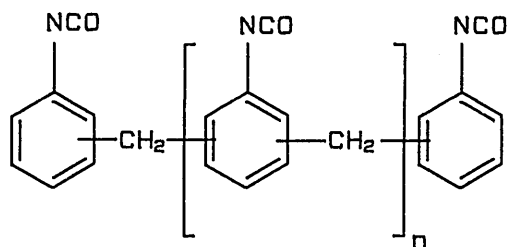


Figure 5.6 Polymeric MDI (DND).

DND has an average of 2.7 $-NCO$ groups per molecule, *i.e.*, a functionality of 2.7.

5.2.5. Polyols in Polyurethane Manufacture

Most polyols used in polyurethane manufacture fall into two classes, hydroxyl terminated polyethers and polyesters. As with the isocyanate, the structure of the polyol is important in determining the nature of the polyurethane. The characteristics of the polyols used in making flexible and rigid polyurethanes are shown below:

Characteristic	Flexible Foams	Rigid Foams
RMM	1000–6500	150–1600
Functionality	2–3	3–8
Hydroxyl Value	28–160	250–1000

The hydroxyl value, expressed as mg KOH per g, is given by:

$$\text{hydroxyl value} = \frac{56.1 \times \text{functionality}}{\text{RMM}} \times 1000$$

Polyols are often characterized by their hydroxyl value.

The majority of polyols, $\approx 90\%$, used in polyurethane manufacture are O—H terminated polyethers. These are synthesized by the addition of alkylene oxides, usually propylene oxide, onto alcohols in the presence of a basic catalyst. For the manufacture of flexible polyurethanes, the alcohols are generally trifunctional, *e.g.*, glycerol or trimethylolpropane, TMP:

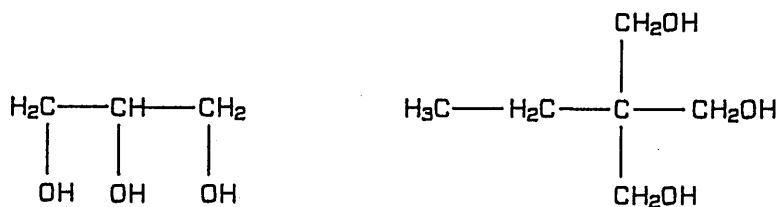


Figure 5.7 Structure of Glycerol and TMP.

The polyols used in flexible polyurethanes typically have RMM's around 3 500, whereas rigid polyurethanes require polyols of lower RMM. Blends of polyols are often made to obtain the best performance. Terathane 1000 was the polyol supplied by for this study.

5.3. Additives

These can include catalysts, chain extenders, cross-linking agents, fillers, surfactants, flame-retarders and pigments.

5.3.1. Catalysts

A number of catalysts can be used in the production of polyurethanes, including aliphatic and aromatic 3° amines and organometallic compounds, especially organotin. Some of the commonly used 3° amine catalysts are shown below in Figure 5.8:

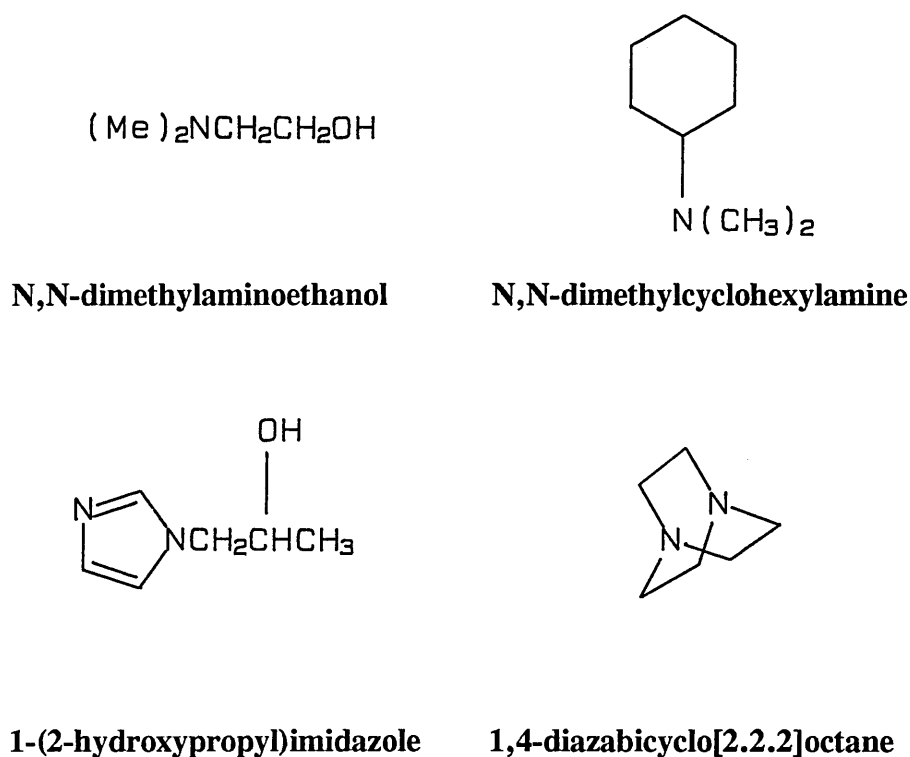


Figure 5.8 Tertiary Amine Catalysts.

The activity of 3° amine catalysts increases with basicity, and decreases with steric hinderance of the aminic N. 1,4-diazabicyclo[2.2.2]octane, or as it is more commonly known, DABCO, is a catalyst of relatively high activity for its basicity. Farkus and Flynn [2] attribute this to the lack of steric hinderance at

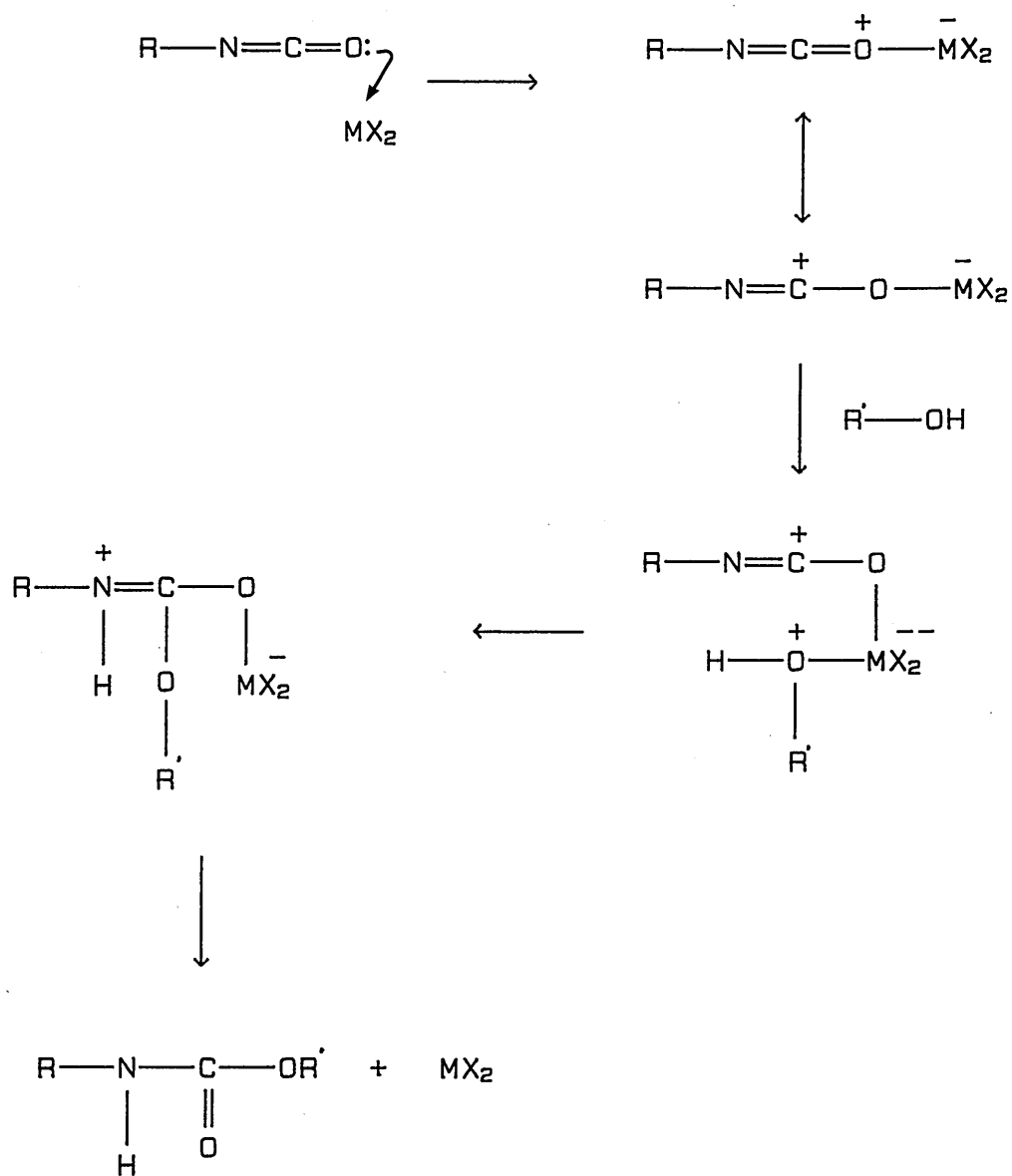
the aminic N in DABCO compared to other 3° amines, thus facilitating deprotonation of the hydroxyl groups (the —NCO carbon is more susceptible to nucleophilic attack by R—O[−], rather than R—OH).

Organometallic catalysts are also commonly employed in the manufacture of polyurethanes (where they enhance the reactivity of 2° alcohols relative to 1° alcohols). The most popular are stannous octoate, (H₃C(CH₂)₆COO)₂Sn and di-n-butyltin dilaurate, Bu₂Sn(OOC(CH₂)₁₀CH₃)₂. In comparison to the catalytic effect shown by 3° amines, that of the organometallics is not well understood. A mechanism was first proposed by Britain and Gemeinhardt [3] in 1960. They studied the effect of various metallic and basic compounds on the gelation time of polyurethanes, made of either aromatic or (less reactive) aliphatic isocyanates. It was found that the catalysts could be divided into three classes:

- (i) 3° amines which did not greatly effect the reaction rate of the aliphatic isocyanates relative to the aromatic isocyanates;
- (ii) tin, lead and bismuth compounds, which activated the aliphatic isocyanates to a reactivity similar to that of the aromatic isocyanates and
- (iii) zinc, cobalt, iron, antimony and titanium compounds which caused the aliphatic isocyanates to react faster than the aromatic isocyanates.

It was also noted that for tin the catalytic activity decreased in the order: SnCl₄ > BuSnCl₃ > Bu₂SnCl₂ > Bu₃SnCl > Bu₄Sn.

Britain and Gemeinhardt proposed the following reaction scheme to account for the observed catalytic activity of the metal compounds:



Reaction 5.7 Proposed Mechanism of MX_2 Catalysis in the Polyurethane Reaction.

As can be seen, the metal compound, MX_2 , forms a complex with the isocyanate and alcohol which brings them into a geometry which facilitates reaction. The isocyanate group is bonded through the oxygen atom to the metal centre, but Bloodworth and Davies [4] proposed that it is the nitrogen of the isocyanate group which bonds to tin.

The mechanism has also been studied by Entelis *et al* [5], with particular interest in tin (IV) compounds. They found that increases in the acceptor capacity of the alkyltin chloride initially leads to an increase in catalytic activity, which then falls sharply. They claim that there is an optimum strength of the hydroxyl-catalyst complex, which allows maximum isocyanate reactivity.

Lipatova *et al* [6] studied the effect of di-n-butyltin dilaurate catalysis of the reaction between hexamethylene diisocyanate and di-/triethylene glycol. Detailed rate calculations were used and the following conclusions were drawn; the isocyanate-tin complex can react with either coordinated or free alcohol, the latter being first or second order and the catalytic mechanism is dependant on reaction conditions, *e.g.* temperature, solvent and catalyst ligand. They concluded that the mechanism is difficult to establish.

The reactions of aryl isocyanates with alcohols in the presence of four organotin compounds; tin (II) dioctanoate, di-n-butyltin dichloride, tri-n-butyltin acetate and di-n-butyltin dilaurate has been studied by Bacaloglu *et al* [7]. The reactants, phenyl isocyanate and n-butanol, were dissolved in CCl₄ and reactions were carried out at 32°C. Catalytic activity was found to decrease in the order:

di-n-butyltin dilaurate >> tri-n-butyltin acetate > di-n-butyltin dichloride > tin (II) dioctanoate. Bacaloglu *et al* concluded that optimum activity is achieved when two carboxylic acid groups and two alkyl chains are present in the tin (IV) species. The authors continue the discussion, assuming the following structure for di-n-butyltin dilaurate:

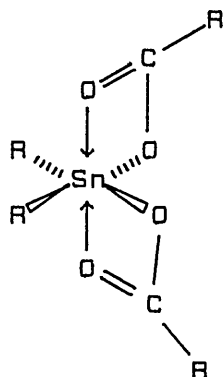


Figure 5.9 Di-n-Butyltin Dilaurate

bond energies:

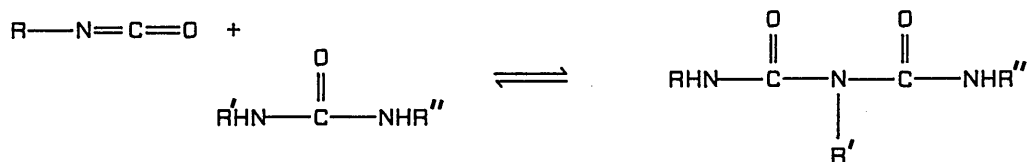
Sn—Cl 76Kcal/mole,

Sn—O 132Kcal/mole and

Sn—C 45Kcal/mole.

On the basis of the bond energy data they claim that the Sn—R bond(s) will be cleaved and bonds to the alcohol and isocyanate will form, thus promoting reaction. The carboxylate groups prevent interference from other moieties, hence facilitating reaction. If the tin atom coordinates to three or more hydroxyl or isocyanate groups, then a decrease in reaction rate is proposed to occur.

Dyer and Pinkerton [8] studied the catalytic effect of organotins on biuret, rather than polyurethane formation:



Reaction 5.8 Biuret Formation.

The standard reactants chosen were 1,1-pentamethylene-3-phenylurea, PMPU, and phenyl isocyanate:

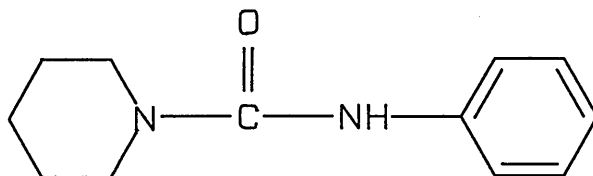


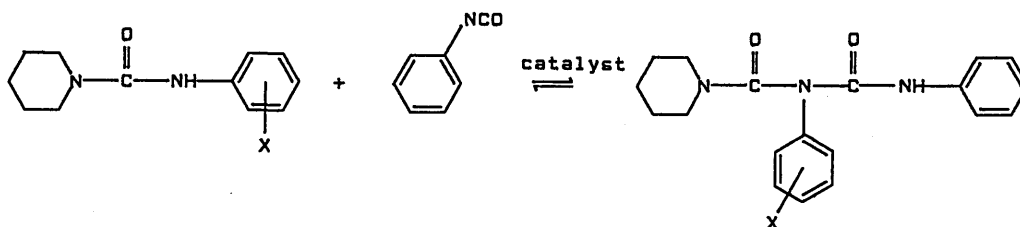
Figure 5.10 1,1-Pentamethylene-3-Phenylurea, PMPU.

PMPU was chosen because it has one active proton, was soluble in chlorobenzene and substituted phenyl derivatives could be produced.

In the absence of catalyst, the biuret reaction will only occur at around 150°C, at which temperature the reverse reaction and other side reactions (*eg* trimerization of the isocyanate) take place. Various organotin compounds were added to the reaction mixture, but only three were catalysts, *viz*, tin (IV)

chloride, butyltin trichloride and triethyltin chloride. Those which did not catalyze the reaction included di-n-butyltin dilaurate, di-n-butyltin diacetate and di-n-butyltin dichloride, which all catalyze polyurethane formation.

The effect of aromatic substituents in PMPU on the rate of reaction was studied:



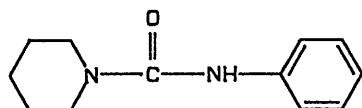
Reaction 5.9 Aromatic Substituent Effect on Biuret Formation.

Reactions were carried out in the presence of n-butyltin trichloride and the following relative rates were observed:

Substituent, X	Relative Rate
<i>para</i> -H	1.00
<i>para</i> -Me	1.13
<i>para</i> -OCH ₃	0.84
<i>para</i> -Cl	0.53
<i>meta</i> -Cl	0.42
<i>para</i> -NO ₂	0.01

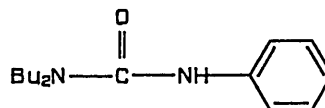
These data reveal that electron withdrawing groups reduce the reaction rate, which indicates that the transition state complex may be associated with an increase of positive charge at the N—H nitrogen of PMPU.

It was also shown that replacement of the pentamethylene group on the urea nitrogen by more bulky groups, *e.g.* di-*n*-butyl reduced the reaction rate tenfold, see Figure 5.12. This demonstrated that substituents on one nitrogen of the urea could influence, by a steric effect, the reactivity of the proton on the second nitrogen atom:



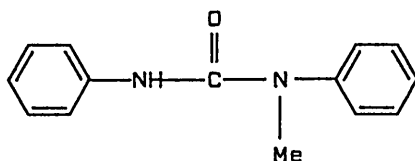
PMPU

relative reaction rate 1.00



1,1-Di-*n*-Butyl Phenylurea

relative reaction rate 0.10



1,3-Diphenyl Methylurea

relative reaction rate 0.06

Figure 5.12 Relative Reaction Rates of Substituted Ureas.

The biurets and ureas described all formed 1:1 complexes with anhydrous tin (IV) chloride on contact. The infrared spectra of the tin (IV) chloride:biuret complexes exhibited large shifts, $\approx 50 \text{ cm}^{-1}$, in the N—H stretching band, with only small changes, $\approx 10 \text{ cm}^{-1}$, in the C=O band. In the neat state there is extensive hydrogen-bonding between these two groups, but if the carbonyl

oxygens are coordinated to the tin atoms this cannot occur. Thus, the infrared data on these complexes suggests that the tin atom is coordinated to the carbonyl oxygen, not the nitrogen, of the urea, see Figure 5.13:

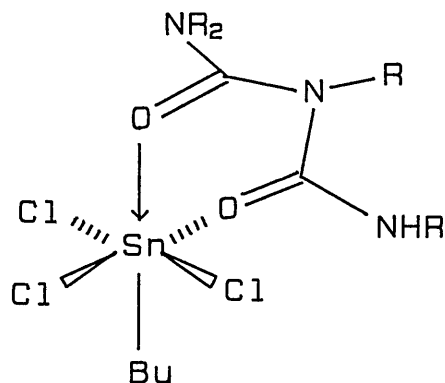
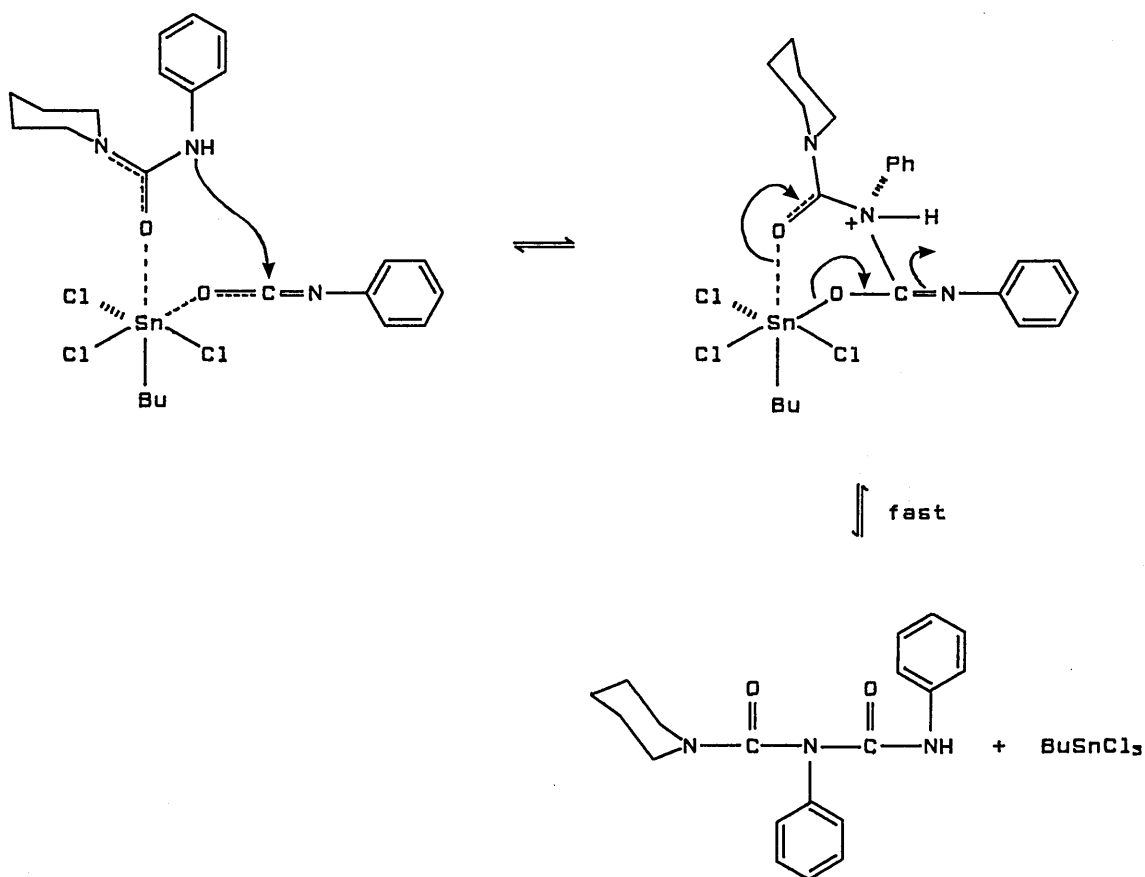


Figure 5.13 Proposed Bonding in Biuret-Butyltin Trichloride Complex.

From the combined results the following reaction mechanism was proposed:



Reaction 5.10 Catalytic Mechanism for the Urea/Isocyanate Reaction.

In Reaction 5.10 the urea and isocyanate are complexed in such a way as to facilitate reaction. The build up of positive charge on the carbonyl urea would be stabilized by the piperidine nitrogen, thus allowing enough electron density for nucleophilic aminic nitrogen to attack the isocyanate carbon. When this occurs, the tertiary nitrogen will be stabilized by electron-donating substituents on the benzene ring, as was described on page 177.

This mechanism explains the observed reaction rates for the different starting materials and catalysts. However, it should be noted that all the mechanistic studies described were carried out on relatively simple systems in solution.

5.3.2. Other Polyurethane Additives

(i) chain extenders and cross-linking agents: these are generally low-weight polyols or polyamines. Chain extenders are usually difunctional, *e.g.* glycols or hydroxyamines, whereas cross-linking agents are at least trifunctional. Chain extenders react with isocyanates to give polyurea or polyurethane segments in the polymer. Cross-linkers increase the amount of covalent bonding resulting in the formation of rigid foams. In the polyurethane mix provided, 2-ethyl-2-(hydroxymethyl)-1,3-propanediol, TMP, was present as a cross-linking agent.

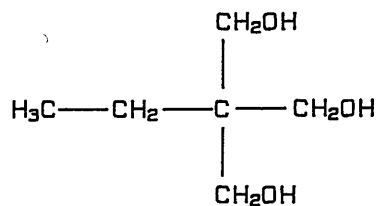


Figure 5.14 2-Ethyl-2-(Hydroxymethyl)-1,3-Propanediol, TMP.

(ii) surfactants: these are essential ingredients in most polyurethanes. They aid the mixing of incompatible components and also help control the size of the foam cells. Most flexible and rigid foams use organosiloxane or silicone based surfactants. A surfactant with the trade name SC120 was a component of the urethane mix.

(iii) colouring: this is generally a cosmetic requirement, and can be achieved with organic or inorganic pigments. Statex N330 Black was the pigment for the urethane mix.

(iv) fillers: these are added to most polyurethanes. Particulate fillers are added to flexible polyurethane foams to reduce flammability, or to increase the bulk, leading to better compression resistance for seating. Fibrous fillers are often used as bulking agents to reduce costs. The polyurethane mix in this study used Grade 1438 Barytes, barium sulphate. This is typically used in flexible and semi-rigid foams for sound absorption.

5.4. Effect of Triorganotin Biocides on the Polyurethane Foams

It was of interest to study the potential of a polyurethane as an antifouling system. From the preceding discussion it is evident that the incorporation of organotin biocides into the polyurethane system might lead to changes in reaction rates. This in turn may cause physical changes in the polymer and chemical modifications in the biocides. The components of the polyurethane are listed in Table 5.1.

Table 5.1 Components of the Polyurethane Mix.

	pilot plant mix	1/25 scale
Terathane 1000 (polyol)	2000 g	8.00g
Barytes 1438 (filler)	4200 g	16.80 g
Aerosil A200 (filler?)	50 g	0.20 g
TMP (cross-linker)	36 g	0.142 g
SC120 (surfactant)	13 g	0.052 g
Statex N330 (pigment)	12 g	0.048 g
Triorganotin (biocide)	/	0.68 g
DABCO (catalyst)	0.8 ml	3 μ l
DND (polyisocyanate)	703 g	2.81 g

The components are listed in order of their addition to the beaker. The pilot plant mix was scaled down $25\times$ to produce a convenient mass of working polymer. All the components, except the isocyanate, were added to the beaker (including, when required, the triorganotin at 2.5%w/w, 0.68g) and warmed to around 40°C. This caused the polyol to melt and the mixture was stirred until it became homogeneous. The polyisocyanate was then added to the mix, which was stirred and poured onto a watch-glass. This was then placed in a vacuum for ten minutes, during which time foaming, if any, occurred.

Addition of certain triorganotin compounds to the urethane mix was known to result in extensive foaming, which was undesirable. The cause of the foaming and subsequent chemical/physical changes in the organotin compounds were unknown at the start of the present study.

5.5. Initial Studies of Triorganotin Biocides in Polyurethane

Five triorganotin biocides have been incorporated into the polyurethane mix, *viz*, *bis*-(tri-*n*-butyltin) oxide, tri-*n*-butyltin chloride, tri-*n*-butyltin acetate, *bis*-(triphenyltin) oxide and triphenyltin chloride. The resultant polyurethanes were compared with a "blank" polyurethane, *i.e.* containing no organotin, by

scanning electron microscopy, SEM. A series of polyurethane foams was also prepared without the cross-linking agent, (TMP), in an attempt to reduce excessive foaming. These polymers were also examined by SEM.

The biocide-containing polyurethanes were also studied by Mößbauer and ^{119}Sn NMR spectroscopy. The latter was carried out on Soxhlet extracts of the foams.

A summary of results is presented in Tables 5.2 and 5.3:

Table 5.2 Mößbauer Parameters of Triorganotins in

Polyurethane with Pure State Parameters for Comparison.

PU sample	phase	$\delta/$ mms^{-1}	$\Delta E_Q/$ mms^{-1}	$\Gamma_1/$ mms^{-1}	$\Gamma_2/$ mms^{-1}	%R.A.	ρ	χ^2
TBTO + TMP	Q1	1.39	2.86	1.24	1.32	100.0	2.1	1.5
TBTO - TMP	Q1	1.45	3.06	1.39	1.73	100.0	2.1	10.3
pure TBTO	Q1	1.21	1.52	1.18	1.18	100.0	1.3	1.2
TBTOAc + TMP	Q1	1.41	3.54	1.00	1.00	100.0	2.5	0.5
TBTOAc - TMP	Q1	1.53	3.61	1.06	1.18	100.0	2.4	4.6
pure TBTOAc	Q1	1.40	3.54	1.02	0.92	100.0	2.5	0.4
TPTO - TMP	Q1	1.22	2.49	1.66	1.19	100.0	2.0	0.9
pure TPTO	Q1	1.09	1.33	0.95	0.95	84.9	1.2	0.6
TPTCl - TMP	Q1	1.36	3.00	0.95	0.98	100.0	2.2	0.6
pure TPTCl	Q1	1.33	2.56	0.97	0.97	100.0	1.9	0.5

1. All spectra recorded at 80K with an error of $\pm 0.02 \text{mms}^{-1}$ for the pure compounds and $\pm 0.05 \text{mms}^{-1}$ for the polyurethane samples. Isomer shifts are relative to CaSnO_3 .
2. %R.A. is the relative area of each phase, *i.e.* quadrupole doublet.
3. $\rho = \Delta E_Q / \delta$.
4. TBTO and TPTO are *bis*-(tri-*n*-butyltin)- and *bis*-(triphenyltin) oxides.
5. TBTOAc is tri-*n*-butyltin acetate.
6. TPTCl and TBTCI are triphenyltin and tri-*n*-butyltin chloride.
7. TMP is the cross-linking agent, its presence is indicated by "+ TMP", its absence by "- TMP".
8. The following polyurethanes gave poor quality spectra which were not fitted: TBTCI + TMP, TBTCI -TMP, TPTO + TMP and TPTCl+TMP.

**Table 5.3 Comparison of Physical Properties of the Triorganotin
Containing Polyurethanes and NMR Data of Soxhlet Extracts.**

polyurethane sample	setting time in minutes	degree of foaming	rigidity	$\delta(^{119}\text{Sn})$ ppm	integral ratio
Blank + TMP	5	1	3	n/a	n/a
Blank - TMP	did not set	n/a	3	n/a	n/a
TBTO + TMP	0.5	5	3	112.4 (80.9)	n/a
TBTO - TMP	0.5	5	2	102.9 92.7	1 4
TBTCl + TMP	1	2	>3	153.7 (153.0)	n/a
TBTCl - TMP	1	1	3	155.3	n/a
TBTOAc + TMP	5	4	1	107.9 (105.7)	n/a
TBTOAc - TMP	5	4	2	147.8 112.0	1 2
TPTO + TMP	2	3	1	-223.4 -118.5 (121.9)	10 1
TPTO - TMP	2	2	1	-223.8 -118.7 -133.9	10 1 1
TPTCl + TMP	>60	<1	2	-224.2 (-224.9)	n/a
TPTCl - TMP	10	<1	3	-223.6	n/a

1. Foaming is on a scale relative to the blank polyurethane, where 1 is the least extent of foaming and 5 the greatest.
2. Rigidity is on a scale relative to the blank polyurethane, where 1 is the least rigid and 3 the most rigid.
3. All ^{119}Sn NMR spectra were recorded in CDCl_3 .
4. Abbreviations as on previous page.
5. Pure state NMR shifts are in parentheses.

5.5.1. The *Bis*-(Tri-*n*-Butyltin) Oxide Containing Polyurethane

The incorporation of *bis*-(tri-*n*-butyltin) oxide into the polyurethane mix results in an exothermic reaction and a fast-setting polymer (<0.5min, *cf.* \approx 5mins in the blank polyurethane). The polymer was a rigid foam with a continuous skin. When the cross-linking agent was omitted from the mix, rapid setting was again observed. The polymer was less rigid than that containing TMP. (It should also be noted that the blank urethane mix without TMP did not set).

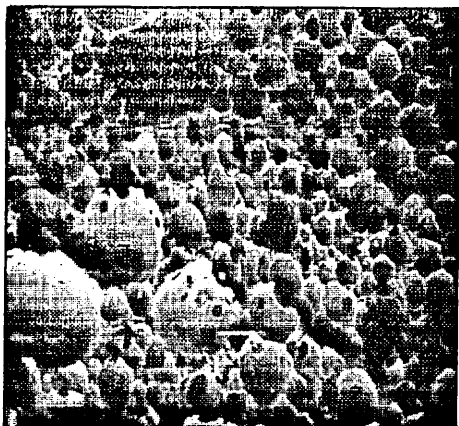
The foams were examined by SEM; the cross-sections of the blank polyurethane and the *bis*-(tri-*n*-butyltin) oxide containing polyurethanes are shown in Figure 5.15.

The micrographs reveal the extensive foaming of the triorganotin-containing polymer relative to that of the blank. It is also evident that the presence of TMP in the triorganotin-containing polymer leads to a larger average bubble-size. Further, the absence of TMP results in a more uniform average bubble-size.

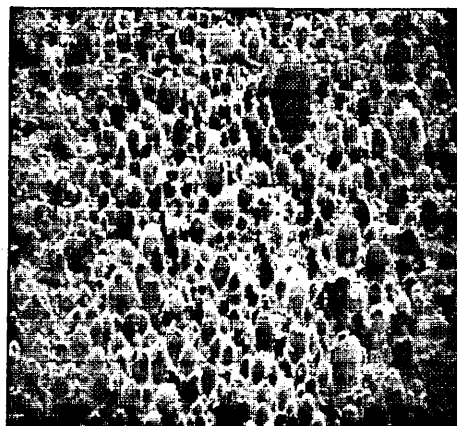
The Mößbauer spectra of the *bis*-(tri-*n*-butyltin) oxide-containing polymers were recorded and the parameters are shown in Table 5.2. In both cases, new tin compounds have been formed, which appear to be five-coordinate, (ρ 2.1), tin (IV) species.

The NMR spectrum of the *bis*-(tri-*n*-butyltin) oxide + TMP extract contains one signal at $\delta(^{119}\text{Sn})$ 112.4 ppm (*cf.* 80.9 ppm for pure *bis*-(tri-*n*-butyltin) oxide). The NMR spectrum of the extract from the polymer without TMP contains two signals at $\delta(^{119}\text{Sn})$ 92.7 and 102.9 ppm, (4:1 integral ratio).

The Mößbauer and NMR data show that *bis*-(tri-*n*-butyltin) oxide is not a catalyst, in the true sense of the term, in polyurethane formation. In fact it would appear to be the unidentified tin species which catalyze the reaction. Since the setting time was less than one minute, it is proposed that *bis*-(tri-*n*-butyltin) oxide reacts rapidly with a component of the polyurethane mix. This reaction and/or the subsequent catalysis was exothermic with a resultant change in polymer structure compared to that of the blank polyurethane (the formation of which was not noticeably exothermic).

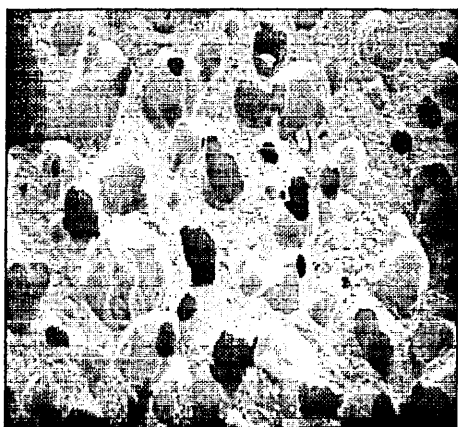


bis-(tri-n-butyltin) oxide
+ TMP (45×)



bis-(tri-n-butyltin) oxide
– TMP (45×)

**Figure 5.15 Micrographs of
Cross-Sections Through *Bis*-
(Tri-n-Butyltin) Oxide
Containing Polyurethanes.**



blank + TMP (48×)

The most likely reactant in the urethane mix is the isocyanate, DND. Model studies of reactions between simple isocyanates, as well as DND, with *bis*-(tri-n-butyltin) oxide have been carried out and these are detailed in Sections 5.7 to 5.11.

5.5.2. The Tri-n-Butyltin Chloride Containing Polyurethane

The presence of tri-n-butyltin chloride in the urethane mix results in an exothermic reaction, with a faster setting time than the blank polyurethane. However, it is not as efficient as the mix originally containing *bis*-(tri-n-butyltin) oxide. The end product, with or without TMP, was a very rigid "tile" with a continuous skin. In cross-section, bubbles were evident and these were photographed using SEM, see Figure 5.16.

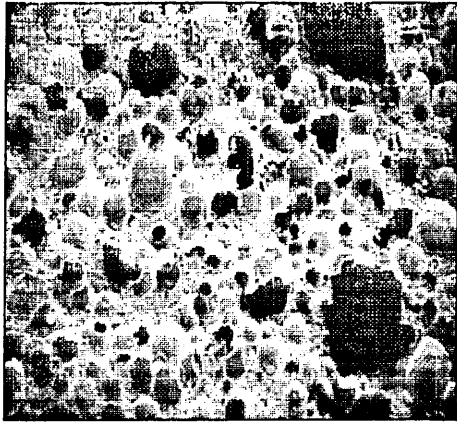
Both tri-n-butyltin chloride-containing polymers show random bubble-size, with a lower bubble density than the polyurethane originally containing *bis*-(tri-n-butyltin) oxide.

The Mößbauer spectra of the two tri-n-butyltin chloride-containing polymers were recorded, but proved to be of very poor quality. However, the NMR spectra of the Soxhlet extracts both exhibited signals at $\delta(^{119}\text{Sn})$ 155 ppm, which is the same as for pure tri-n-butyltin chloride.

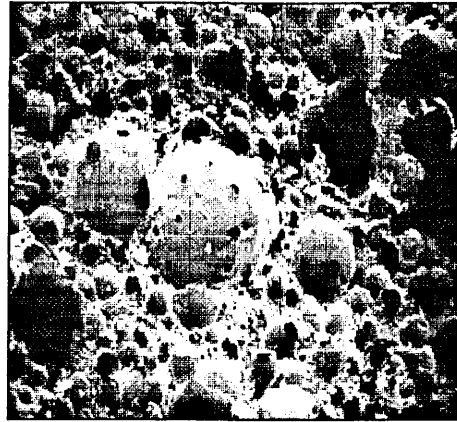
It can be concluded that tri-n-butyltin chloride is a catalyst for polyurethane formation, providing a polyurethane which is less foam-like than the blank.

5.5.3. The Tri-n-Butyltin Acetate Containing Polyurethane

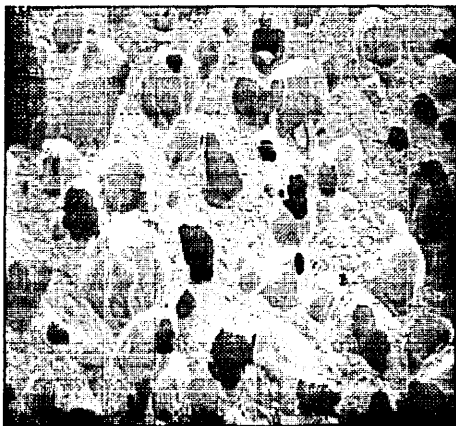
The incorporation of tri-n-butyltin acetate into the urethane mix did not reduce the setting time compared to the blank. The end product, whether TMP was present or not, was a foam more flexible than the blank. Micrographs of cross-sections through the foam are shown in Figure 5.17.



tri-n-butyltin chloride
+ TMP (46×)

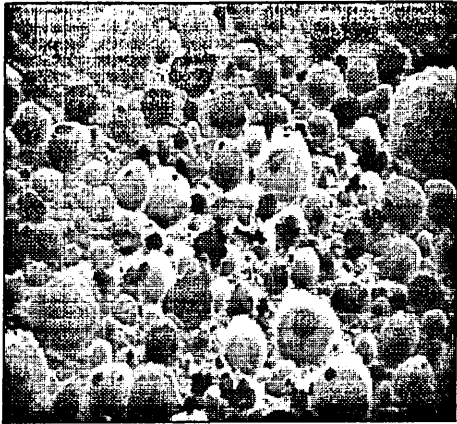


tri-n-butyltin chloride
- TMP (44×)

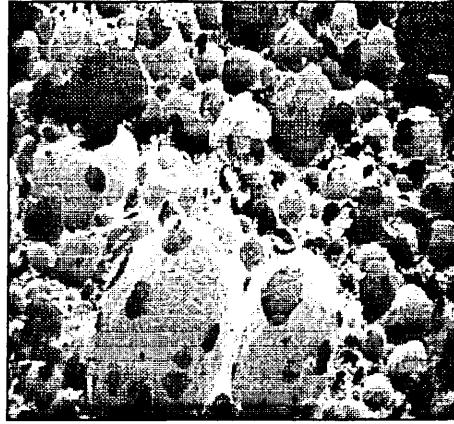


blank + TMP (48×)

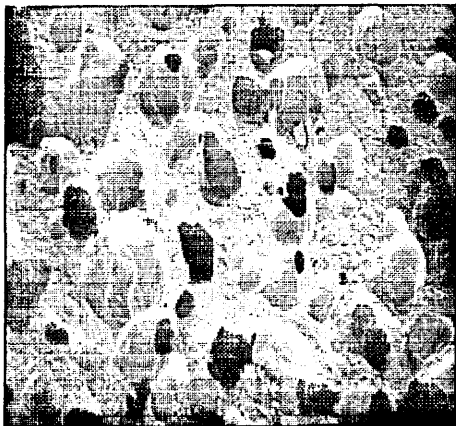
**Figure 5.16 Micrographs of
Cross-Sections Through
Tri-n-Butyltin Chloride
Containing Polyurethanes.**



tri-n-butyltin acetate
+ TMP (47×)



tri-n-butyltin acetate
- TMP (44×)



blank + TMP (48×)

**Figure 5.17 Micrographs of
Cross-Sections Through
Tri-n-Butyltin Acetate
Containing Polyurethanes.**

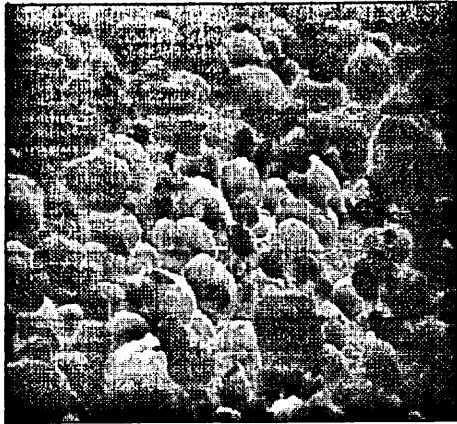
They reveal the more extensive foaming in the triorganotin-containing polymer compared to the blank. It is also apparent that the polyurethane with TMP has a more uniform bubble-size compared to that without the cross-linking agent (this is in contrast to the *bis*-(tri-*n*-butyltin) oxide-containing foams).

The Mößbauer and NMR spectra of the TMP-containing polyurethane reveal that the triorganotin is unmodified. However, when the cross-linking agent is not present in the mixture, tri-*n*-butyltin acetate appears to be transformed in the polyurethane. The Mößbauer spectrum exhibits one quadrupole doublet with parameters differing from those of the pure tri-*n*-butyltin acetate by more than experimental error. The NMR spectrum of the extract exhibits two signals at $\delta(^{119}\text{Sn})$ 112.0 and 147.8 ppm (2:1 integral ratio). The major signal has a similar shift to that observed in the polymer originally containing *bis*-(tri-*n*-butyltin) oxide, (without TMP). The minor signal did not correspond to pure tri-*n*-butyltin acetate and could not be identified from literature values.

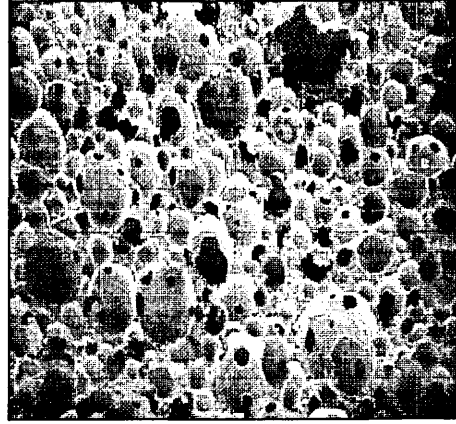
Model studies of reactions between simple isocyanates, as well as DND, with tri-*n*-butyltin acetate have been carried out and are detailed in Section 5.7 to 5.11.

5.5.4. The *Bis*-(Triphenyltin) Oxide Containing Polyurethane

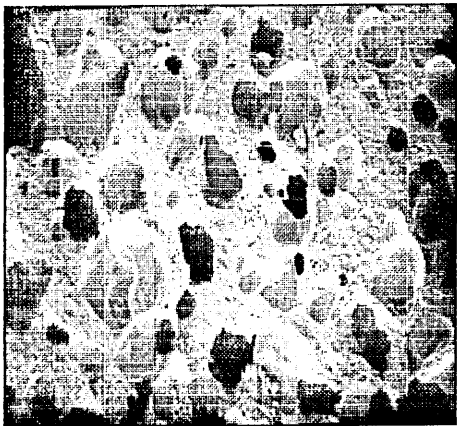
The presence of *bis*-(triphenyltin) oxide in the urethane mix reduces the setting time, though not as significantly as the corresponding tri-*n*-butyltin oxide. The two polymers produced, with or without TMP, were more foam-like than the blank and the least rigid of all the foams made. Micrographs of the *bis*-(triphenyltin) oxide-containing polyurethanes are shown in Figure 5.18. Both exhibit more extensive bubble formation than the blank polyurethane. There do not appear to be any significant difference in the bubble sizes in the foams with, or without, TMP.



bis-(triphenyltin) oxide
+ TMP (44×)

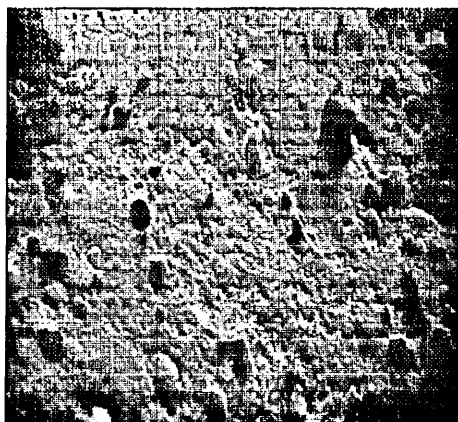


bis-(triphenyltin) oxide
- TMP (47×)



blank + TMP (48×)

**Figure 5.18 Micrographs of
Cross-Sections Through *Bis*-
(Triphenyltin) Oxide
Containing Polyurethanes.**

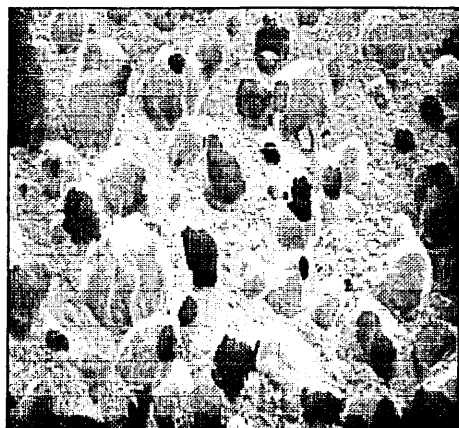


triphenyltin chloride
+ TMP (44×)



triphenyltin chloride
- TMP (45×)

**Figure 5.19 Micrographs of
Cross-Sections Through
Triphenyltin Chloride
Containing Polyurethanes.**



blank + TMP (48×)

The Mößbauer spectrum of the polyurethane containing TMP was of poor quality. However, the spectrum of the composition without TMP was fitted and revealed a quadrupole doublet of dissimilar parameters to those of the pure triorganotin. The NMR spectra of both extracts exhibit a major signal at $\delta(^{119}\text{Sn}) -223$ ppm, with a minor signal at $\delta(^{119}\text{Sn}) -118$ ppm, (*cf.* pure *bis*-(triphenyltin) oxide $\delta(^{119}\text{Sn}) -122$ ppm). The most intense signal in the spectrum corresponds closely to pure triphenyltin chloride $\delta(^{119}\text{Sn}) -225$ ppm, although its formation can not be readily accounted for.

5.5.5. The Triphenyltin Chloride Containing Polyurethane

Triphenyltin chloride was the only one of the five organotins which increased the time taken for the polymer to set, relative to the blank. When set, the polyurethanes were rigid and the least foam-like of those made. Micrographs of the polyurethanes are shown in Figure 5.19 and reveal an almost complete lack of bubble structure.

The Mößbauer spectra of the two triphenyltin chloride-containing polymers were of poor quality. However, the spectrum of the foam without TMP was fitted as a quadrupole doublet with an isomer shift the same as that of pure triphenyltin chloride, but with a larger quadrupole splitting. The NMR spectra of both the polyurethane extracts exhibited single peaks at $\delta(^{119}\text{Sn}) -224$ ppm, corresponding to unreacted triphenyltin chloride.

The larger than expected quadrupole splitting observed may be due either to the coordination chemistry of the triorganotin in the polyurethane, or simply the increased error associated with the poor quality of the spectrum.

5.6. Conclusions of the Initial Study

The incorporation of certain triorganotin compounds into the urethane mix resulted in decreased setting times with resultant modifications to the polymer. Tri-*n*-butyltin acetate and triphenyltin chloride did not increase the rate of

reaction, the latter, in fact, slowed the reaction, but their presence did have an effect on the physical nature of the polyurethane. In addition, all the organotins, apart from the chlorides, undergo chemical transformations within the polymer. The most reactive component of the urethane mix is the isocyanate, DND. The chemistry of DND and three relatively simple isocyanates with the triorganotins was investigated in a model study, which is detailed below. It was hoped that such a study might account for the physical differences in the triorganotin-containing foams, compared to the blank, and also to identify the catalytic tin-containing species formed.

5.7. Model Studies of Reactions Between Triorganotin Compounds and Isocyanates

Three isocyanates were used in the model study, viz, phenyl isocyanate, 1,6-diisocyanatohexane and 1,4-phenylene diisocyanate, see Figure 5.20:

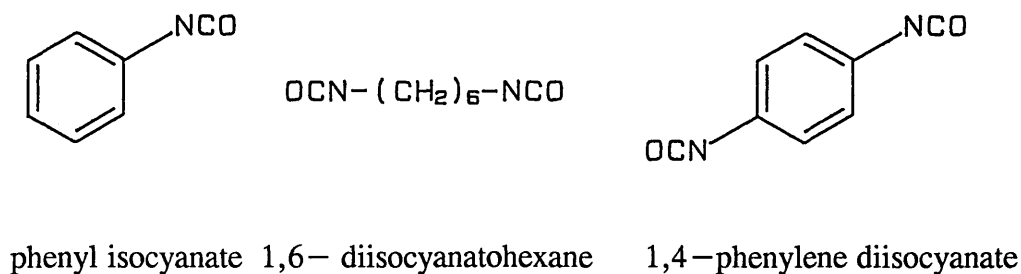


Figure 5.20 Isocyanates used in the Model Study.

Initial reactions were carried out with these three isocyanates, rather than DND, since the latter was thought likely to result in complex products. Conditions for the initial reactions were refluxing chloroform solution for one hour, under dinitrogen (isocyanates are moisture-sensitive).

5.7.1. The Reaction Between *Bis*-(Tri-*n*-Butyltin) Oxide and Phenyl Isocyanate

1 mol equivalent of the organotin was heated with 2 mol equivalents of the isocyanate. The product of the reaction was a cloudy liquid which was isolated by rotary evaporation of the solvent.

The infrared spectrum of the product did not contain the —N=C=O stretching band at 2280 cm^{-1} . A number of strong bands were evident between 1700 and 1220 cm^{-1} , some of which (1595 and 1550 cm^{-1}) were thought to be due to amide carbonyls.

The NMR spectrum of the product was recorded (in CDCl_3) and the following signals were present: 113.1 , 110.9 , 102.9 , 87.4 , 52.9 and 38.1 ppm (2:1:3:5:11:9 integral ratio). Pure *bis*-(tri-*n*-butyltin) oxide, $\delta(^{119}\text{Sn})$ 92 ppm, was not evident in the product and it appears that the two starting materials are fully reacted to yield a complex mixture of organotin compounds.

5.7.2. The Reaction Between *Bis*-(Tri-*n*-Butyltin) Oxide and 1,6-Diisocyanatohexane

Equimolar quantities of the reactants were heated together. The product isolated, after rotary evaporation of the solvent, was a clear liquid. The infrared spectrum of the product was very similar to that of the phenyl isocyanate product, as described in the previous section.

The NMR spectrum (in CDCl_3) contained a number of signals at $\delta(^{119}\text{Sn})$ 96.0 , 74.6 , 27.1 and the most intense at -198.6 ppm. It is evident that the starting materials are fully reacted to yield several tin-containing species.

5.7.3. The Reaction Between *Bis*-(Tri-*n*-Butyltin) Oxide and 1,4-Phenylene Diisocyanate

Equimolar amounts of the triorganotin and diisocyanate were heated together, the solution turning pale green once the diisocyanate had dissolved. Solvent evaporation yielded a pale green liquid.

The infrared spectrum was very similar to those of the products of *bis*-(tri-*n*-butyltin) oxide with phenyl isocyanate and 1,6-diisocyanatohexane. Similarly, the NMR spectrum exhibited several, rather weak, signals at $\delta(^{119}\text{Sn})$ 114.6, 102.6, 82.9, 78.3, 51.8, 38.6 and -11.2 ppm.

5.7.4. The Reaction Between Tri-*n*-Butyltin Acetate and Phenyl Isocyanate

The two compounds were heated together in equimolar quantities in chloroform solution. Rotary evaporation of the solvent isolated a white solid. The infrared spectrum exhibited the strong $-\text{N}=\text{C}=\text{O}$ stretching band at 2260 cm^{-1} . A broad resonance at $\approx 3300\text{ cm}^{-1}$ was also present, indicative of $\text{N}-\text{H}$ stretching. A number of strong bands were present between 1710 and 1010 cm^{-1} . The ^{119}Sn NMR spectrum of the product contained one signal at 105 ppm, indicative of unreacted tri-*n*-butyltin acetate.

5.7.5. The Reaction Between Tri-*n*-Butyltin Acetate and 1,4-Phenylene Diisocyanate/1,6-Diisocyanatohexane

2 mol equivalents of the triorganotin were heated together with 1 mol equivalent of each of the diisocyanates. In each case, a white solid was isolated, whose infrared and NMR spectra were virtually identical to those described for the product of tri-*n*-butyltin acetate/phenyl isocyanate, in the previous section.

5.7.6. The Reaction Between Tri-*n*-Butyltin Chloride and Phenyl Isocyanate

Equimolar quantities of the organotin and isocyanate were heated together. Two products were isolated, after solvent evaporation, a clear liquid (98% yield) and a white solid (2% yield).

The infrared spectrum of the liquid contained a strong —N=C=O stretching band at 2260 cm^{-1} . The spectrum was essentially the same as that of a combination of the starting materials, but with additional strong bands between $1710\text{—}1740\text{ cm}^{-1}$ and at 1220 cm^{-1} . The ^{119}Sn NMR spectrum of the liquid contained a single peak at 155 ppm, indicative of tri-*n*-butyltin chloride.

The solid had a high melting point, ($\approx 250^\circ\text{C}$), suggestive of a polymeric and/or highly coordinated compound. No isocyanate band was observed in the infrared spectrum, but below 2000 cm^{-1} , the spectrum was very similar to that of the liquid product. The solid was insoluble in chloroform, the NMR spectrum in $\text{d}_6\text{-DMSO}$, exhibited one signal at 6.6 ppm (*cf.* tri-*n*-butyltin chloride $\delta(^{119}\text{Sn})$ 18.9 ppm in $\text{d}_6\text{-DMSO}$).

5.7.7. The Reaction Between Tri-*n*-Butyltin Chloride and 1,6-Diisocyanatohexane

2 mol equivalents of the organotin were heated together with 1 mol equivalent of the diisocyanate in chloroform. The reaction mixture became cloudy after five minutes. Solvent evaporation yielded a cloudy liquid whose infrared spectrum appeared to be a combination of the starting materials, except for a broad resonance at 1700 cm^{-1} . The NMR spectrum contained one signal indicative of unreacted tri-*n*-butyltin chloride.

5.7.8. The Reaction Between Tri-*n*-Butyltin Chloride and 1,4-Phenylene Diisocyanate

2 mol equivalents of the organotin were heated together with 1 mol equivalent of the diisocyanate in chloroform. The reaction mixture turned pink as soon as refluxing commenced and a pink solid was isolated after rotary evaporation of the solvent. The solid decomposed at around 260°C , 1,4-phenylene diisocyanate melts at $97\text{—}100^\circ\text{C}$. The product was insoluble in the available NMR solvents.

The infrared spectrum contained a strong $-\text{N}=\text{C}=\text{O}$ stretching resonance at 2260 cm^{-1} , as well as a band at 3300 cm^{-1} . The latter was observed in the tri-*n*-butyltin/isocyanate reaction products. The Mößbauer spectrum of the solid was recorded and the parameters are shown below:

**Table 5.4 Mößbauer Parameters of Tri-*n*-Butyltin Chloride/
1,4-Phenylene Diisocyanate Product.**

	δ/mms^{-1}	$\Delta E_Q/\text{mms}^{-1}$	Γ_1/mms^{-1}	Γ_2/mms^{-1}	χ^2
pure tri- <i>n</i> -butyltin chloride	1.51	3.43	1.04	1.04	0.4
tri- <i>n</i> -butyltin chloride/ isocyanate product	1.58	3.51	1.01	1.03	0.5

All spectra recorded at 80K with an error of $\pm 0.02\text{mms}^{-1}$. Isomer shifts are relative to CaSnO_3 .

These parameters suggest that a species very similar in nature to tri-*n*-butyltin chloride is present in the solid product. This is confirmed by the mass spectrum, see Figure 5.21, which is dominated by fragmentation species of the organotin, (note the characteristic splitting pattern of the tin isotopes). Evidence of the aromatic component of the product can be seen at m/z 76, $[\text{C}_6\text{H}_4]^+$, but isocyanate containing fragments are not evident.

5.8. Discussion of Results from the Initial Study

Bis-(tri-*n*-butyltin) oxide clearly reacts with the three isocyanates yielding liquid products which contain several tin sites. The infrared data suggests the presence of amide carbonyl groups. Bloodworth and Davies [9] studied the reactions of tin alkoxides with isocyanates and proposed the following reaction:

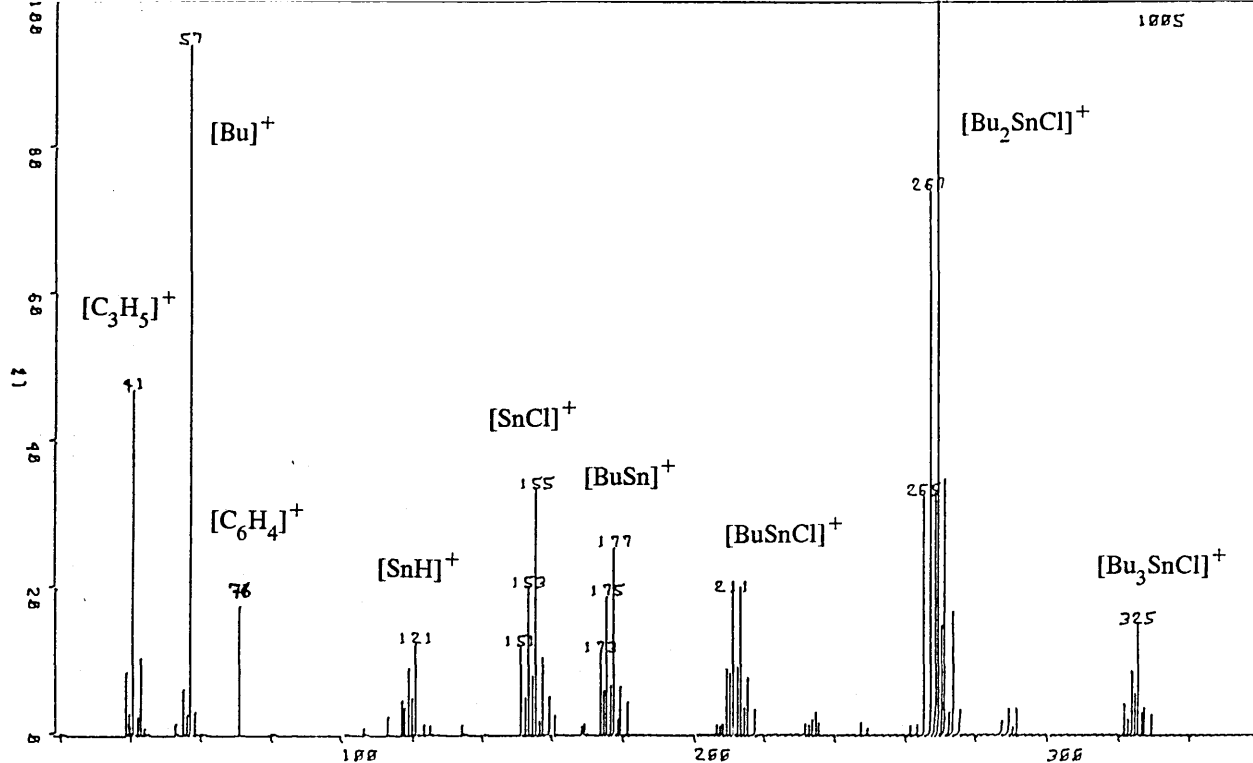


Figure 5.21 Mass Spectrum of the Solid Product of the Tri-n-Butyltin Chloride/1,4-Phenylene Diisocyanate Reaction.

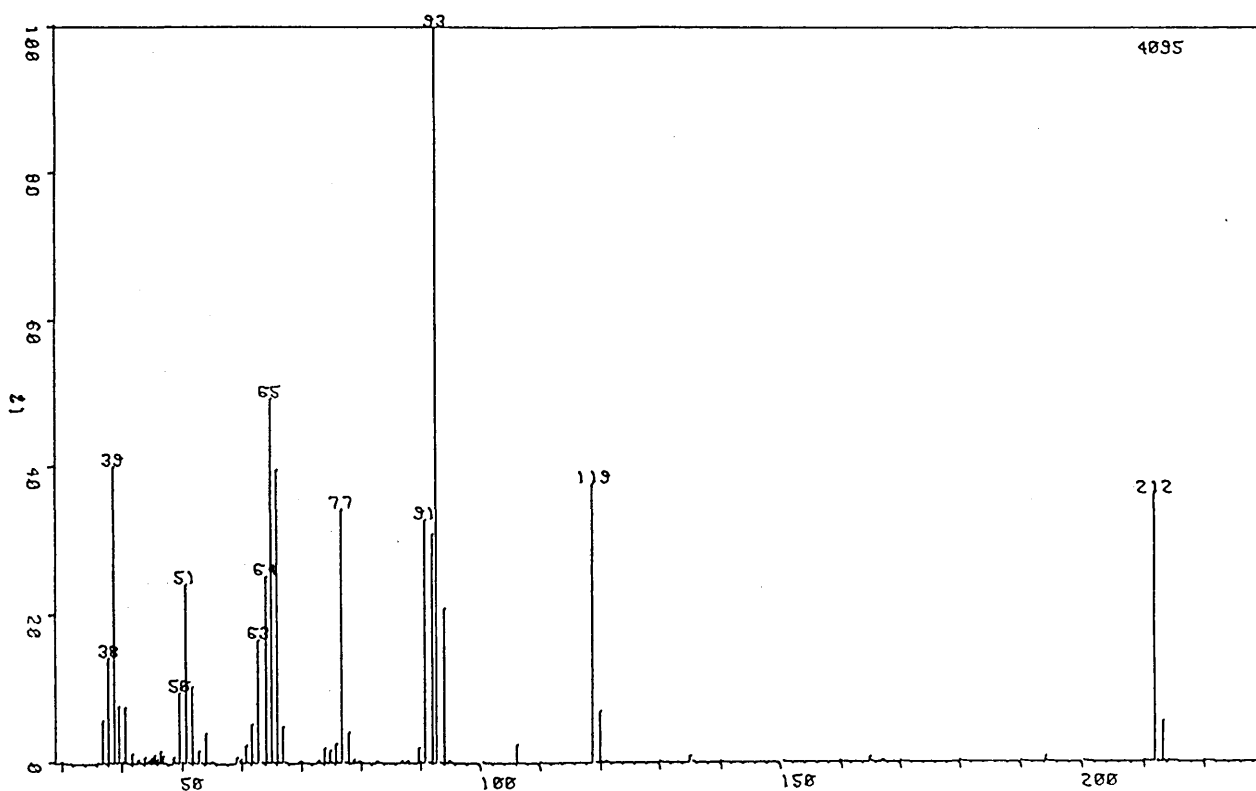
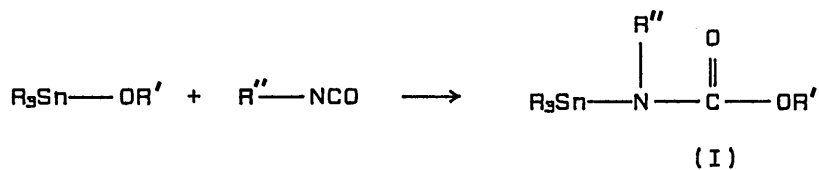


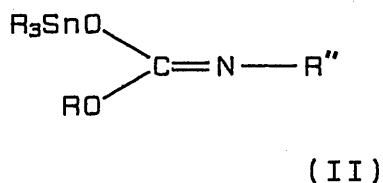
Figure 5.23 Mass Spectrum of the Solid Product of the *Bis*-(Tri-n-Butyltin) Oxide/Phenyl Isocyanate RT Reaction.



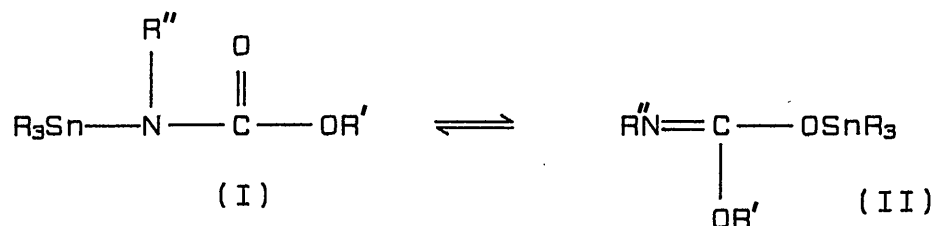
where R=Bu, Et; R'=Me, Et, Ph and R''=Et, Bu, Ph or naphthyl.

Reaction 5.11 The Reaction Between Tin Alkoxides and Isocyanates.

In Reaction 5.11 it is assumed that addition of the Sn—O bond occurs across the N=C rather than the C=O bond. The latter would yield (II):

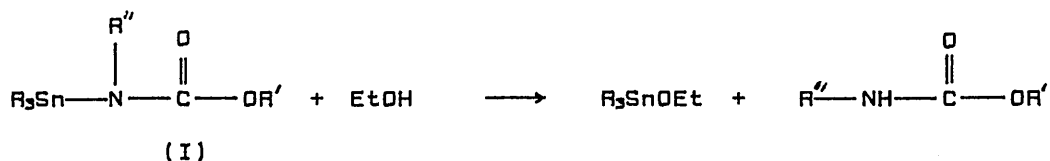


Infrared data supported the formation of (I), an N-stannylcarbamate. It was also suggested that the following interconversion may occur:



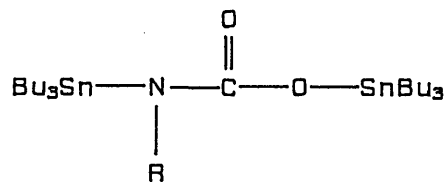
Reaction 5.12 Interconversion of N-Stannylcarbamates.

Compound (I) was shown to react rapidly with alcohols to yield a urethane:



Reaction 5.13 Urethane Formation.

It is suggested, from the results of this study, that Reaction 5.11 may occur when $R = \text{Bu}$ and $R' = \text{SnBu}_3$ to give:



Organotin Ester of N-Stannylcarbamate, (III).

(III) contains two four-coordinate tin sites, with the possibility of five-coordinate tin sites *via* intermolecular dative bonding with the carbonyl oxygen (interconversion as proposed in Reaction 5.12 would result in more tin sites). This may explain the multiple signals observed in the ^{119}Sn NMR spectra of the *bis*-(tri-*n*-butyltin) oxide/isocyanate products.

Tri-*n*-butyltin acetate does not appear to react with the isocyanates, the ^{119}Sn NMR spectra of the products containing signals due only to the starting material. Further, the infrared spectra of the products retain the isocyanate bands at 2260 cm^{-1} . However, a number of strong resonance bands were observed between 1710 and 1010 cm^{-1} which were not apparent in the starting materials. It is not unreasonable to suggest that some coordination may occur between the organotin and isocyanates:

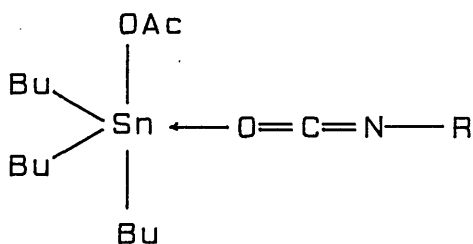


Figure 5.22 Proposed Coordination Between Tri-*n*-Butyltin Acetate and Isocyanates.

The diisocyanates may act as bidentate ligands.

Tri-n-butyltin acetate was not a catalyst for polyurethane formation, which may indicate that a complex, if formed, is very stable and/or its coordination geometry does not facilitate attack by the hydroxyl oxygen.

The reaction of tri-n-butyltin chloride with phenyl isocyanate yielded a liquid and a trace of solid. The ^{119}Sn NMR spectrum of the former contained one signal indicative of the unreacted organotin. However, the infrared spectrum contained bands which suggest that some interaction may occur between the reactants. The solid product contained tin, but not tri-n-butyltin chloride, and no isocyanate absorption was observed in the infrared spectrum. The identity of the solid was not investigated further due to its very low yield.

No significant reaction was observed between tri-n-butyltin chloride and 1,6-diisocyanatohexane. However, with 1,4-phenylene diisocyanate a solid was isolated, which retained the strong isocyanate resonance band in the infrared spectrum. The Mößbauer parameters were indicative of a tin species very similar to pure tri-n-butyltin chloride. It is proposed that a complex is formed between the two starting materials. In contrast to the complex formed by the acetate, the tri-n-butyltin chloride complex facilitates polyurethane formation, as was evident from the reduced setting time when this triorganotin is incorporated into the polymer mix.

It is concluded that tri-n-butyltin acetate and chloride may form complexes with isocyanates which are readily dissociated by the NMR solvent (*i.e.* CDCl_3). In contrast, *bis*-(tri-n-butyltin) oxide reacts with the isocyanates to yield a number of tin-containing products and it is these which are likely to be catalysts for polyurethane formation. In an attempt to identify some of these products, the reaction of *bis*-(tri-n-butyltin) oxide with the three isocyanates was repeated under milder conditions. These reactions are detailed in the following section.

5.9. Further Model Reactions

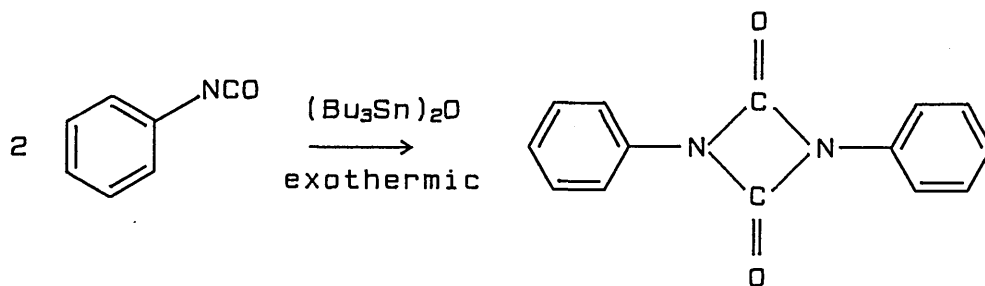
The following reactions were carried out in chloroform at room temperature under an inert atmosphere. The products were isolated after a one hour reaction period.

5.9.1. The Reaction Between *Bis*-(Tri-*n*-Butyltin) Oxide and Phenyl Isocyanate

The reaction was noticeably exothermic, solvent evaporation and condensation occurring on the flask wall. This ceased after about ten minutes. The product isolated was a clear viscous liquid in >100% yield. Trituration with petroleum spirit resulted in the precipitation of a white solid (8%). This was filtered off and a pale green liquid (82%) was isolated after rotary evaporation of the filtrate.

The solid had a high melting point ($\approx 244^\circ\text{C}$) and the infrared spectrum revealed that no isocyanate groups were present. Bands at 1600 and 1550 cm^{-1} suggested the presence of secondary amide and carboxylate groups. The ^{119}Sn NMR spectrum of the solid was devoid of signals and the absence of tin was also confirmed by the mass spectrum, see Figure 5.23, page 200. The latter exhibited an apparent molecular ion at m/z 212 with other peaks at m/z 119, $[\text{C}_6\text{H}_5\text{NCO}]^+$, m/z 93, m/z 91, $[\text{C}_6\text{H}_5\text{N}]^+$, m/z 77, $[\text{C}_6\text{H}_5]^+$, m/z 65, m/z 51, $[\text{C}_4\text{H}_3]^+$ and m/z 39, $[\text{C}_3\text{H}_3]^+$. The most intense peaks, m/z 93 and 65, could not be easily assigned, but loss of 26 mass units from m/z 119 and 91 respectively would result in such signals. It is known that aromatic compounds may lose an ethyne unit and the peaks at m/z 93 and 65 may, therefore be due to $[\text{C}_4\text{H}_3\text{NCO}]^+$ and $[\text{C}_4\text{H}_3\text{N}]^+$.

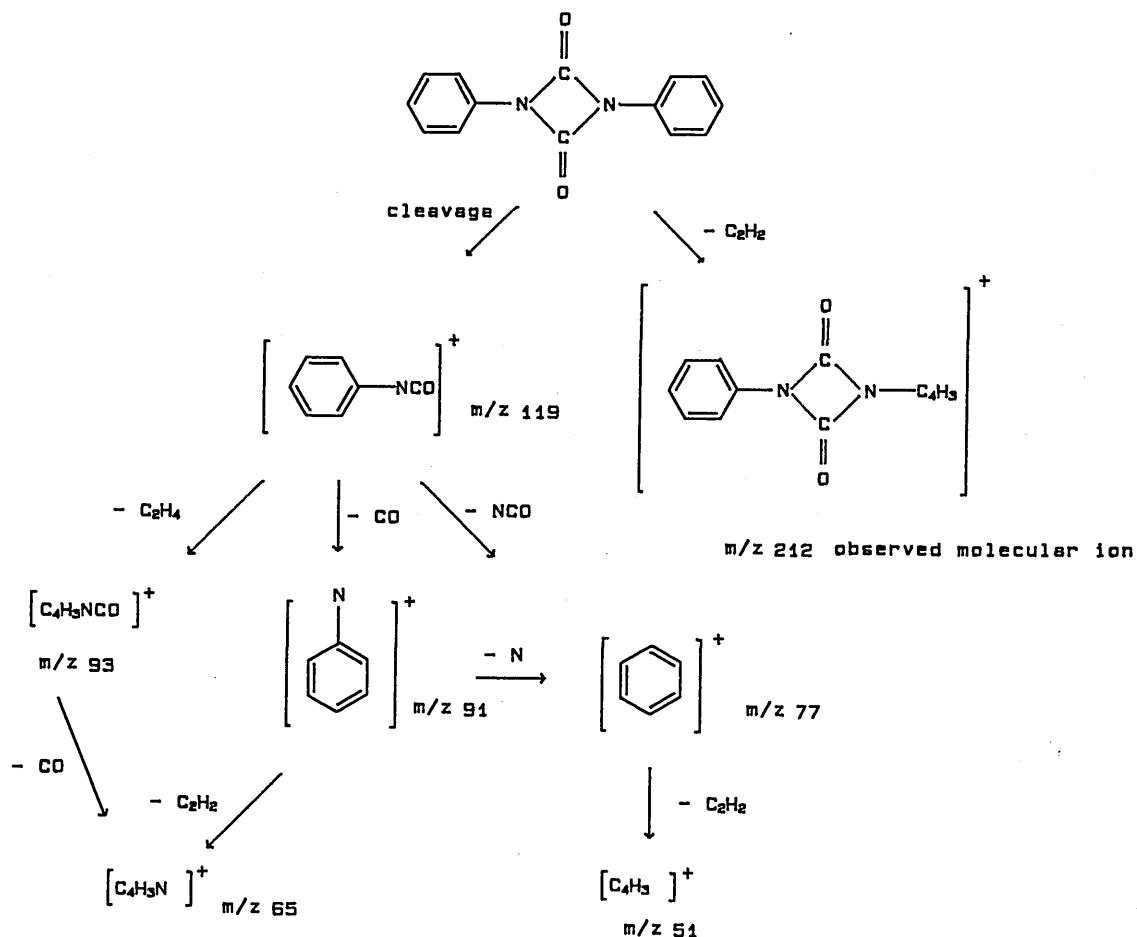
It was noted in Section 5.2.2 that in the presence of a catalyst, isocyanates may dimerize to form a uretidinedione. It is suggested that such a reaction occurs with phenyl isocyanate in the presence of *bis*-(tri-*n*-butyltin) oxide:



Reaction 5.14 Dimerization of Phenyl Isocyanate.

During electron impact in the mass spectrometer, the loss of ethyne from diphenyl uretidinedione would yield an apparent molecular ion with m/z 212.

The proposed breakdown is shown fully in Scheme 5.1:



Scheme 5.1 Proposed Fragmentation Products of Diphenyl Uretidinedione During Electron Impact.

Microanalytical data was in good agreement with that expected of diphenyl uretidinedione.

The liquid product, like the solid, was found not to contain isocyanate groups, but N—H bands (3300 cm^{-1}) and various C=O bands (1730 , 1650 , 1600 and 1550 cm^{-1}) were evident in the infrared spectrum. The ^{119}Sn NMR spectrum contained several signals:

Table 5.5 NMR Data of Liquid Products from *Bis*-(Tri-*n*-Butyltin) Oxide/Phenyl Isocyanate Reaction.

room temperature reaction		60°C reaction	
$\delta(^{119}\text{Sn})$	integral ratio	$\delta(^{119}\text{Sn})$	integral ratio
105.2	3	113.1	2
96.5	3	110.9	1
88.8	5	102.9	3
77.3	1	87.4	5
55.1	6	52.9	11
39.8	4	38.1	9
-8.8	1		

In fact, one more signal is observed in the room temperature reaction product than in the 60°C reaction product. The Mößbauer spectrum of the frozen liquid from the room temperature reaction was recorded at 80K and fitted as three quadrupole doublets, see Figure 5.24:

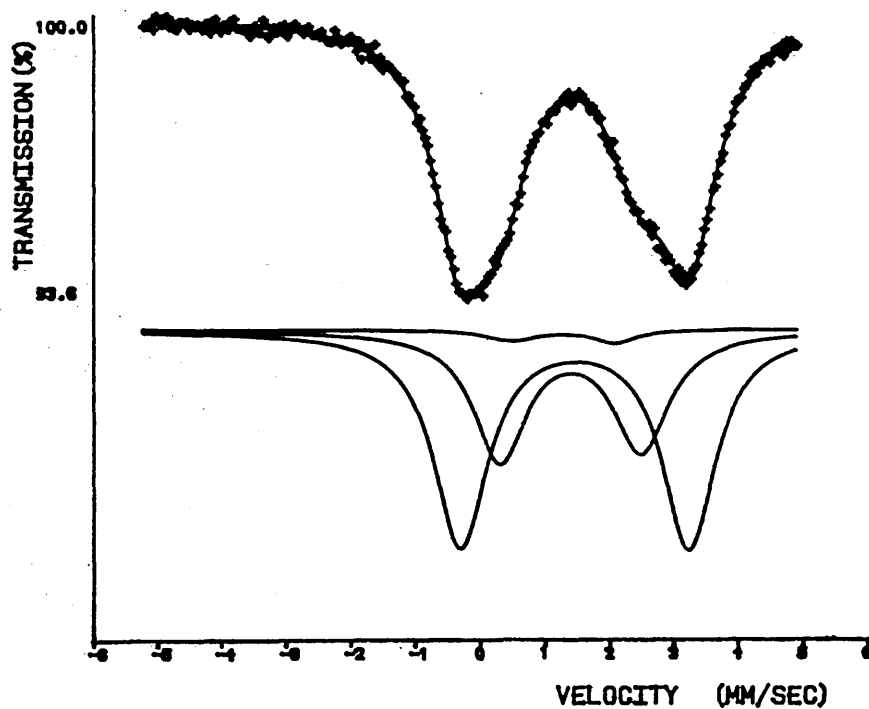


Figure 5.24 Mößbauer Spectrum of the Liquid Product from *Bis*-(Tri-*n*-Butyltin) Oxide/Phenyl Isocyanate RT Reaction.

The parameters for the Mößbauer spectrum are shown below in Table 5.6:

Table 5.6 Mößbauer Data for the Liquid Product from the Room Temperature *Bis*-(Tri-*n*-Butyltin) Oxide/Phenyl Isocyanate Reaction.

sample	phase	$\delta/$ mms ⁻¹	$\Delta E_Q/$ mms ⁻¹	$\Gamma_1/$ mms ⁻¹	$\Gamma_2/$ mms ⁻¹	%R.A.	ρ	χ^2
TBTO/PI	Q1	1.27	1.58	0.94	0.78	2.9	1.2	1.1
	Q2	1.40	2.18	0.98	1.06	35.5	1.6	
	Q3	1.47	3.53	1.01	1.01	61.6	2.4	

1. All spectra recorded at 80K with an error of $\pm 0.02 \text{mms}^{-1}$. Isomer shifts are relative to CaSnO_3 .
2. %R.A. is the relative area of each phase, *i.e.* quadrupole doublet.
3. $\rho = \Delta E_Q / \delta$.
4. TBTO is *bis*-(tri-*n*-butyltin) oxide and PI is phenyl isocyanate.

It is not valid to fit the spectrum with more doublets, (despite the NMR data), since the three phase fit with a χ^2 of around 1 is as statistically probable as any below this value. Only if constraints could be applied to the additional doublets, *i.e.* their identity and, therefore the Mößbauer parameters, would such fitting be statistically meaningful.

The most likely components of the liquid product are the N-stannylcarbmates, as suggested in Section 5.8.

5.9.2. The Reaction Between *Bis*-(Tri-*n*-Butyltin) Oxide and 1,6-Diisocyanatohexane

Equimolar quantities were added together in chloroform and an exothermic reaction occurred. Removal of the solvent left a clear liquid which was triturated with petroleum spirit. A white precipitate formed which was filtered off, (5% yield). Rotary evaporation of the filtrate left a cloudy, gelatinous product, (54% yield).

The solid product had a high melting point, (around 232°C), and its infrared spectrum was similar to that of the phenyl isocyanate solid product. However, unlike the latter, the 1,6-diisocyanatohexane solid product contained tin, with a weak signal at $\delta(^{119}\text{Sn}) -1.6$ ppm (in d_6 -DMSO) in the NMR spectrum. The presence of tin was confirmed by the mass spectrum, see Figure 5.25:

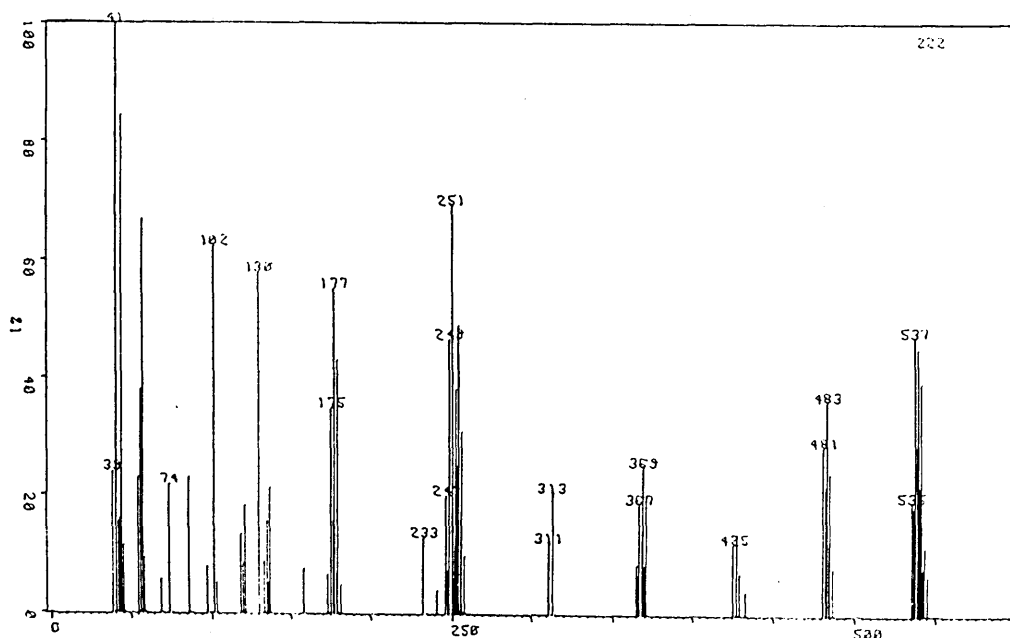


Figure 5.25 Mass Spectrum of the Solid Product of the *Bis*-(Tri-*n*-Butyltin Oxide/1,6-Diisocyanatohexane RT Reaction.

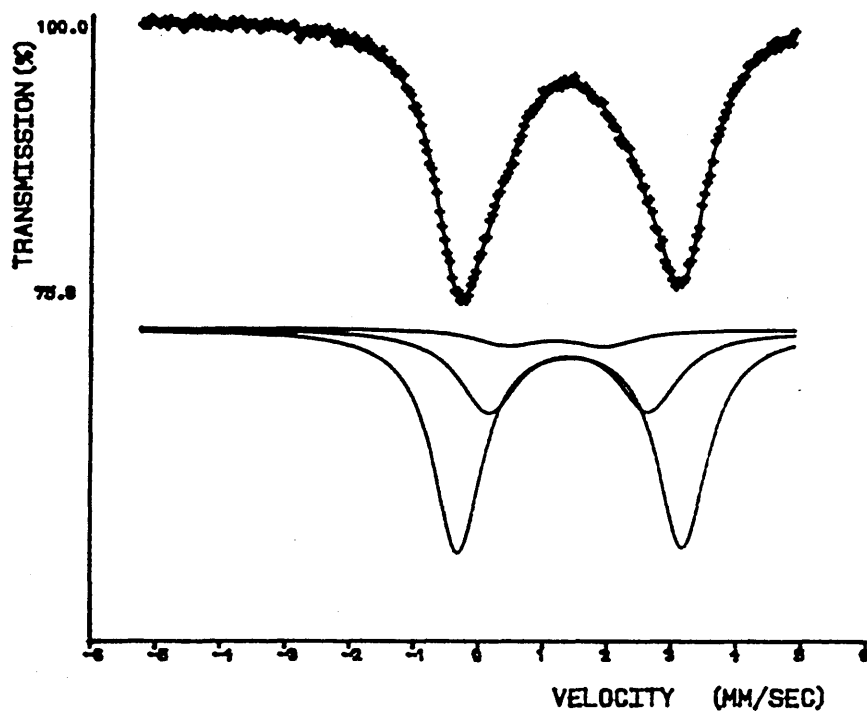
Tin containing fragments are evident at m/z 537, 483, 425, 369, 251 and 177. It was noted that a loss of 74 mass units from m/z 251 would result in a peak at m/z 177 and a peak at m/z 74 is present in the spectrum. The signal at m/z 177 is almost certainly $[\text{BuSn}]^+$, but assignment of m/z 74 and, therefore, m/z 251, cannot be easily made (one possible stoichiometry is $[\text{CNO}_3]^+$).

The observed molecular ion is not *bis*-(tri-*n*-butyltin) oxide, (RMM 598), although fragments of m/z 57, $[\text{Bu}]^+$, are progressively lost from m/z 537 \rightarrow m/z 483 \rightarrow m/z 425 \rightarrow m/z 369 \rightarrow m/z 313. A peak at m/z 57 is present. The mass spectrum of this solid product is more complex and hence more difficult to interpret than that of the *bis*-(tri-*n*-butyltin) oxide/phenyl isocyanate solid product.

The infrared spectrum of the gelatinous product does not contain the isocyanate stretching band, but N—H and urethane/imide C=O stretching bands are both present. C—O absorption bands are also evident. The ^{119}Sn NMR spectrum (in CDCl_3) exhibited three signals at 95.6, 92.4 and 75.4 ppm (3:4:1 integral ratio). The most intense signal corresponds to unchanged *bis*-(tri-*n*-butyltin) oxide.

The Mößbauer spectrum was fitted as three quadrupole doublets, one of which was constrained to the parameters of *bis*-(tri-*n*-butyltin) oxide, see Figure 5.26(a) and Table 5.7.

5.26 (a)



5.26 (b)

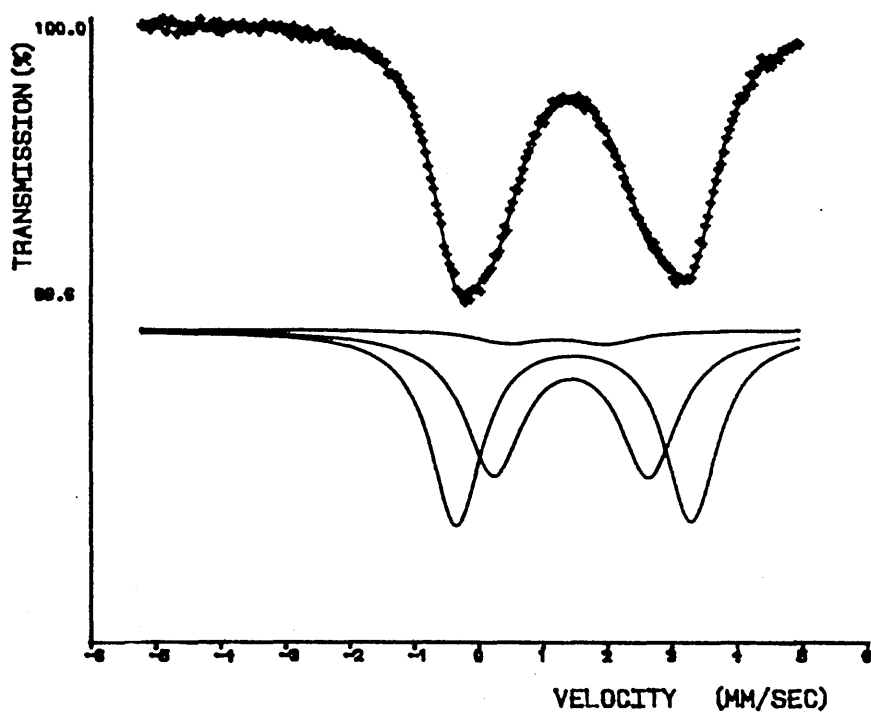


Figure 5.26 (a) Mössbauer Spectrum of the Gelatinous Product from the RT Reaction of *Bis*-(Tri-*n*-Butyltin) Oxide with 1,6-Diisocyanatohexane and 5.26 (b) Mössbauer Spectrum of the Liquid Product from the RT Reaction of *Bis*-(Tri-*n*-Butyltin) Oxide with 1,4-Phenylene Diisocyanate.

Table 5.7 Mößbauer Data for the Gelatinous Product from the Room Temperature *Bis*-(Tri-*n*-Butyltin) Oxide/1,6-Diisocyanatohexane Reaction.

sample	phase	$\delta/$ mms ⁻¹	$\Delta E_Q/$ mms ⁻¹	$\Gamma_1/$ mms ⁻¹	$\Gamma_2/$ mms ⁻¹	%R.A.	ρ	χ^2
TBTO/DIH	Q1	1.21	1.52	1.20	1.20	6.0	1.3	1.7
	Q2	1.41	2.48	1.13	1.15	29.0	1.8	
	Q3	1.43	3.49	0.92	0.95	65.0	2.4	

1. All spectra recorded at 80K with an error of $\pm 0.02\text{mms}^{-1}$. Isomer shifts are relative to CaSnO_3 .
2. %R.A. is the relative area of each phase, *i.e.* quadrupole doublet.
3. $\rho = \Delta E_Q / \delta$.
4. TBTO is *bis*-(tri-*n*-butyltin) oxide and DIH is 1,6-diisocyanatohexane.

It is interesting to note that the relative area of the *bis*-(tri-*n*-butyltin) oxide doublet is just 6%, whereas in the NMR spectrum it is the most intense signal. This is unlikely to be due to differences in the recoil-free fractions of Q1, Q2 and Q3 alone; some additional factor(s) must also be at work. The parameters of Q3 are very similar to those of tri-*n*-butyltin chloride, although that compound cannot be present in the gel.

5.9.3. The Reaction Between *Bis*-(Tri-*n*-Butyltin) Oxide and 1,4-Phenylene Diisocyanate

Mixing equimolar quantities of the starting materials in chloroform gave rise to an exothermic reaction. As with the previous two reactions, a viscous liquid was isolated, which when triturated with petroleum spirit yielded two products. The first was a cream-coloured solid (5% yield) and a thick yellow oil (66% yield). The latter darkened after two days.

The solid product did not melt, but charred at around 250°C and decomposed above 300°C. The infrared spectrum showed evidence of N—H, amide C=O and C—O groups, but no —N=C=O moieties. The ^{119}Sn NMR spectrum was devoid of signals, but the mass spectrum contains several peaks with the tin isotopic splitting pattern, see Figure 5.27.

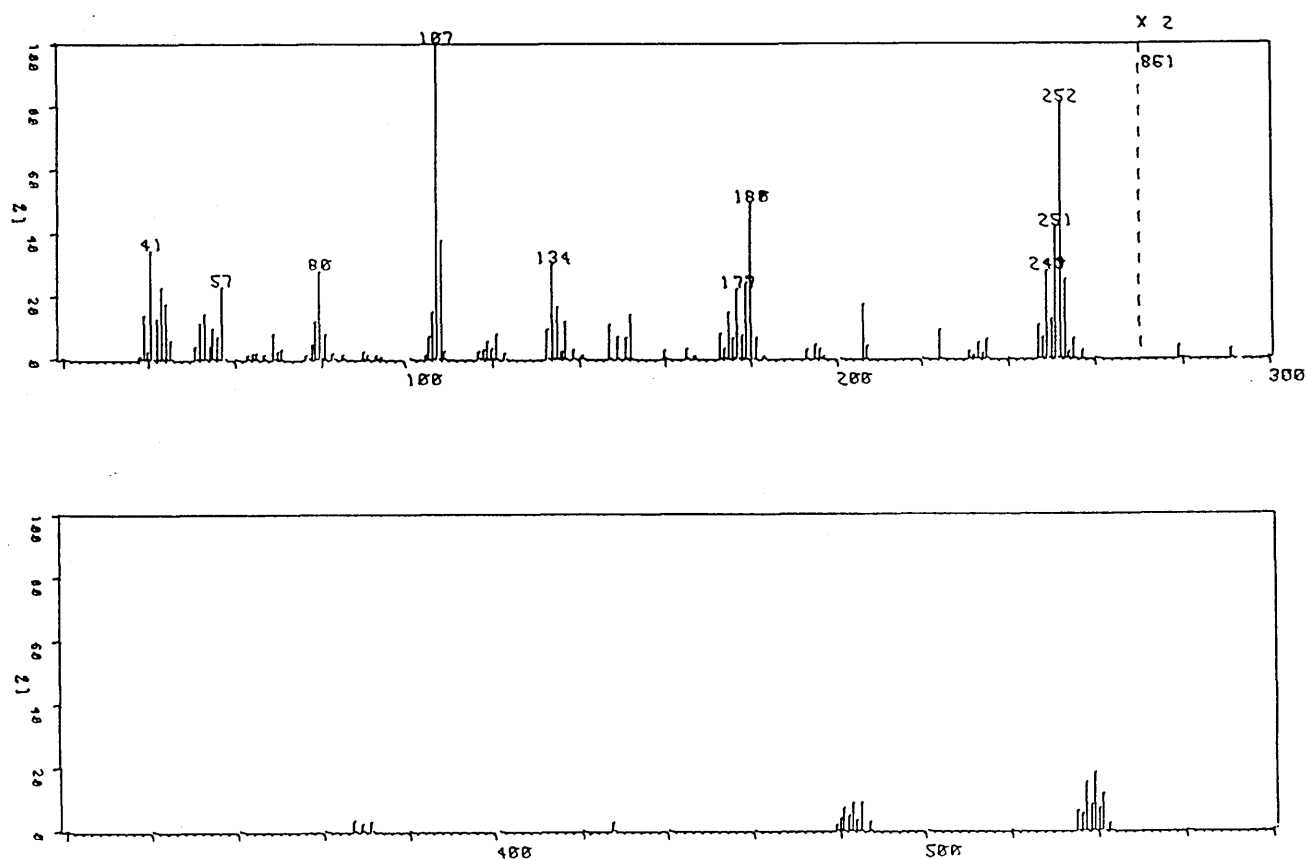


Figure 5.27 Mass Spectrum of the Solid Product of the *Bis*-(Tri-n-Butyltin Oxide)/1,4-Phenylene Diisocyanate RT Reaction.

The spectrum is rather similar to that of the solid product of *bis*-(tri-n-butyltin) oxide/1,6-diisocyanatohexane, the major differences being the relatively weak intensities of the higher m/z signals. This suggests that these species are very easily fragmented during electron impact. Assignments to the higher m/z signals have not been made.

The infrared spectrum of the liquid product, like that of the solid, contained N—H, amide C=O and C—O stretching bands, but not those of —N=C=O. The ^{119}Sn NMR spectrum of the product exhibited several peaks:

Table 5.8 NMR Data of Liquid Products from *Bis*-(Tri-*n*-Butyltin) Oxide/1,4-Phenylene Diisocyanate Reaction.

room temperature reaction		60°C reaction	
$\delta(^{119}\text{Sn})$	integral ratio	$\delta(^{119}\text{Sn})$	integral ratio
		114.6	n/a
102.1	2	102.6	n/a
93.1	4		
81.4	2	82.9	n/a
61.3	1	76.5	n/a
50.4	3	51.8	n/a
45.5	2		
38.6	1	38.6	n/a
-11.5	1	-11.2	n/a

The room temperature reaction has resulted in the formation of one more tin species than the equivalent reaction at 60°C. Unreacted *bis*-(tri-*n*-butyltin) oxide appears to be present in the product and this is confirmed by the Mößbauer spectrum, see Figure 5.26(b), p.211. The parameters for the fit are shown in Table 5.9.

Table 5.9 Mößbauer Data for the Liquid Product from the Room Temperature *Bis*-(Tri-*n*-Butyltin) Oxide/Phenylene 1,4-Diisocyanate Reaction.

sample	phase	$\delta/$ mms^{-1}	$\Delta E_Q/$ mms^{-1}	$\Gamma_1/$ mms^{-1}	$\Gamma_2/$ mms^{-1}	%R.A.	ρ	χ^2
TBTO/PDI	Q1	1.21	1.52	1.20	1.20	6.0	1.3	1.8
	Q2	1.44	2.41	1.11	1.10	43.3	1.7	
	Q3	1.47	3.65	0.97	0.99	52.5	2.5	

1. All spectra recorded at 80K with an error of $\pm 0.02\text{mms}^{-1}$. Isomer shifts are relative to CaSnO_3 .
2. %R.A. is the relative area of each phase, *i.e.* quadrupole doublet.
3. $\rho = \Delta E_Q / \delta$.
4. TBTO is *bis*-(tri-*n*-butyltin) oxide and PDI is 1,4-phenylene diisocyanate.

The parameters of Q2 and Q3 of the gelatinous product of *bis*-(tri-*n*-butyltin) oxide/1,6-diisocyanatohexane are very similar to those of the liquid product with 1,4-phenylene diisocyanate.

5.10. Discussion of Results of the Room Temperature Reactions Between *Bis*-(Tri-*n*-Butyltin) Oxide and the Isocyanates

It has been shown that *bis*-(tri-*n*-butyltin) oxide reacts rapidly and exothermically with the three isocyanates. In all cases a small amount of solid was isolated ($\approx 5\%$ yield), together with a liquid or gel ($\approx 50-80\%$ yield). The former all had high melting points and exhibited amide carbonyl bands, but no isocyanate absorption. From the spectroscopic evidence, the solid product of the phenyl isocyanate reaction has been identified as the dimer, diphenyl uretidinedione (Reaction 5.14).

The solid products from the diisocyanate reactions have not been identified, due to the increased complexity of their mass spectra. These have shown that a tin species is present which is progressively debutylated by electron impact. It is assumed that the difunctional nature of 1,6-diisocyanatohexane and 1,4-phenylene diisocyanate results in a more complex reaction scheme than with phenyl isocyanate.

The liquid/gelatinous products from the three reactions are also complex. With the aromatic isocyanates at least seven tin signals are observed in the NMR spectra. Only three are evident in the 1,6-diisocyanatohexane gel. The TLC behaviour of the liquid products is very similar, each resulting in a single spot. An attempt was made to separate the three components of the gel by GC (for GC/MS analysis), but just one peak was apparent.

From the NMR and Mößbauer data it is clear that similar types of species are present in the liquid/gelatinous products, but it is only possible to speculate on their identity. It is thought that the species described in Section 5.8 (pp. 201-202) are present in these products.

5.11. Triorganotin Reactions with DND

One further series of experiments was carried out, the reaction of the triorganotin biocides with the authentic polyurethane isocyanate, DND. The stoichiometry of DND is not well defined, all reactions were with an excess of the isocyanate. Conditions were the same as those in the previous section, *i.e.* room temperature for one hour in chloroform solution.

5.11.1. The Reaction Between *Bis*-(Tri-*n*-Butyltin) Oxide and DND

The reaction was exothermic for around five minutes after the starting materials were placed in solution. Solvent evaporation yielded an orange oil, which, when triturated with petroleum spirit, yielded a small amount of white solid, (#1). The latter was isolated by filtration (0.6g) and rotary evaporation of the filtrate produced a yellow solid (5.6g, #2).

Both solids had high melting points ($>220^{\circ}\text{C}$) and both were insoluble in the available NMR solvents. The infrared spectra of both products contained weak amide N—H and $-\text{N}=\text{C}=\text{O}$ stretching bands, as well as strong amide C=O bands. The Mößbauer spectra of both products were recorded and the parameters are shown below in Table 5.10:

Table 5.10 Mößbauer Data for the *Bis*-(Tri-*n*-Butyltin) Oxide/DND Reaction Products.

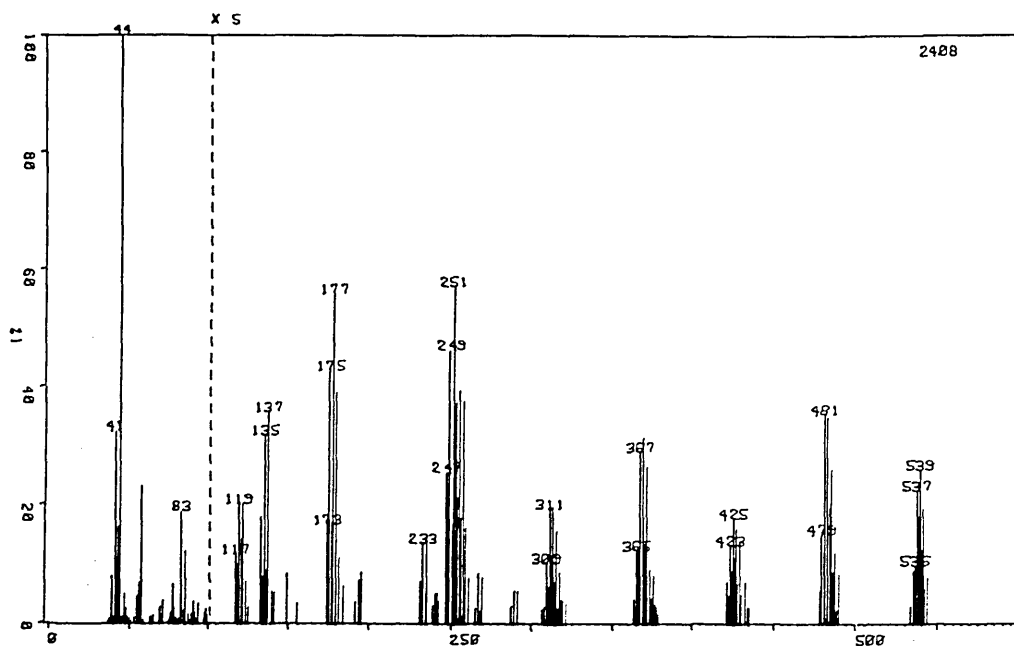
sample	phase	δ/mms^{-1}	$\Delta E_Q/\text{mms}^{-1}$	Γ_1/mms^{-1}	Γ_2/mms^{-1}	%R.A.	ρ	χ^2
solid #1	Q1	1.43	2.45	1.09	1.16	92.8	1.7	0.9
	Q2	1.63	2.85	0.81	0.70	7.2	1.7	
solid #2	Q1	1.43	3.52	1.22	1.26	100.0	2.3	0.9
pure TBTO	Q1	1.21	1.52	1.18	1.18	100.0	1.3	1.2

1. All spectra recorded at 80K with an error of $\pm 0.02\text{mms}^{-1}$. Isomer shifts are relative to CaSnO_3 .
2. %R.A. is the relative area of each phase, *i.e.* quadrupole doublet.
3. $\rho = \Delta E_Q/\delta$.
4. TBTO is *bis*-(tri-*n*-butyltin) oxide.

It is evident that neither solid #1 or #2 contain pure *bis*-(tri-*n*-butyltin) oxide, but, rather, a more highly coordinate tin (IV) species.

The mass spectra of both solids were recorded. The samples were placed in the volatilization chamber at 240°C and two ion current maxima were observed for both solids, the first at around seven minutes, the second at around twenty-five minutes. The spectra are shown in Figures 5.28 and 5.29. Both sets of spectra contain similar fragmentation products:

5.28 (a)



5.28 (b)

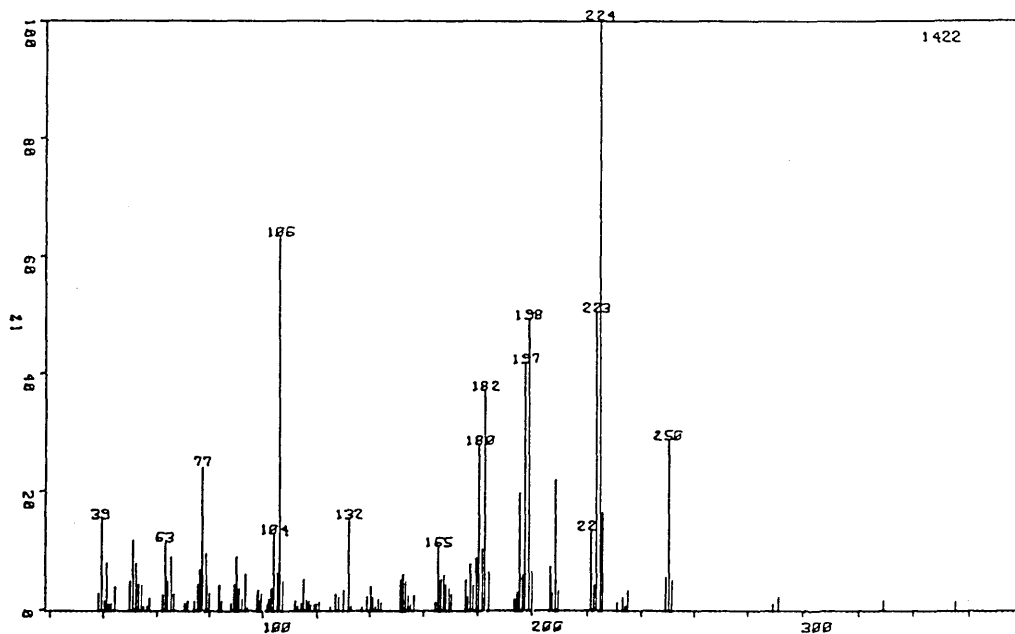


Figure 5.28 Mass Spectra of Solid Product #1 of the *Bis*-(Tri-*n*-Butyltin) Oxide/DND Room Temperature Reaction after 6 minutes, (a) and 24 minutes, (b).

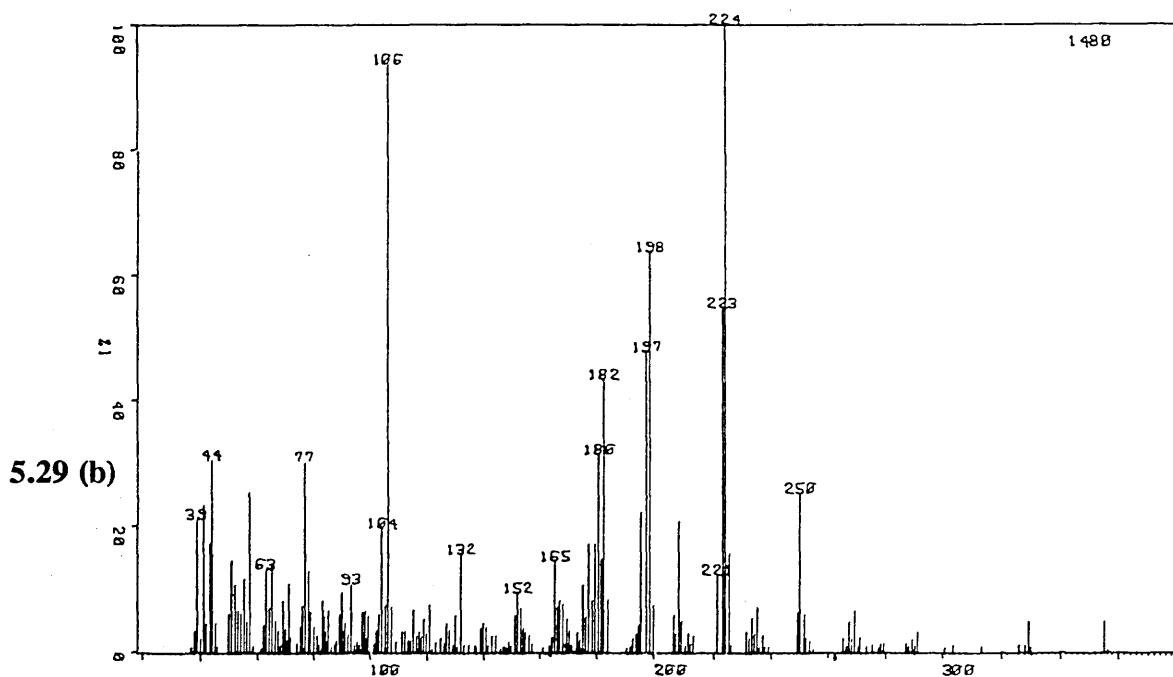
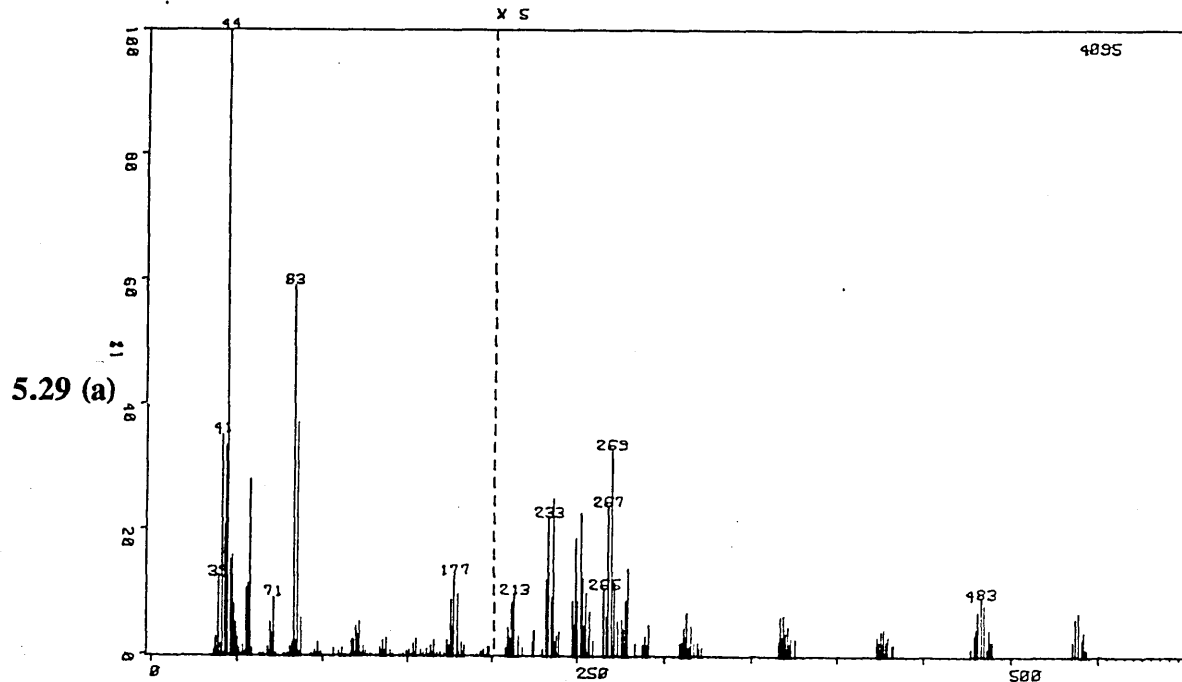


Figure 5.29 Mass Spectra of Solid Product #2 of the *Bis*-(Tri-*n*-Butyltin) Oxide/DND Room Temperature Reaction after 7 minutes, (a) and 25 minutes, (b).

6/7 minute spectra of solids #1 and #2:

<u>m/z signal</u>	<u>assignment</u>
535/537/539	$[\text{Bu}_3\text{SnOSn}(\text{C}_4\text{H}_8)_2]^+$
479/481	$[\text{BuSnOSn}(\text{C}_4\text{H}_8)_3]^+$
423/425	$[\text{BuSnOSn}(\text{C}_4\text{H}_8)_2]^+$
365/367	$[\text{C}_4\text{H}_8\text{SnOSnC}_4\text{H}_7]^+$
309/311	$[\text{C}_4\text{H}_7\text{SnOSn}]^+$
265/267/269	$[\text{CHSnOSn}]^+$
247/249/251	$[\text{Bu}_2\text{SnOH}]^+$
233	
173/175/177	$[\text{BuSn}]^+$
83	$[\text{C}_4\text{H}_9\text{NC}]^+$ or $[\text{C}_4\text{H}_9\text{C}_2\text{H}_2]^+$
57	$[\text{Bu}]^+$
44	$[\text{C}_3\text{H}_8]^+$
41	$[\text{C}_3\text{H}_5]^+$

It is clear that the more volatile species in solids #1 and #2 contain tin fragments almost certainly derived from *bis*-(tri-n-butyltin) oxide. The most intense peaks in both spectra occur at *m/z* 44 and 83. The former is due to $[\text{C}_3\text{H}_8]^+$, a fragment of the butyl group. The latter is more difficult to account for; two possibilities are $[\text{C}_4\text{H}_9\text{NC}]^+$ and $[\text{C}_4\text{H}_9\text{C}_2\text{H}_2]^+$.

The less volatile species in solids #1 and #2 again have very similar mass spectra:

<u>m/z signal</u>	<u>assignment</u>
250	$[(C_6H_4NCO)_2CH_2]^+$
224	$[C_6H_4N_2Sn]^+$ or $[C_6H_5NHCSn]^+$
223	$[C_6H_5NCSn]^+$ or $[C_6H_4NHCSn]^+$
208	$[C_6H_4CH_2C_6H_4NCO]^+$
198	$[C_6H_5SnH]^+$
197	$[C_6H_5Sn]^+$
182	$[H_2NC_6H_4CH_2C_6H_5]^+$
180	$[NC_6H_4CH_2C_6H_4]^+$
165	$[C_3H_8SnH]^+$
132	$[SnC]^+$ or $[CH_2C_6H_4NCO]^+$
118/120	$[Sn]^+$
106	$[C_6H_4CH_2NC]^+$ or $[C_6H_4(NH)_2]^+$
104	$[C_6H_4N_2]^+$ or $[C_6H_5NHC]^+$
77	$[C_6H_5]^+$
63	
57	$[Bu]^+$
44	$[C_3H_8]^+$
39	$[C_3H_3]^+$

The later evaporating species would seem to contain the isocyanate and its reaction products. Traces of tin are present in both spectra and assignments are made to most of the observed *m/z* peaks. Those of most interest are perhaps *m/z* 83, $[C_4H_9NC]^+/[C_4H_9C_2H_2]^+$; *m/z* 224, $[C_6H_4N_2Sn]^+$ or $[C_6H_5NHCSn]^+$; *m/z* 223, $[C_6H_5NCSn]^+/[C_6H_4NHCSn]^+$ and *m/z* 197, $[C_6H_5Sn]^+$, since these fragments are made up of components of both starting materials.

(It must be noted that other assignments may exist for the observed *m/z* peaks observed in these spectra).

5.11.2. The Reaction Between Tri-n-Butyltin Chloride and DND

No heat was evolved when the two compounds were brought together in chloroform. The product isolated was an orange oil, (as is pure DND), the Mößbauer and NMR parameters of which indicated that the only tin species present was the starting material. The infrared spectrum was almost identical to that of pure DND.

5.11.3. The Reaction Between Tri-n-Butyltin Acetate and DND

The reaction was exothermic, though less so than that of *bis*-(tri-n-butyltin) oxide. Solvent evaporation resulted in a yellow mass, which, when triturated with petroleum spirit yielded a cream-coloured solid (0.4g, #1). The filtrate was reduced on a rotary evaporator to yield a yellow amorphous solid (4.8g, #2). Both solids were insoluble in the available NMR solvents and both had high melting points ($>300^{\circ}\text{C}$). The infrared spectra of the two products were also very similar, with strong N—H, —N=C=O, amide C=O and C—O— bands. The Mößbauer spectra of both solids were recorded, but that of solid #1 showed no absorbance.

Table 5.11 Mößbauer Data for the *Bis*-(Tri-n-Butyltin) Acetate/DND Reaction Products.

sample	phase	δ/mms^{-1}	$\Delta E_Q/\text{mms}^{-1}$	Γ_1/mms^{-1}	Γ_2/mms^{-1}	%R.A.	ρ	χ^2
solid #2 pure TBTOAc	Q1	1.51	3.59	0.95	0.93	100.0	2.4	0.7
	Q1	1.40	3.54	1.02	0.92	100.0	2.2	0.4

1. All spectra recorded at 80K with an error of $\pm 0.02\text{mms}^{-1}$. Isomer shifts are relative to CaSnO_3 .
2. %R.A. is the relative area of each phase, *i.e.* quadrupole doublet.
3. $\rho = \Delta E_Q/\delta$.
4. TBTOAc is tri-n-butyltin acetate.

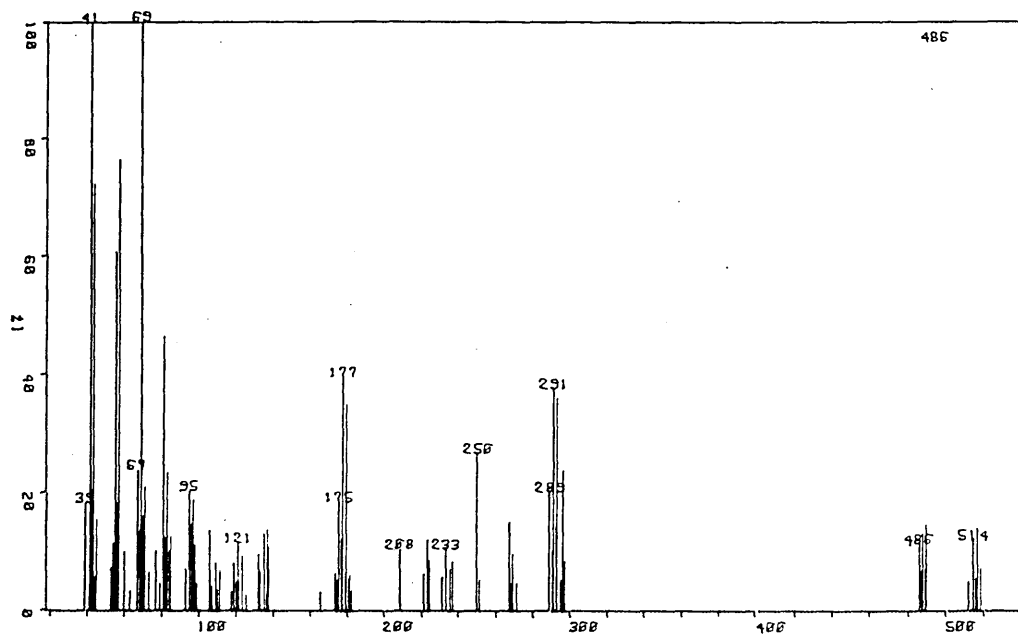
The Mößbauer data suggests that the tin species present in solid #2, if not unreacted organotin, is very similar in nature.

The mass spectra of both solids were recorded. As with the solids from the *bis*-(tri-*n*-butyltin) oxide reaction, two ion current maxima were observed at similar time intervals. The spectra are shown in Figures 5.30 and 5.31 and possible assignments are listed below:

9 minute spectrum of solid #1:

<u>m/z signal</u>	<u>assignment</u>
514	$[(C_6H_4NCO)_4(CH_2)_3]^+$
485	$[M-HCO]^+$
291/289	$[Bu_3Sn]^+$
250	$[(C_6H_4NCO)_2CH_2]^+$
233	$[BuSnC_4H_8]^+$ or $[OCNC_6H_4CH_2C_6H_4NH]^+$
208	$[OCNC_6H_4CH_2C_6H_4]^+$
175/177	$[BuSn]^+$
121	$[SnH]^+$
95	
77/76	$[C_6H_5]^+/[C_6H_4]^+$
69	
57	$[Bu]^+$
41	$[C_3H_5]^+$

5.30 (a)



5.30 (b)

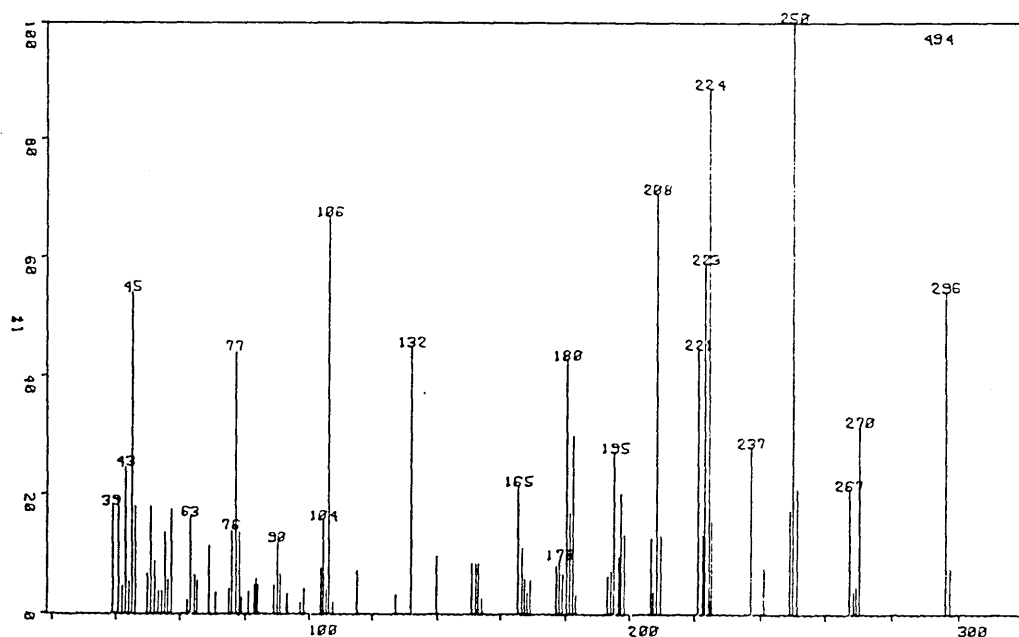
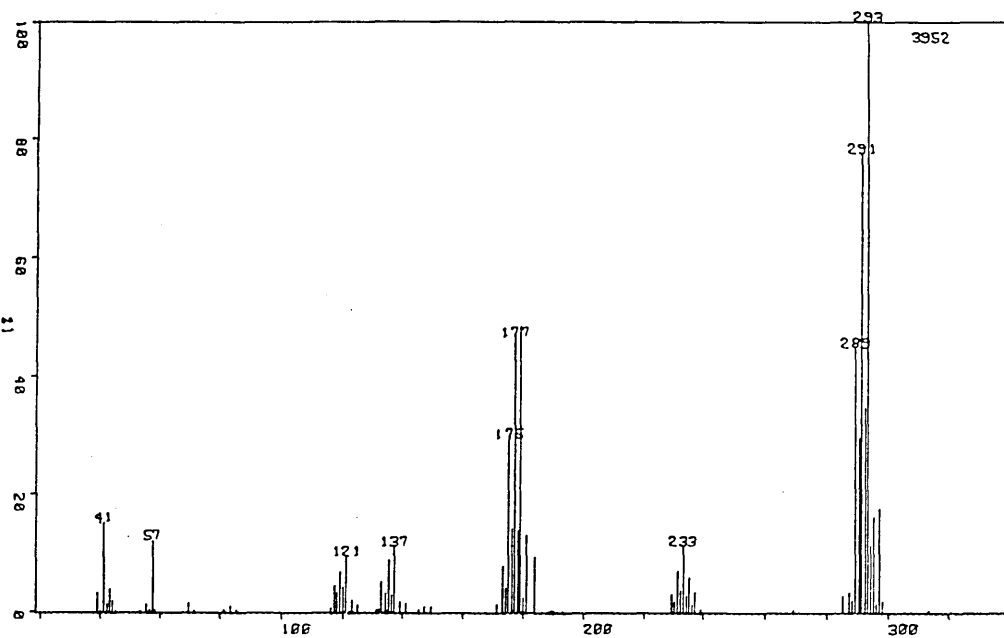


Figure 5.30 Mass Spectra of Solid Product #1 of the Tri-n-Butyltin Acetate/DND Room Temperature Reaction after 9 minutes, (a) and 24 minutes, (b).

5.31 (a)



5.31 (b)

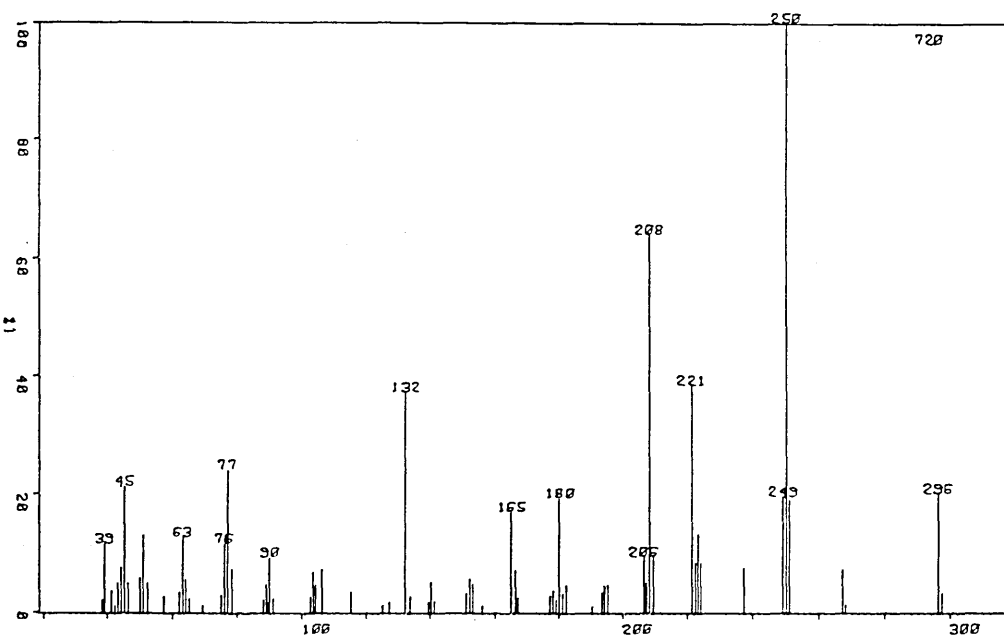


Figure 5.31 Mass Spectra of Solid Product #2 of the Tri-n-Butyltin Acetate/DND Room Temperature Reaction after 4 minutes, (a) and 22 minutes, (b).

24 minute spectrum of solid #1:

<u>m/z signal</u>	<u>assignment</u>
296	
267/270	
250	$[(C_6H_4NCO)_2CH_2]^+$
237	
224/223/221	
208	$[OCNC_6H_4CH_2C_6H_4]^+$
195	
180	$[NC_6H_4CH_2C_6H_4]^+$
178	
165	loss of NH from m/z 180?
132	$[CH_2C_6H_4NCO]^+$ or $[NC_6H_4NCO]^+$
106	$[C_6H_4CH_2NC]^+$ or $[C_6H_4(NH)_2]^+$
104	$[C_6H_4N_2]^+$ or $[C_6H_5NHC]^+$ or $[C_6H_4(CH_2)_2]^+$
90	$[C_6H_4N]^+$ or $[C_6H_4(CH_2)]^+$
76/77	$[C_6H_5]^+/[C_6H_4]^+$
63	
45	
43	
39	$[C_3H_3]^+$

It is evident that the earlier evaporating component of solid #1 contains both unreacted isocyanate, (m/z 514) and a tri-n-butyltin species. The second component shows no evidence of tin. These observations are also true of the two components of solid #2 from the tri-n-butyltin acetate/DND reaction (see Figure 5.31). Very similar m/z peaks are evident in the two spectra of solid #2 and solid #1.

5.11.4. The Reaction Between *Bis*-(Triphenyltin) Oxide and DND

The reaction was noticeably exothermic. A cream-coloured solid (11.6g) was isolated after solvent evaporation and trituration with petroleum spirit. It was insoluble in the available NMR solvents and melted at 165–180°C. The infrared spectrum contained amide/amine N—H, amide C=O and C—O stretching bands. No isocyanate absorption was observed.

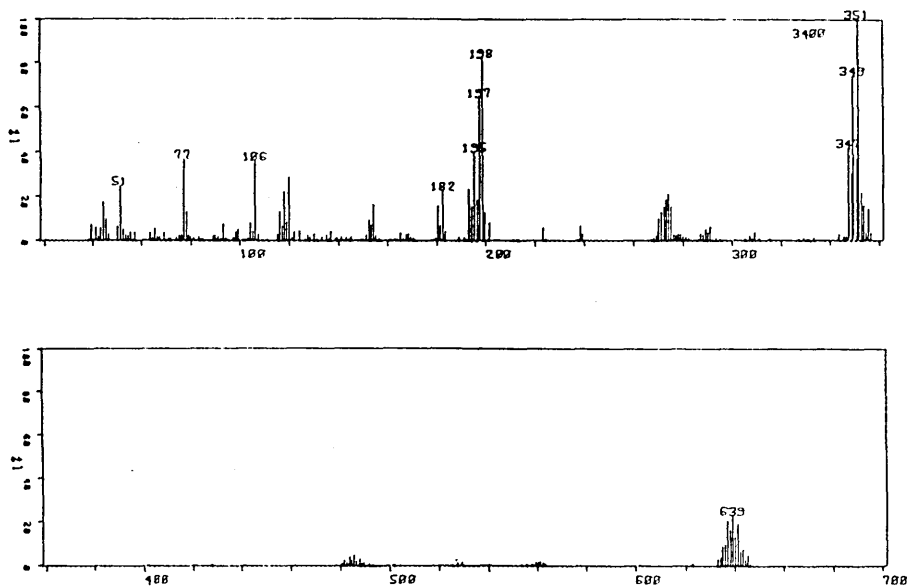
The Mößbauer spectrum of the solid was recorded and the parameters are shown below:

Table 5.12 Mößbauer Data for the *Bis*-(Triphenyltin) Oxide/DND Reaction Products.

sample	phase	$\delta/$ mms^{-1}	$\Delta E_Q/$ mms^{-1}	$\Gamma_1/$ mms^{-1}	$\Gamma_2/$ mms^{-1}	%R.A.	ρ	χ^2
TPTO/DND	Q1	1.19	2.96	1.04	1.15	75.2	2.5	0.7
	Q2	1.41	2.98	0.99	0.88	24.8	2.1	
pure TPTO	Q1	1.09	1.33	0.95	0.95	84.9	1.2	0.6
	Q2	1.16	2.66	1.13	1.13	15.1	2.3	

1. All spectra recorded at 80K with an error of $\pm 0.02 \text{mms}^{-1}$. Isomer shifts are relative to CaSnO_3 .
2. %R.A. is the relative area of each phase, *i.e.* quadrupole doublet.
3. $\rho = \Delta E_Q / \delta$.
4. TPTO is *bis*-(triphenyltin) oxide.

The Mößbauer parameters indicate that *bis*-(triphenyltin) oxide is not present in the reaction product. The mass spectrum, in contrast, is dominated by tin-containing fragments typical of the pure organotin, see Figure 5.32:



**Figure 5.32 Mass Spectra of the *Bis*-(Triphenyltin) Oxide/
DND Room Temperature Reaction Product.**

<u>m/z signal</u>	<u>assignment</u>
639/641	$[(\text{Ph}_3(\text{C}_6\text{H}_4)_2\text{Sn})_2\text{O}]^+ / [\text{Ph}_5\text{Sn}_2\text{O}]^+$
487	$[\text{Ph}_3\text{Sn}_2\text{O}]^+$
347/349/351	$[\text{Ph}_3\text{Sn}]^+$
274	$[\text{Ph}_2\text{Sn}]^+$
195/197/198	$[\text{PhSn}]^+ / [\text{PhSnH}]^+$
182	
118/120	$[\text{Sn}]^+$
106	$[\text{H}_2\text{N}_2\text{C}_6\text{H}_4]^+ / [\text{ONH}_2\text{C}_6\text{H}_4]^+$
77	$[\text{Ph}]^+$
51	$[\text{C}_4\text{H}_3]^+$

5.11.5. The Reaction Between Triphenyltin Chloride and DND

The reaction was slightly exothermic, but not to the same degree as with the *bis*-(triorganotin) oxides. Solvent evaporation and trituration yielded just one product, an orange sticky mass (6.2g). The product decomposed at around 350°C and was insoluble in the available NMR solvents. The Mößbauer spectrum exhibited one quadrupole doublet with parameters very similar to those of the pure organotin. The infrared spectrum exhibited a strong isocyanate absorbance, as well as N—H, amide C=O and C—O stretching bands.

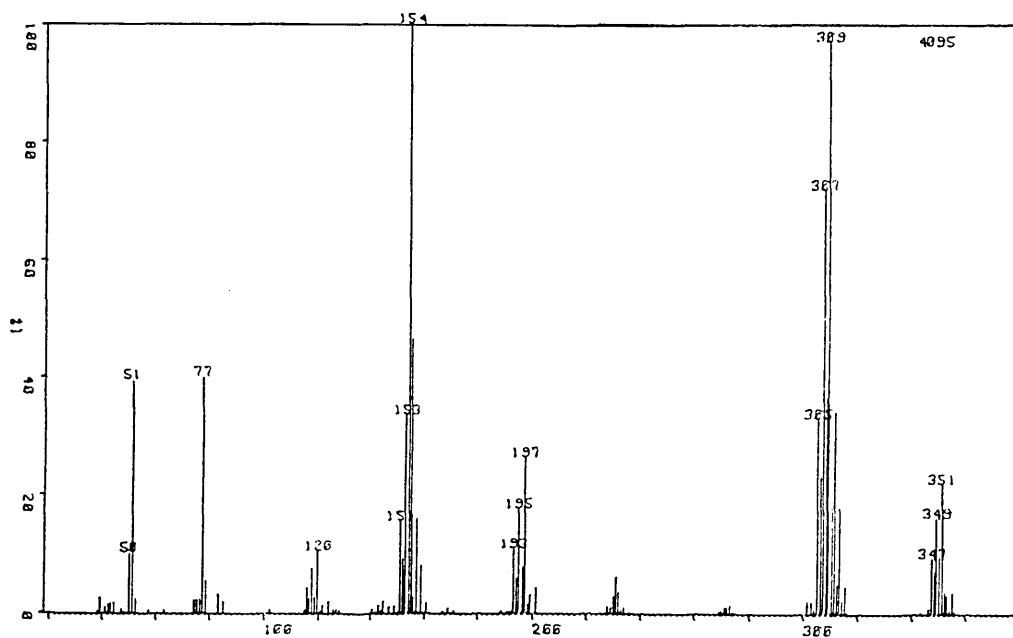
Two maxima in the ion current were observed when the mass spectrum was recorded (Figure 5.33). Assignments to the observed *m/z* peaks are listed below:

7 minute mass spectrum of triphenyltin chloride/DND reaction product:

<u><i>m/z</i> signal</u>	<u>assignment</u>
347/349/351	[Ph ₃ Sn] ⁺
305/307/309	[Ph ₂ SnCl] ⁺
193/195/197	[PhSn] ⁺
151/153/154	[SnCl] ⁺
116/118/120	[Sn] ⁺
77	[Ph] ⁺
51	[C ₄ H ₃] ⁺

The spectrum consists entirely of fragments of triphenyltin chloride. The less volatile component of the product contains both tin and isocyanate fragments:

5.33 (a)



5.33 (b)

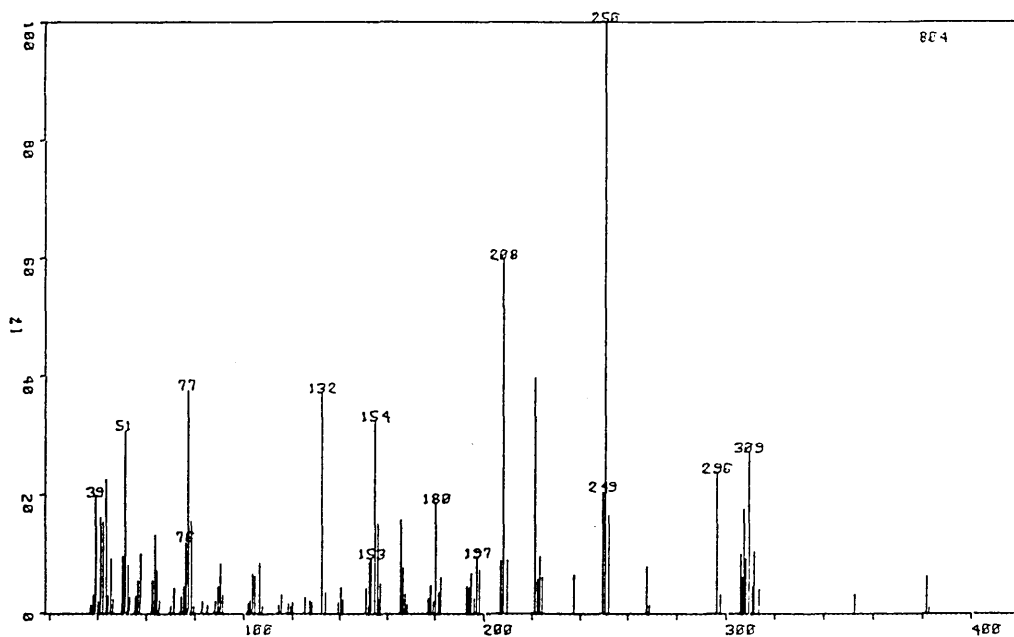


Figure 5.33 Mass Spectra of the Triphenyltin Chloride/DND Room Temperature Reaction Product after 7 minutes, (a) and 19 minutes, (b).

<u>m/z signal</u>	<u>assignment</u>
307/309	$[\text{Ph}_2\text{SnCl}]^+$
296	
250	$[(\text{C}_6\text{H}_4\text{NCO})_2\text{CH}_2]^+$
221	
208	$[\text{C}_6\text{H}_4\text{CH}_2\text{C}_6\text{H}_4\text{NCO}]^+$
195/197	$[\text{PhSn}]^+$
180	$[\text{NC}_6\text{H}_4\text{CH}_2\text{C}_6\text{H}_4]^+ / [\text{CH}_2\text{C}_6\text{H}_4\text{CH}_2\text{C}_6\text{H}_4]^+$
153/154	
132	$[\text{CH}_2\text{C}_6\text{H}_4\text{NCO}]^+ / [\text{NC}_6\text{H}_4\text{NCO}]^+$
76/77	$[\text{C}_6\text{H}_4]^+ / [\text{C}_6\text{H}_5]^+$
51	$[\text{C}_4\text{H}_3]^+$
39	$[\text{C}_3\text{H}_3]^+$

5.12. Discussion and Conclusion of the Model Studies

Apart from tri-n-butyltin chloride, all of the triorganotins studied interact or react with the polymeric isocyanate, DND. However, this would not appear to be a prerequisite of catalytic activity, since tri-n-butyltin chloride reduced the polymer setting time, which triphenyltin chloride and tri-n-butyltin acetate did not. It was stated in Section 5.2.2 that isocyanates can, in the presence of catalysts, form oligomers *viz*, uretidinediones, isocyanurates, carbodiimides and uretonimines. Mass spectral evidence for the presence of a uretidinedione in the solid product of the room temperature reaction between *bis*-(tri-n-butyltin) oxide and phenyl isocyanate was found. However, the triorganotins may themselves also react with the isocyanates to yield N-stannylcarbamates (Section 5.8).

Bis-(tri-n-butyltin) oxide and tri-n-butyltin acetate both behaved in a similar way with DND, each yielding two solids. The solids, when analyzed by mass spectrometry, all exhibited two ion current maxima. The first was associated with the triorganotins and their fragmentation products, the second with the

higher boiling isocyanate components. These observations suggest that the organotins are complexed to the isocyanates (and their reaction products), rather than covalently bonded.

It is apparent from this study that triorganotin-isocyanate interactions are complex, with several reaction pathways available. With respect to the formulation of antifouling coatings, the most appropriate triorganotins to incorporate would appear to be tri-*n*-butyltin chloride and tri-*n*-butyltin acetate which are unchanged in the polymer. The presence of the latter does, however, lead to rather excessive foaming. The foaming observed in the *bis*-(tri-*n*-butyltin) oxide polymers is probably due to the formation of isocyanate oligomers which act as branch points, thus aiding foam development. A similar effect is proposed for the *bis*-(triphenyltin) oxide, which again yields highly foamed polymers.

The increased setting time observed for the triphenyltin chloride containing polymer is not readily explained. The spectral evidence suggests that the organotin is unchanged after mixing with DND, which itself appears to be modified. It is assumed that the chemical changes which triphenyltin chloride induces in the isocyanate results in a lack of reactivity with the polyol. Certainly, the triphenyltin chloride containing polyurethane was physically very different to the others made.

Chapter 5 References.

1. Woods, G., The ICI Polyurethanes Book, Wiley and Sons, 1987.
2. Farkus, A. and Flynn, K.G., J. Am. Chem. Soc., 1960, 82, 645.
3. Britain, J.W. and Gemeinhardt, P.G., J. Appl. Poly. Sci., 1960, 4, (11), 207.
4. Bloodworth, A.J. and Davies, A.G., Proc. Chem. Soc., 1963, 264.
5. Entelis, S.G., Nesterov, O.V. and Tiger, R.P., J. Cell. Plast., 1976, 360.
6. Lipatova, T.E., Bakalo, L.A., Niselsky, Y.N. and Sirotinskaya, A.L., J. Macromol. Sci.-Chem., 1970, A4, (8), 1743.
7. Bacaloglu, R., Cotarca, L., Marcu, N. and Tölgyi, S., J. Prakt. Chem., 1988, 330, (4), 541.
8. Dyer, E. and Pinkerton, R.B., J. Appl. Polym. Sci., 1965, 9, 1713.
9. Bloodworth, A.J. and Davies, A.G., J. Chem. Soc., 1965, 5238.

6. Summary of Conclusions and Suggestions for Future Work

6.1. Conclusions from Studies of Triorganotins in Hypalon Paint

It was found that tri-*n*-butyltin chloride, tri-*n*-butyltin acetate, *bis*-(tri-*n*-butyltin) carbonate and *bis*-(triphenyltin) oxide are essentially unmodified when they are incorporated into Hypalon paint. There was some evidence, (from solvent extraction/NMR studies), to suggest that tri-*n*-butyltin chloride may be bonded coordinately to the polymer. This may result in a lower than expected release-rate of biocide from the paint.

Bis-(tri-*n*-butyltin) oxide was entirely converted into two new species, one of which was identified as tri-*n*-butyltin chloride, (from Mößbauer and NMR parameters). It was thought that *bis*-(tri-*n*-butyltin) oxide may react with chlorosulphonyl side groups of the Hypalon polymer. This would result in the formation of tri-*n*-butyltin chloride and a tri-*n*-butyltin sulphonate ester. The latter was thought to be the second tin component in the dried paint originally containing *bis*-(tri-*n*-butyltin) oxide. However, when such compounds were synthesized in a model study, the Mößbauer and NMR parameters did not support such a theory.

Two other potentially reactive components of the paint mix were also treated with *bis*-(tri-*n*-butyltin) oxide in model studies, *viz*, stearic acid and thiuram disulphide. However, the Mößbauer and NMR parameters of the products were, again, dissimilar to those observed in the dried paint. The identity of the second component remains unknown.

Triphenyltin acetate undergoes some dephenylation upon incorporation into Hypalon paint, with a diphenyltin species detected by GC after derivatization/solvent extraction. Triphenyltin chloride experiences more severe dephenylation, with di- and monophenyltin species present in the dried paint. In contrast, *bis*-(triphenyltin) oxide was unmodified when incorporated into the paint.

The model studies with the triorganotin sulphonate esters showed them to be species of high coordination number, (and 1:1 electrolytes in DMSO). The Mößbauer spectra of the triphenyltin sulphonate esters exhibit significant line asymmetry, even after grinding with graphite or aluminium oxide. This was thought to be due, not to the Gol'danskii-Karyagin effect, but rather a distribution of tin sites within the products. There is no literature, to date, on such systems and further work is required to gain a better understanding of their structural chemistry. One approach might be to study the structure of these and other synthesized triphenyltin sulphonate esters, by X-ray crystallography.

6.2. Conclusions from the Release-Rate Studies

The eight Hypalon paint samples were found to have release-rates around the $0.05 \mu\text{gSn}/\text{cm}^2/\text{day}$ level. This is two orders of magnitude too low for effective antifouling performance, but this can only be confirmed by raft panel tests. The cause of the low release-rates may be due to the the levels of triorganotins originally incorporated into the the paint. Additionally, it may also be a result of coordinate bonding between the biocide and the polymer. This assertion is based upon Mößbauer and NMR spectroscopic evidence.

6.3. Conclusions from Studies of Triorganotins in Polyurethane

Apart from tri-n-butyltin chloride, all of the triorganotins studied interact or react with the polymeric isocyanate, DND. Certain organotins were also shown to catalyze the polyurethane reaction, viz, tri-n-butyltin chloride, *bis*-(triphenyltin) oxide and triphenyltin chloride, (the latter actually decreasing the rate of reaction, *i.e.* an inhibitor).

The polyurethane originally containing *bis*-(tri-n-butyltin) oxide was the fastest setting, but *bis*-(tri-n-butyltin) oxide was not present in the final polymer. It is proposed that *bis*-(tri-n-butyltin) oxide reacts rapidly with isocyanates to yield N-stannylcarbamate derivatives and it is these species which catalyze the

reaction. The excessive foaming caused by *bis*-(tri-*n*-butyltin) oxide (and its reaction products), is thought to be due to the catalytic formation of isocyanate oligomers which act as branch-points for polymer cross-linking.

The most suitable triorganotins for the incorporation into polyurethane are tri-*n*-butyltin chloride and tri-*n*-butyltin acetate. However, release-rate studies and/or raft panel tests are necessary in order to determine their efficiency as antifouling coatings. Other work should include a more detailed study into the structural and chemical nature of the triorganotins and their relationship to catalytic activity, *e.g.* the marked differences in catalytic behaviour of triphenyltin chloride and tri-*n*-butyltin chloride and their effect on polyurethane structure. There is very little data reported in the literature on this industrially significant area of chemistry.

Courses and Conferences Attended.

1. Conferences:

The Royal Society of Chemistry Mößbauer Discussion Group meetings at:

- (i) UMIST 8th to the 9th September 1988,
- (ii) University of Essex 5th to the 7th July 1989 and
- (iii) University of Sheffield 2nd to the 4th July 1990, where I presented a paper entitled "¹¹⁹Sn Mößbauer Studies of Triorganotin Biocides in Antifouling Paints".

2. Courses:

- (i) Introduction to Mößbauer Spectroscopy, 10×2 hour lectures held at Sheffield City Polytechnic, February 1988 and
- (ii) Introduction to Word Processing held at Sheffield City Polytechnic, June 1988.

Acknowledgements

I should like to thank my supervisors, Dr D W Allen and Professor J S Brooks, for their considerable help and guidance throughout the past three years. I should also like to acknowledge financial support from Sheffield City Polytechnic and supplies of samples and the tin source from the Admiralty Research Establishment.

Thanks also go to various members of staff at the polytechnic for helpful discussions and practical advice, in particular, Roger Smith and Alan Cox. Mention should also be made of the Department of Chemistry Research Staff Tea Club and its contribution towards social development.

Finally, I should like to thank Antony Dewar of Raytek Scientific Ltd for his incalculable assistance during the conversion of this thesis from its original draft form and Katharine Taylor for her patience.